

**PHYTOPLANKTON CHANGE FROM POPULATION TO ECOSYSTEMS:  
INTEGRATING THE EFFECTS OF NUTRIENT DYNAMICS,  
TEMPERATURE AND ENVIRONMENTAL VARIABILITY**

Dissertation zur Erlangung des akademischen Grades  
Doktorin der Naturwissenschaften

*Dr. rer. nat.*



Erstgutachterin: PD Dr. Maren Striebel  
Zweitgutachterin: Prof. Dr. Sonja Jähnig

Anika Happe

1. September 2025





## Table of contents

Abstract .....	III
Zusammenfassung .....	V
1 Introduction.....	1
1.1 Changing the rules: how the climate crisis reshapes the aquatic environment .....	2
1.2 Scales of environmental change: local to global, from cells to ecosystems .....	3
1.3 The central role of phytoplankton in the aquatic ecosystem.....	4
1.3.1 Phytoplankton growth and stoichiometry in a changing environment.....	6
1.3.2 Up the food web: Stoichiometric links from microalgae to birds .....	9
1.4 How is phytoplankton currently studied and assessed? .....	10
1.5 Aims and outline of the thesis .....	11
1.6 List of publications of the thesis and author contributions .....	14
2 Publication I.....	17
<i>Synthesis of Population Trends Reveals Seascape-Wide Reorganisation of Biodiversity From Microalgae to Birds</i>	
3 Publication II .....	35
<i>Warming increases the compositional and functional variability of a temperate protist community</i>	
4 Publication III .....	49
<i>The experimental implications of the rate of temperature change and timing of nutrient availability on growth and stoichiometry of a natural marine phytoplankton community</i>	
5 Publication IV .....	63
<i>Nutrient pulse scenarios drive contrasting patterns in the functional stability of freshwater phytoplankton</i>	
6 Publication V .....	77
<i>The effects of nutrient pulse scenarios on the stoichiometry of a freshwater plankton community across sites and seasons</i>	
7 Synthesis .....	101
7.1 Mechanistic effects on phytoplankton biomass and growth across studies .....	103
7.2 Mechanistic effects on phytoplankton community stoichiometry across studies ..	104
7.3 Transferring mechanistic effects to the ecosystem scale.....	107
7.4 Implications for the food-web and ecosystem.....	110
7.5 Future perspectives.....	112

7.5.1	Policy: Missing aspects in standard monitoring and assessment .....	112
7.5.2	Experimental gaps and biases .....	113
7.5.3	Concluding remarks .....	115
	References .....	117
	Appendix Publication I.....	127
	Appendix Publication II .....	137
	Appendix Publication III.....	147
	Appendix Publication IV.....	155
	Appendix Publication V .....	161
	Acknowledgements .....	181
	Declaration .....	182

## **Abstract**

Climate change is massively reshaping aquatic ecosystems, for example, by altering nutrient cycles, increasing water temperatures and intensifying the frequency and intensity of extreme events such as heatwaves and heavy rainfall events. These environmental changes have far-reaching consequences for the structure and functioning of phytoplankton communities which determine the food quantity (biomass) and quality (stoichiometry) available to higher trophic levels and thus, form the foundation of aquatic food-webs. Even though significant progress has been made to understand how phytoplankton respond to shifts in its environment, critical knowledge gaps remain. For example, experimental studies often focus on mean warming levels or nutrient concentrations, even though nature is determined by more complex facets of these parameters. Furthermore, despite their pivotal role, phytoplankton communities are often underrepresented in ecosystem-level assessments, leading to an incomplete understanding of how climate-induced changes at the base of the food web cascade through trophic levels. This thesis addresses these gaps by integrating long-term monitoring data with targeted experiments to unravel the effects of a wide range of facets of climate change on phytoplankton communities and link experimental insights to monitoring findings.

After a general introduction (chapter 1), chapter 2 synthesizes population trends and highlights the current status of phytoplankton relative to other ecosystem components in the natural environment. The results demonstrate that phytoplankton as a group show as many positive as negative population trends, whereas fish and zooplankton show overall decreasing population trends. However, as several phytoplankton classes demonstrate overall decreasing trends, this clearly shows a drastic reorganization of coastal communities, including phytoplankton. The reasons for these alterations are based on an interplay of local pressures (e.g., shifts in the nutrient regime) and global stressors (e.g., global warming) which are individually and in interaction addressed in chapters 3-6. In chapter 3, I conducted an indoor mesocosm experiment and showed that warming increased the compositional and functional variability (biomass, gross oxygen productivity) of a temperate protist community, whereas its stoichiometry remained largely unaffected by temperature. This is in line with the findings from a laboratory experiment in chapter 4 in which no effect of warming or the rate of temperature change on the community stoichiometry was found. In turn, I experimentally showed that phytoplankton community stoichiometry is strongly influenced by nutrient dynamics (chapter 4-6). However, the stoichiometric response goes beyond prevailing nutrient conditions and associated limitation patterns (chapter 4) but is additionally shaped by the nutrient supply ratio, the relative

timing and interaction with temperature (chapter 4). Additionally, varying the temporal pattern of nutrient pulses during in-situ mesocosm experiments (chapter 5-6) showed that phytoplankton biomass fully recovered from an extreme nutrient and cDOM pulse, whereas multiple pulses of higher frequency gradually increased the biomass. In terms of stoichiometry, however, the extreme pulse led to the lowest stability (chapter 5). The direction of phytoplankton responses was consistent across seasonal and spatial settings, whereas the magnitude of changes was strongly influenced by seasonal and site-specific characteristics, such as the trophic status of a system (chapter 6). Overall, this highlights that extreme rainfall events, which are predicted to increase in frequency in the future, may destabilize phytoplankton stoichiometry, potentially leading to shifts in the consumer community composition (chapter 5) and thus, likely cascade through the food-web.

In the synthesis of this thesis (chapter 7), I summarise these mechanistic findings (chapter 7.1 and 7.2), transfer them to the ecosystem scale to use this knowledge for interpreting findings from long-term monitoring data (chapter 7.3) and highlight implications of phytoplankton changes for the food-web (chapter 7.4). Most dominantly, the here evidenced alterations of phytoplankton food quantity and quality impact higher trophic levels, for example, by inducing quality starvation, constraining the energy transfer efficiency and promoting shifts in grazer community composition which eventually impact fish and bird populations and communities. Ultimately, this thesis points to conducting ecologically relevant and transferable experiments, for example by using multi-driver and scenario-based approaches, alternative facets of environmental change or/and natural phytoplankton communities to increase our understanding of the fate of aquatic systems in the future. Beyond experimental implications, this thesis strongly highlights the importance of monitoring phytoplankton stoichiometry in environmental assessments to be aware of changes at the base of the food-web and potential critical thresholds that induce food quality limitation for higher trophic levels.

## **Zusammenfassung**

Der Klimawandel setzt aquatische Ökosysteme unter massiven Druck, indem er z.B. die Wassertemperaturen erhöht, Nährstoffkreisläufe verändert oder die Häufigkeit und Intensität von Extremereignissen wie Hitzewellen und Starkregenereignissen verstärkt. Diese Umweltveränderungen führen zu weitreichenden Folgen für die Struktur und Funktionsweise von Phytoplanktongemeinschaften, die die Menge (Biomasse) und Qualität (Stöchiometrie) der Nahrung bestimmen, die höheren trophischen Ebenen zur Verfügung steht und somit die Grundlage der Nahrungsnetze in aquatischen Systemen bildet. Obwohl in den letzten Jahrzehnten bereits große Fortschritte erzielt wurden, um die Veränderungen des Phytoplanktons infolge von Umweltveränderungen zu verstehen, bestehen noch entscheidende Wissenslücken. Beispielsweise konzentrieren sich experimentelle Studien häufig auf mittlere Veränderungen in der Temperatur oder Nährstoffverfügbarkeit, obwohl die Natur durch komplexere Facetten dieser Parameter bestimmt wird. Während Phytoplankton in der Wissenschaft eine zentrale Rolle in der Klimawandelforschung zugeschrieben wird, sind sie in Bewertungen über den Zustand von Ökosystemen, die an politische Entscheidungsträger herangetragen werden, häufig unterrepräsentiert. Die vorliegende Doktorarbeit schließt diese Lücken, indem sie zielgerichtete Experimente mit Langezeitbeobachtungsdaten verbindet, um die Auswirkungen einer Vielzahl von Facetten an Umweltveränderungen auf Phytoplanktongemeinschaften zu entschlüsseln.

Nach einer allgemeinen Einführung (Kapitel 1), präsentiere ich eine Synthese von Populationstrends, um den aktuellen Status von Phytoplankton im Vergleich zu anderen Organismengruppen im Ökosystem zu betrachten (Kapitel 2). Die Ergebnisse zeigen, dass Phytoplankton als Gruppe sowohl positive als auch negative Populationstrends aufweist, während beispielsweise Zooplankton und Fische insgesamt rückläufige Trends zeigen. Gleichzeitig weisen jedoch eine Vielzahl von Phytoplanktonklassen negative Populationstrends auf, womit ich insgesamt eine drastische Umstrukturierung von Küstengemeinschaften, einschließlich des Phytoplanktons zeige. Die Gründe für diese Umstrukturierung beruhen auf einem Zusammenspiel aus lokalen (z.B. Verschiebungen in der Nährstoffverfügbarkeit) und globalen Stressoren (z.B. Klimaerwärmung), die einzeln und in Kombination in den Kapiteln 3-6 behandelt werden. In Kapitel 3 zeige ich anhand eines Mesokosmos-Experiments, dass wärmere Temperaturen die Variabilität der Gemeinschaftszusammensetzung und Funktionsweise vom Phytoplankton erhöhen, während ihre Stöchiometrie weitgehend unbeeinflusst von der Temperatur bleibt. Dies spiegelt sich auch in einem Laborexperiment in

Kapitel 4 wider, bei dem keine Effekte von der Intensität oder Rate der Temperaturveränderung auf die Stöchiometrie der Phytoplanktongemeinschaft gefunden wurden. Allerdings zeigen Kapitel 4-6 eindeutig, dass die Nährstoffverfügbarkeit der wichtigste Treiber für die Stöchiometrie der Phytoplanktongemeinschaft ist. Dies geht jedoch über vorherrschende Nährstoffkonzentrationen oder Limitierungsmuster hinaus (Kapitel 4) und wird zusätzlich durch das Verhältnis von verfügbaren Nährstoffen zueinander, der Interaktion und dem relativen Zeitpunkt zu Temperaturveränderungen bestimmt (Kapitel 4). Die Variation des zeitlichen Musters von Nährstoffpulsen während in-situ Mesokosmos-Experimenten (Kapitel 5-6) zeigt zudem, dass sich die Phytoplanktonbiomasse von einem extremen Puls (als simuliertes Extremregenereignis) vollständig erholen kann, während die Stöchiometrie eine hohe langfristige Instabilität aufweist. Pulse mit höherer Frequenz, hingegen, zeigen ein gegensätzliches Muster von graduell ansteigender Biomasse und stabilerer Stöchiometrie (Kapitel 5). Die Richtung der Phytoplanktonreaktion war über getestete Jahreszeiten und Seen hinweg konsistent, während die Intensität der Veränderung im Phytoplankton eine hohe Kontextabhängigkeit zeigte (Kapitel 6). Insgesamt können also extreme Niederschlagsereignisse, deren Häufigkeit in Zukunft zunehmen wird, die Stöchiometrie von Phytoplankton destabilisieren, was zu Verschiebungen in der Zooplanktongemeinschaft führen (Kapitel 5) und sich entlang des Nahrungsnetz übertragen kann.

In der Synthese der Doktorarbeit (Kapitel 7) fasse ich die experimentellen Ergebnisse zusammen (Kapitel 7.1 und 7.2), übertrage sie auf die Ökosystemskala, um diese Erkenntnisse für die Interpretation von Langzeitbeobachtungsdaten zu nutzen (Kapitel 7.3) und zeige die Auswirkungen von Phytoplanktonveränderungen auf das Nahrungsnetz auf (Kapitel 7.4). Die gezeigten Veränderungen der Quantität und Qualität von Phytoplankton wirken sich zunächst auf höhere trophische Ebenen aus, indem sie beispielsweise die Effizienz des Energietransfers einschränken oder zu Verschiebungen in der Zusammensetzung der Zooplanktongemeinschaft führen. Abschließend empfehle ich die Durchführung von ökologisch relevanten und auf natürliche Systeme übertragbaren Experimenten, z.B. durch die Verwendung von mehreren Treibern oder Szenario-basierten Ansätzen, alternativen Facetten von Umweltveränderungen und/oder natürlichen Phytoplanktongemeinschaften, um unser Verständnis für Ökosystemveränderungen zu verbessern. Neben experimentellen Empfehlungen unterstreiche ich die Bedeutung von Phytoplankton für Umweltbewertungen, um Veränderungen an der Basis des Nahrungsnetzes, die zur Einschränkung der Nahrungsbedingungen für höhere trophische Ebenen führen, frühzeitig zu erkennen.

# **1 Introduction**

# 1 INTRODUCTION

## 1.1 Changing the rules: how the climate crisis reshapes the aquatic environment

Aquatic systems are increasingly exposed to cumulative pressures from local anthropogenic activities, such as tourism or fisheries, interacting with the large-scale pressures of climate change and eutrophication (Ramírez et al. 2018, IPBES 2019, Mazaris et al. 2019). On a global scale, greenhouse gas emissions following industrialization led to an average global temperature increase of 1.1°C at a mean warming rate of 0.06°C per decade since 1850 (IPCC 2023). Anthropogenic activities have also significantly altered the global cycles of phosphorus and nitrogen, for instance, by increasing the phosphorus concentrations from wastewater and agriculture, and nitrogen compounds from the agricultural use of fertilizers that ultimately accumulate in aquatic ecosystems, especially in lakes and coastal ecosystems (Vitousek et al. 1997, Filippelli 2008). Beyond their concentration, also the ratio between nutrients in the environment is significantly impacted by imbalanced anthropogenic inputs (Wu et al. 2022) as, for example, the global average nitrogen:phosphorus ratio in fertilizers has increased by 51% since 1975 (Peñuelas et al. 2013). However, climate change is not only altering mean levels of environmental parameters but also the frequency and intensity of extreme events such as heatwaves, droughts, or heavy rainfall (IPCC 2023) which is accompanied by terrestrial run-off of nutrients into lakes and coastal ecosystems.

Understanding the effects of global change on aquatic ecosystems, however, requires considering the interplay of multiple environmental drivers to provide a comprehensive and realistic prediction of future scenarios. For example, rising surface water temperatures increase stratification globally by 0.9% per decade (Li et al. 2020), which weakens mixing and thus reduces nutrient supply to surface waters (Thomas et al. 2012). In lakes, in turn, increased stratification can reduce the oxygen content in the hypolimnion, causing internal fertilization as chemical processes release and accumulate nutrients that were previously bound in the sediment (Song et al. 2013). Strong eutrophication again can severely limit light availability (Wilhelm and Adrian 2008). To account for this interconnectedness and complexity of drivers, studies investigating the response of aquatic organisms to global change should aim to realistically mimic the changing environment, for example, by including a multi-driver perspective or the variability around changes in the mean within their study designs.



# 1 INTRODUCTION

## 1.2 Scales of environmental change: local to global, from cells to ecosystems

The anthropogenic activities that impact aquatic ecosystems through interconnected pressures operate across different temporal and spatial scales (Petersen et al. 2009), from local over regional to global pressures (Figure 1.1). For example, pollution and nutrient input from a single sewage outfall are local stressors, while land use management, the agricultural landscape and the associated large-scale use of fertilizers can be classified as regional pressures, as they depend on national or regional regulations. Climate change and hence, global warming, can be classified as global pressures, although the effects of climate change are not evenly distributed across the globe (IPCC 2023) and aquatic systems (O'Reilly et al. 2015). Additionally, there are cross-scale feedbacks in which a global pressure, such as warming interacts with regional pressures, such as eutrophication (Petersen et al. 2009).

Pressures from anthropogenic activities across temporal and spatial scales, in turn, affect aquatic systems on various ecological scales, from single cells over populations to entire ecosystems (Petersen et al. 2009) (Figure 1.1). Understanding these scales is necessary to adequately address environmental responses resulting from local, regional and global pressures and assigning them to logical management levels. Scientific studies experimentally mimic these pressures in laboratory experiments, which typically target small and short-lived species such as phytoplankton and zooplankton, whereas mesocosms allow for the incubation of more complex aquatic communities (Gerhard et al. 2023). Both experimental approaches usually address pressures on shorter time scales (Petersen et al. 2009) or test the effects of pressures that occur on long time scales (e.g., warming) in a compressed experimental duration (Peck et al. 2009). Long-term monitoring fills this gap and provides a realistic picture of the past and present derived from the natural environment.

By integrating these approaches, we can build a mechanistic understanding of individual and multiple pressure effects on specific ecosystem components, relate the findings from populations to communities, and ultimately, use this knowledge to interpret long-term monitoring data and enhance our holistic understanding of climate change effects on aquatic ecosystems.

# 1 INTRODUCTION

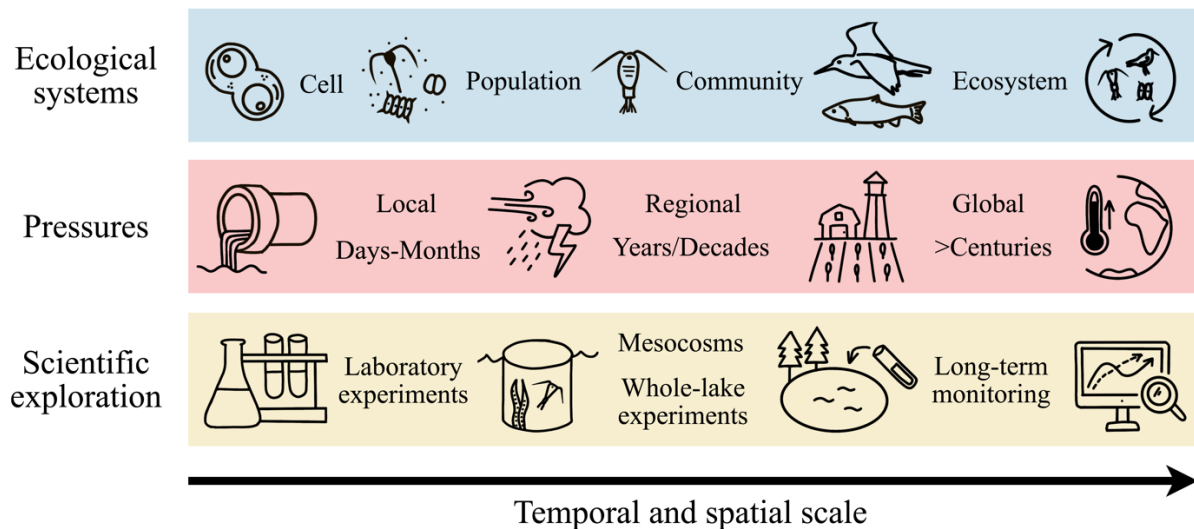


**Fig. 1.1:** Ecological systems, pressures and scientific exploration across temporal and spatial scales. Ecological systems range from biochemical reactions on cell-level over populations of small, short-lived organisms to communities and larger organisms (such as birds and fish) to the entire ecosystem perspective. Pressures act on local scales (such as wastewater outlets), on regional scale (such as extreme events and agricultural use of fertilizers) and with climate change on the global scale. Scientific studies explore the responses of ecological systems to these pressures, for example, in laboratory experiments, mesocosm studies, whole-lake experiments or via long-term monitoring and time series analyses. Along these scales, the complexity and realism that these scientific approaches address increases. Modified after Petersen et al. (2009).

## 1.3 The central role of phytoplankton in the aquatic ecosystem

Although phytoplankton only contribute between 1 and 2% to the total global plant carbon biomass (Falkowski 1994), they hold global relevance as major primary producers (Field et al. 1998) and play a vital role in the Earth's climate by driving the cycling of carbon and oxygen (Falkowski 1994, Falkowski et al. 2008). In the process of photosynthesis, phytoplankton produces a large proportion of the world's oxygen and simultaneously transforms atmospheric carbon dioxide into organic matter which later contributes to carbon sequestration in the deep sea and lake sediments, or fuels the aquatic food web (Falkowski 1994, Li et al. 2023).

However, phytoplankton react sensitively to changes in their environment such as seasonal changes, short-term disturbances or long-term climate change. Their extraordinarily high diversity in physiology (dominant pigment type, light and nutrient uptake parameters, temperature optima) and morphology (shape, size, biovolume, mucilage) (Litchman and Klausmeier 2008, Weithoff and Beisner 2019) contains a variety of strategies to cope with those changes via shifts in community composition or intracellular acclimation. For example, inherent nutrient acquisition traits, including maximum uptake rates and subsistence quotas directly regulate phytoplankton elemental assimilation, creating a critical bridge to cellular stoichiometry (Edwards et al. 2012).

# 1 INTRODUCTION

Phytoplankton stoichiometry is defined as the cellular elemental composition of essential macromolecules, most commonly carbon (C), nitrogen (N) and phosphorus (P) for example bound into proteins, lipids, carbohydrates and nucleic acids of the cell (Geider and La Roche 2002, Liefer et al. 2019). The structural stoichiometry i.e., the composition of the functional machinery of the cell, is rather constant and determines the species' nutrient requirements (Sterner and Elser 2002). However, phylogenetic differences in the composition of macromolecular compounds into which C, N and P are bound among major phytoplankton groups lead to group-specific, but also species-specific, variations in the C:nutrient ratios (Rhee and Gotham 1980, Finkel et al. 2009, Finkel et al. 2016). For example, cyanobacteria exhibit comparably low cellular C:N ratios, whereas *Bacillariophyta* and *Chlorophyta* fall within the intermediate range and *Dinophyta* demonstrate the highest cellular C:N ratios (Finkel et al. 2016).

During the onset of stoichiometry research, Redfield (1958) proposed the key concept of a mean universal C:N:P ratio of 106:16:1 in marine phytoplankton. However, more recent studies show that a strong latitudinal pattern underlies this generalization with ratios of 195:28:1 in the nutrient-deplete, warm low-latitude gyres, 137:18:1 in nutrient-rich, warm upwelling zones, and 78:13:1 in nutrient-rich, cold high-latitude regions (Martiny et al. 2013). Further important elements such as iron (Fe) or silicate (Si) were proposed to be included in the stoichiometric framework (Quigg et al. 2003), but still receive scarce consideration in studies on elemental ratios, although these micronutrients limit phytoplankton growth in certain regions (e.g., Martin et al. 1990). Nonetheless, this underlines that phytoplankton stoichiometry is not static but systematically varies depending on environmental conditions.

Over the years, more underlying processes have been identified to lead to plasticity in the cellular stoichiometry of phytoplankton. For example, the physiological demands for the allocation of nutrients depend on the growth phase of the phytoplankton as explained by the *growth-rate hypothesis* (Sterner and Elser 2002). During the exponential growth phase, such as the onset of a bloom event, a higher assimilation of phosphorus-rich ribosomes, and thus a lower N:P supply ratio, is required for protein synthesis (Klausmeier et al. 2004, Gerhard et al. 2019). During the stationary phase, phytoplankton cells prioritize the synthesis of nitrogen-rich proteins to facilitate metabolic processes (Klausmeier et al. 2004, Gerhard et al. 2019). At these low growth rates, phytoplankton stoichiometry often matches their nutrient supply (Sterner and Elser 2002, Klausmeier and Litchman 2004). Besides nutrient acquisition traits, also the cell size or the ability to store excess nutrients, influence the stoichiometry of a population (Litchman and Klausmeier 2008, Marañón et al. 2013).

# 1 INTRODUCTION

Thus, both the stoichiometric plasticity of the present species in response to environmental conditions (Geider and La Roche 2002) and shifts in group composition (Finkel et al. 2016) can explain shifts in community stoichiometry in space and time.

## 1.3.1 Phytoplankton growth and stoichiometry in a changing environment

Phytoplankton grows in the euphotic zone of aquatic systems where the concentration of inorganic nutrients, light, and temperature naturally vary in space and time (Tanioka and Matsumoto 2020). Even though they can cope with these natural variations within their habitat-specific conditions, they are increasingly stressed by long-term environmental changes (press disturbances) and fluctuations with increased intensity and frequency (pulse disturbances) imposed by anthropogenic climate change. These pressures do not only alter mean conditions (e.g., average temperature, nutrient conditions), but also the temporal and spatial variance around these conditions.

Generally, phytoplankton populations follow genotype-specific performance curves along environmental gradients. For example, growth in response to warming follows a unimodal, left-skewed curve that increases exponentially or linearly under colder temperatures and decreases sharply after its temperature optimum (Eppley 1972, Kontopoulos et al. 2024). Under increasing light, the growth curve initially increases linearly, saturates at an optimum light intensity and then slowly decreases due to photo-inhibition (Langdon 1988, Litchman and Klausmeier 2008). Nutrients show a typical saturation function with a rapid increase in low nutrient concentrations (Eppley et al. 1969).

Phytoplankton stoichiometry, as a second major performance parameter, shows an increased C:P and a stable C:N ratio in response to warming (Fig. 1.2, Yvon-Durocher et al. 2017, Verbeek et al. 2018, Tanioka and Matsumoto 2020). The mechanisms behind this are still under debate but include an increased metabolic stimulation of carbon versus phosphorus uptake or an enhanced resource use efficiency under warming (Paul et al. 2015). With increasing light, both C:nutrient ratios increase as phytoplankton down-regulates the production of light-harvesting nitrogen-rich pigments and proteins to avoid photooxidative stress while increased carbon fixation enhances the storage of lipids and polysaccharides (Berman-Frank and Dubinsky 1999, Tanioka and Matsumoto 2020, Heinrichs et al. 2024). Similarly, rapid carbon fixation at high light conditions outpaces phosphorus uptake and thus, decouples carbon and phosphorus assimilation leading to increased carbon relative to phosphorus (Hessen et al. 2002, Hessen et al. 2008, Tanioka and Matsumoto 2020). Additionally, both C:nutrient ratios decrease with the

# 1 INTRODUCTION

concentration of the respective nutrient until reaching a saturation which is largely controlled by nutrient storage strategies (Tanioka and Matsumoto 2020).

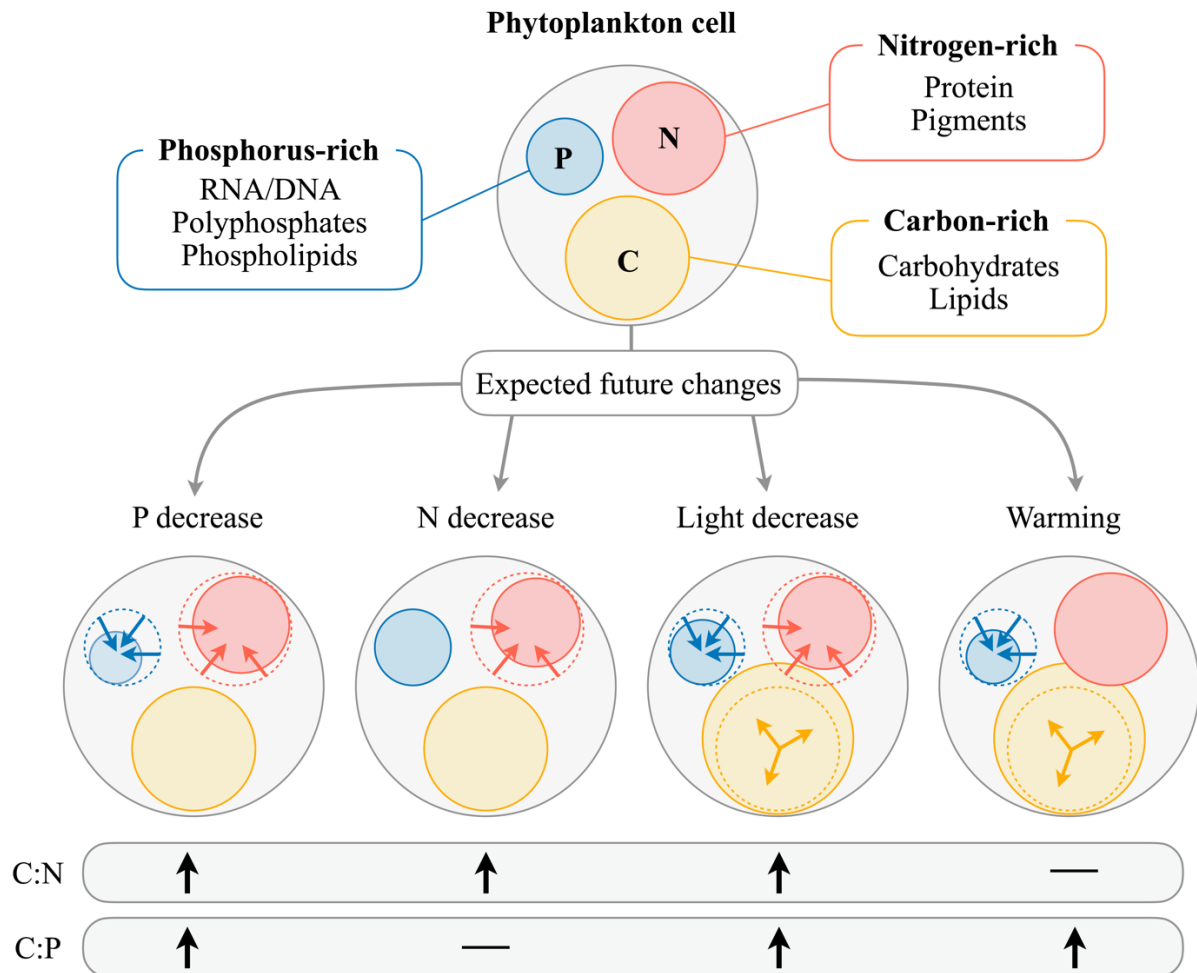


**Fig. 1.2:** Illustration of how expected future environmental changes affect the cellular allocation of volume between phosphorus-rich (blue), nitrogen-rich (red), and carbon-rich (orange) pools and modulate phytoplankton C:N and C:P ratios. Decreasing P supply leads to a decrease in P and N pools and thus, an increase in both C:nutrient ratios. A decrease in N supply negatively affects cellular N pools and decreases the C:N ratio. Decreasing light increases the C pool, while decreasing both nutrient pools which lead to increases in both C:nutrient ratios. Warming increases the C pool but decreases the P pool and by this induces an increase in C:P ratios. Modified based on Tanioka and Matsumoto (2020).

The past decades have been used to extensively study the response of phytoplankton performance to individual drivers. However, the natural world is multi-factorial and its drivers never act in isolation. Therefore, to make ecologically relevant estimates and predictions of climate change, it is important to consider the interaction of effects between environmental drivers (e.g., Thomas et al. 2017, Heinrichs et al. 2025). Multiple experiments demonstrated interactive effects of two environmental factors on phytoplankton performance, e.g., temperature and light (Dauta et al. 1990, Edwards et al. 2016), temperature and nutrients

# 1 INTRODUCTION

(Thomas et al. 2017, Thrane et al. 2017, Marañón et al. 2018, Verbeek et al. 2018) or even threefold interactions (Spilling et al. 2015, Heinrichs et al. 2024, Heinrichs et al. 2025).

For the temperature-light interaction, light limitation was shown to decrease the temperature optimum of phytoplankton populations by  $\sim 5^{\circ}\text{C}$  compared to optimum light conditions and the growth rate no longer increases with temperature under these light-limited conditions (Edwards et al. 2016). Similarly, highlighting the importance of temperature-nutrient interactions, nitrate limitation was found to decrease the temperature optimum by  $\sim 4^{\circ}\text{C}$  compared to unlimited conditions (Thomas et al. 2017). Thus, nutrients alter the curvature and height of a population growth curve at a set temperature (Thomas et al. 2017). In addition, thermal dependence of phytoplankton metabolism was shown to accentuate with increasing nutrient concentration (and vice versa) (Thrane et al. 2017, Marañón et al. 2018).

Stoichiometry is inherently combining the effects of multiple stressors as each component of the elemental composition is differently influenced by environmental parameters. For example, light availability predominantly drives carbon uptake, while nutrient supply mainly regulate the nitrogen and phosphorus quotas, and temperature modulates these processes by determining metabolic rates and growth efficiency (Tanioka and Matsumoto 2020). However, despite also being applicable to stoichiometry, multiple stressor research is still an underrepresented topic in the field. Still, recent research has shown that the thermal response of phytoplankton stoichiometry can be suppressed under nutrient limitation (Verbeek et al. 2018) and that the magnitude of the increase in C:nutrient ratios in response to increased irradiance is also nutrient-dependent (Dickman et al. 2006). This is in support of the *light-nutrient hypothesis* (Sterner and Elser 2002) predicting C:nutrient ratios to be a function of the light:nutrient supply ratio.

To date, the vast majority of mechanistic understanding of single-driver and multi-driver impacts on phytoplankton performance is based on single-species experiments. Although the here described response curves and surfaces are widely applicable, performance metrics (e.g., range or optima) along environmental gradients are species-dependent (Heinrichs et al. 2025). Additionally, community response curves and surfaces are not simply aggregated species responses, but are shaped by complex species interactions, such as competition and species selection (e.g., Anderson et al. 2022, Breton et al. 2022). Environmental gradients act as filters favoring certain species over others and thus, both the plasticity of the present species to environmental changes (Geider and La Roche 2002) as well as shifts in community composition (Finkel et al. 2016) shape the community performance across environmental conditions.

# 1 INTRODUCTION

## 1.3.2 Up the food web: Stoichiometric links from microalgae to birds

The biomass and stoichiometry of phytoplankton set the quantity and quality of food available to consumers at higher trophic levels. Not only a low food quantity but also a reduced nutritional content or a low digestibility of the dominating phytoplankton species can cause declines in grazer populations (Elser et al. 2000, Sterner and Elser 2002, Striebel et al. 2012). In contrast to the plastic stoichiometry of primary producers, consumers like zooplankton at higher trophic levels maintain relatively stable elemental body ratios (Andersen and Hessen 1991, Elser et al. 2000). However, since they acquire essential nutrients by feeding on prey with a plastic balance of these, elemental mismatches may emerge. For example, low C:nutrient ratios in the prey may evoke an energy limitation, while the nutrient content in high C:nutrient ratios potentially becomes too dilute and induces nutrient limitation for consumers (Urabe and Sterner 1996, Hodapp et al. 2019). However, zooplankton – as the primary consumers of phytoplankton – possess physiological mechanisms and feeding strategies to cope with such mismatches. For example, some can regulate their own elemental balance and thus, effectively reduce the mismatch, by digesting or retaining essential elements in ratios independent from the ratio in the prey (Elser et al. 2001, Kooijman et al. 2004). Unselectively feeding *Daphnia* increase their consumption rate as compensation for low food quality (Mandal et al. 2018), while copepods can select for nutritionally valuable food (Meunier et al. 2015).

Additionally, the nutritional quantity and quality of phytoplankton are heterogeneously distributed in space and can fluctuate over time, even more profoundly in response to environmental disturbances. Even though phytoplankton is capable of compensating for short-term fluctuations in environmental parameters through biochemical adjustments and changing the balance between photosynthesis and respiration (Padfield et al. 2016), their performance metrics (e.g., growth or stoichiometry) often respond sensitively to environmental variability depending on the fluctuation frequency (Svensen et al. 2002, Kunze et al. 2022). However, these fluctuations – which translate into temporally and spatially variable resources for consumers – are subsequently attenuated while spreading through the food web (Noy-Meir 1973, Schwinning and Sala 2004) as a dynamic averaging process occurs at each trophic level (Simon and Vasseur 2021). Strategies employed at the zooplankton level to mitigate the impact of fluctuations in resources or nutrient limitation include the increase in the individual ingestion rate in daphnids referred to as "compensatory feeding" (Koussoroplis et al. 2012) or "selective feeding" on nutrient-rich cells, a strategy employed by copepods (Cowles et al. 1988, Meunier et al. 2015).

# 1 INTRODUCTION

Nonetheless, elemental mismatches may be accompanied by a reduced trophic transfer efficiency between primary and secondary producers (Urabe et al. 2003) and thus, may impact the entire aquatic food web by strengthening or creating stoichiometric bottlenecks (van de Waal et al. 2010). Within this, zooplankton plays a key role as being positioned in the center of the food web, while the mid-trophic level is often dominated by a few abundant species of pelagic schooling fish, channeling the produced energy and nutrients to top predators such as predatory fish, marine birds or mammals (Frederiksen et al. 2006). For example, in the North Sea ecosystem, the abundance of zooplankton (Richardson et al. 2004, Frederiksen et al. 2006), recruitment of fish (Beaugrand et al. 2003, Frederiksen et al. 2006), and seabird breeding productivity (Aebischer et al. 1990, Frederiksen et al. 2006) were all shown to be bottom-up controlled. Systems in which bottom-up control is the predominant mechanism are particularly vulnerable to environmental change, as the impact on each trophic level accumulates and cascades up the food web. Understanding the impacts of climate change on bottom-up controlled systems is therefore crucial for predicting and attenuating negative cascading effects.

## 1.4 How is phytoplankton currently studied and assessed?

To achieve the overarching goal of estimating and predicting the effects of global change on phytoplankton as the base of the aquatic food web, researchers employ a diverse array of methodological approaches. These range from gaining a mechanistic understanding of the effects of specific drivers and driver combinations in small-scale laboratory experiments and more complex mesocosm experiments, to long-term time series analysis that capture the current status of change and explore the complex web of naturally interacting drivers (Fig. 1.1). Understanding phytoplankton responses to global change requires experimental and observational science to inform each other to identify patterns in real-world data by linking it to mechanistic understanding.

Observational studies that build on long-term monitoring provide essential insights for detecting trends and changes in species composition and biomass and identify causalities between biotic changes and environmental parameters or anthropogenic disturbances over time (e.g., Di Pane et al. 2022, Rönn et al. 2023). The collection of such data relies on sustained funding for monitoring and continuous data processing which often limits the time series length or the range of monitored species. For example, in the Wadden Sea, while phytoplankton has been monitored for decades (Rönn et al. 2023) and regularly informs eutrophication assessments as bulk biomass (van Beusekom et al. 2019), zooplankton monitoring was only established 5 years ago and has not yet been incorporated in official assessments that guide



# 1 INTRODUCTION

conservation efforts (Jak and Slijkerman 2023). Additionally, interpreting patterns found between environmental parameters and species changes requires linking them to experimentally derived mechanistic understanding.

Experimental studies typically select certain species or assemble artificial communities in laboratory experiments, whereas mesocosm studies more frequently test natural communities with one or two trophic levels. These studies usually manipulate specific environmental drivers in isolation or a controlled multi-driver setting which enables to gain mechanistic insights into cellular responses and community dynamics which collectively inform how phytoplankton may respond to future conditions of global change. However, due to the compromise between controllability and complexity in experimental design (Gerhard et al. 2023), these studies are a simplistic representation of natural processes and cannot fully capture the complexity of nature in which even more environmental parameters, their variability, interactions with higher trophic levels and dispersal drive the ecosystem-level response.

Despite considerable advancements, plankton communities are still underrepresented in ecosystem assessments and thus, a crucial link from the base of the food web to changes on higher trophic levels is often overlooked. Additionally, several aspects that allow for a more realistic representation of climate change effects on natural plankton communities are currently critically understudied, such as applying a certain rate of temperature change or data-derived future precipitation patterns.

## 1.5 Aims and outline of the thesis

In this thesis, I aim to (1) mechanistically disentangle the effects of classical and overlooked facets of future temperature and nutrient changes in moderating phytoplankton community biomass and stoichiometry; (2) map phytoplankton change in a whole-ecosystem perspective and identify potential effect on trophic dynamics; (3) and address methodological issues in observational and experimental studies on phytoplankton in the face of climate change to improve their ecological relevance. Five interconnected studies form the core chapters of this thesis (chapters 2–6), moving from a data analysis of long-term monitoring data to identify how plankton communities are restructuring in comparison with other ecosystem components, to then mechanistically and experimentally disentangle the effects of various facets of environmental change on phytoplankton performance.

In chapter 2 (**publication I**), I applied a new systematic and quantitative approach to generalize population trends across all ecosystem components within the Wadden Sea and thus, present a

# 1 INTRODUCTION

seascape-wide assessment of population status. To fill a critical gap in governmental assessment strategies, I aimed to include a community perspective of phytoplankton and zooplankton, as important basal trophic levels, and thus, to provide a holistic view of biodiversity re-organization in the Wadden Sea which complements existing assessments.

In the subsequent chapters, I aimed to experimentally understand the effects of the most important drivers behind these changes in natural plankton communities. To upscale the changes on the base of the food web, I focused on food quality (stoichiometry) and quantity which allowed to estimate potential effects for higher trophic levels and draw conclusions from a broader ecological viewpoint.

Specifically, chapter 3 (**publication II**), mimics the effect of future temperature increases on a natural phytoplankton community in the spring-summer transition phase to assess how warming altered the compositional and functional variability of the community.

Conducted alongside the mesocosm experiment in chapter 3, chapter 4 (**publication III**) includes gradients of nitrogen and phosphorus concentrations in addition to warming as drivers of growth and stoichiometry in a natural phytoplankton community. Additionally, this chapter studies novel facets of these drivers by testing different rates of temperature change and timings of nutrient input relative to warming and with this aims to identify biases in the experimental design of temperature change experiments to ultimately improve the comparability across studies and the transfer of the results to natural systems.

Chapter 5 (**publication IV**) and chapter 6 (**publication V**) pick up the topic of nutrient fluctuations introduced into natural aquatic systems by terrestrial run-off following heavy rainfall events. In these chapters, different scenarios of future rainfall, from regularly small events to extreme events, were applied as nutrient and cDOM pulses to a natural plankton community. By this, I aimed to disentangle the effect of different fluctuations of nutrients and light on phytoplankton and zooplankton growth and stoichiometry (chapter 5 and 6) and to understand seasonal and spatial dependencies to identify general patterns (chapter 6).

# 1 INTRODUCTION

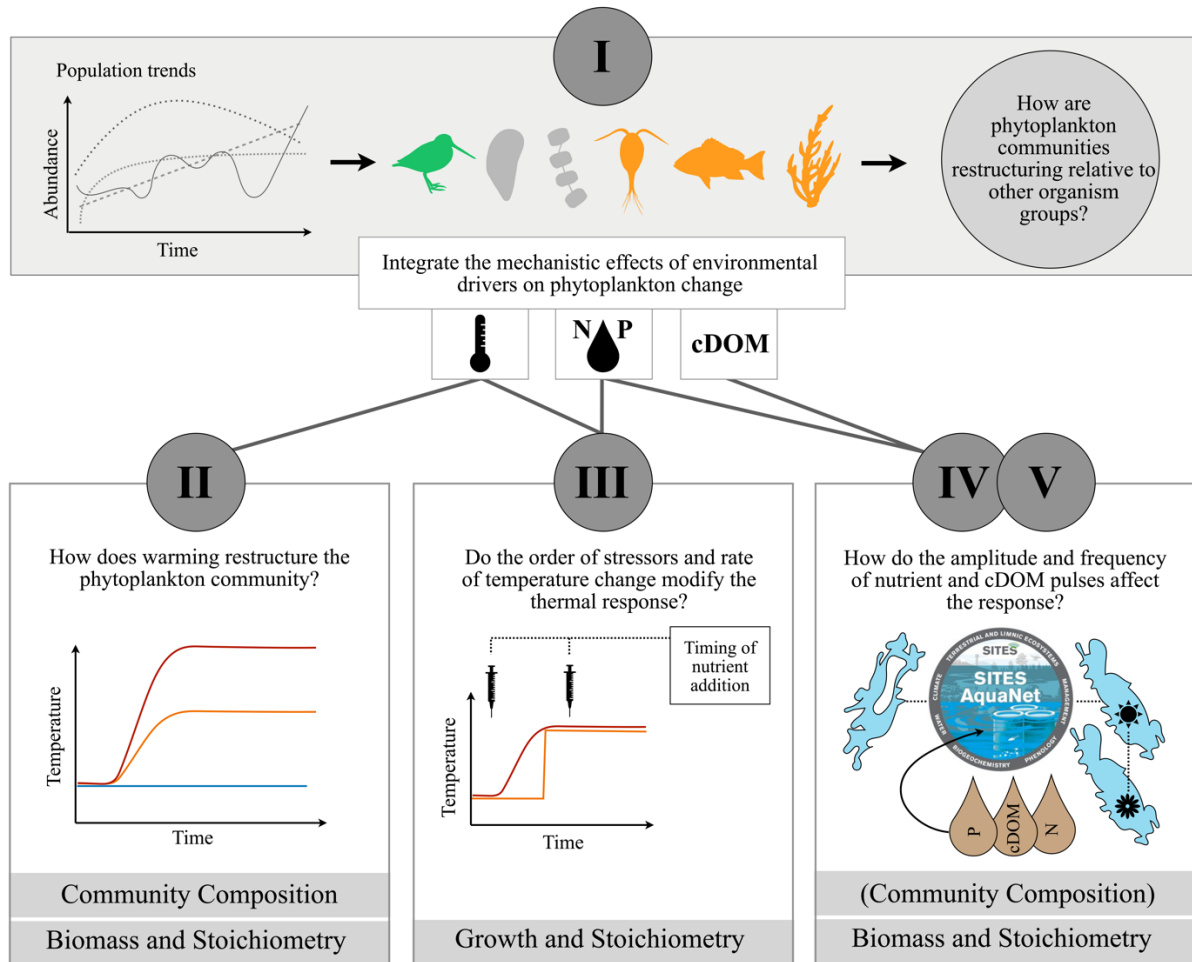


**Fig. 1.3:** Overview of the five publications of this thesis. The box of the first publication (I) shows the idea of generalizing population trends in which each line represents one population and the outcome of a subsequent meta-analysis as organism group symbols identifying saltmarsh plants and seagrasses, fish and zooplankton as having overall negative trends (orange), macrozoobenthos and phytoplankton with neutral trends (grey) and birds with overall positive trends (green). The second publication (II) displays the three temperature treatments that were applied to the phytoplankton community to test their effect on phytoplankton community composition, biomass and stoichiometry. The box of the third (III) publication presents the experimental treatments that were applied i.e., gradual versus acute temperature change and nutrient addition before or after the temperature change. The box of the fourth and fifth (IV, V) publication shows the input of nitrogen, phosphorus and colored dissolved organic matter (cDOM) that were applied with different frequencies, intensities and chronologies mimicking different run-off scenarios across two different lakes and seasons.

# 1 INTRODUCTION

## 1.6 List of publications of the thesis and author contributions

**Publication I**                      **Happe, A.\***, K. J. Meijer\*, J.-C. Dajka, O. Franken, H. Haslob, L. Chapter 2                      L. Govers, M. Kleyer, A. C. M. Kok, L. Kuczynski, K. Löhmus, S. E. T. van der Meij, H. Olff, L. Rönn, A. Ryabov, A. F. Sell, D. W. Thieltges, B. K. Eriksson†, H. Hillebrand† (*accepted*): Synthesis of population trends reveals seascape-wide reorganisation of biodiversity from microalgae to birds. *Global Change Biology*.

The study was conceptualized by myself, KJM, BKE and HHi. The data used in the analysis was curated by myself, HHa, MK, KL, SETVDM, HO, LR, AFS, BKE and HHi. The methodology was developed by myself, KJM, JCD, OF, HHa, ACMK, SETVDM, HO, AR, AFS, BKE and HHi. The formal analysis was conducted by myself and KJM. The results were visualized by myself and KJM. The original draft was written by myself and KJM. The manuscript was reviewed and edited by myself, KJM, JCD, OF, HHa, ACMK, LK, LLG, SETVDM, HO, LR, AR, AFS, DWT, BKE and HHi.

\* KJM and me contributed equally to this work and share first authorship.

† BKE and HHi contributed equally to this work and share senior authorship.

**Publication II**                      Ahme, A., **A. Happe**, M. Striebel, M. J. Cabrerizo, M. Olsson, J. Chapter 3                      Giesler, R. Schulte-Hillen, A. Sentimenti, N. Kuhne, and U. John. 2024. Warming increases the compositional and functional variability of a temperate protist community. *Science of the Total Environment* 926:171971.

The experiment was planned by AA with support of myself, UJ and MS. The on-site coordination of the mesocosm infrastructure and transnational access to the experiment was led by myself. The experiment was conducted by AA with the help of myself and all co-authors. The samples were processed by AA and myself. The data analysis was performed by AA, MC and JG. Results were interpreted by AA with the help of myself and all co-authors. The manuscript was written by AA, and revised with the help of myself and all co-authors.

# 1 INTRODUCTION

## Publication III

### Chapter 4

**Happe, A.,** A. Ahme, M. J. Cabrerizo, M. Gerhard, U. John, and M. Striebel. 2024. The experimental implications of the rate of temperature change and timing of nutrient availability on growth and stoichiometry of a natural marine phytoplankton community. *Limnology and Oceanography* 69:1769-1781.

The experiment was planned by myself and MS with the help of AA. The experiment was conducted by myself with the help of AA. The samples were processed by myself. The data analysis was performed by myself with support of MS and MG. Results were interpreted by myself with the help of all co-authors. The manuscript was written by myself and revised by all co-authors.

## Publication IV

### Chapter 5

**Happe, A.,** B. Buttyán, B. Gergác, S. Langenheder, S. A. Berger, J. C. Nejstgaard, and M. Striebel. 2025. Nutrient pulse scenarios drive contrasting patterns in the functional stability of freshwater phytoplankton. *Limnology and Oceanography*, 9999: 1-14.

The overarching mesocosm experiment was planned conceptualized by SL with support of myself, SAB, JCN and MS. The specific study was conceptualized by myself and MS. The specific study was coordinated by myself with support of MS and SL. The mesocosm study was implemented by myself, BB, BG, SL, SAB and JCN. The sample analysis was conducted by myself with the help of BB, BG and SL. The data analysis and interpretation of results was done by myself with the help of MS. The original draft was written by myself. The manuscript was reviewed and edited by myself and all co-authors.

## Publication V

### Chapter 6

**Happe, A.,** J. Exner, B. Buttyán, E. A. Charmpila, B. Gergác, C. Mangold, S. Neun, J. C. Oppong, M. M. Yaqoob, J. C. Nejstgaard, S. A. Berger, S. Langenheder, and M. Striebel. (*in prep*). The effects of nutrient pulse scenarios on the stoichiometry of a freshwater plankton community across sites and seasons.

The overarching mesocosm study on the network-level was coordinated by SL with support of MS, SAB and JCN. The idea for the specific study was conceived by myself, MS and SL. The specific study was coordinated by myself with support of MS, JE, SL,

## 1 INTRODUCTION

EC, CM and SN. The mesocosm study was implemented by myself, SL, AH, JE, JCO, MMY, SAB, JCN, BB, BG, EC and CM. The sample analysis for the specific studies was conducted by myself, SL, BB, BG, CM and SN. The data analysis was conducted by myself with support of JE, JCO and MMY analyzed the data. The data was interpreted by myself with the help of SN, MS and SL. The original draft was written by myself with input of JE, BB, EC, BG, CM, JCO, MMY. All authors contributed to reviewing and editing the manuscript.

† SL and MS contributed equally to this work and share senior authorship.

## 2 Publication I

Synthesis of population trends reveals seascape-wide reorganisation of biodiversity from microalgae to birds

Published in *Global Change Biology* (2025)



## RESEARCH ARTICLE OPEN ACCESS

# Synthesis of Population Trends Reveals Seascape-Wide Reorganisation of Biodiversity From Microalgae to Birds

Anika Happe<sup>1</sup>  | Kasper J. Meijer<sup>2</sup>  | Jan-Claas Dajka<sup>1,3,4</sup>  | Oscar Franken<sup>2,5</sup>  | Holger Haslob<sup>6</sup>  | Laura L. Govers<sup>2,5</sup>  | Michael Kleyer<sup>7</sup>  | Annebelle C. M. Kok<sup>2</sup>  | Lucie Kuczynski<sup>1,8</sup>  | Kertu Löhmus<sup>7</sup>  | Sancia E. T. van der Meij<sup>2,9</sup>  | Han Olff<sup>2</sup>  | Lena Rönn<sup>10</sup>  | Alexey Ryabov<sup>1,4</sup>  | Anne F. Sell<sup>6</sup>  | David W. Thielges<sup>2,5</sup>  | Britas Klemens Eriksson<sup>2</sup>  | Helmut Hillebrand<sup>1,3,4</sup> 

<sup>1</sup>Institute for Chemistry and Biology of the Marine Environment (ICBM), School of Mathematics and Science, Carl von Ossietzky Universität Oldenburg, Oldenburg, Germany | <sup>2</sup>Groningen Institute for Evolutionary Life-Sciences, University of Groningen, Groningen, AG, the Netherlands | <sup>3</sup>Helmholtz-Institute for Functional Marine Biodiversity at the University of Oldenburg [HIFMB], Oldenburg, Germany | <sup>4</sup>Alfred Wegener Institute, Helmholtz-Centre for Polar and Marine Research [AWI], Bremerhaven, Germany | <sup>5</sup>Department of Coastal Systems, NIOZ Royal Netherlands Institute for Sea Research, Den Burg, the Netherlands | <sup>6</sup>Thünen Institute of Sea Fisheries, Bremerhaven, Germany | <sup>7</sup>Institute of Biology and Environmental Sciences, School of Mathematics and Science, Carl von Ossietzky Universität Oldenburg, Oldenburg, Germany | <sup>8</sup>UMR ENTROPIE, Lucie Kuczynski IRD, IFREMER, CNRS, University of La Reunion, University of New Caledonia, Noumea, New Caledonia | <sup>9</sup>Naturalis Biodiversity Center, Leiden, CR, the Netherlands | <sup>10</sup>Lower Saxony Water Management, Coastal and Nature Protection Agency (NLWKN, Brake-Oldenburg), Oldenburg, Germany

**Correspondence:** Britas Klemens Eriksson ([b.d.h.k.eriksson@rug.nl](mailto:b.d.h.k.eriksson@rug.nl)) | Helmut Hillebrand ([helmut.hillebrand@uni-oldenburg.de](mailto:helmut.hillebrand@uni-oldenburg.de))

**Received:** 15 January 2025 | **Revised:** 14 March 2025 | **Accepted:** 24 March 2025

**Funding:** This work was supported by European Union HORIZON EUROPE program ACTNOW: Advancing understanding of Cumulative Impacts on European marine biodiversity, ecosystem functions and services for human wellbeing (101060072).

**Keywords:** biodiversity assessment | conservation | ecosystem functioning | monitoring | North Sea | temporal population trends | Wadden Sea | winners and losers

## ABSTRACT

Many monitoring programs aim to understand regional biodiversity patterns in relation to global and regional conservation targets, using either community-wide biodiversity metrics to describe the community status or trends of pre-selected “key” species as biodiversity change indicators. However, the former often lacks information on which species are changing, and the latter is heavily skewed towards specific taxa, potentially overlooking changes in other, functionally important taxa. We gathered an extensive set of monitoring data with over 3000 population trends (ranging from 5 to 91 years in duration) for a wide range of taxa across the Wadden Sea. We combined a systematic and quantitative categorization of population trends (weighted vote count) with a meta-analysis on different taxonomic levels. This allowed the first cross-taxa synopsis of species declines and increases and determined their directionalities throughout time. Our meta-analysis showed an overall decrease in population size for fish, zooplankton, and plant species, while birds showed an overall increase. However, these increases mask recent negative trends within specific bird groups since the late 1990s. In contrast, fish populations exhibited declines over the entire monitoring period. Species with declining populations (losers) were phylogenetically related, whereas species with increasing populations (winners) represented various organismal groups. Directionality and onsets of change in population trends were temporally synchronized throughout several groups, such as bivalves, fish, and birds, and may provide warning signals for future local extinctions in these taxa. Our analysis moves beyond typical indicator species by including the entire species inventory of the system. Basal trophic levels of aquatic ecosystems, such as zooplankton and phytoplankton, are often missing from policy assessments but are

Anika Happe and Kasper J. Meijer contributed equally to this work and share first authorship. Britas Klemens Eriksson and Helmut Hillebrand contributed equally to this work and share senior authorship.

This is an open access article under the terms of the [Creative Commons Attribution](https://creativecommons.org/licenses/by/4.0/) License, which permits use, distribution and reproduction in any medium, provided the original work is properly cited.

© 2025 The Author(s). *Global Change Biology* published by John Wiley & Sons Ltd.



among the most important organism groups for ecosystem functioning. Here, we show that without additional monitoring effort, a systematic analysis of population trends adds to our understanding of trophic and compositional restructuring of ecosystems.

## 1 | Introduction

The global biodiversity crisis is an increasing concern as shifts in species ranges and relative abundances not only restructure biodiversity but also impact ecosystem functioning and human well-being (Pecl et al. 2017). However, as biodiversity comprises aspects of genetic, taxonomic, phylogenetic, and ecosystem diversity, unifying and generalizing this multifacetedness (Pereira et al. 2013) in biodiversity assessments is complex. Also, diversity can be captured on different scales as in alpha (within-sample diversity), beta (between-sample diversity), and gamma (regional) diversity. Moreover, biodiversity metrics do not always reflect ecologically meaningful processes, and some only provide a limited perspective of changes (Santini et al. 2017). For instance, the widely used species richness metric is sensitive to sampling effort and taxonomic resolution and does not align with rates of compositional turnover (Hillebrand et al. 2018). Simpson and Shannon diversity specifically capture both species richness and evenness (Hillebrand et al. 2018), but do not intuitively scale with species gain and loss (Roswell et al. 2021). To overcome these conceptual issues of traditional biodiversity metrics, the Hill number series (Hill 1973) provides a simple but more robust and logically reasonable approach to biodiversity by focusing more on dominant species and taking abundances into account (Chase and Knight 2013; Roswell et al. 2021; Antonucci Di Cavalho et al. 2023).

Analysing temporal trends with alpha diversity measures (e.g., species richness or the effective number of species) has provided insights into biodiversity dynamics (Dornelas et al. 2014; Rishworth et al. 2020), but this approach has limitations for inferring ecological mechanisms or informing policy. Ecologically, changes in local (i.e., alpha) biodiversity reflect only net changes in species number and not identity (Hillebrand et al. 2018). These changes, or the lack thereof, may not accurately reflect the actual changes in ecosystem properties and processes if, for instance, the declining species are replaced by functionally similar or different colonisers (Hillebrand et al. 2018; Eriksson and Hillebrand 2019). Also, analyses of changes in richness are strongly affected by the concept of extinction debt, when extinction is delayed after habitat deterioration (Tilman et al. 1994). Imbalances in temporal occurrences of colonisations and extinctions can bias biodiversity trends for decades (Jackson and Sax 2010; Kuczynski et al. 2023). More fundamentally, local species extirpation is the final step of decline, which is ideally detected much earlier.

An alternative approach is summarising population trends across species, which estimates population declines and increases. For example, the Living Planet Index (LPI) assesses trends in the relative abundance of vertebrate populations. However, the LPI has been criticised for not being an accurate, fully representative biodiversity indicator for planetary health; besides the fact that it only assesses vertebrates, it has been questioned as being sensitive to a multitude of mathematical assumptions (Jaspers 2020). For example, extreme individual trends can disproportionately influence aggregated indices (Finn et al. 2023). Moreover, the LPI relies on a geometric mean of trends across species (Loh

et al. 2005) and does not specifically aim to identify increasing populations (winners) alongside decreasing populations (losers) (Finn et al. 2023). Here, we propose a synthesis of population trends within and across taxonomic groups to fully capture the ecosystem-wide reorganisation of biodiversity.

In long-term monitoring data sets, species populations may fluctuate over time due to natural or anthropogenic perturbation events (Figure 1). Such fluctuations in spatially separated locations may cause populations of the same species to respond differently across regions and ecological settings (Figure 1a). However, spatial differences are often not incorporated within population assessments, although understanding the timing of changes on larger scales may help to understand the drivers behind population trends. Closely connected populations might show similar trends (Folmer et al. 2014), while opposite trends in spatially separated populations might cancel each other out, resulting in an overall neutral trend. Our approach uses a comparison of statistical models to assign each time series (population trend of each species at individual measurement stations) to one of five defined trend types (Figure 1b). Targeted meta-analyses enable the calculation of overall trends across and within taxonomic groups (Figure 1c), while time-specific trend analyses help identify critical points of change.

We use the Wadden Sea as a case study to highlight the benefits of a systematic and quantitative analysis of population trends to assess ecosystem reorganisation. Spanning the North Sea coastal regions of the Netherlands, Germany, and Denmark, the Wadden Sea is the world's largest connected sedimentary intertidal system (Kloepper et al. 2022). Its diverse habitats and high productivity support over 100 wetland bird species, over 150 fish species, three marine mammal species, and numerous benthic invertebrates (Kloepper et al. 2022). The Wadden Sea was declared a UNESCO World Heritage Site in 2009 and hosts Natura 2000 sites designated under the European Birds and Habitats Directives (Directive 2009/147/EC; Directive 92/43/EEC) as well as a range of National Parks. The area is managed as separate units, corresponding to different countries and protection zones, whereas, in reality, it is one connected seascape. Therefore, assessing the conservation status of the Wadden Sea benefits from a holistic area-wide assessment of population trends. Ecological change is monitored in the Trilateral Monitoring and Assessment Programme (TMAP) as well as in national and international monitoring programmes. To date, the analysis of these data has focused on trends in traditional biodiversity metrics (e.g., richness) or selected populations (CWSS 2008; Kloepper et al. 2022), but a synthesis of these trends remains lacking.

We present generalised population trends across a wide range of organism groups and trophic levels throughout the Wadden Sea. We describe the temporal reorganisation of biodiversity in the Wadden Sea and identify clear winners and losers among taxonomic groups. Finally, we discuss how the added benefits of the approach provide a more holistic overview of the population dynamics in the Wadden Sea and thus facilitate targeted conservation practices.

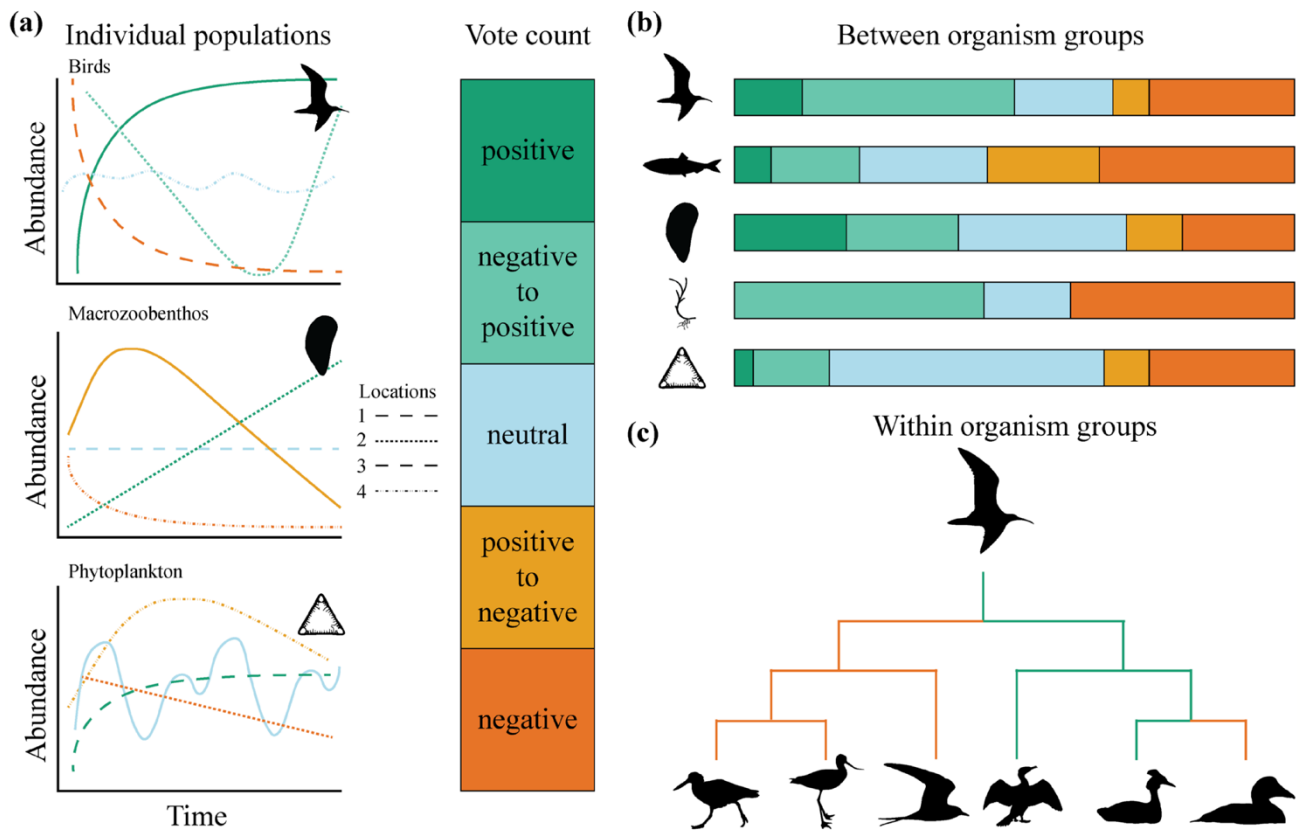


**FIGURE 1** | Conceptual figure of (a) individual populations temporally fluctuating in population response. The different panels represent theoretical examples of abundance trends of spatially separated populations per organism group. Different types of trends can be delineated here. Population trends can differ (b) between and (c) within organism groups. This figure does not represent actual data or results.

## 2 | Materials and Methods

### 2.1 | Data Collection

We combined 20 data sets from national monitoring programs and scientific studies, covering 401 species covering microalgae to birds throughout the Wadden Sea (Figure 2). Monitoring periods of the datasets ranged from 5 to 91 years (with a median of 30 years). Data on birds were collected on the Dutch parts from Netwerk Ecologische Monitoring ([www.sovon.nl](http://www.sovon.nl)) and DeltaMilieu Projecten (Sluijter et al. 2023) and the German parts from Lower Saxony National Park monitoring efforts (Kleefstra et al. 2022). Fish data from the entire Wadden Sea were downloaded from the ICES database on trawl surveys (ICES, n.d.; [www.ices.dk](http://www.ices.dk)), supplemented with additional survey data from Thünen Institute of Sea Fisheries for the German parts (ICES DYFS and survey database: GASEEZ—German Autumn Survey in the Exclusive Economic Zone). Macrozoobenthos data were obtained from a long-term sampling program of the Royal Netherlands Institute for Sea Research on the tidal flat Balgzand (Beukema and Dekker 2020) and national monitoring programs (MWTl) collected by Rijkswaterstaat in the Netherlands (Van der Jagt et al. 2023) and in Germany (Rishworth et al. 2020; Dajka et al. 2022). Phytoplankton data were derived from Dutch and German monitoring programs as described in Antonucci Di Cavalho et al. (2023). The phytoplankton data

also include two taxa of cyanobacteria. Zooplankton data originated from the Lower Saxony Water Management, Coastal and Nature Protection Agency (NLWKN). Finally, plant data were obtained from long-term saltmarsh studies on the islands of Schiermonnikoog (Oloff et al. 1997), Spiekeroog (Balke et al. 2017; Löhmus et al. 2020) and Mellum (Kleyer et al. 2014) and a national seagrass monitoring program in the Dutch Wadden Sea (Folmer 2015). For a more detailed description of the study site, see Supporting Information and Kloepper et al. (2017).

We standardised all taxon names across datasets, checked synonyms, and updated their taxonomic classification based on WoRMS Editorial Board (2024) and AlgaeBase (Guiry and Guiry 2024). When needed, primary taxonomic literature was consulted to reflect the most recent classification of the species (Table S1).

### 2.2 | Statistical Analysis

#### 2.2.1 | Fitting Population Trends

We conducted all statistical analyses in R version 4.3.1 (R Core Team 2023) and all data and code are provided in Happe and Meijer et al. (2025). We first aggregated all monitoring data to annual means per location. Only species recorded for at least

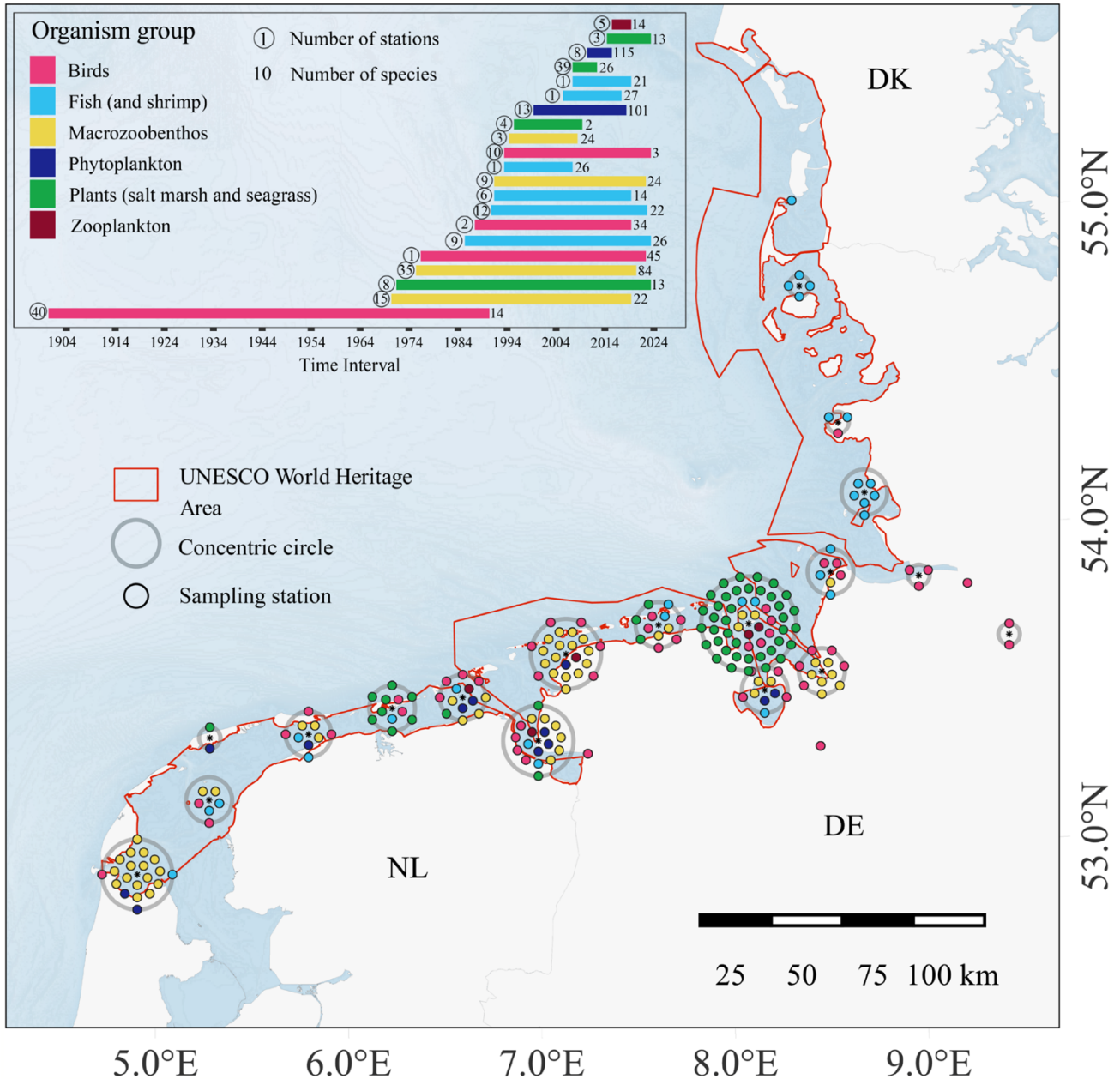


**FIGURE 2** | Overview of monitoring stations and periods for each organism group. Points reflect individual stations for the respective group (colour) within the radius of the concentric circle. The red outline indicates the official UNESCO World Heritage boundaries. Map lines delineate study areas and do not necessarily depict accepted national boundaries.

5 years and present in at least 50% of the monitoring period were included in subsequent analyses to avoid biases by infrequent observations of extreme population differences. We then fitted population trends separately for each species at each location using linear and second-order polynomial regressions with year as the predictor and abundance measure as the response variable. Since data distributions can differ, Gaussian, Poisson, and negative binomial models were applied to all species. Abundance data was  $\ln(x+1)$  transformed for the Gaussian models, and values were rounded off to the nearest integer for Poisson and negative binomial models. We tested Gaussian and Poisson models for normality and homoscedasticity of the residuals. Poisson models were also checked

for overdispersion. In the case of overdispersion, negative binomial models were used. The Akaike information criterion (AIC) was used to select the most parsimonious model in case multiple models indicated significant trends and met model assumptions.  $p$ -values and AIC were used to choose between the best-fitting trends (linear or second-order polynomial). Nine trend types were identified based on the coefficients of the best model (Figure S1). A unimodal trend (as negative to positive or positive to negative) was assigned if the polynomial model was the most parsimonious, coefficients had opposite signs (negative and positive) and the mode fell within the observation period, verified by the MOSTest (Mitchell-Olds and Shaw 1987). Accelerating or decelerating, positive or negative



trends were assigned in case the polynomial model did not meet these requirements but was the most parsimonious (Figure S1). Linear negative or positive trends were concluded in case the linear model was the most parsimonious. Neutral trends were assigned if no significant annual trend was detected despite conforming to model assumptions (Figure S1).

To evaluate the probability of detecting non-neutral trends, we performed a binomial analysis using monitoring duration as a predictor variable. To account for pseudo-replication, sampling station and species were included as separate random factors. Only neutral and non-neutral trends that met model assumptions were included. Additionally, we performed a binomial analysis to assess the probability of finding a model that meets assumptions using the same predictor and random factors to determine whether linear model assumptions hold for longer time series.

### 2.2.2 | Weighted Vote Count

To assess the relative distribution of trend directions, we grouped positive directional trends (positive accelerating, positive decelerating and positive linear) and negative directional trends (negative accelerating, negative decelerating and negative linear) into 'positive' and 'negative' trend types, respectively. We then weighed the relative distribution of the types of trends by the number of years with observations (Wirth et al. 2024) across all population trends or separated by ecosystem components. Species representation in the meta-analyses reflects their representation in the dataset, that is, species monitored at more locations have higher representation. The total number of monitoring locations for each species is provided in Table S1.

### 2.2.3 | Meta-Analyses on Multiple Organisational Levels

To test for significant overall trends within and across ecosystem components, we conducted subsequent meta-analyses in which we only included the population trends that fitted a linear regression without violating assumptions (2298 out of 3058 trends, 75%), regardless of whether polynomial predictors, Poisson or negative binomial error distributions, lowered AIC. For the meta-analyses, we used multi-level random-effects models using the '*rma.mv*' function from the '*metafor*' package (Viechtbauer 2010). The slope of the linear regression was used as the effect size, and the squared standard errors as the corresponding sampling variance, giving more weight to reliable trends, typically from longer time series. Station identity was included as a random effect, and the model was fitted using the restricted maximum likelihood (REML) estimation method for unbiased variance component estimates under random effects. To extract group-specific trends, the ecosystem component was added as a moderator variable in a following meta-analysis. To determine overall directionality across all ecosystem components (i.e., slopes differing from zero) and account for the cancellation of positive and negative trends, we repeated the ecosystem-wide meta-analysis using the absolute values of the slopes.

To identify taxonomic groups as winners and losers, we repeated the meta-analysis using the slopes as the effect size (as described above) but added the taxonomic rank class as a moderator variable in a model without intercept. This provided class-wide effect sizes with 95% confidence intervals (CIs); if a CI did not overlap with 0, the entire class either increased or declined in population sizes. Class rank was chosen to get a deep enough insight into structural changes while ensuring sufficient entries per group (Table S3). We also performed the same analyses on group-specific subsets of the dataset on genus, family, and order level to get an insight into specific genera, families, or orders driving class-level trends. A dendrogram was created using the '*ggtree*' function from the '*ggtree*' package (Yu 2022) to visualize the winners and losers across taxonomic ranks. The branches were colored based on the meta-analysis results, with positive or negative trends assigned if the CI did not overlap 0.

### 2.2.4 | Time-Specific Analysis

To analyse the timing of trend directionality, we used coefficients from the most parsimonious models to calculate the annual rate of change in each population trend using the derivative as a proxy for the slope of the population trend in each year. With this rate of change (negative, positive or equal to zero), we assigned a yearly trend direction (negative, positive, or neutral) for each population during the monitoring period. Neutral trends were assigned if the rate equalled zero or if no trend was detected in the first step. Thereby, each population has three possible states each year. We applied multinomial random logit models using the '*mblogit*' function from the '*mclogit*' package (Elff 2022) to estimate the probability of each state for different taxonomic groups over time. These models estimate the probability of one state (here, positive or negative trends, respectively) against a reference state (here, a neutral trend). A binomial distribution was used in case only two types of trends were found for a taxonomic group, where then the probability of one state was modelled against the probability of the second state. Species and locations were included as random effects to account for repeated measures. Only models where the variable 'year' significantly predicted the trend state were considered. AIC was used to determine whether a second-order polynomial should be included in the model. We calculated 95% CIs by bootstrapping the estimated values. Estimated probabilities and CIs for positive and negative states were compared to deduce predominant trend directions. The state with the highest probability was considered the predominant state unless both were below 50%, in which case a neutral trend was assigned. If the probability and the CIs overlapped, the trend was considered cancelled out by equal positive and negative trends (see Figure S2 for an example).

## 3 | Results

### 3.1 | Trends and Weighted Vote Count

We analysed a total of 3058 population trends, of which 1862 showed no clear directionality, 355 were positive, 104 shifted from negative to positive, 167 shifted from positive to negative, and 570 were negative. Thus, population trends across all

organism groups show a much higher percentage of significant trends (38.2% i.e., the share of directional trends in the total number of trends) than predicted by chance ( $p$ -value and type I error  $\alpha = 5\%$ ), with more negative than positive trends at the end of the monitoring period (737 and 459, respectively).

Weighting the trend types by the number of observation years increased the proportion of significant trends to 66.2% across organism groups (Figure 3). The proportion of positive and negative trends was roughly similar (Figure 3), and consequently, the overall slope of the quantitative meta-analysis was close to zero (Table 1). When using absolute slopes (i.e., the direction of signs removed), the overall slope showed a highly significant deviation from 0 (Table 1), reflecting the large weighted proportion of significant trends. When separating the meta-analysis for organism groups, marine birds showed significantly positive trends in population size overall. In contrast, zooplankton, fish, and plants displayed a negative directionality of population trends. No consistent trend was found for phytoplankton and macrozoobenthos.

The probability of finding a significant trend for a population increased with the monitoring duration (Binomial regression,  $B = 0.015$ , 95% CI = [0.007, 0.022],  $\chi^2 = 15.47$ ,  $p < 0.001$ ; Figure S3a). However, the probability of detecting a trend using linear regression that fits model assumptions under Gaussian, Poisson, or negative binomial error distributions, including the possibility of a second-order polynomial, decreases with monitoring duration (Binomial regression,  $B = -0.048$ , 95% CI = [-0.060, -0.036],  $\chi^2 = 65.13$ ,  $p < 0.001$ ; Figure S3b).

### 3.2 | Meta-Analysis: Winners vs. Losers

Identifying winners and loser class ranks reveals a high abundance of primary producers on the loser side (estimate and  $CI_{\max} < 0$ ), with 10 out of 13 significantly negative classes belonging to either plants or phytoplankton, whereas phytoplankton represents the five classes with the most negative trends (Figure 4). Negative trends appear to group taxonomically for all classes within the

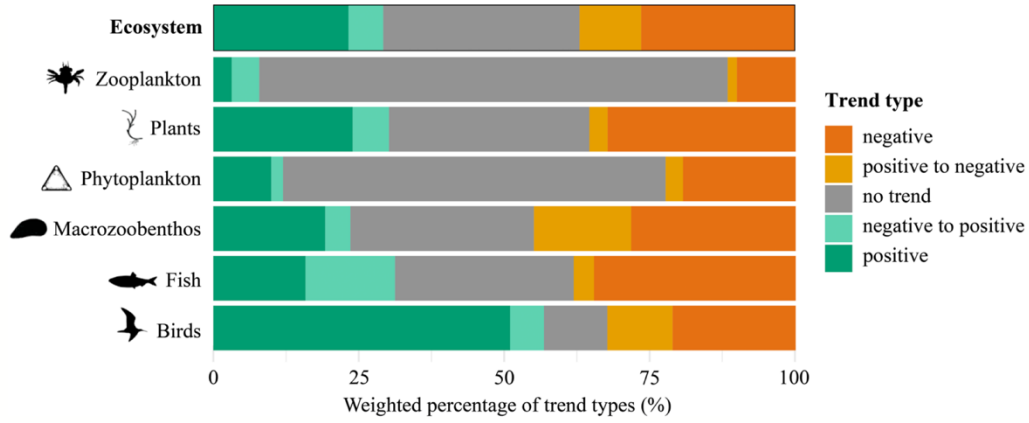


**FIGURE 3** | The weighted vote count as the percentage of each trend type in all ecosystem components together (top row) and separately (for the groups specified on the left axis) is weighted by the number of years with observations. Numbers of trends and species per organism group: Zooplankton (56 trends, 14 species), plants (205 trends, 33 species), phytoplankton (1111 trends, 161 species), macrozoobenthos (938, 96 species), fish (382 trends, 40 species), and birds (350 trends, 57 species). The organism group of “Plants” includes salt marsh plants and seagrasses. Table S2 provides an overview of the number of entries in each taxonomic level and organism group.

**TABLE 1** | Top: Meta-analysis output testing the slope (All) or absolute slope (All (absolute)) of the linear regression from all populations as the effect size with squared standard errors as the corresponding sampling variance and the station identifier as a random effect; Bottom: Meta-analysis output testing the signed slope of the linear regression moderated by the ecosystem components at the class level.

	Estimate	SE	Zval	CI, lower	CI, upper	p
All (absolute)	0.0632	0.0031	20.5501	0.0571	0.0692	<0.0001*
All	-0.0052	0.0044	-1.1979	-0.0137	0.0033	0.2309
Phytoplankton	-0.0071	0.0104	-0.6820	-0.0275	0.0133	0.4953
Zooplankton	-0.0468	0.0200	-2.3378	-0.0861	-0.0076	0.0194*
Macrozoobenthos	0.0043	0.0046	0.9409	-0.0047	0.0133	0.3468
Fish	-0.0150	0.0049	-3.0428	-0.0247	-0.0053	0.0023*
Birds	0.0243	0.0060	4.0437	0.0125	0.0360	<0.0001*
Plants	-0.0468	0.0200	-2.3378	-0.0563	-0.0356	<0.0001*

Note: The category “plants” includes salt marsh plants and seagrasses.

\*Significance level of <0.05.

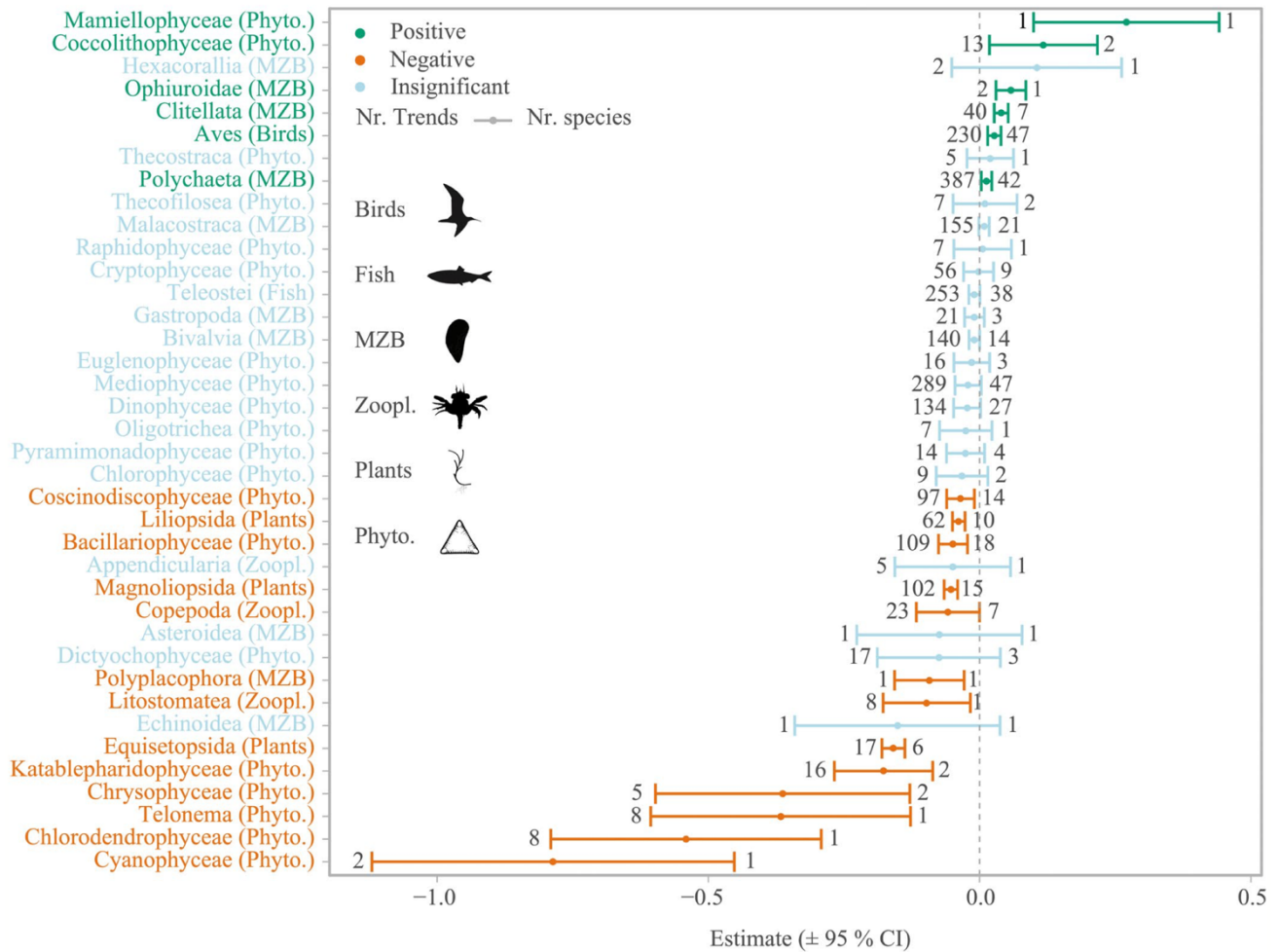


**FIGURE 4** | Estimates and 95% confidence intervals (CI) derived from the meta-analysis to identify winners (green) and losers (orange) for classes. Blue indicates no significant difference from 0. The abbreviations refer to phytoplankton (Phyto.), macrozoobenthos (MZB), and zooplankton (Zoopl.). The number left of the lower CI indicates the number of trends in the analysis, and the number to the right of the upper CI indicates the number of species. Significance ( $p < 0.05$ ) is indicated by CI not crossing 0. Detailed figures for birds (Figure S5), zooplankton (Figure S6) and macrozoobenthos (Figure S7) on family level can be found in the supplements.

phylum Tracheophyta (vascular plants) and all families within the class Cryptophyceae (unicellular flagellates) (Figure 5). In the kingdom Animalia, negative trends are found in several genera (11/32) of the class Teleostei (fish). The class Aves (birds), however, displays positive trends for most genera (24/28) (Figure 5). The phyla Annelida (segmented worms), Arthropoda, and Mollusca present a more balanced pattern with winners and losers within the same classes and orders (Figure 5). The macrozoobenthos class Polyplacophora (chitons) and the two zooplankton classes Litostomatea (here consisting only of the ciliate *Mesodinium rubrum*) and Copepoda belong to the losers, whereas the three macrozoobenthos classes Ophiuroidae (brittle stars), Clitella, and Polychaeta (both annelid worms) were identified as winners. On the family level, we find more nuance in which families perform well or poorly (see Supporting Information).

### 3.3 | Temporal Trend Analysis

Trends and directional changes of trends for 16 out of 32 analysed classes were temporally synchronised over all populations within

(Figures 6 and 7; Table S3). The birds (Aves) shift from initially positive to negative trends with a turning point in trend direction around the mid-1990s to early 2000s. Within the Aves, trends for four of seven families were temporally synchronised (Figure 6b; Table S3). Most families show similar patterns as on class level, specifically for the families Scolopacidae (e.g., sandpipers and snipes), Charadriidae (e.g., plovers and lapwings), and Laridae (including gulls and terns) (Figure 6b). In contrast, the Anatidae (ducks, geese, and swans) remain positive overall (Figure 6b). The Thecostraca (barnacles, two families), Malacostraca (malacostracan crustaceans, 16 families), Gastropoda (five families), and Bivalvia (nine families) show overall consistently neutral trends (Figure 6a). Within these classes, the Semelidae (clams) diverged from the class trend and instead showed mostly positive trends (Figure 6c). Temporal trends within the class Polychaeta were neutral overall (Figure 6a) but showed high variability between families. While most families shifted from negative to neutral trends, the Cirratulidae shifted from positive to neutral, whereas the Phyllodocidae (paddle worms) and Capitellidae remained consistently negative (Figure 6d). Lastly, fish (Teleostei) showed negative trends overall, with an intermediate period of



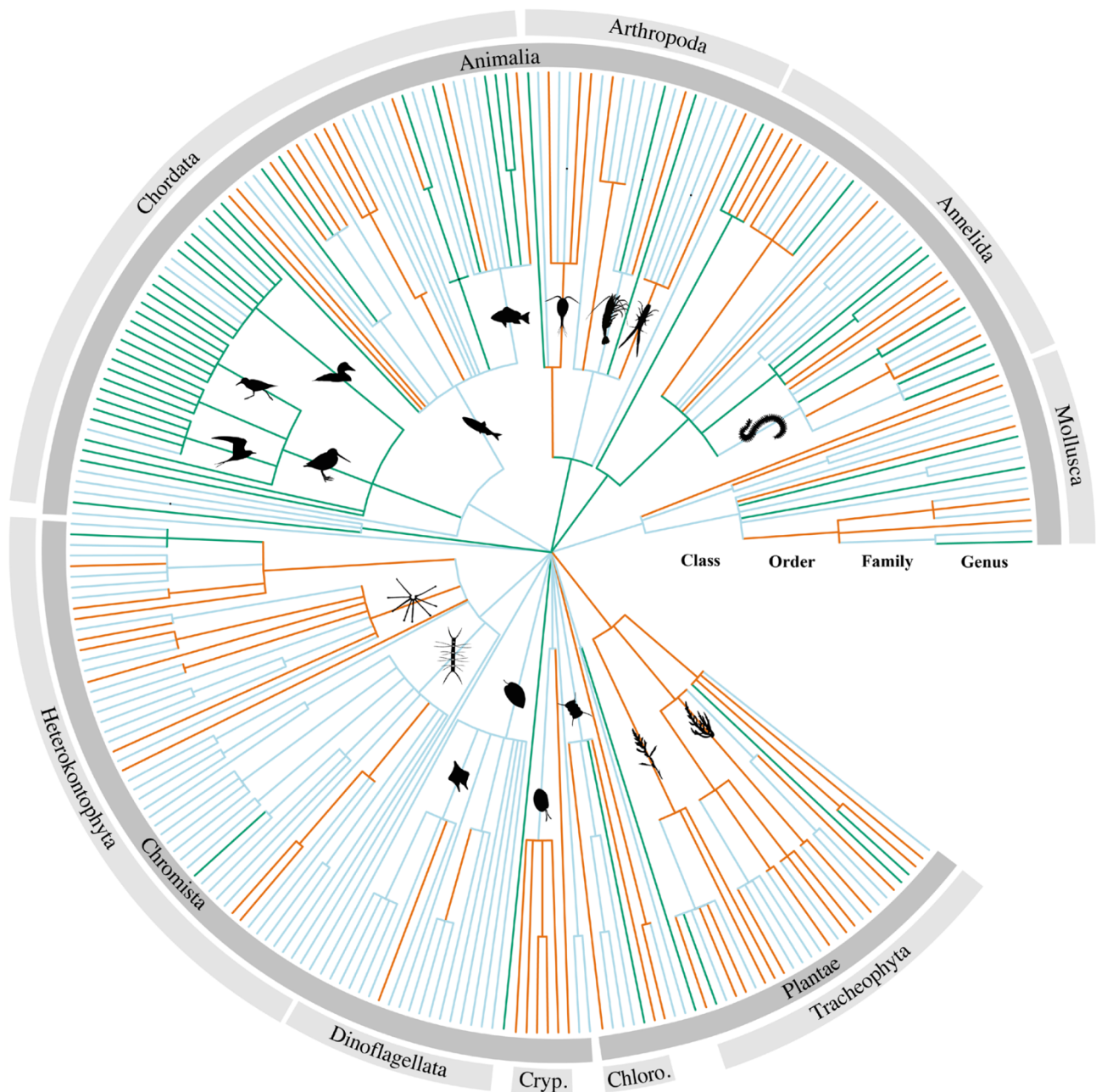


**FIGURE 5** | Dendrogram of the meta-analysis results (coloured branches). The colour indicates an overall significantly positive trend (green), negative trend (orange) or a non-significant overall trend (blue). The dark grey circle indicates the kingdom, and the light grey circle indicates the phylum. Abbreviations are as follows: Cryptophyta (Cryp.) and Chlorophyta (Chloro.). The dendrogram does not represent phylogenetic distances. Figure S3 shows the dendrogram with genus labels. The estimates and 95% confidence intervals for each taxonomic level are presented in Table S3.

neutral trends (Figure 6a). Temporal trends could be predicted significantly for four out of ten families (Figure 6e; Table S3). The Syngnathidae (represented by pipefishes, *Syngnathus* spp.) remain neutral, the Pleuronectidae (righteye flounders) showed negative trends, and the Clupeidae (herrings) remained positive within the monitored time series (Figure 6e). The Gadidae (cod-fish) showed largely negative trends except for a neutral period between 2002 and 2009 (Figure 6e).

Trends remained largely neutral within the Bacteria, Chromista, and Protozoa (Figure 7a), which also were consistently reflected

within their families (Figure 7a–d). Only the Plantae showed variable trends over time. The Equisetopsida (horsetails, five families) showed neutral trends over time, whereas Liliopsida (including grasses, three families) shifted from a positive to a negative trend in the early 2000s (Figure 7a). Within these classes, Poaceae (grasses) were negative overall, similar to Plantaginaceae (plantains) but had an intermediate positive period, while Plumbaginaceae (leadworts) and Amaranthaceae remained neutral across time (Figure 7e). The Compositae also showed neutral trends until its shift into a negative trend in the last monitoring year (Figure 7e).

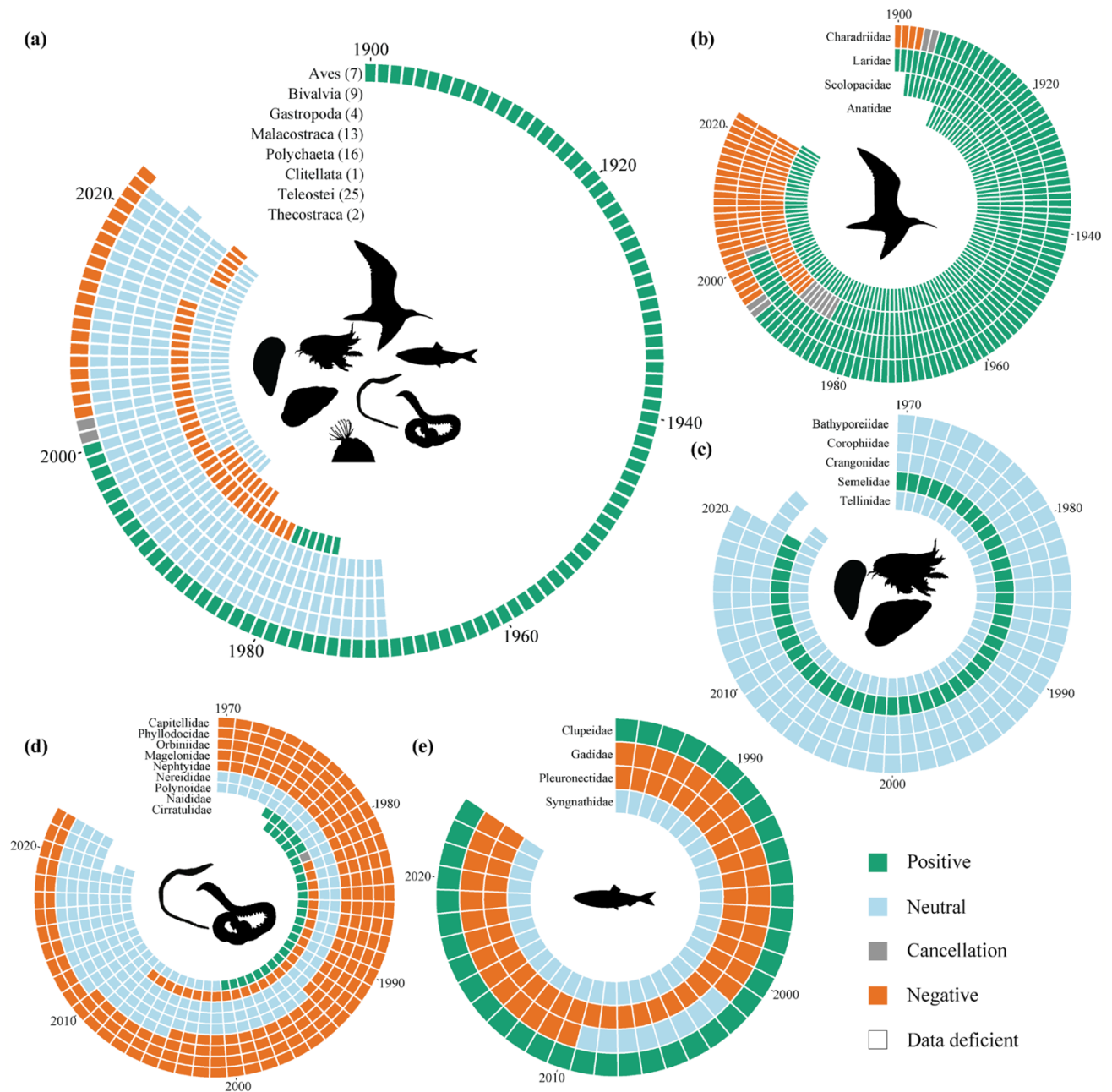


**FIGURE 6** | Significant temporal population trends for animals. Trend timeline on (a) class-level aggregation (number of families within the class in brackets), (b) families within the Aves class, (c) families within the classes Bivalvia, Gastropoda and Malacostraca, (d) families within the classes Clitellata and Polychaeta, (e) families within the Teleostei class. Trend timelines are only shown for taxa where “year” was a significant predictor for the trend in multinomial models. No families within the Thecostraca class had significant models (Table S3). A cancellation is assigned if equal positive and negative trends cancel each other out.

#### 4 | Discussion

Our systematic generalisation of 3058 populations across six ecosystem components revealed a continued reorganisation of marine biodiversity in the Wadden Sea. We find general declines for zooplankton, fish, and plants, whereas birds exhibited an overall positive trend in population size. Many of these overarching organism groups exhibit both positive and negative trends of smaller taxonomic units within the same group. Moreover, a temporal trend analysis revealed shifts

in trend signs over time, a result often obscured by general trend analysis. For example, the generally positive trend for marine birds masks the drastic shift to a population decline between the late 1990s and early 2000s, giving early warning signals for local species extinctions. The clear directionality of changes in several ecosystem components and the temporal changes of trend directions allow for the identification of both winners and losers on multiple taxonomic resolutions to guide conservation efforts and better understand the reorganisation of biodiversity.



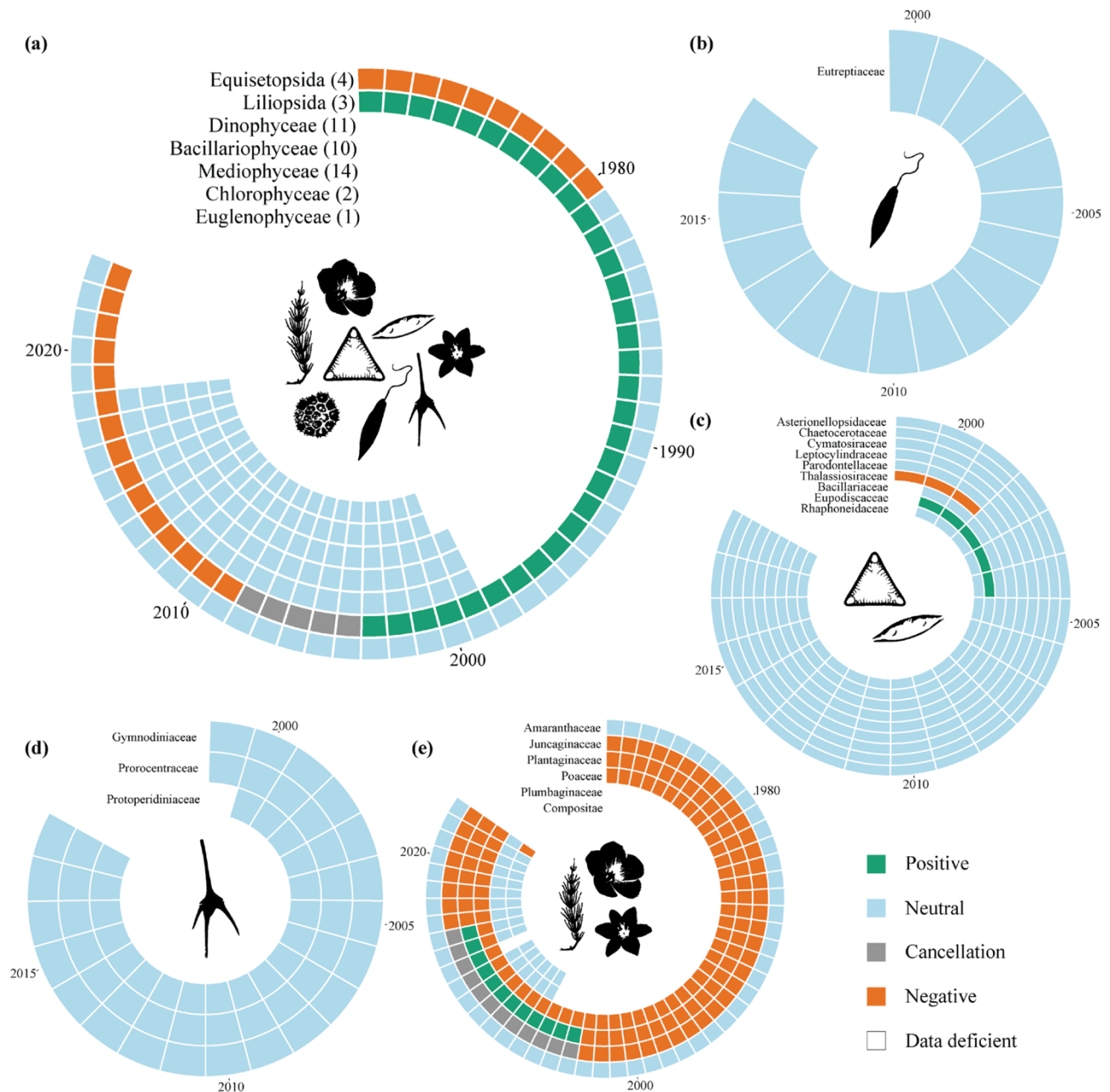


**FIGURE 7** | Significant temporal population trends for plants and phytoplankton. Trend timelines on (a) class-level aggregation (number of families within the class in brackets), (b) families within the Euglenophyceae class, (c) families within the Bacillariophyceae and Mediophyceae classes, (d) families within the Dinophyceae class, (e) families within the classes Equisetopsida, Liliopsida and Magnoliopsida. Trend timelines are only shown for taxa where “year” was a significant predictor for the trend in multinomial models. No families within the Chlorophyceae classes had significant models (Table S3). A cancellation is assigned if equal positive and negative trends cancel each other out.

#### 4.1 | Population Trends and Biodiversity Changes

Our results generally align with the individual species trends reported in the quality status reports (QSR) for the Wadden Sea produced by the trilateral monitoring and assessment programme (TMAP) (Kloepper et al. 2022). However, a holistic biodiversity assessment for the Wadden Sea through the TMAP is complicated as species groups are assigned to different expert groups. This causes varying methodological approaches to determining population trends depending on the species group.

For example, generalized additive models (GAMs) are grouped by tidal basins or regions to assess trends for macrozoobenthos and fish. In contrast, for breeding birds, the mean annual rate of population change and for migratory birds, a “flexible trend” obtained via TrendSpotter is used (Visser 2004; Kloepper et al. 2017, 2022). In addition, not all species groups are represented equally within these assessments. Following the water framework directive (WFD), marine phytoplankton is currently not assessed on a community level by TMAP, which only considers phytoplankton via chlorophyll-a as a biomass indicator

for eutrophication and water quality and blooms of the indicator species *Phaeocystis* sp. (Kloepper et al. 2022). Moreover, microphytobenthos, an important driver of the intertidal food web (Christianen et al. 2017), is currently not monitored (Wirth et al. 2024). This monitoring gap has also resulted in microphytobenthos not being included within our data sets. Still, our results indicate structural changes by a decrease in various phytoplankton classes, with potential functional implications at the base of the food web. A standardized approach categorizing population trends across taxonomic groups allows for more direct comparisons of biodiversity reorganization in all trophic levels.

The temporal trend analysis reveals shifts in trend directions between and within organism groups otherwise overshadowed by dominant trends. For example, the meta-analysis classifies birds as winners, whereas the temporal trend analysis on the family level shows that this classification only holds until the early 2000s. The probabilistic direction of their trend switched from positive to negative in this period. The decline in Scolopacidae (e.g., sandpipers and snipes) since 1992 was followed by a decline in Charadriidae (e.g., oystercatchers, plovers, and lapwings) in 1996 and subsequently in Laridae (e.g., gulls, and terns) in 2003. Pressures that led to these changes could be linked to pressures in breeding or wintering areas for migratory species but may be exacerbated by changes within the Wadden Sea. Drastic declines in food resources, for example crashes in local intertidal mussel and cockle populations (Herlyn and Millat 2000; Imeson and Van den Bergh 2006) likely reinforced negative trends of shellfish-eating birds in the 1990s (Beukema et al. 2015). For breeding birds, the number of declining species rises (Kloepper et al. 2022) likely resulting from poor breeding success (Van der Jeugd et al. 2014) due to increased predation risk (e.g., by mustelids, and racoons) and increasing intensity and frequency of heavy flooding (Van de Pol et al. 2010; Kloepper et al. 2022). Incorporating temporal analysis of changes within a time series allows for identifying critical time points of drastic reorganization.

Population trends heavily depend on the spatial scale at which populations are followed. On a global scale, trends tend to become muddled (Johnson et al. 2024). However, too small scales may give inaccurate perspectives of systemic changes. For example, Beukema and Dekker (2020) conclude that Wadden Sea-wide decreases in the Baltic clam *Macoma balthica* and increases in the sand gaper *Mya arenaria* are likely caused by trophic changes and warming based on data from the tidal flat Balgzand. However, using Wadden Sea-wide monitoring data, we find decreasing trends for both species. Still, even the entire Wadden Sea ecosystem might be too small-scale to contextualize pressures driving population trends, especially for migratory fish and birds with additional pressures along their migration pathways or overwintering habitats (Shaw 2016). In this context, it is important to consider the scale at which a population is defined and monitored. For example, the local populations of migratory birds in our analyses represent a subset of a larger global population, while macrozoobenthos comprises smaller local meta-populations forming a larger population within the connected ecosystem. The pressures acting upon these populations also vary, where highly mobile and migratory species are more susceptible to changes over larger spatial scales, and less mobile species are more subject to local pressures (Runge et al. 2014).

These pressures can also change throughout ontogeny and drive the observed population trends.

The Wadden Sea is an important nursery area for many fish (Kloepper et al. 2022; van der Veer et al. 2022), but adult and juvenile populations undergo different pressures. Although the function of the Wadden Sea as a nursery for fish has stabilised over the last decade after declining since the 1980s (van der Veer et al. 2022; Kloepper et al. 2022), we still find declining trends among many fish families. For example, the flatfish families Pleuronectidae (righteye flounders) and Soleidae (true soles; represented by one species: *Solea solea*) that use the Wadden Sea during juvenile life stages (van der Veer et al. 2022) were identified as clear losers, even though a species-specific analysis in Kloepper et al. (2022) has shown that the decrease in juvenile flatfish species has recently levelled off. Whether this is driven by local pressures or by pressures off-shore remains unclear (van der Veer et al. 2022). Identifying the pressures behind the observed population trends is beyond the scope of this research, but it is an obvious next step in order to also implement targeted management interventions.

Interestingly, we find that losers are phylogenetically related, whereas winners are more heterogeneously spread across organism groups. Shared life history strategies within organism groups might explain this phylogenetically related decline. Moreover, life history traits associated with both winners and losers might give insights into generalizations of characteristics that make certain species groups more vulnerable to population decline (Chichorro et al. 2019). For example, we find declines for larger-bodied, predatory, and long-lived fish species (e.g., *Gadus morhua*, *Trachurus trachurus*), for which declines might be caused from outside the Wadden Sea but also larger-bodied polychaetes and bivalves such as *Ampharete* sp. and *Mya* sp. Moreover, our meta-analysis indicates that the reorganization of macrozoobenthos is largely driven by the strong increase of alien species, such as the Ostreidae (Pacific oysters, *Magallana gigas*) and the Pharidae (American jackknife clams, *Ensis leei*) (Kloepper et al. 2022). In contrast, groups containing native species, such as the Tellinidae (*Macoma balthica* and *Fabulina fabula*), are revealed as clear losers. In general, we find a positive trend for the Polychaeta, whereas the Bivalvia remain neutral. This overall shift in macrozoobenthic communities towards a more polychaete-dominated community was also described by Eriksson et al. (2010) who found these shifts to be also reflected by higher trophic levels in shifts in bird communities. However, this general increase in Polychaeta is not uniform across all families. The polychaete families showing the strongest declines, such as the Ampharetidae, Magelonidae, and Polynoidae, are mostly less mobile or sessile carnivores, filter feeders, or sub-surface deposit feeders (Fauchald and Jumars 1979). In contrast, those showing positive trends, such as the Pectinariidae and Cirratulidae, are highly mobile surface deposit feeders or carnivores (Fauchald and Jumars 1979). Less mobile species are more susceptible to sediment dynamics and natural bottom perturbations (Meijer et al. 2023), which impose similar stress gradients as human-induced bottom perturbations like bottom trawling and promote carrion feeding species (van Denderen et al. 2015; McLaverty et al. 2024). Shifts in functional groups of macrozoobenthic species might have been induced by the increasing intensity of human-induced bottom perturbations in

the system (Kloepper et al. 2017, 2022). Notably, we find losers among functionally important species for the stability of coastal ecosystems, such as seagrasses and salt marsh plants (McLeod et al. 2011). Combining functional and taxonomic aspects to identify winners and losers may highlight urgent conservation needs for threatened ecosystem functions and their associated species, thus allowing for early management interventions to preserve ecological integrity.

## 4.2 | Methodological Considerations

The inaccessibility of monitoring data from governmental programs and scientific institutions remains a major obstacle to large-scale analyses of population trends (Eriksson and Hillebrand 2019). Although the recently developed BioTIME database (Dornelas et al. 2018) collects global biodiversity time series data as a community-led and open-source approach, many relevant time series are still missing. This limitation is also mirrored in our analyses, where, despite considerable efforts, we could not access broad data for the Danish part of the Wadden Sea and other known monitoring programs. Moreover, the apparent spatial clustering of sampling stations might introduce a bias through spatial autocorrelation of population trends (Folmer et al. 2014), especially for more mobile species. Marine mammals are one such highly mobile species group that is also missing within our dataset. Only three species of marine mammals occur in the Wadden Sea, of which the harbour porpoise is more a guest than a resident. The population trends of both the harbour and grey seal populations are detailed in the QSR (Unger et al. 2022). The report highlights the recovery of harbour and grey seal populations following severe declines caused by large-scale hunting in the mid-20th century. Currently, both seal species present the highest population sizes since the beginning of monitoring. Nevertheless, in addition to the detailed trends on marine mammals in the QSR, we can conclude drastic changes for many species groups in the Wadden Sea based on the current data.

Our findings indicate that the probability of finding a population trend increases with the length of the time series, and thus, short time series may fail to detect changes. This is in line with previous studies on species diversity trends for which the duration-related bias was shown to underestimate diversity loss (Zhang et al. 2021; Kuczynski et al. 2023). Minimum periods to reliably detect changes are estimated to range between 5 and 30 years, depending on the taxonomic group, with generally a minimum of 10 years (White 2019). Still, these have been estimated from vertebrate populations, and invertebrate species with faster life cycles require shorter periods (Rueda-Cediel et al. 2015; Wauchope et al. 2019). Moreover, the detection of trends from short-term time series is quite reliable in terms of sign direction, though the scale of the trend does require longer periods to be estimated reliably (Wauchope et al. 2019). The time series used in the present study have an average length of 32 years but also include three time series shorter than 10 years. These comprise a time series on salt marsh plants, one on phytoplankton, and a short time series of 5 years for the only available zooplankton data. This reflects the general lack of area-wide monitoring for this species group until recent efforts (Jak and Slijkerman 2023). However, even average durations do not capture important

structural changes such as the increasing eutrophication until the 1980s (Kloepper et al. 2017), which is known to have dramatically decreased seagrass meadows (Burkholder et al. 2007) and influenced phytoplankton community structure (Philippart et al. 2000; van Beusekom et al. 2019). Species with fast life cycles, like phytoplankton, have high within-year variability that might mask long-term structural changes. To overcome this, we have aggregated the community data to annual means, similar to Antonucci Di Cavalho et al. (2023). Nevertheless, asynchronous sampling by different programmes for species with fast life cycles complicates comparisons. Additionally, a common limitation in time series data is the lack of information on rare species whose capturing highly depends on the sampling effort (Bunge and Fitzpatrick 1993; Chase and Knight 2013) and cannot be reliably incorporated in trend assessments. This is also partly due to changes in taxonomic expertise over the years and between programs. We have standardised taxonomy between the datasets, but this does not remove initial misidentification, which might influence generalisations beyond rare species and influence long-term trends. To overcome this, we have limited the analyses to higher-level taxonomic groups and have excluded rare species from our analysis based on the criterion that a species must have been present in five data points to calculate regressions. These limitations highlight the need for standardised monitoring methods across borders and validation of taxonomic resolution (Antonucci Di Cavalho et al. 2023).

This systematic assessment of population trends complements biodiversity analyses focusing on classic diversity metrics or selected species. IUCN Red List and LPI assessments are specifically aimed at identifying populations of conservation concern. However, IUCN Red List and LPI assessments often focus on key or endangered species and do not aim to identify winners alongside losers (Finn et al. 2023). Additionally, the LPI assessment focuses solely on vertebrate populations (Loh et al. 2005), ignoring functionally important parts of the ecosystem, such as invertebrates and primary producers, which often are more directly affected by environmental change (Behrenfeld et al. 2006; Prather et al. 2013). While diversity metrics and population trends of selected species are easily communicated, they may overlook changes in functionally important but neglected groups, resulting in distorted perceptions of the effects of biodiversity change (Lamb et al. 2009). Our analysis does not replace other assessments, as it comes with its own advantages and disadvantages (Table 2). However, using the Wadden Sea as a case study, we show that this systematic and normalized approach can provide important additional insights.

## 5 | Conclusions

In contrast to static conservation categories (e.g., IUCN), population trend analyses offer a dynamic assessment of biodiversity change that can serve as early warning signals for local extinctions (Finn et al. 2023). Except for marine mammals and specific microbes (microphytobenthos, bacteria), the assessment presented here covers all species groups that comprise the Wadden Sea ecosystem and identifies both winners and losers across time. Losers are phylogenetically related, hinting at shared life history traits that may explain vulnerabilities to environmental change. Non-native species are identified as winners, especially

TABLE 2 | Comparison of assessment approaches.

Approach	Advantages	Disadvantages
Classical biodiversity assessment: e.g., species richness, Shannon or Simpson indices	<ul style="list-style-type: none"> <li>• Directly comparable between areas and applicable to situations without abundance data</li> </ul>	<ul style="list-style-type: none"> <li>• Does not give insight into turnover of communities or which species respond to changes (Hillebrand et al. 2018)</li> <li>• Susceptible to immigration/extinction debt (Jackson and Sax 2010)</li> </ul>
Assessment of Trilateral Wadden Sea Monitoring Programme (TMAP): Mostly based on selected species trends	<ul style="list-style-type: none"> <li>• Comprehensive assessment of many components of the Wadden Sea ecosystem (holistic view)</li> </ul>	<ul style="list-style-type: none"> <li>• Differences in assessment strategy between taxonomic groups (and thus, expert groups), no direct comparison of changes possible</li> <li>• Some taxonomic groups are overlooked (e.g., phytoplankton communities, zooplankton)</li> <li>• Selected species trends (e.g., for birds) mask the change in neglected species</li> </ul>
IUCN Red List of Species: Analysis and categorisation of extinction risk based on population size and geographic range	<ul style="list-style-type: none"> <li>• Practical value: Aids in informing conservation priorities (Hoffmann et al. 2008)</li> </ul>	<ul style="list-style-type: none"> <li>• Only available for a few taxonomic groups, high number of species classified as “Data Deficient” which may neglect them from conservation planning (Borgelt et al. 2022)</li> <li>• Time consuming process requiring a lot of data</li> <li>• Classically focuses on “losers” rather than “winners” (although improvements are on the way) (Finn et al. 2023)</li> <li>• Criteria are not universally applicable across ecological contexts, thus inconsistencies between national and global assessments may arise which need to be connected with special care (Karam-Gemael et al. 2020)</li> <li>• Static categories (rather than a dynamic assessment)</li> </ul>
Living Planet Index (LPI): Population trends for assessing conservation status of selected species groups	<ul style="list-style-type: none"> <li>• Can be used on multiple spatial scales e.g., national, regional, and international (Currie et al. 2022)</li> </ul>	<ul style="list-style-type: none"> <li>• Only considers vertebrates (Loh et al. 2005)</li> <li>• Focus on “losers” and missing “winners” (Finn et al. 2023), thus no holistic assessment</li> <li>• Extreme population trends and random fluctuations can skew global LPI (Buschke et al. 2021)</li> </ul>
Generalisation of population trends: (with time-specific analysis)	<ul style="list-style-type: none"> <li>• Holistic view on diversity in terms of including all taxonomic groups (some of which are underrepresented in current assessments)</li> <li>• Allows direct comparisons between taxonomic groups</li> <li>• Allows for identification of “winners and losers”</li> <li>• Role of species identities can be interpreted (e.g., non-native species)</li> <li>• Identification of critical time points of re-organisation</li> <li>• Dynamic assessment</li> </ul>	<ul style="list-style-type: none"> <li>• Depends on spatial scale, monitoring effort and taxonomic resolution of monitoring</li> <li>• Probability of finding a trend depends on the length of the time series (as shown in Figure S3)</li> <li>• Excludes rare species</li> <li>• Trends are dependent on baselines. Introduced species can only increase whereas species at carrying capacity can only stay neutral or decrease</li> </ul>



among the macrozoobenthos. Moreover, the majority of losers are phytoplankton, which are currently not addressed in monitoring programs beyond bulk biomass and thus overlooked from a species perspective in assessment strategies. Therefore, signs of biodiversity change may be represented by less charismatic organism groups not usually included in management schemes. Finally, our assessment reveals clear losses in the functionality of the ecosystem, indicated by population declines in fish groups that use the Wadden Sea as a nursery area, bird groups that use the Wadden Sea as a feeding and breeding area, and plant groups that stabilize the coastline. This work can thus serve as a stepping stone for further analyses focusing on functional or food web perspectives and quantitatively linking pressures with the shown biological reorganization. This holistic approach captures the dynamic and interconnected nature of seascapes and provides a near-complete representation of the regional biodiversity status that goes beyond the assessment of key indicator species, which may help to guide ecosystem-wide conservation and management strategies.

#### Author Contributions

**Anika Happe:** conceptualization, data curation, formal analysis, methodology, visualization, writing – original draft, writing – review and editing. **Kasper J. Meijer:** conceptualization, data curation, formal analysis, methodology, visualization, writing – original draft, writing – review and editing. **Jan-Claas Dajka:** methodology, writing – review and editing. **Oscar Franken:** methodology, writing – review and editing. **Holger Haslob:** data curation, methodology, writing – review and editing. **Laura L. Govers:** writing – review and editing. **Michael Kleyer:** data curation. **Annebelle C. M. Kok:** methodology, writing – review and editing. **Lucie Kuczynski:** writing – review and editing. **Kertu Löhmus:** data curation. **Sancia E. T. van der Meij:** data curation, methodology, writing – review and editing. **Han Olff:** data curation, methodology, writing – review and editing. **Lena Rönn:** data curation, writing – review and editing. **Alexey Ryabov:** methodology, writing – review and editing. **Anne F. Sell:** data curation, methodology, writing – review and editing. **David W. Thielges:** writing – review and editing. **Britas Klemens Eriksson:** conceptualization, data curation, methodology, writing – review and editing. **Helmut Hillebrand:** conceptualization, data curation, methodology, writing – review and editing.

#### Acknowledgements

The authors would like to thank all data contributors. We thank the Center for Information Technology of the University of Groningen for their support and for providing access to the Hábrók high performance computing cluster. Anika Happe was supported by the European Union HORIZON EUROPE program ACTNOW: Advancing understanding of Cumulative Impacts on European marine biodiversity, ecosystem functions, and services for human wellbeing (Grant no. 101060072).

#### Conflicts of Interest

The authors declare no conflicts of interest.

#### Data Availability Statement

The data and code that support the findings of this study are openly available in the dataverseNL (DANS) repository at <https://doi.org/10.34894/LJNSYR>. Long-term saltmarsh data were obtained from DataverseNL at <https://doi.org/10.34894/FASXGR> (Schiermonnikoog), and <https://doi.org/10.5061/dryad.gxd2547z3> (Mellum and Spiekeroog). Phytoplankton monitoring data were obtained from Zenodo at <https://doi.org/10.5281/zenodo.8192381>. Macrozoobenthos data were obtained

from the Balgzand long-term monitoring program via NIOZ at <https://doi.org/10.25850/nioz/7b.b.sh>. A list of the sources of fish data (stow net) data used in this study can be found in Table S9. Demersal Young Fish Survey (DYFS) data were obtained from the ICES DATRAS database at <https://gis.ices.dk/geonetwork/srv/metadata/87ea4d4d-6798-4c06-b001-7b59ad1ea916>. Macrozoobenthos data were obtained from MUDAB at <https://geoportal.bafg.de/MUDABAnwendung/> (Germany) and AquaDesk at <https://live.aquadesk.nl> (Dutch Rijkswaterstaat MWT). Phytoplankton data were obtained from MUDAB at <https://geoportal.bafg.de/MUDABAnwendung/>. Zooplankton data were obtained from the Lower Saxony Water Management Agency at <https://geoportal.bafg.de/MUDABAnwendung/>. Bird data for the Netherlands were obtained from Netwerk Ecologische Monitoring at <https://stats.sovon.nl/stats/gebied/1000001>.

#### References

- Antonucci Di Cavalho, J., L. Rönn, T. C. Prins, and H. Hillebrand. 2023. “Temporal Change in Phytoplankton Diversity and Functional Group Composition.” *Marine Biodiversity* 53: 72. <https://doi.org/10.1007/s12526-023-01382-9>.
- Balke, T., K. Löhmus, H. Hillebrand, et al. 2017. “Experimental Salt Marsh Islands: A Model System for Novel Metacommunity Experiments.” *Estuarine, Coastal and Shelf Science* 198: 288–298. <https://doi.org/10.1016/j.ecss.2017.09.021>.
- Behrenfeld, M. J., R. T. O'Malley, D. A. Siegel, et al. 2006. “Climate-Driven Trends in Contemporary Ocean Productivity.” *Nature* 444, no. 7120: 752–755. <https://doi.org/10.1038/nature05317>.
- Beukema, J. J., and R. Dekker. 2020. “Half a Century of Monitoring Macrobenthic Animals on Tidal Flats in the Dutch Wadden Sea.” *Marine Ecology Progress Series* 656: 1–18. <https://doi.org/10.3354/meps13555>.
- Beukema, J. J., R. Dekker, M. R. Van Stralen, and J. De Vlas. 2015. “Large-Scale Synchronization of Annual Recruitment Success and Stock Size in Wadden Sea Populations of the Mussel *Mytilus edulis* L.” *Helgolander Marine Research* 69, no. 4: 327–333. <https://doi.org/10.1007/s10152-015-0440-9>.
- Borgelt, J., M. Dorber, M. A. Høiberg, and F. Verones. 2022. “More Than Half of Data Deficient Species Predicted to Be Threatened by Extinction.” *Communications Biology* 5, no. 1: 679. <https://doi.org/10.1038/s42003-022-03638-9>.
- Bunge, J., and M. Fitzpatrick. 1993. “Estimating the Number of Species: A Review.” *Journal of the American Statistical Association* 88, no. 421: 364–373. <https://doi.org/10.1080/01621459.1993.10594330>.
- Burkholder, J. M., D. A. Tomasko, and B. W. Touchette. 2007. “Seagrasses and Eutrophication.” *Journal of Experimental Marine Biology and Ecology* 350: 46–72. <https://doi.org/10.1016/j.jembe.2007.06.024>.
- Buschke, F. T., J. G. Hagan, L. Santini, and B. W. T. Coetzee. 2021. “Random Population Fluctuations Bias the Living Planet Index.” *Nature Ecology & Evolution* 5, no. 8: 1145–1152. <https://doi.org/10.1038/s41559-021-01494-0>.
- Chase, J. M., and T. M. Knight. 2013. “Scale-Dependent Effect Sizes of Ecological Drivers on Biodiversity: Why Standardised Sampling Is Not Enough.” *Ecology Letters* 16: 17–26. <https://doi.org/10.1111/ele.12112>.
- Chichorro, F., A. Juslén, and P. Cardoso. 2019. “A Review of the Relation Between Species Traits and Extinction Risk.” *Biological Conservation* 237: 220–229. <https://doi.org/10.1016/j.biocon.2019.07.001>.
- Christianen, M. J. A., J. J. Middelburg, S. J. Holthuisen, et al. 2017. “Benthic Primary Producers Are Key to Sustain the Wadden Sea Food Web: Stable Carbon Isotope Analysis at Landscape Scale.” *Ecology* 98, no. 6: 1498–1512. <https://doi.org/10.1002/ecy.1837>.
- Currie, J., J. B. Burant, V. Marconi, et al. 2022. “Assessing the Representation of Species Included Within the Canadian Living Planet Index.” *Facets* 7: 1121–1141. <https://doi.org/10.1139/facets-2022-0063>.

- CWSS. 2008. "TMAP Handbook. TMAP guidelines for an integrated Wadden Sea monitoring." Version 0.9. Common Wadden Sea Secretariat (CWSS), Wilhelmshaven, Germany.
- Dajka, J.-C., J. Antonucci Di Cavalho, A. Ryabov, et al. 2022. "Modeling Drivers of Biodiversity Change Emphasizes the Need for Multivariate Assessments and Rescaled Targeting for Management." *Conservation Science and Practice* 4: e12794. <https://doi.org/10.1111/csp2.12794>.
- DATRAS. n.d. "ICES Database on Trawl Surveys (DATRAS)." Accessed 11-01-2024. ICES, Copenhagen, Denmark. <https://datras.ices.dk>.
- Dornelas, M., L. H. Antao, F. Moyes, et al. 2018. "BioTIME: A Database of Biodiversity Time Series for the Anthropocene." *Global Ecology and Biogeography* 27: 760–786. <https://doi.org/10.1111/geb.12729>.
- Dornelas, M., N. J. Gotelli, B. McGill, et al. 2014. "Assemblage Time Series Reveal Biodiversity Change but Not Systematic Loss." *Science* 344: 296–299. <https://doi.org/10.1126/science.1248484>.
- Elff, M. 2022. "mclgit: Multinomial Logit Models, with or without Random Effects or Overdispersion." R Package Version 0.9.6. <https://CRAN.R-project.org/package=mclgit>.
- Eriksson, B. K., and H. Hillebrand. 2019. "Rapid Reorganization of Global Biodiversity." *Science* 366, no. 6463: 308–309. <https://doi.org/10.1126/science.aaz4520>.
- Eriksson, B. K., T. van der Heide, J. van de Koppel, T. Piersma, T. van de Veer, H. W. and H. Olff (2010). "Major Changes in the Ecology of the Wadden Sea: Human Impacts, Ecosystem Engineering and Sediment Dynamics." *Ecosystems* 13, 752–764. <https://doi.org/10.1007/s10021-010-9352-3>
- Fauchald, K., and P. A. Jumars. 1979. "The Diet of Worms: A Study of Polychaete Feeding Guilds." *Oceanography and Marine Biology* 17: 193–284.
- Finn, C., F. Grattarola, and D. Pincheira-Donoso. 2023. "More Losers Than Winners: Investigating Anthropocene Defaunation Through the Diversity of Population Trends." *Biological Reviews* 98, no. 5: 1732–1748. <https://doi.org/10.1111/brv.12974>.
- Folmer, E. O. 2015. *Ontwikkelingen en Vestigingsmogelijkheden Voor Litoraal Zeegras in de Trilaterale Waddenzee*, 31. Programma naar een Rijke Waddenzee.
- Folmer, E. O., J. Drent, K. Troost, et al. 2014. "Large-Scale Spatial Dynamics of Intertidal Mussel (*Mytilus edulis* L.) bed Coverage in the German and Dutch Wadden Sea." *Ecosystems* 17: 550–566. <https://doi.org/10.1007/s10021-013-9742-4>.
- Guiry, M. D., and G. M. Guiry. 2024. "AlgaeBase. World-Wide Electronic Publication." University of Galway. Accessed July 2024. <https://www.algaebase.org>.
- Happe, A., K. J. Meijer, J.-C. Dajka, et al. 2025. "Replication Data for: Synthesis of Population Trends Reveals Seascape-Wide Reorganisation of Biodiversity From Microalgae to Birds." DataaverseNL, 10.34894/LJNSYR.
- Herlyn, M., and G. Millat. 2000. "Decline of the Intertidal Blue Mussel (*Mytilus edulis*) Stock at the Coast of Lower Saxony (Wadden Sea) and Influence of Mussel Fishery on the Development of Young Mussel Beds." In *Life at Interfaces and Under Extreme Conditions*, edited by G. Liebezeit, S. Dittmann, and I. Kröncke, 203–210. Springer Netherlands. [https://doi.org/10.1007/978-94-011-4148-2\\_20](https://doi.org/10.1007/978-94-011-4148-2_20).
- Hill, M. O. 1973. "Diversity and Evenness: A Unifying Notation and Its Consequences." *Ecology* 54: 427–432.
- Hillebrand, H., B. Blasius, E. T. Borer, et al. 2018. "Biodiversity Change Is Uncoupled From Species Richness Trends: Consequences for Conservation and Monitoring." *Journal of Applied Ecology* 55, no. 1: 169–184. <https://doi.org/10.1111/1365-2664.12959>.
- Hoffmann, M., T. M. Brooks, G. A. B. Fonseca, et al. 2008. "Conservation Planning and the IUCN Red List." *Endangered Species Research* 6: 113–125. <https://doi.org/10.3354/esr00087>.
- Imeson, R. J., and J. C. J. M. Van den Bergh. 2006. "Policy Failure and Stakeholder Dissatisfaction in Complex Ecosystem Management: The Case of the Dutch Wadden Sea Shellfishery." *Ecological Economics* 56: 488–507. <https://doi.org/10.1016/j.ecolecon.2005.02.007>.
- Jackson, S. T., and D. F. Sax. 2010. "Balancing Biodiversity in a Changing Environment: Extinction Debt, Immigration Credit and Species Turnover." *Trends in Ecology & Evolution* 25, no. 3: 153–160. <https://doi.org/10.1016/j.tree.2009.10.001>.
- Jak, R. G., and D. M. E. Slijkerman. 2023. "Short Review on Zooplankton in the Dutch Wadden Sea: Considerations for Zooplankton Monitoring." Wageningen Marine Research Report; No. C003/23. Wageningen Marine Research. <https://doi.org/10.18174/586428>.
- Jaspers, A. 2020. "Can a Single Index Track the State of Global Biodiversity?" *Biological Conservation* 246: 108524. <https://doi.org/10.1016/j.biocon.2020.108524>.
- Johnson, T. F., A. P. Beckerman, D. Z. Childs, et al. 2024. "Revealing Uncertainty in the Status of Biodiversity Change." *Nature* 628: 788–794. <https://doi.org/10.1038/s41586-024-07236-z>.
- Karam-Gemael, M., P. Decker, P. Stoev, M. I. Marques, and A. Chagas Jr. 2020. "Conservation of Terrestrial Invertebrates: A Review of IUCN and Regional Red Lists for Myriapoda." In *Proceedings of the 18th International Congress of Myriapodology*, edited by Z. Korsós and L. Dányi, vol. 930, 221–229. ZooKeys. <https://doi.org/10.3897/zookeys.930.48943>.
- Kleefstra, R., T. Bregnballe, J. Frikke, et al. 2022. "Trends of Migratory and Wintering Waterbirds in the Wadden Sea 1987/1988–2019/2020." Common Wadden Sea Secretariat, Expert Group Migratory Birds. <https://www.waddensea-worldheritage.org/resources/ecosystem-41-trends-migratory-birds>.
- Kleyer, M., T. Balke, V. Minden, et al. 2014. "Mellum: A Highly Dynamic Landscape, Though Not for Plants." In *Dynamic Islands in the Wadden Sea. Ecosystem No. 33:1–134*, edited by U. Hellwig and M. Stock. Common Wadden Sea Secretariat.
- Kloepper, S., M. J. Baptist, A. Bostelmann, et al. 2017. *Wadden Sea Quality Status Report*. Common Wadden Sea Secretariat.
- Kloepper, S., A. Bostelmann, T. Bregnballe, et al. 2022. *Wadden Sea Quality Status Report*. Common Wadden Sea Secretariat.
- Kuczynski, L., V. J. Ontiveros, and H. Hillebrand. 2023. "Biodiversity Time Series Are Biased Towards Increasing Species Richness in Changing Environments." *Nature Ecology & Evolution* 7: 994–1001. <https://doi.org/10.1038/s41559-023-02078-w>.
- Lamb, E. G., E. Bayne, G. Holloway, et al. 2009. "Indices for Monitoring Biodiversity Change: Are Some More Effective Than Others?" *Ecological Indicators* 9, no. 3: 432–444. <https://doi.org/10.1016/j.ecoli.2008.06.001>.
- Loh, J., R. E. Green, T. Ricketts, et al. 2005. "The Living Planet Index: Using Species Population Time Series to Track Trends in Biodiversity." *Philosophical Transactions of the Royal Society, B: Biological Sciences* 360, no. 1454: 289–295. <https://doi.org/10.1098/rstb.2004.1584>.
- Löhmus, K., T. Balke, and M. Kleyer. 2020. "Spatial and Temporal Patterns of Initial Plant Establishment in Salt Marsh Communities." *Journal of Vegetation Science* 31, no. 6: 1122–1132. <https://doi.org/10.1111/jvs.12915>.
- McLaverty, C., E. D. Beukhof, K. Bromhall, G. E. Dinesen, A. C. Erichsen, and O. R. Eigaard. 2024. "The Relative Effects of Bottom Trawling, Organic Enrichment, and Natural Environmental Factors on Coastal Seabed Communities." *Marine Pollution Bulletin* 209: 117169. <https://doi.org/10.1016/j.marpolbul.2024.117169>.
- McLeod, E., G. L. Chmura, S. Bouillon, et al. 2011. "A Blueprint for Blue Carbon: Toward an Improved Understanding of the Role of Vegetated Coastal Habitats in Sequestering CO<sub>2</sub>." *Frontiers in Ecology and the Environment* 9, no. 10: 552–560. <https://doi.org/10.1890/110004>.

- Meijer, K. J., O. Franken, T. Van Der Heide, et al. 2023. "Characterizing Bedforms in Shallow Seas as an Integrative Predictor of Seafloor Stability and the Occurrence of Macrozoobenthic Species." *Remote Sensing in Ecology and Conservation* 9, no. 3: 323–339. <https://doi.org/10.1002/rse2.312>.
- Mitchell-Olds, T., and R. G. Shaw. 1987. "Regression Analysis of Natural Selection: Statistical Inference and Biological Interpretation." *Evolution* 41, no. 6: 1149–1161.
- Oloff, H., J. de Leeuw, J. P. Bakker, R. J. Platerink, H. J. Van Wijnen, and W. De Munck. 1997. "Vegetation Succession and Herbivory on a Salt Marsh: Changes Induced by Sea Level Rise and Silt Deposition Along an Elevational Gradient." *Journal of Ecology* 85, no. 6: 799–814. <https://doi.org/10.2307/2960603>.
- Pecl, G. T., M. B. Araújo, J. D. Bell, et al. 2017. "Biodiversity Redistribution Under Climate Change: Impacts on Ecosystems and Human Well-Being." *Science* 355: aai9214. <https://doi.org/10.1126/science.aai9214>.
- Pereira, H. M., S. Ferrier, M. Walters, et al. 2013. "Essential Biodiversity Variables." *Science* 339: 277–278. <https://doi.org/10.1126/science.1229931>.
- Philippart, C. J. M., G. C. Cadée, W. van Raaphorst, and R. Riegman. 2000. "Long-Term Phytoplankton-Nutrient Interactions in a Shallow Coastal Sea: Algal Community Structure, Nutrient Budgets, and Denitrification Potential." *Limnology and Oceanography* 45, no. 1: 131–144. <https://doi.org/10.4319/lo.2000.45.1.0131>.
- Prather, C. M., S. L. Pelini, A. Laws, et al. 2013. "Invertebrates, Ecosystem Services and Climate Change." *Biological Reviews* 88, no. 2: 327–348. <https://doi.org/10.1111/brv.12002>.
- R Core Team. 2023. *R: A Language and Environment for Statistical Computing* (4.3.1). R Foundation for Statistical Computing.
- Rishworth, G. M., J. B. Adams, M. S. Bird, et al. 2020. "Cross-Continental Analysis of Coastal Biodiversity Change." *Philosophical Transactions of the Royal Society B* 375: 20190452. <https://doi.org/10.1098/rstb.2019.0452>.
- Roswell, M., J. Dushoff, and R. Winfree. 2021. "A Conceptual Guide to Measuring Species Diversity." *Oikos* 130: 321–338.
- Rueda-Cediel, P., K. E. Anderson, T. J. Regan, J. Franklin, and H. M. Regan. 2015. "Combined Influences of Model Choice, Data Quality, and Data Quantity When Estimating Population Trends." *PLoS One* 10, no. 7: e0132255. <https://doi.org/10.1371/journal.pone.0132255>.
- Runge, C. A., T. G. Martin, H. P. Possingham, S. G. Willis, and R. A. Fuller. 2014. "Conserving Mobile Species." *Frontiers in Ecology and the Environment* 12, no. 7: 395–402. <https://doi.org/10.1890/130237>.
- Santini, L., J. Belmaker, M. J. Costello, et al. 2017. "Assessing the Suitability of Diversity Metrics to Detect Biodiversity Change." *Biological Conservation* 213: 341–350. <https://doi.org/10.1016/j.biocon.2016.08.024>.
- Shaw, A. K. 2016. "Drivers of Animal Migration and Implications in Changing Environments." *Evolutionary Ecology* 30, no. 6: 991–1007. <https://doi.org/10.1007/s10682-016-9860-5>.
- Sluijter, M., S. J. Lilipaly, and P. A. Wolf. 2023. "Midwintertelling van Zee-Eenden in de Waddenzee en Nederlandse Kustwateren in November 2022, Januari en Maart 2023 (Rapport RWS – Centrale Informatievoorziening)." Rapport BM 23.24/Deltamilieu Projecten Rapport 2023-08. p.38.
- Tilman, D., R. M. May, C. L. Lehman, and M. A. Nowak. 1994. "Habitat Destruction and the Extinction Debt." *Nature* 371: 65–66. <https://doi.org/10.1038/371065a0>.
- Unger, B., J. Baltzer, J. Brackmann, et al. 2022. "Marine mammals." In *Wadden Sea Quality Status Report*, edited by S. Kloepper et al. Common Wadden Sea Secretariat.
- van Beusekom, J. E. E., J. Carstensen, T. Dolch, et al. 2019. "Wadden Sea Eutrophication: Long-Term Trends and Regional Differences." *Frontiers in Marine Science* 6: 370. <https://doi.org/10.3389/fmars.2019.00370>.
- Van de Pol, M., B. J. Ens, D. Heg, et al. 2010. "Do Changes in the Frequency, Magnitude and Timing of Extreme Climatic Events Threaten the Population Viability of Coastal Birds?" *Journal of Applied Ecology* 47: 720–730. <https://doi.org/10.1111/j.1365-2664.2010.01842.x>.
- van Denderen, P. D., S. G. Bolam, J. G. Hiddink, et al. 2015. "Similar Effects of Bottom Trawling and Natural Disturbance on Composition and Function of Benthic Communities Across Habitats." *Marine Ecology Progress Series* 541: 31–43. <https://doi.org/10.3354/meps11550>.
- Van der Jagt, H. A., O. Duijts, R. Middelveld, and D. B. Kruijt. 2023. *Macrozoöbenthosbemonstering in de Zoute Rijkswateren 2022-Waterlichamen: Waddenzee en Overgangswateren Noordzeekanaal, Nieuwe Waterweg en Haringvliet-west. Rapport 23–266*. Waardenburg Ecology.
- Van der Jeugd, H. P., B. J. Ens, M. Versluijs, and H. Schekkerman. 2014. "Geïntegreerde monitoring vangvogels van de Nederlandse Waddenzee." Vogeltrekstation Rapport 2014–01. Vogeltrekstation, Wageningen; CAPS-Rapport 2014–01; Sovon-Rapport 2014/18, Sovon Vogelonderzoek Nederland, Nijmegen.
- van der Veer, H. W., I. Tulp, J. I. Witte, S. Poiesz, and L. Bolle. 2022. "Changes in Functioning of the Largest Coastal North Sea Flatfish Nursery, the Wadden Sea, Over the Past Half Century." *Marine Ecology Progress Series* 693: 183–201. <https://doi.org/10.3354/meps14082>.
- Viechtbauer, W. 2010. "Conducting Meta-Analyses in R With the Metafor Package." *Journal of Statistical Software* 36, no. 3: 1–48. <https://doi.org/10.18637/jss.v036.i03>.
- Visser, H. 2004. "Estimation and Detection of Flexible Trends." *Atmospheric Environment* 38: 4135–4145. <https://doi.org/10.1016/j.atmosenv.2004.04.014>.
- Wauchope, H. S., T. Amano, W. J. Sutherland, and A. Johnston. 2019. "When Can We Trust Population Trends? A Method for Quantifying the Effects of Sampling Interval and Duration." *Methods in Ecology and Evolution* 10, no. 12: 2067–2078. <https://doi.org/10.1111/2041-210X.13302>.
- White, E. R. 2019. "Minimum Time Required to Detect Population Trends: The Need for Long-Term Monitoring Programs." *Bioscience* 69, no. 1: 40–46. <https://doi.org/10.1093/biosci/biy144>.
- Wirth, C., H. Bruehlheide, N. Farwig, J. M. Marx, and J. Settele. 2024. *Faktencheck Artenvielfalt. Bestandsaufnahme Und Perspektiven für den Erhalt der Biologischen Vielfalt in Deutschland*. Oekom-Verlag.
- WoRMS Editorial Board. 2024. "World Register of Marine Species." Accessed July 2024. <https://www.marinespecies.org> at VLIZ. <https://doi.org/10.14284/170>.
- Yu, G. 2022. *Data Integration, Manipulation and Visualization of Phylogenetic Trees*. 1st ed. Chapman and Hall/CRC.
- Zhang, W., B. C. Sheldon, R. Grenyer, and K. J. Gaston. 2021. "Habitat Change and Biased Sampling Influence Estimation of Diversity Trends." *Current Biology* 31: 3656–3662. <https://doi.org/10.1016/j.cub.2021.05.066>.

## Data Sources

- Behm-Berkelmann, K., and H. Heckenroth. 1991. "Übersicht Brutbestandsentwicklung Ausgewählter Vogelarten 1900–1990 an der Niedersächs. Nordseeküste." In *Naturschutz und Landschaftspflege in Niedersachsen*, vol. 27, 97. Nds. Landesbetrieb für Wasserwirtschaft, Küsten- und Naturschutz.
- Dänhardt, A., J. Riechert, S. Bouwhuis, G. Millat, C. Abel, and P. H. Becker. 2018. "Nahrungsnetzbeziehungen zwischen Flussschwalben und Fischen an der Jade. Forschungsergebnisse 2006–2015." In *Schriftenreihe der Nationalparkverwaltung*, vol. 16. Nationalparkverwaltung Niedersächsisches Wattenmeer.

## 2 PUBLICATION I

Folmer, E. O. 2015. *Ontwikkelingen en Vestigingsmogelijkheden Voor Litoraal Zeegras in de Trilaterale Waddenzee*, 31. Programma Naar een Rijke Waddenzee.

Kleefstra, R., T. Bregnballe, J. Frikke, et al. 2022. "Trends of Migratory and Wintering Waterbirds in the Wadden Sea 1987/1988–2019/2020." Common Wadden Sea Secretariat, Expert Group Migratory Birds. <https://www.waddensea-worldheritage.org/resources/ecosystem-41-trends-migratory-birds>.

### **Supporting Information**

Additional supporting information can be found online in the Supporting Information section.



### 3 Publication II

Warming increases the compositional and functional  
variability of a temperate protist community

Published in *Science of the Total Environment* (2024)





Contents lists available at ScienceDirect

Science of the Total Environment

journal homepage: [www.elsevier.com/locate/scitotenv](http://www.elsevier.com/locate/scitotenv)

## Warming increases the compositional and functional variability of a temperate protist community

Antonia Ahme<sup>a,\*</sup>, Anika Happe<sup>b</sup>, Maren Striebel<sup>b</sup>, Marco J. Cabrerizo<sup>c,d</sup>, Markus Olsson<sup>e</sup>, Jakob Giesler<sup>a</sup>, Ruben Schulte-Hillen<sup>f</sup>, Alexander Sentimenti<sup>f</sup>, Nancy Kühne<sup>a</sup>, Uwe John<sup>a,g</sup>

<sup>a</sup> Alfred-Wegener-Institute, Helmholtz Centre for Polar and Marine Research, Am Handelshafen 12, 27570 Bremerhaven, Germany

<sup>b</sup> Institute for Chemistry and Biology of the Marine Environment (ICBM), University of Oldenburg, Schleusenstraße 1, 26382 Wilhelmshaven, Germany

<sup>c</sup> Department of Ecology, University of Granada, Campus Fuentenueva s/n 1, 18071 Granada, Spain

<sup>d</sup> Department of Ecology and Animal Biology, University of Vigo, Campus Lagoas Marcosende s/n, 36310 Vigo, Spain

<sup>e</sup> Department of Ecology, Environment and Plant Sciences, Stockholm University, Svante Arrhenius väg 20A, 106 91 Stockholm, Sweden

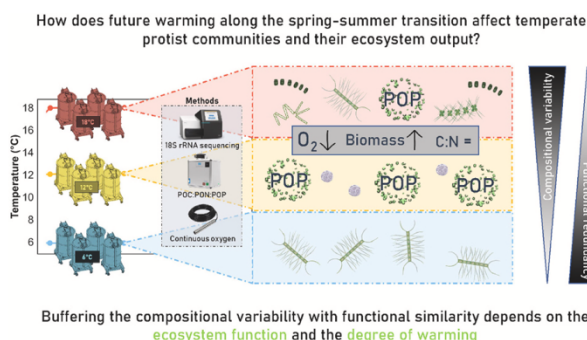
<sup>f</sup> Albert-Ludwigs-Universität Freiburg, Fahnbergplatz, 79104 Freiburg i.Br., Germany

<sup>g</sup> Helmholtz Institute for Functional Marine Biodiversity at the University of Oldenburg, Ammerländer Heersstraße 231, 26129 Oldenburg, Germany

### HIGHLIGHTS

- The species' thermal traits primarily drive community reorganisation under warming
- Many North Sea protists tolerate and coexist at temperatures of + 12 °C
- Biomass accumulation in- and oxygen production decreases with warming
- Temperature increases the compositional and functional variability
- *Phaeocystis globosa* drives functional dissimilarity regarding the C:P but not the C:N ratio

### GRAPHICAL ABSTRACT



### ARTICLE INFO

Editor: Jay Gan

#### Keywords:

Diatoms  
Ecosystem services  
Functional redundancy  
Haptophytes  
Indoor mesocosm incubation  
Marine phytoplankton  
Temperature increase  
Primary producers

### ABSTRACT

Phototrophic protists are a fundamental component of the world's oceans by serving as the primary source of energy, oxygen, and organic nutrients for the entire ecosystem. Due to the high thermal seasonality of their habitat, temperate protists could harbour many well-adapted species that tolerate ocean warming. However, these species may not sustain ecosystem functions equally well. To address these uncertainties, we conducted a 30-day mesocosm experiment to investigate how moderate (12 °C) and substantial (18 °C) warming compared to ambient conditions (6 °C) affect the composition (18S rRNA metabarcoding) and ecosystem functions (biomass, gross oxygen productivity, nutritional quality – C:N and C:P ratio) of a North Sea spring bloom community. Our results revealed warming-driven shifts in dominant protist groups, with haptophytes thriving at 12 °C and diatoms at 18 °C. Species responses primarily depended on the species' thermal traits, with indirect temperature effects on grazing being less relevant and phosphorus acting as a critical modulator. The species *Phaeocystis globosa* showed highest biomass on low phosphate concentrations and relatively increased in some replicates of

\* Corresponding author.

E-mail address: [antonia.ahme@awi.de](mailto:antonia.ahme@awi.de) (A. Ahme).

<https://doi.org/10.1016/j.scitotenv.2024.171971>

Received 2 February 2024; Received in revised form 22 March 2024; Accepted 23 March 2024

Available online 26 March 2024

0048-9697/© 2024 The Authors. Published by Elsevier B.V. This is an open access article under the CC BY license (<http://creativecommons.org/licenses/by/4.0/>).

both warming treatments. In line with this, the C:P ratio varied more with the presence of *P. globosa* than with temperature. Examining further ecosystem responses under warming, our study revealed lowered gross oxygen productivity but increased biomass accumulation whereas the C:N ratio remained unaltered. Although North Sea species exhibited resilience to elevated temperatures, a diminished functional similarity and heightened compositional variability indicate potential ecosystem repercussions for higher trophic levels. In conclusion, our research stresses the multifaceted nature of temperature effects on protist communities, emphasising the need for a holistic understanding that encompasses trait-based responses, indirect effects, and functional dynamics in the face of exacerbating temperature changes.

## 1. Introduction

Phototrophic protists play a central role in the ecosystem by providing energy, oxygen and organic nutrients for organisms higher up the food chain (Naselli-Flores and Padisák, 2023). Especially in coastal temperate areas, their habitat is characterised by a high seasonality in temperature. For instance, a typical North Sea spring bloom spans from early March to late April, during which the temperature gradually increases from around 6 °C to approximately 12 °C (Käse et al., 2020). A few months later in August, temperature peaks near 18 °C (Wiltshire and Manly, 2004). Many species are adapted to this wide temperature range and therefore often reside below their optimum temperature for growth (Boyd et al., 2013; Giesler et al., 2023). Despite this variability, most experiments investigating warming effects on temperate plankton employ treatments of +3 °C to +6 °C (Happe et al., 2024), which fall well within the range of what they naturally experience (Wiltshire and Manly, 2004). These temperatures may represent the average increases projected for the North Sea (IPCC, 2021); however, they do not encompass heatwaves, which are anticipated to become more frequent, intense, and long-lasting in the upcoming decades (Oliver et al., 2019; Sánchez-Benítez et al., 2022). Many studies also tend to overlook the seasonal dynamics in the field (Gerhard et al., 2023) and, instead, capture a snapshot of a specific point in the year (but see Staehr and Sand-Jensen, 2006). Consequently, the outcomes of these experiments heavily depend on the selection of the starting point, possibly failing to fully represent the actual temperature variations that temperate protist communities will encounter in the future.

Temperature can affect protist community structure via different ways. One of them is through its direct effect on the physiology of single organisms by increasing all metabolic rates until they reach an optimum temperature and then drop (Raven and Geider, 1988). This relationship is described by thermal performance curves (TPCs) and mostly expressed in terms of growth rate (Thomas et al., 2012). Although it can be expected that many temperate phototrophic species tolerate a wide range of temperatures in single strain incubations (Boyd et al., 2013), interspecific competition may alter the response on the community level (Huertas et al., 2011; Denny, 2017). The reason for this lies in species-specific TPC characteristics such as the temperature optimum, the thermal breadth and the maximum growth rate at a given temperature, leading to different growth increments under warming and ultimately entailing species sorting (Bestion et al., 2018; Anderson et al., 2021; Wiczyński et al., 2021). Furthermore, warming can have indirect effects such as stronger grazing (Gibert, 2019) or the acceleration of nutrient incorporation causing earlier limitation (Berges et al., 2002), which in turn affects the TPC of organisms by lowering their thermal optimum or limits (Thomas et al., 2017). Variations in all relevant traits can translate into temperature-induced community shifts, reflected in the compositional transition from spring to summer and between years with different mean temperatures (Alvarez-Fernandez et al., 2012; Bruhn et al., 2021).

Shifts in the community composition of phototrophic protists may mediate a changed output for the ecosystem (Di Pane et al., 2022). But even when the composition remains the same, temperature can alter attributes relevant for higher trophic levels such as the provision of oxygen, energy and organic nutrients (Naselli-Flores and Padisák,

2023). These ecosystem functions stem from a variety of cellular processes and could therefore respond differently to changes in temperature. Functions that are mainly driven by biophysical mechanisms, such as oxygen production, may be affected less strongly compared to functions that rather depend on biochemical reactions, like biomass accumulation (Falkowski and Raven, 2007; Rehder et al., 2023). Another trait tightly linked to temperature is the stoichiometry, specifically the cellular carbon to nutrient ratios (i.e. C:N and C:P), which are used as proxies for the nutritional quality for heterotrophic organisms (van de Waal et al., 2010). While warming favours the investment in nitrogen-rich proteins over phosphorus-rich ribosomes and thus may raise the cellular C:P ratio more than the C:N ratio (Woods et al., 2003; Armin and Inomura, 2021), both ratios could generally increase due to indirect temperature effects such as faster nutrient drawdown (De Senerpont Domis et al., 2014; Matsumoto et al., 2020). Ultimately, all of these processes depend on the environmental context, leading to great variations between the warming responses observed for ecosystem functions (Lewandowska et al., 2014; Striebel et al., 2016).

Differences in functional traits in combination with warming can increase the variability of a system. For example, small variations in the abundance of a species with a high nutrient uptake affinity can quickly build up to large differences when temperatures rise and then affect the surrounding conditions, e.g. induce earlier nutrient limitation (Serra-Pompei et al., 2019). In a setting where this species was slightly less abundant, another species with different traits could outcompete it and nutrient limitation might be induced later. The lag between these scenarios creates a phase with varying competition conditions and could shift the system to fundamentally different compositional states. Consequently, the existing stochasticity within planktonic systems can create several different trajectories and thereby lead to a higher unpredictability (Huisman and Weissing, 2001; Pálffy et al., 2021; Rogers et al., 2022). However, an increased compositional variability does not necessarily result in a higher variability of the respective ecosystem functions as it might be buffered by functional similarity between different species (Eisenhauer et al., 2023). While this has been shown to increase ecosystem stability to abiotic stressors (Biggs et al., 2020), temperature may context-dependently compromise this capacity (García et al., 2018; Zhong et al., 2020).

Despite the urgent need to understand warming responses for projecting future ecosystem properties, current studies on temperate communities do not cover the full potential natural temperature range (Gerhard et al., 2023). To fill this gap, we mechanistically investigated the effect of warming on temperate protist communities in an indoor-mesocosm setting, covering three temperatures from the start of the spring bloom up to the summer peak. The aim was to experimentally determine the compositional output including its variability and to assess potential consequences for ecosystem functions provided to the North Sea by the spring bloom community. We hypothesized that warming leads to a relative increase in species with the respective thermal niche; a higher oxygen production and biomass accumulation but lower nutritional quality; and finally, an increasing compositional and functional variability that depends on the temperature increment, resulting in functional similarity of the communities under moderate but not under substantial warming.

## 2. Material & methods

### 2.1. Seawater collection and experimental set-up

The experiment was carried out in the mesocosm facility of the Institute for Chemistry and Biology of the Marine Environment (ICBM) in Wilhelmshaven in March/April 2022. Experimental units were the Planktotrons – twelve stainless steel indoor-mesocosms (Gall et al., 2017). A total of 8000 L of surface seawater was collected from the open North Sea, 60 km off the German coast at the long-term ecological research station Helgoland Roads (DEIMS ID: <https://deims.org/1e96ef9b-0915-4661-849f-b3a72f5aa9b1>) during a cruise with the German RV *Heincke* on March 6th, 2022. The water was pumped with a diaphragm pump through a 200  $\mu\text{m}$  mesh (reducing the abundance of larger grazers) into eight acid-cleaned 1000 L polyethylene Intermediate Bulk Containers (IBC, AUER Packaging GmbH, Amerang, Germany). On March 7th, we filled the mesocosms by evenly spreading 75 L from each IBC tank into each mesocosm via gravity, resulting in a total of 600 L per mesocosm.

The experiment was conducted using three different temperature treatments, with a replication of four. Upon incubation, the water temperature of all twelve tanks was set to 6 °C, which is representative of the water temperature for the North Sea in March over the last 12 years (based on Helgoland Roads LTER time series) and close to the field temperature during water collection (5.4 °C). As we wanted to cover a wide temperature range, we aimed our highest temperature treatment to be around the optimum temperature for growth (e.g. the highest possible temperature before community growth deteriorates). Therefore, we determined the temperature reaction norm of the phototrophic community at the start of the incubation with a thermal performance curve (TPC) assay. This was started one day after filling the mesocosms (March 8th) by taking a pooled water sample from all mesocosms that was filled into 40 mL cell culture flasks (SARSTEDT, Nümbrecht, Germany) and randomly spread across ten temperatures (3 °C to 30 °C in 3 °C steps) in triplicates. The incubation of the units was achieved by placing them on heating/cooling mats (Inkbird, Shenzhen, China) in different temperature rooms under the same light conditions as the mesocosms. Fluorescence (395/680 nm excitation/emission) was measured daily for eight days to determine growth using a SYNERGY H1 microplate reader (BioTek, Winooski, Vermont, USA) and the thermal performance curve was fitted according to the model by Thomas et al. (2017) using the “rTPC” package (Padfield and O’Sullivan, 2022). We chose the treatment temperatures to span the minimum (6 °C) and optimum temperature (18 °C) for growth, as well as an intermediate temperature (12 °C; Fig. S1). We performed a gradual temperature increase by 1 °C per day starting 24 h after the mesocosms have been filled (incubation days 0–12; Fig. S2). During this phase, temperatures and replicates behaved similarly in terms of community composition as well as ecosystem functions (Figs. S10–14). Therefore, and for comparability, we focus on the period from day 13 onwards.

All parameters that required water to be taken out (DNA, particulate nutrients, dissolved nutrients) were sampled every 3rd day using a self-built tube of the same height as the mesocosms to equally obtain water from all depths. This water was poured into a sample-rinsed bucket, from which subsamples were taken for each parameter after gentle hand-stirring. The starting conditions were assessed on the 8th of March by combining ~4 L of water from each mesocosm and taking technical triplicates from this pool for each parameter. From then onwards, each mesocosm was sampled individually.

### 2.2. Abiotic conditions

Non-invasive parameters (temperature, pH, salinity) were sampled daily at 10 am. To promote water convection, an integrated, mechanically driven mixing paddle with silicone lips homogenised the water column every two hours at a slow speed to prevent disturbing fragile

organisms. Water temperatures were measured constantly with built-in PT100 sensors (Temperature Control, Donaueschingen, Germany) to confirm and adjust the target temperatures in each tank (Fig. S2). Two LED units (IT2040, Evergrow, Shenzhen, China) above each mesocosm were set to a 12:12 h day-night cycle (07:00–19:00 UTC light) with an intensity of 180  $\mu\text{mol photons m}^{-2} \text{ s}^{-1}$  (spherical PAR-sensor (US-SQS/L, Walz, Effeltrich, Germany) connected to a LI-250 A (Li-Cor, Lincoln, NE, USA)). These settings were selected based on the natural conditions at Helgoland Roads during this time of the year (Wiltshire, 2008, 2010). Although the light intensity changed in all mesocosms over time (potentially due to biomass accumulation), we observed no differences between the treatments, excluding light as a confounding factor (Fig. S3). Translucent float glass plates (Pilkington Optiwhite, Tokyo, Japan) were placed on top of the mesocosms to prevent evaporation, outgassing, and contamination. Daily salinity measurements (WTW IDS TetraCon, Xylem Analytics, Rye Brook, NY, USA) indicated no differences between temperatures (Fig. S4).

The experiment was conducted under ambient nutrient conditions. To monitor the concentrations of dissolved nitrate and phosphate, a subsample was filtered through a 0.2  $\mu\text{m}$  polyethersulfon syringe filter (Sartorius, Göttingen, Germany) every third day and stored at –20 °C until the colorimetric measurement on a continuous flow analyser (Euro EA 3000, HEKAtech GmbH, Wegberg, Germany). Samples for dissolved silicate were taken every other day and quantified by molybdate reaction according to Wetzel and Likens (2003).

The pH was measured daily (WTW Multi 3630 IDS, Xylem Analytics, Rye Brook, NY, USA). Samples for total alkalinity were taken at the beginning, middle (day 15), and end (day 27) of the incubation by filtering a 100 mL subsample through a 0.2  $\mu\text{m}$  polyethersulfon syringe filter (Sartorius, Göttingen, Germany) into a borosilicate bottle. The sample was kept at 4 °C until it was measured by duplicate potentiometric titration using a TitroLine alphaplus autosampler (Schott Instruments, Mainz, Germany) and subsequent correction with certified reference materials from A. Dickson (Scripps Institution of Oceanography, San Diego, CA, USA). The concentration of dissolved inorganic carbon (DIC) was calculated for incubation day 0, 15, and 27 using the software CO<sub>2</sub>sys (Pierrot et al., 2011) with dissociation constants of carbonic acid by Mehrbach et al. (1973), refitted by Dickson and Millero (1987).

### 2.3. Grazing assessment

Despite the initial filtering procedure, mesozooplankton appeared in all mesocosms, possibly due to early developmental stages (<200  $\mu\text{m}$ ) passing the mesh during water collection. Therefore, ~8 L water from each mesocosm were filtered through a 200  $\mu\text{m}$  mesh and any mesozooplankton were transferred into 250 mL brown glass bottles before being fixed with Lugol's iodine solution at the end of the experiment (incubation day 27). Mesozooplankton was enumerated and identified to the lowest possible taxonomic level based on scientific literature (Conway, 2012) using a stereo-microscope (S8 AP00, Leica, Wetzlar, Germany).

Additionally, protist herbivorous-induced mortality ( $m$ ) rates were measured with the dilution method (Landry and Hassett, 1982) in a two-point modification (Chen, 2015a; Landry et al., 2022) using undiluted (100 %) and diluted (30 %) seawater. Samples from each mesocosm were pooled together for each temperature treatment. From the original water, we prepared 500 mL undiluted (100 %) and diluted (30 %) samples (two technical replicates per temperature treatment at 0 h (t<sub>0</sub>) and one for 24 h (t<sub>f</sub>)). Following Landry and Hassett (1982) and Chen (2015a) net phototrophic growth rate ( $k$ ) was calculated as:

$$k = \ln (\text{Chla}_{\text{tf}} / \text{Chla}_{\text{t0}}) / t$$

where  $\text{Chla}_{\text{tf}}$  and  $\text{Chla}_{\text{t0}}$  are the Chla concentration measured at the end (t<sub>f</sub>) and at the beginning (t<sub>0</sub>) of the incubation period, respectively, and t

represents the duration of the incubation period (24 h). From both rates (that is,  $k_{30}$  and  $k_{100}$ ), we calculated grazing of protist herbivores as:

$$m = (k_{30} - k_{100}) / (1 - \times)$$

with  $\times$  being the dilution factor used.

#### 2.4. Community composition and diversity

Protist community composition was assessed via 18S rRNA gene amplicon sequencing of the V4 region as described by Ahme et al. (2023) and the results were validated qualitatively using light microscopy (fixed with 1 % Lugol's solution). Briefly, a subsample of 500 mL was gently vacuum-filtered ( $< -200$  mbar) onto 0.8  $\mu$ m polycarbonate filters (Nucleopore, Whatman, Maidstone, UK), which were stored in extraction buffer at  $-80^\circ\text{C}$ . DNA extraction was performed according to the manufacturer's protocol (NucleoSpin Soil extraction kit, Macherey-Nagel GmbH, Düren, Germany). All samples were normalised to 5 ng  $\mu\text{L}^{-1}$  before generating amplicons of the variable region 4 (V4) of the 18S rRNA gene following the standard protocol (16S Metagenomic Sequencing Library Preparation, Part #15044223 Rev. B. Illumina, San Diego, CA, USA). To best target the phototrophic community, we chose the forward and reverse primers of Bradley et al. (2016). Using the Nextera XT Index Kit v2 Set A primers (Illumina, San Diego, CA, USA), single samples were indexed and the barcoded amplicons were pooled equimolarly into one library. The library was sequenced with a  $2 \times 300$  bp paired-end setup on a MiSeq sequencer (Illumina, San Diego, CA, USA) and generated amplicon reads which were demultiplexed by the Generate FASTQ workflow of the MiSeq software.

Primers were removed with v2.8 cutadapt (Martin, 2011) and the data was further processed with v1.18 DADA2 (Callahan et al., 2016). Forward reads were quality-trimmed after 240 and reverse reads after 210 base pairs. Sequences were denoised and paired-end reads merged with a minimum overlap of 20 base pairs. Subsequently, chimeras were predicted and removed (Table S1). The resulting amplicon sequence variants (ASVs) were taxonomically annotated using the protist reference databases v4.12.0 PR2 (Guillou et al., 2013). Samples with a sequencing depth outside of the 90 % quantile range were removed, sufficient depth was confirmed using rarefaction curves (Fig. S5) and all samples were scaled to the lowest depth (Beule and Karlovsky, 2020). ASVs with a count of fewer than ten reads in replicate sample means were excluded, as well as metazoans, fungi, plastids and nuclei. All larger hetero- and mixotrophic taxa were separately analysed and grouped based on their primary feeding strategy (de Vargas et al., 2015; Ramond et al., 2018; Adl et al., 2019). For an assessment of diversity of each sample, we calculated species richness as number of species in each sample, species evenness (Pielou, 1966) and the Shannon index (Ortiz-Burgos, 2016). Processing of the data was performed using R v4.21 (RCoreTeam, 2022) with RStudio v2022.07.2 (RStudioTeam, 2022) and the packages v0.2.3 SRS (Heidrich et al., 2021), v1.40.0 phyloseq (McMurdie and Holmes, 2013), v0.0.22 microbial (Guo and Gao, 2022), and v4.2.6 propr (Quinn et al., 2017).

The replicates diverged in terms of their community composition and therefore no analyses were performed to compare mean compositions between temperature treatments. To get a measure for compositional dissimilarity between replicates, the pairwise Aitchinson distances were calculated between all replicates for each temperature and day. Then, the distances of the replicates to their centroids in multivariate space of a principal coordinate ordination were calculated with the betadisper function (vegan v2.6–2) as described by Anderson et al. (2006) and Pálffy et al. (2021). The compositional variability at a constant temperature of  $6^\circ\text{C}$  represents the “baseline”-variability within our experimental incubation. An increase in variability under warming (to  $12^\circ\text{C}$  or  $18^\circ\text{C}$ ) compared to  $6^\circ\text{C}$  indicates a temperature-driven effect rather than experimental duration/bottle effects. Therefore, we consider compositional variability to be driven by temperature if the beta-

dispersion at a given warming treatment is significantly higher than at  $6^\circ\text{C}$ .

#### 2.5. Ecosystem functions

To assess the effect of temperature on different ecosystem functions, we chose several proxies: the concentration of particulate organic carbon (POC) for community biomass (Andersson and Rudehäll, 1993), the molar ratios between POC and particulate organic nitrogen (PON)/phosphorus (POP) for nutritional quality (Thomas et al., 2022), as well as the rate of change of dissolved oxygen per POC for gross oxygen productivity (GOP; Sanz-Martín et al., 2019). Furthermore, samples for chlorophyll *a* (Chl*a*) were taken as a proxy to track the development of the phototrophic biomass throughout the experiment.

For Chl*a*, POC/PON and POP, subsamples were filtered onto pre-combusted glass-fibre filters (GF/F Whatman, Maidstone, UK), and kept frozen until processing. Filters for Chl*a* were extracted according to the method of Thrane et al. (2015) and measured using a microplate reader (614 nm/680 nm; SYNERGY H1, BioTek, Winooski, Vermont, USA). For POC/PON, filters were dried and measured with an elemental analyser (Flash EA 1112, Thermo Scientific, Waltham, MA, USA). The POP filters were quantified by molybdate reaction after digestion with a potassium peroxydisulfate solution (Wetzel and Likens, 2003). Particulate nutrient ratios were calculated by dividing the molar masses of the respective nutrients.

Dissolved oxygen concentration in  $\text{mmol m}^{-3}$  was measured continuously by the built-in OXYBase WR-RS485-L5 sensors (PreSens, Regensburg, Germany), calibrated by PreSens. Daily community production and respiration were calculated via the slope of the linear regression of oxygen concentration over the light period (09:00–19:00) and dark period (19:00–09:00), respectively. Daily GOP was then obtained by summing community production and respiration for each day, as described by Sanz-Martín et al. (2019). To account for differences in biomass, we normalised the daily GOP to POC.

#### 2.6. Statistics

A two-way repeated measures ANOVA (rmANOVA) was conducted to assess the effect of temperature, time and their interaction on the Shannon diversity, Chl*a*, ecosystem functions and the compositional variability. Normality was confirmed visually using quantile-quantile-plots. Sphericity was tested using Mauchly's test, and whenever it was violated, a Greenhouse-Geisser correction was applied. In analysing the beta-dispersion and Shannon diversity, day 24 had to be excluded because of too few data points. If a main effect of either temperature or time and no interaction was observed, pairwise *t*-tests were performed and the *p*-values were adjusted using the Bonferroni correction. For both, a main effect and a significant interaction, a one-way ANOVA of the main effect variable was performed before pairwise *t*-testing. All data are shown as arithmetic mean with one standard deviation in parentheses and analyses were conducted with a significance level of 0.05, using the v0.7.0 R package rstatix (Kassambara, 2021).

### 3. Results

#### 3.1. Bloom development and abiotic conditions

Chl*a* was significantly higher at  $18^\circ\text{C}$  than both at  $6^\circ\text{C}$  ( $p < .001$ ) and  $12^\circ\text{C}$  ( $p < .001$ ) without any effect of time (Table 1, Fig. 1). Both phosphate and nitrate concentrations showed no temperature effect but decreased over time, while silicate concentrations showed both main effects of temperature and time and an interaction (Table 1, Fig. 1). Silicate concentrations showed significant effects of temperature and time as well as an interaction (Table 1, Fig. 1). They decreased slightly at  $6^\circ\text{C}$  and strongest at  $18^\circ\text{C}$  (all  $p < .001$ ), whereas the concentrations at  $12^\circ\text{C}$  remained constant over time. Between replicates, phosphate and



**Table 1**

Results of the two-way rmANOVA for temperature, time, and their interactive effects on chlorophyll *a*, dissolved nutrients, diversity parameter and ecosystem functions. Dfn is the degree of freedom for the numerator of the F ratio, and DFd is for the denominator. Significant effects are highlighted in bold.

Parameter	Effect	DFn	DFd	F	p
Chlorophyll <i>a</i>	Temperature	2.00	9.00	30.5	<b>&lt;0.001</b>
	Time	1.99	17.89	2.3	0.134
	Temperature:Time	3.98	17.89	1.3	0.293
	Temperature	2.00	9.00	1.5	0.275
Nitrate	Time	1.88	16.91	8.3	<b>0.003</b>
	Temperature:Time	3.76	16.91	1.9	0.158
	Temperature	2.00	9.00	2.0	0.197
	Time	4.00	36.00	6.0	<b>&lt;0.001</b>
Phosphate	Temperature:Time	8.00	36.00	0.2	0.995
	Temperature	2.00	9.00	15.8	<b>0.001</b>
	Time	2.07	18.61	55.4	<b>&lt;0.001</b>
	Temperature:Time	4.13	18.61	10.2	<b>&lt;0.001</b>
Silicate	Temperature	2.00	3.00	2.1	0.268
	Time	1.00	3.00	1.3	0.343
	Temperature:Time	2.00	3.00	384.7	<b>&lt;0.001</b>
	Temperature	2.00	8.00	0.097	0.909
Micrograzing rate	Time	3.00	24.00	9.497	<b>&lt;0.001</b>
	Temperature:Time	6.00	24.00	7.572	<b>&lt;0.001</b>
	Temperature	2.00	8.00	1.118	0.373
	Time	3.00	24.00	7.576	<b>&lt;0.001</b>
Shannon index	Temperature:Time	6.00	24.00	0.616	0.715
	Temperature	2.00	8.00	0.056	0.946
	Time	3.00	24.00	5.635	<b>0.005</b>
	Temperature:Time	6.00	24.00	9.818	<b>&lt;0.001</b>
Richness	Temperature	2.00	9.00	4.9	<b>0.037</b>
	Time	4.00	36.00	14	<b>&lt;0.001</b>
	Temperature:Time	8.00	36.00	2.1	0.059
	Temperature	2.00	8.00	7.3	<b>0.015</b>
Evenness	Time	4.00	32.00	6.2	<b>0.005</b>
	Temperature:Time	8.00	32.00	1.4	0.220
	Temperature	2.00	9.00	3.6	0.070
	Time	4.00	36.00	11.8	<b>&lt;0.001</b>
Biomass	Temperature:Time	8.00	36.00	3.4	<b>0.006</b>
	Temperature	2.00	9.00	0.2	0.791
	Time	4.00	36.00	33.5	<b>&lt;0.001</b>
	Temperature:Time	8.00	36.00	3.9	<b>0.002</b>

silicate concentrations remained similar but they diverged in terms of nitrate, with replicates C and D at 12 °C and C at 18 °C decreasing more (Fig. S6). The pH increased from 8.09 (sd 0.01) to 8.36 (sd 0.05) in all mesocosms during the whole incubation period, but again replicates C and D at 12 °C and replicate C at 18 °C stood out by increasing the pH to 8.55–8.63 (Fig. S7). The same replicates additionally had the strongest decrease of DIC down to a minimum of 1920.17–1823.79 mmol kg SW<sup>-1</sup> (Fig. S7). The DIC concentration in all other mesocosms decreased to a lesser extent, i.e. 2032.87 (sd 31.75) mmol kg SW<sup>-1</sup>.

### 3.2. Grazing impact

In terms of mesozooplankton, we found no significant differences between the temperature treatments regarding their abundances (Kruskal-Wallis test,  $\chi^2(2) = 1.08$ ,  $p = .5836$ ) or composition (Fig. S8). The micro-grazing rates showed a significant interaction between temperature and time (Table 1, Fig. S9). Pairwise t-tests revealed a significant decrease over time at 6 °C ( $p = .008$ ) but an increase at 12 °C ( $p = .053$ ) and 18 °C ( $p = .061$ ). Thus, the micro-grazing rates at 6 °C were initially higher compared to 12 and 18 °C ( $p_{6-12} = 0.021$ ,  $p_{6-18} = 0.012$ ) but lower at the end ( $p_{6-12} = 0.039$ ,  $p_{6-18} = 0.012$ ). Between the two warming treatments, we found no significant differences at any time ( $p_{15} = 0.669$ ,  $p_{27} = 0.198$ ). The community composition was consistent between replicates at 6 °C, but became more variable under warming (Fig. S10).

### 3.3. Community composition and diversity

On phylum level, the main response pattern showed diatoms to be dominant at 6 °C and 18 °C, whereas they relatively decreased at 12 °C and instead haptophytes and dictyochophytes increased their relative abundance (Fig. S11). At 18 °C, either green algae or haptophytes comprised the rest of the community. Dinoflagellates showed similarly low relative abundances between all temperatures except for larger shares in the warming treatments, especially replicate C and D at 18 °C (*Prorocentrum* sp.; Fig. S12).

On lower taxonomic levels, the responses were more complex (Fig. 2). At 6 °C, the species *Chaetoceros debilis* relatively increased during the incubation while *Minidiscus variabilis*, *Skeletonema marinoi*, and *Thalassiosira punctigera* relatively decreased (Fig. S12). Additionally, the haptophyte *Phaeocystis globosa* had a low but stable relative contribution (Fig. S12). At 12 °C, *Dictyocha speculum* relatively increased in replicates A and B while the haptophytes were either dominated by *Gephyrocapsa oceanica* (replicate B), by *P. globosa* (replicates C & D) or switched from *P. globosa* to *G. oceanica* over time (replicate A; Fig. 2 & S12). At 18 °C, diatoms comprised more different species compared to 6 °C (several *Chaetoceros* species, *Ditylum brightwellii*, *T. punctigera* etc.; Fig. S12). In replicate A, *G. oceanica* was the main residual species whereas in replicate C it was *P. globosa*. In replicates B and D, *Pyr- amimonas* sp. made up a major part (Fig. 2, S12).

The Shannon diversity showed a significant effect of time and an interaction between time and temperature (Table 1, Fig. 3a). It stayed stable under warming and decreased over time at 6 °C ( $p_{15-27} = 0.002$ ,  $p_{18-27} = 0.003$ ), leading to 6 °C having an initially higher but at the end lower Shannon diversity compared to the warming treatments. This was mainly driven by differences in species evenness (Fig. 3c) as opposed to species richness (Fig. 3b), which only showed significant decreases over time at all temperatures (Table 1). The mean beta-dispersion was significantly higher at 18 °C but not at 12 °C compared to 6 °C (Table S2). Ellipsoids in multivariate space were more circular at 6 °C compared to 12, indicating that the differences between replicates at 6 °C were equal while at 12 °C two replicates each were more similar to each other but more dissimilar to the other pair (Fig. S13).

### 3.4. Ecosystem functions

Biomass (as POC) and gross oxygen productivity (GOP) were the only two ecosystem functions that significantly differed between temperatures (Table 1, Fig. 4a & b). Pairwise comparisons between the temperatures revealed biomass to be significantly higher at 18 °C than both at 6 °C ( $p < .001$ ) and 12 °C ( $p = .018$ ), but similar between 6 and 12 °C ( $p = .340$ ). GOP was significantly higher at 6 °C compared to 12 °C ( $p < .001$ ) and 18 °C ( $p = .002$ ).

All four ecosystem functions showed a significant effect of time (Table 1). Pairwise t-tests for biomass across the timepoints showed an increase at all temperatures from the first two sampling days (day 15 and 18) towards the last two sampling days (day 24 and 27;  $p_{15-24} = 0.032$ ,  $p_{15-27} = 0.013$ ,  $p_{18-24} = 0.024$ ,  $p_{18-27} = 0.005$ ). GOP decreased over time but only from sampling day 21 to sampling day 27 ( $p = .035$ ). Both particulate nutrient ratios additionally exhibited a significant interaction between time and temperature (Table 1). The C:N ratio only significantly decreased over time at 12 °C (Fig. 4c;  $p = .003$ ), while the C:P significantly increased over time at all temperatures (Fig. 4d; 6 °C:  $p_{C:P} = .003$ , all other  $p < .001$ ).

Inspecting differences within the temperatures, the mesocosms in which *P. globosa* made up a large proportion (12 °C C & D, 18 °C C) had higher values of biomass, the C:P ratio and pH and lower concentrations of nitrate compared to the other replicates at the same temperature (Fig. S14). Towards the end, replicate A at 18 °C also increased its biomass more compared to other replicates of the same temperature.

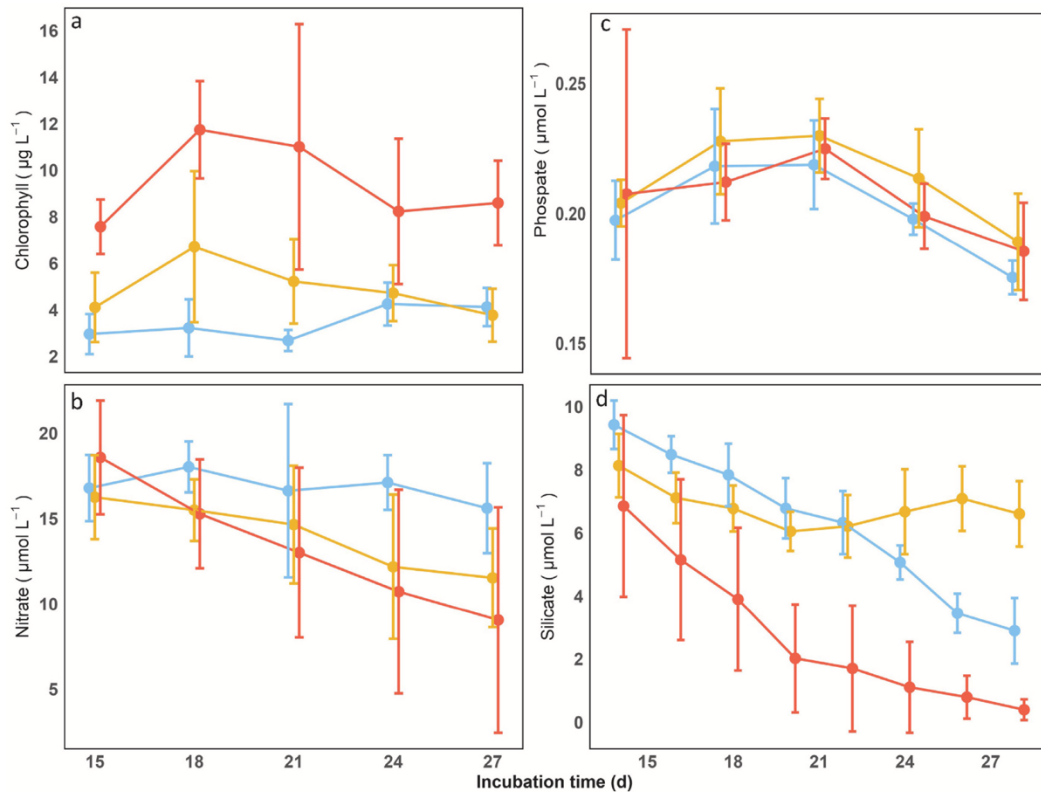


**Fig. 1.** Chlorophyll a (a), nitrate (b), phosphate (c), and silicate (d) of each temperature over time. Dots represent the arithmetic mean of the temperatures (6 °C: blue, 12 °C: yellow, 18 °C: red) and error bars the standard deviation.

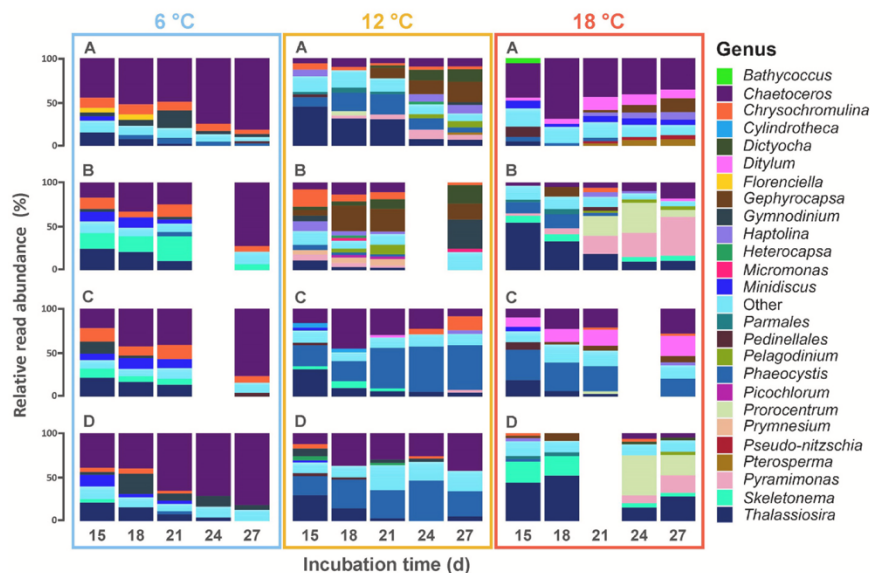


**Fig. 2.** Metabarcoding-based phototrophic community composition on genus level over time for all replicates (A-D; vertical alignment) and temperatures (6–18 °C; horizontal alignment). For readability, ASVs with an abundance of fewer than 150 reads among temperatures were categorized as “other”.

#### 4. Discussion

The aim of this study was to mechanistically investigate warming effects on the composition and resulting ecosystem functions of a temperate protist community. Our results indicate that thermal traits are the most important factor for community reorganisation but can be

amended by nutrients (here phosphorus) as modulators. Overall, we observed a high capacity of many North Sea species to tolerate and coexist at increased temperatures. Resulting ecosystem functions showed both warming-driven as well as species-specific responses and, due to reduced functional similarity, consequences for the ecosystem may be severe.

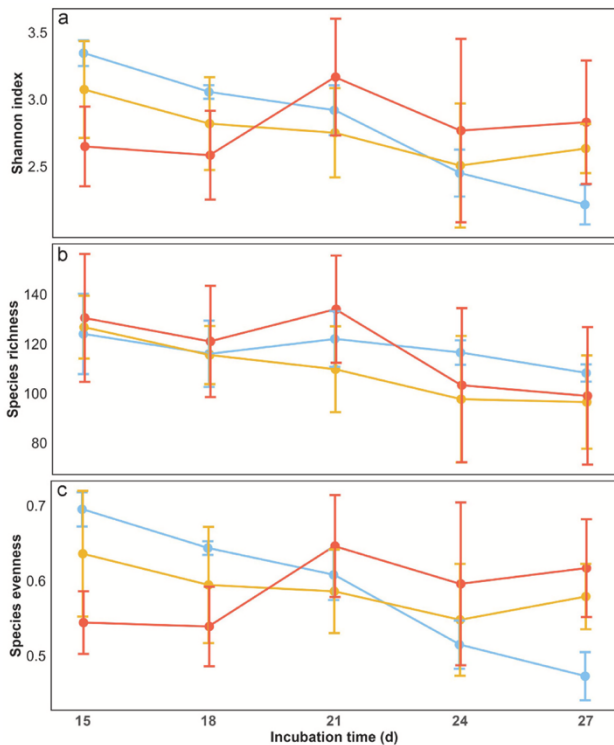


**Fig. 3.** Shannon index (a), species richness (b), and species evenness (c) of each temperature over time. Dots represent the arithmetic mean of the temperatures (6 °C: blue, 12 °C: yellow, 18 °C: red) and error bars the standard deviation.

#### Thermal traits are the main driver of community reorganisation under warming

At 6 °C, the species evenness was lower than under warming towards the end of the incubation. This indicates that 6 °C low temperatures to pose a higher selective pressure for species-sorting and dominance. A study by Anderson and Ryneason (2020) on temperate diatoms supports this argument by showing that community dynamics were driven more by thermal limits than thermal optima. Furthermore, we could not confirm previous projections on declining diversity with warming (Benedetti et al., 2021; Henson et al., 2021; Ahme et al., 2023). A potential explanation is that most of these studies depict Arctic communities with narrower thermal breadths, while temperate species usually reside far below their optimum temperature (Thomas et al., 2012). This likely enables many species to prevail under warming, as long as their (comparably high) thermal limits are not reached.

We observed a clear separation of the community composition at the phylum level. Diatoms dominated the communities at 6 °C and 18 °C while at 12 °C, it was largely haptophytes (either *P. globosa* or *Gephyrocapsa oceanica*). *Phaeocystis* spp. are known to decrease grazing pressure via large mucus-embedded colonies or potential toxicants (Stelfox-Widdicombe et al., 2004; Nejstgaard et al., 2007; Liang et al., 2020) and some studies pose that warming disproportionately favours heterotrophs, increasing top-down control (Chen et al., 2012; Boscolo-Galazzo et al., 2018). However, there were no significant differences in micro-grazing or mesozooplankton abundances and neither a clear pattern of certain grazer groups between 12 and 18 °C. In our experiment, grazing pressure can thus be excluded to drive the community composition under warming, consistent with the idea that the temperature-grazing relationship depends on other factors like nutrient levels (Chen et al., 2012).

The ability of diatoms to dominate communities both at low and high temperatures might be indicative of the high thermal niche diversity and a wider thermal breadth compared to haptophytes (Chen, 2015b;

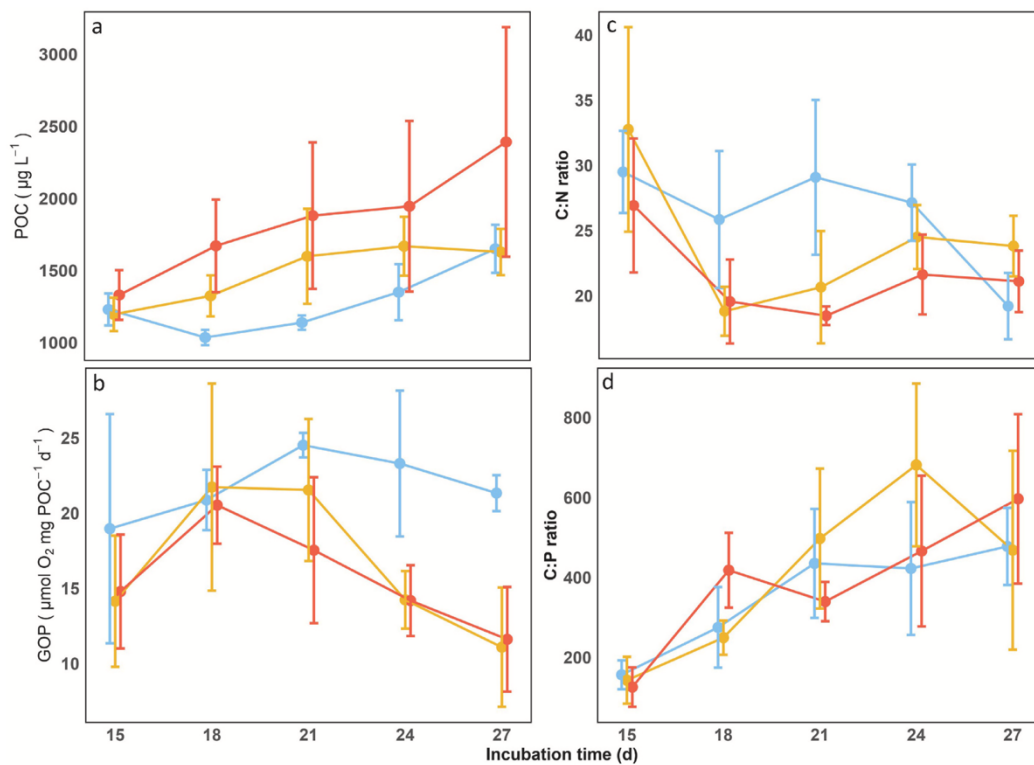


**Fig. 4.** Ecosystem function values of each temperature over time for (a) biomass, (b) GOP, (c) the C:N ratio, and (d) the C:P ratio. Dots represent the arithmetic mean of the temperatures (6 °C: blue, 12 °C: yellow, 18 °C: red) and error bars the standard deviation.



Anderson et al., 2021). For haptophytes, warming may have alleviated potential temperature limitation at 6 °C explaining their dominance at 12 °C (Wang et al., 2010; Wang et al., 2024). However, they could not outcompete diatoms anymore at 18 °C, despite having their optima at temperatures >15 °C (Wang et al., 2010; Müller et al., 2021). Indeed, diatoms are known to deal better with temperatures that exceed the multiyear upper temperature limit of the community at a given point of year (Kling et al., 2020), which could be reflected in the high number of different diatom species at 18 °C. Furthermore, the highest competitive abilities for nutrients are shown to be at colder temperatures compared to growth rate optima (Sunday et al., 2023). Considering the low phosphate concentrations in our experiment, this could have contributed to the dominance of haptophytes at 12 °C. Coccolithophores and *Phaeocystis* are known for thriving under low inorganic phosphorus concentrations (McKew et al., 2015; Moreno et al., 2022) and several studies indicate *Phaeocystis* to outcompete diatoms under inorganic phosphorus depletion under intermediate temperatures (Mori et al., 2021; Breton et al., 2022; Chai et al., 2023). At 18 °C, the competitive ability of haptophytes for low nutrient concentrations may have diminished and the higher growth rates of diatoms became more prevalent (Kremer et al., 2017; Sunday et al., 2023). Therefore, we found the main compositional patterns to arise from thermal traits, while nutrients acted as modulators.

Further support for the importance of thermal traits arises from the species level composition. At 6 °C, the diatom *C. debilis* increasingly dominated over time, reflecting its thermal niche as it is mainly found in colder waters (Ahyong et al., 2022). On the other hand, the decreasing *T. punctigera* is rather common in warmer waters (Ahyong et al., 2022). This is in line with *T. punctigera* being the dominant species in one replicate at 18 °C (C) while in two other replicates (B & D) *Pyramimonas* sp. and *Prorocentrum* sp. made up a large share, consistent with their thermal optima near 18 °C (Thomas et al., 2012; Edullantes et al., 2023). Furthermore, *D. speculum* is known to grow between 11 °C and 15 °C (Henriksen et al., 1993) and had a large contribution in two replicates (A & B) at 12 °C. Overall, our results show that literature-derived thermal traits can be considered a good predictor for community reorganisation under warming.

#### Temperature-dependence of ecosystem functions is mediated by the presence of *Phaeocystis*

The higher biomass accumulation under warming is consistent with other studies (De Senerpont Domis et al., 2014; Lewandowska et al., 2014) and reflects the seasonal dynamics in the field (González-Gil et al., 2022). Taken together with the higher species evenness, it may indicate a higher niche complementarity (Zhang et al., 2012). Another explanation could be temperature-stimulated higher carbon fixation rates of all community members taken together as shown by De Senerpont Domis et al. (2014) who also observed increased biomass despite changes in community composition.

The response of gross oxygen productivity (GOP) deviated from expectations. Instead of increasing with temperature, it was significantly lower at 12 °C and 18 °C compared to 6 °C towards the end of the incubation. One potential reason is an enhanced respiration rate of heterotrophs (Yvon-Durocher et al., 2012), exceeding the oxygen production by phototrophs. Indeed, the higher grazing rates observed at 12 °C and 18 °C can be a proxy for higher heterotrophic biomass (Freibott et al., 2016; Cabrerizo and al., in prep.) and therefore might underpin this theory. But even in phototrophs, the ratio of respiration to photosynthesis can increase with temperature (Bozzato et al., 2019; Bestion et al., 2020). Interestingly, there was no further decrease in GOP with temperature. As there were no differences in grazing rates or heterotrophic community composition between 12 °C and 18 °C, this can only be explained by differences in phototrophic community composition based on species- and size-specific variations in metabolic rates (López-Sandoval et al., 2014; Chen and Laws, 2017).

The C:N ratio was observed to be unresponsive to warming, confirming other studies (Yvon-Durocher et al., 2017; Verbeek et al., 2018). This may be based on the tight coupling between nitrate uptake and carbon assimilation as well as a limited ability to store surplus nitrogen in many species (Frost et al., 2023). On the other hand, the C:P ratio showed no mean differences among temperatures but consistently increased over time, implying an enhanced resource use efficiency over the incubation period (Breton et al., 2022) that could be based on species sorting (Verbeek et al., 2018). However, considering the higher C:P ratio of *Phaeocystis*-containing mesocosms which increased under warming, consequences regarding the nutritional quality for higher trophic levels cannot be ruled out (Bukovinszky et al., 2012).

Generally, the mesocosms with major proportions of *P. globosa* behaved differently compared to the other replicates. With higher relative amounts of *P. globosa*, more biomass was built up via more DIC uptake from the water, which resulted in a higher pH. The C:N ratio remained similar to the other replicates via a higher nitrate uptake. However, the C:P ratio was much higher, indicating that *P. globosa* could build up more organic carbon and nitrogen on the same amount of phosphorus compared to other species. This is consistent with other studies (Smith and Trimborn, 2024) and stresses *P. globosa*'s high capability of growing on low inorganic phosphorus levels, potentially because it better exploits the advantages of alkaline phosphatases (van Boekel and Veldhuis, 1990; Veldhuis et al., 1991). While the biomass of the *Phaeocystis*-dominated replicate at 18 °C was much higher than at 12 °C, the C:P ratio was similar between them, indicating a potential upper threshold of phosphorus resource use efficiency.

#### Temperature increases compositional variability and decreases functional similarity

The compositional variability increased with warming, which confirms the expectation that the enhanced growth rates until the community  $T_{opt}$  increase the potential for small differences in abundances to amplify. This is supported by the results of Pálffy et al. (2021), as they observed higher compositional variability of pioneer communities with warming. We also found an increased functional variability, which was mainly induced by *P. globosa*. But also the non-*Phaeocystis* containing replicate A at 18 °C experienced a stronger biomass increase than the other replicates towards the end (Fig. S14). This indicates that substantial warming (i.e. +12 °C) lowered the functional similarity even more than a moderate temperature increase (i.e. +6 °C). Consistently, modelling studies have observed increased functional uncertainty with warming (Laufkötter et al., 2015; Dutkiewicz et al., 2013; Sarker et al., 2020). Considering the high patchiness of plankton communities in the ocean (Robinson et al., 2021), this stresses the importance of experimentally covering a broad range of potential starting communities that may yield different functional outputs.

Overall, we observed that some functional responses appear universal between different organisms, while others exhibit species-dependence. Especially the C:N ratio can be considered robust across different community compositions. The communities additionally appeared to be functionally similar in terms of GOP under warming, which is in line with the findings of López-Sandoval et al. (2014). However, biomass and the C:P ratio depended on the exact community composition, consistent with the idea that functional and taxonomic diversity can covary (Ramond et al., 2019). A balanced nutrient supply to higher trophic levels under warming can therefore only be assumed for nitrogen, but not for phosphorus. Accordingly, functional similarity can buffer compositional differences only for specific functions (Biggs et al., 2020). However, it has to be kept in mind that the nutrient regime may modulate responses (Fetzer et al., 2015), yielding different results when nutrients are replete (Hoppe et al., 2018). We thus support the notion that functional similarity depends on the ecological context and can differ between ecosystem functions (Meyer et al., 2018; Eisenhauer et al., 2023).

## 5. Ecological implications and conclusion

From our study, we can derive several implications for resulting ecosystem processes. Firstly, higher temperatures may induce nutrient limitation of either nitrogen or phosphorus, depending on the community composition and the nutrient availability. Considering that phosphorus limitation is increasingly common for the North Sea (Grizzetti et al., 2012; Breton et al., 2022; Rönn et al., 2023), we expect the C:P ratio to increase, potentially limiting the growth of organisms higher up the food chain. Secondly, gross oxygen production could decrease, although this is likely no major problem in most areas of the shallow and well-mixed North Sea. Lastly, we discovered that the presence of *P. globosa* has the potential to shift the ecosystem to an alternative state with implications for the entire food web and biogeochemical cycles. It has to be noted that our incubation only lasted for a month so that we could not capture the aspect of evolution. As this can change the outcome of warming responses (Barton et al., 2020), longer-term incubations and field monitoring are needed to complement our results and infer consequences for the future North Sea more realistically.

In conclusion, our study demonstrates that thermal traits well explain community restructuring, modulated by nutrient-related traits. Considering the strong selective pressure posed by the lowest temperature, the temperature drop at the end of potential heatwaves requires more scientific attention. Furthermore, the degree of warming also determined the development of haptophyte vs. diatom-dominated communities and thereby may affect higher trophic levels and biogeochemical cycles, but the mechanisms for this are still poorly understood and need further investigation. While warming partly affected the mean differences between temperatures, the most striking result of this study was the increased compositional and partly functional variability at higher temperatures. Overall, we can conclude that stronger warming likely results in a less predictable ecosystem and an increased probability of fundamental shifts.

## Funding

This research was funded by the Helmholtz research program “Changing Earth, Sustaining our Future” (subtopic 6.2 “Adaptation of marine life: from genes to ecosystems” in topic 6 “Marine and Polar Life”) in the INSPIRES call I of the Alfred Wegener Institute Helmholtz Centre for Polar and Marine Research, Germany and AQUACOSM-plus (Project No. 871081) through the European Commission EU H2020-INFRAIA. MJC was supported by programa de proyectos de investigación para la incorporación de jóvenes doctores a nuevas líneas de investigación - Universidad de Granada, and his visit at ICBM by a Transnational Access granted through the AQUACOSM+ plus project (no. 871081).

## CRedit authorship contribution statement

**Antonia Ahme:** Writing – review & editing, Writing – original draft, Visualization, Software, Resources, Project administration, Methodology, Investigation, Formal analysis, Data curation, Conceptualization. **Anika Happe:** Writing – review & editing, Validation, Methodology, Investigation, Data curation, Conceptualization. **Maren Striebel:** Writing – review & editing, Validation, Supervision, Resources, Project administration, Funding acquisition, Conceptualization. **Marco J. Cabrerizo:** Writing – review & editing, Visualization, Methodology, Investigation, Data curation. **Markus Olsson:** Writing – review & editing, Validation, Methodology, Investigation, Formal analysis, Data curation. **Jakob Giesler:** Writing – review & editing, Validation, Formal analysis, Data curation. **Ruben Schulte-Hillen:** Writing – review & editing, Methodology, Investigation. **Alexander Sentimenti:** Writing – review & editing, Methodology, Investigation. **Nancy Kühne:** Writing – review & editing, Methodology, Investigation. **Uwe John:** Writing – review & editing, Validation, Supervision, Resources, Funding

acquisition, Conceptualization.

## Declaration of competing interest

Anika Happe, Marco J. Cabrerizo, Markus Olsson reports financial support was provided by European Commission. If there are other authors, they declare that they have no known competing financial interests or personal relationships that could have appeared to influence the work reported in this paper.

## Data availability

The DNA data are available from the European Nucleotide Archive at EMBL-EBI under the accession ID PRJEB72441 (<https://www.ebi.ac.uk/ena/browser/view/PRJEB72441>) and was submitted via GFBio (Diepenbroek et al., 2014). The TPC data can be obtained from Ahme et al. (2023a) and all other data from Ahme et al. (2023b). Abiotic conditions at Helgoland Roads are available in the Data Publisher for Earth & Environmental Science PANGAEA, at <https://doi.pangaea.de/10.1594/PANGAEA.960375>, or will be shared on reasonable request to LTER. HRSR@awi.de. Code to produce the graphs and results of the manuscript can be found online on GitHub: <https://github.com/AntoniaAhme/TopTronsMesocosmIncubation> (accessed on 06.11.2023).

## Acknowledgements

We thank the whole ICBM and Aquacosm+ team for their help during the experiment, in particular Simon Hasselø Kline, Lutz Ter Hell, Heike Scheele, Sebastian Neun and Lennart-Kilian Wenke. We also acknowledge Stefan Neuhaus for his help with bioinformatic processing of the 18S rRNA metabarcoding data. We thank Klara Wolf, Linda Rehder and Kristof Möller for their valuable input regarding the oxygen data and statistics. Furthermore, we are grateful for the data provided by Helgoland Roads that assisted in tuning the experimental design. We thank the cruise lead Jennifer Dannheim as well as the crew of the RV Heincke HE593 expedition for collecting the water sample. Finally, we would like to thank the anonymous reviewers of this manuscript, whose feedback greatly improved its quality.

## Appendix A. Supplementary data

Supplementary data to this article can be found online at <https://doi.org/10.1016/j.scitotenv.2024.171971>.

## References

- Adl, S.M., Bass, D., Lane, C.E., Lukeš, J., Schoch, C.L., Smirnov, A., et al., 2019. Revisions to the classification, nomenclature, and diversity of eukaryotes. *The Journal of Eukaryotic Microbiology* 66 (1), 4–119. <https://doi.org/10.1111/jeu.12691>.
- Ahme, A., Von Jackowski, A., McPherson, R.A., Wolf, K.K.E., Hoppmann, M., Neuhaus, S., et al., 2023. Winners and losers of atlantification: the degree of ocean warming affects the structure of arctic microbial communities. *Genes [Online]* 14 (3).
- Ahyong, S., Boyko, C.B., Bailly, N., Bernot, J., Bieler, R., Brandão, S.N., et al., 2022. World Register of Marine Species (WoRMS). WoRMS Editorial Board.
- Alvarez-Fernandez, S., Lindeboom, H., Meesters, E., 2012. Temporal changes in plankton of the North Sea: community shifts and environmental drivers. *Marine Ecology Progress Series* 462, 21–38. <https://doi.org/10.3354/meps09817>.
- Anderson, M.J., Ellingsen, K.E., McArdle, B.H., 2006. Multivariate dispersion as a measure of beta diversity. *Ecology Letters* 9 (6), 683–693. <https://doi.org/10.1111/j.1461-0248.2006.00926.x>.
- Anderson, S.I., Rynearson, T.A., 2020. Variability approaching the thermal limits can drive diatom community dynamics. *Limnology and Oceanography* 65 (9), 1961–1973. <https://doi.org/10.1002/lno.11430>.
- Anderson, S.I., Barton, A.D., Clayton, S., Dutkiewicz, S., Rynearson, T.A., 2021. Marine phytoplankton functional types exhibit diverse responses to thermal change. *Nature Communications* 12 (1), 6413. <https://doi.org/10.1038/s41467-021-26651-8>.
- Andersson, A., Rudehäll, Å., 1993. Proportion of plankton biomass in particulate organic carbon in the northern Baltic Sea. *Marine Ecology Progress Series* 95, 133–139. <https://doi.org/10.3354/meps095133>.
- Armin, G., Inomura, K., 2021. Modelled temperature dependencies of macromolecular allocation and elemental stoichiometry in phytoplankton. *Computational and*

- Structural Biotechnology Journal 19, 5421–5427. <https://doi.org/10.1016/j.csbj.2021.09.028>.
- Barton, S., Jenkins, J., Buckling, A., Schaum, C.E., Smirnov, N., Raven, J.A., Yvon-Durocher, G., 2020. Evolutionary temperature compensation of carbon fixation in marine phytoplankton. *Ecology Letters* 23, 722–733.
- Benedetti, F., Vogt, M., Elizondo, U.H., Righetti, D., Zimmermann, N.E., Gruber, N., 2021. Major restructuring of marine plankton assemblages under global warming. *Nature Communications* 12 (1), 5226. <https://doi.org/10.1038/s41467-021-25385-x>.
- Berges, J., Varela, D., Harrison, P., 2002. Effects of temperature on growth rate, cell composition and nitrogen metabolism in the marine diatom *Thalassiosira pseudonana* (Bacillariophyceae). *Marine Ecology Progress Series* 225, 139–146. <https://doi.org/10.3354/meps225139>.
- Bestion, E., García-Carreras, B., Schaum, C.E., Pawar, S., Yvon-Durocher, G., 2018. Metabolic traits predict the effects of warming on phytoplankton competition. *Ecology Letters* 21 (5), 655–664. <https://doi.org/10.1111/ele.12932>.
- Bestion, E., Barton, S., Garcia, F.C., Warfield, R., Yvon-Durocher, G., 2020. Abrupt declines in marine phytoplankton production driven by warming and biodiversity loss in a microcosm experiment. *Ecology Letters* 23 (3), 457–466. <https://doi.org/10.1111/ele.13444>.
- Beule, L., Karlovsky, P., 2020. Improved normalization of species count data in ecology by scaling with ranked subsampling (SRS): application to microbial communities. *PeerJ* 8, e9593. <https://doi.org/10.7717/peerj.9593>.
- Biggs, C.R., Yeager, L.A., Bolser, D.G., Bonsell, C., Dichiera, A.M., Hou, Z., et al., 2020. Does functional redundancy affect ecological stability and resilience? A review and meta-analysis. *Ecosphere* 11 (7), e03184. <https://doi.org/10.1002/ecs2.3184>.
- van Boekel, W.H.M., Veldhuis, M.J.W., 1990. Regulation of alkaline phosphatase synthesis in *Phaeocystis* sp. *Marine Ecology Progress Series* 61 (3), 281–289.
- Boscolo-Galazzo, F., Crichton, K.A., Barker, S., Pearson, P.N., 2018. Temperature dependency of metabolic rates in the upper ocean: a positive feedback to global climate change? *Global and Planetary Change* 170, 201–212. <https://doi.org/10.1016/j.gloplacha.2018.08.017>.
- Boyd, P.W., Rynearson, T.A., Armstrong, E.A., Fu, F., Hayashi, K., Hu, Z., et al., 2013. Marine phytoplankton temperature versus growth responses from polar to tropical waters—outcome of a scientific community-wide study. *PLoS One* 8 (5), e63091. <https://doi.org/10.1371/journal.pone.0063091>.
- Bozzato, D., Jakob, T., Wilhelm, C., 2019. Effects of temperature and salinity on respiratory losses and the ratio of photosynthesis to respiration in representative Antarctic phytoplankton species. *PLoS One* 14 (10), e0224101. <https://doi.org/10.1371/journal.pone.0224101>.
- Bradley, I.M., Pinto, A.J., Guest, J.S., 2016. Design and evaluation of illumina MiSeq-compatible, 18S rRNA gene-specific primers for improved characterization of mixed phototrophic communities. *Applied and Environmental Microbiology* 82 (19), 5878–5891. <https://doi.org/10.1128/AEM.01630-16>.
- Breton, E., Goberville, E., Sautour, B., Ouadi, A., Skouroliaou, D.-I., Seuront, L., et al., 2022. Multiple phytoplankton community responses to environmental change in a temperate coastal system: a trait-based approach. *Frontiers in Marine Science* 9. <https://doi.org/10.3389/fmars.2022.914475>.
- Bruhn, C.S., Wohlrab, S., Krock, B., Lundholm, N., John, U., 2021. Seasonal plankton succession in accordance with phycotoxin occurrence in Disko Bay, West Greenland. *Harmful Algae* 103. <https://doi.org/10.1016/j.hal.2021.101978>.
- Bukovinsky, T., Verschoor, A.M., Helmsing, N.R., Bezemer, T.M., Bakker, E.S., Vos, M., et al., 2012. The good, the bad and the plenty: interactive effects of food quality and quantity on the growth of different daphnia species. *PLoS One* 7 (9), e42966. <https://doi.org/10.1371/journal.pone.0042966>.
- Callahan, B.J., McMurdie, P.J., Rosen, M.J., Han, A.W., Johnson, A.J., Holmes, S.P., 2016. DADA2: high-resolution sample inference from Illumina amplicon data. *Nature Methods* 13 (7), 581–583. <https://doi.org/10.1038/nmeth.3869>.
- Chai, X., Zheng, L., Liu, J., Zhan, J., Song, L., 2023. Comparison of photosynthetic responses between haptophyte *Phaeocystis globosa* and diatom *Skeletonema costatum* under phosphorus limitation. *Frontiers in Microbiology* 14. <https://doi.org/10.3389/fmicb.2023.1085176>.
- Chen, B., 2015a. Assessing the accuracy of the “two-point” dilution technique. *Limnology and Oceanography: Methods* 13 (10), 521–526. <https://doi.org/10.1002/lom3.10044>.
- Chen, B., 2015b. Patterns of thermal limits of phytoplankton. *Journal of Plankton Research* 37 (2), 285–292. <https://doi.org/10.1093/plankt/fbv009>.
- Chen, B., Laws, E.A., 2017. Is there a difference of temperature sensitivity between marine phytoplankton and heterotrophs? *Limnology and Oceanography* 62 (2), 806–817. <https://doi.org/10.1002/lno.10462>.
- Chen, B., Landry, M.R., Huang, B., Liu, H., 2012. Does warming enhance the effect of microzooplankton grazing on marine phytoplankton in the ocean? *Limnology and Oceanography* 57 (2), 519–526. <https://doi.org/10.4319/lo.2012.57.2.0519>.
- Conway, D.V.P., 2012. Identification of the copepodite developmental stages of twenty-six North Atlantic copepods. In: *Occasional Publication of the Marine Biological Association*.
- De Senerpont Domis, L.N., Van de Waal, D.B., Helmsing, N.R., Van Donk, E., Mooij, W. M., 2014. Community stoichiometry in a changing world: combined effects of warming and eutrophication on phytoplankton dynamics. *Ecology* 95 (6), 1485–1495. <https://doi.org/10.1890/13-1251.1>.
- Denny, M., 2017. The fallacy of the average: on the ubiquity, utility and continuing novelty of Jensen's inequality. *The Journal of Experimental Biology* 220 (Pt 2), 139–146. <https://doi.org/10.1242/jeb.140368>.
- Di Pane, J., Wiltshire, K.H., McLean, M., Boersma, M., Meunier, C.L., 2022. Environmentally induced functional shifts in phytoplankton and their potential consequences for ecosystem functioning. *Global Change Biology* 28 (8), 2804–2819. <https://doi.org/10.1111/gcb.16098>.
- Dickson, A.G., Millero, F.J., 1987. A comparison of the equilibrium constants for the dissociation of carbonic acid in seawater media. *Deep Sea Research Part A. Oceanographic Research Papers* 34 (10), 1733–1743. [https://doi.org/10.1016/0198-0149\(87\)90021-5](https://doi.org/10.1016/0198-0149(87)90021-5).
- Dutkiewicz, S., Scott, J.R., Follows, M.J., 2013. Winners and losers: ecological and biogeochemical changes in a warming ocean. *Global Biogeochemical Cycles* 27 (2), 463–477. <https://doi.org/10.1002/gbc.20042>.
- Edulantes, B., Low-Decarie, E., Steinke, M., Cameron, T., 2023. Comparison of thermal traits between non-toxic and potentially toxic marine phytoplankton: implications to their responses to ocean warming. *Journal of Experimental Marine Biology and Ecology* 562, 151883. <https://doi.org/10.1016/j.jembe.2023.151883>.
- Eisenhauer, N., Hines, J., Maestre, F.T., Rillig, M.C., 2023. Reconsidering functional redundancy in biodiversity research. *npj Biodiversity* 2 (1), 9. <https://doi.org/10.1038/s44185-023-00015-5>.
- Falkowski, P.G., Raven, J.A., 2007. *Aquatic Photosynthesis*, Second edition. Princeton University Press.
- Fetzer, I., Johst, K., Schawe, R., Banitz, T., Harms, H., Chatzinotas, A., 2015. The extent of functional redundancy changes as species' roles shift in different environments. *Proceedings of the National Academy of Sciences* 112 (48), 14888–14893. <https://doi.org/10.1073/pnas.1505587112>.
- Freibott, A., Taylor, A.G., Selph, K.E., Liu, H., Zhang, W., Landry, M.R., 2016. Biomass and composition of protistan grazers and heterotrophic bacteria in the Costa Rica dome during summer 2010. *Journal of Plankton Research* 38 (2), 230–243. <https://doi.org/10.1093/plankt/fbv107>.
- Frost, P.C., Pearce, N.J.T., Berger, S.A., Gessner, M.O., Makower, A.K., Marzetz, V., et al., 2023. Interactive effects of nitrogen and phosphorus on growth and stoichiometry of lake phytoplankton. *Limnology and Oceanography* 68 (5), 1172–1184. <https://doi.org/10.1002/lno.12337>.
- Gall, A., Uebel, U., Ebensen, U., Hillebrand, H., Meier, S., Singer, G., et al., 2017. Planktotrons: a novel indoor mesocosm facility for aquatic biodiversity and food web research. *Limnology and Oceanography: Methods* 15 (7), 663–677. <https://doi.org/10.1002/lom3.10196>.
- Garcia, F.C., Bestion, E., Warfield, R., Yvon-Durocher, G., 2018. Changes in temperature alter the relationship between biodiversity and ecosystem functioning. *Proceedings of the National Academy of Sciences of the United States of America* 115 (43), 10989–10999. <https://doi.org/10.1073/pnas.1805518115>.
- Gerhard, M., Koussoroplis, A.-M., Raatz, M., Pansch, C., Fey, S.B., Vajedsamiee, J., et al., 2023. Environmental variability in aquatic ecosystems: avenues for future multifactorial experiments. *Limnology and Oceanography Letters* 8 (2), 247–266. <https://doi.org/10.1002/lo2.10286>.
- Gibert, J.P., 2019. Temperature directly and indirectly influences food web structure. *Scientific Reports* 9 (1), 5312. <https://doi.org/10.1038/s41598-019-41783-0>.
- Giesler, J.K., Harder, T., Wohlrab, S., 2023. Microbiome and photoperiod interactively determine thermal sensitivity of polar and temperate diatoms. *Biology Letters* 19 (11), 20230151. <https://doi.org/10.1098/rsbl.2023.0151>.
- González-Gil, R., Banas, N.S., Bresnan, E., Heath, M.R., 2022. The onset of the spring phytoplankton bloom in the coastal North Sea supports the disturbance recovery hypothesis. *Biogeosciences* 19 (9), 2417–2426. <https://doi.org/10.5194/bg-19-2417-2022>.
- Grizzetti, B., Bouraoui, F., Aloe, A., 2012. Changes of nitrogen and phosphorus loads to European seas. *Global Change Biology* 18 (2), 769–782. <https://doi.org/10.1111/j.1365-2486.2011.02576.x>.
- Guillou, L., Bachar, D., Audic, S., Bass, D., Berney, C., Bittner, L., et al., 2013. The Protist ribosomal reference database (PR2): a catalog of unicellular eukaryote small subunit rRNA sequences with curated taxonomy. *Nucleic Acids Research* 41 (Database issue), D597–D604. <https://doi.org/10.1093/nar/gks1160>.
- Guo, K., Gao, P., 2022. *microbial: Do 16s Data Analysis and Generate Figures*.
- Happe, A., Ahme, A., Cabrerizo, M.J., Gerhard, M., John, U., Striebel, M., 2024. Do the Rate of Temperature Change and Timing of Nutrient Availability Impact the Growth and Stoichiometry of a Natural Marine Phytoplankton Community? (under review).
- Heidrich, V., Karlovsky, P., Beule, L., 2021. ‘SRS’ R package and ‘q2-SRS’ QIIME 2 plugin: normalization of microbiome data using scaling with ranked subsampling (SRS). *Applied Sciences* 11 (23), 11473. <https://doi.org/10.3390/app112311473>.
- Henriksen, P., Knipschildt, F., Moestrup, Ø., Thomsen, H.A., 1993. Autecology, life history and toxicology of the silicoflagellate *Dictyocha speculum* (Silicoflagellata, Dictyochophyceae). *Phycologia* 32 (1), 29–39. <https://doi.org/10.2216/10031-8884-32-1-29-1>.
- Henson, S.A., Cael, B.B., Allen, S.R., Dutkiewicz, S., 2021. Future phytoplankton diversity in a changing climate. *Nature Communications* 12 (1), 5372. <https://doi.org/10.1038/s41467-021-25699-w>.
- Hoppe, C.J.M., Wolf, K.K.E., Schuback, N., Tortell, P.D., Rost, B., 2018. Compensation of ocean acidification effects in Arctic phytoplankton assemblages. *Nature Climate Change* 8 (6), 529–533. <https://doi.org/10.1038/s41558-018-0142-9>.
- Huertas, I.E., Rouco, M., López-Rodas, V., Costas, E., 2011. Warming will affect phytoplankton differently: evidence through a mechanistic approach. *Proceedings of the Royal Society B: Biological Sciences* 278 (1724), 3534–3543. <https://doi.org/10.1098/rspb.2011.0160>.
- Huisman, J., Weissing, F.J., 2001. Biological conditions for oscillations and chaos generated by multispecies competition. *Ecology* 82 (10), 2682–2695. [https://doi.org/10.1890/0012-9658\(2001\)082\[2682:BCFOAC\]2.0.CO;2](https://doi.org/10.1890/0012-9658(2001)082[2682:BCFOAC]2.0.CO;2).
- IPCC, 2021. In: Masson-Delmotte, V., Zhai, P., Pirani, A., Connors, S.L., Péan, C., Berger, S., Caud, N., Chen, Y., Goldfarb, L., Gomis, M.I., Huang, M., Leitzell, K., Lonnoy, E., Matthews, J.B.R., Maycock, T.K., Waterfield, T., Yelekçi, O., Yu, R., Zhou, B. (Eds.), *Climate Change 2021: The Physical Science Basis. Contribution of*

- Working Group I to the Sixth Assessment Report of the Intergovernmental Panel on Climate Change.
- Käse, L., Kraberg, A.C., Metfies, K., Neuhaus, S., Sprong, P.A.A., Fuchs, B.M., et al., 2020. Rapid succession drives spring community dynamics of small protists at Helgoland roads, North Sea. *Journal of Plankton Research* 42 (3), 305–319. <https://doi.org/10.1093/plankt/fbaa017>.
- Kassambara, A., 2021. rstatix: pipe-friendly framework for basic statistical tests.
- Kling, J.D., Lee, M.D., Fu, F., Phan, M.D., Wang, X., Qu, P., et al., 2020. Transient exposure to novel high temperatures reshapes coastal phytoplankton communities. *ISME* 14 (2), 413–424. <https://doi.org/10.1038/s41396-019-0525-6>.
- Kremer, C.T., Thomas, M.K., Litchman, E., 2017. Temperature- and size-scaling of phytoplankton population growth rates: reconciling the Eppley curve and the metabolic theory of ecology. *Limnology and Oceanography* 62 (4), 1658–1670. <https://doi.org/10.1002/lno.10523>.
- Landry, M.R., Hassett, R.P., 1982. Estimating the grazing impact of marine microzooplankton. *Marine Biology* 67, 283–288. <https://doi.org/10.1007/BF00397668>.
- Landry, M.R., Selph, K.E., Hood, R.R., Davies, C.H., Beckley, L.E., 2022. Low temperature sensitivity of picophytoplankton P: B ratios and growth rates across a natural 10°C temperature gradient in the oligotrophic Indian Ocean. *Limnology and Oceanography Letters* 7, 112–121. <https://doi.org/10.1002/lol2.10224>.
- Laufkötter, C., Vogt, M., Gruber, N., Aita-Noguchi, M., Aumont, O., Bopp, L., et al., 2015. Drivers and uncertainties of future global marine primary production in marine ecosystem models. *Biogeosciences* 12 (23), 6955–6984. <https://doi.org/10.5194/bg-12-6955-2015>.
- Lewandowska, A.M., Boyce, D.G., Hofmann, M., Matthiessen, B., Sommer, U., Worm, B., 2014. Effects of sea surface warming on marine plankton. *Ecology Letters* 17 (5), 614–623. <https://doi.org/10.1111/ele.12265>.
- Liang, Y., Guo, H., Liao, Q., Zhang, X., Huang, K., 2020. Growth performance, phenotypic traits, and antioxidant responses of the rotifer *Brachionus plicatilis* under different proportions of *Phaeocystis globosa*. *Ecotoxicology and Environmental Safety* 202, 110963. <https://doi.org/10.1016/j.ecoenv.2020.110963>.
- López-Sandoval, D.C., Rodríguez-Ramos, T., Cermeño, P., Sobrino, C., Marañón, E., 2014. Photosynthesis and respiration in marine phytoplankton: relationship with cell size, taxonomic affiliation, and growth phase. *Journal of Experimental Marine Biology and Ecology* 457, 151–159. <https://doi.org/10.1016/j.jembe.2014.04.013>.
- Martin, M., 2011. Cutadapt removes adapter sequences from high-throughput sequencing reads. *Next Generation Sequencing Data Analysis* 17 (1). <https://doi.org/10.14806/ej.17.1.200>.
- Matsumoto, K., Tanioka, T., Rickaby, R., 2020. Linkages between dynamic phytoplankton C:N:P and the ocean carbon cycle under climate change. *Oceanography* 33 (2), 44–52. <https://doi.org/10.5670/oceanog.2020.203>.
- McKew, B.A., Metodieva, G., Raines, C.A., Metodieva, M.V., Geider, R.J., 2015. Acclimation of *Emiliania huxleyi* (1516) to nutrient limitation involves precise modification of the proteome to scavenge alternative sources of N and P. *Environmental Microbiology* 17 (10), 4050–4062. <https://doi.org/10.1111/1462-2920.12957>.
- McMurdie, P.J., Holmes, S., 2013. Phyloseq: an R package for reproducible interactive analysis and graphics of microbiome census data. *PLoS One* 8 (4), e61217.
- Mehrbach, C., Culbertson, C.H., Hawley, J.E., Pytkowicz, R.M., 1973. Measurement of the apparent dissociation constants of carbonic acid in seawater at atmospheric pressure. *Limnology and Oceanography* 18 (6), 897–907. <https://doi.org/10.4319/lno.1973.18.6.0897>.
- Meyer, S.T., Ptacnik, R., Hillebrand, H., Bessler, H., Buchmann, N., Ebeling, A., Eisenhauer, N., Engels, C., Fischer, M., Halle, S., Klein, A.-M., Oelmann, Y., Roscher, C., Rottstock, T., Scherber, C., Scheu, S., Schmid, B., Schulze, E.-D., Temperton, V.M., Tschamtk, T., Voigt, W., Weigelt, A., Wilcke, W., Weisser, W.W., 2018. Biodiversity-multifunctionality relationships depend on identity and number of measured functions. *Nature Ecology & Evolution* 2, 44–49.
- Moreno, H.D., Köring, M., Di Pane, J., Tremblay, N., Wiltshire, K.H., Boersma, M., et al., 2022. An integrated multiple driver mesocosm experiment reveals the effect of global change on planktonic food web structure. *Communications Biology* 5 (1), 179. <https://doi.org/10.1038/s42003-022-03105-5>.
- Mori, C., Beck, M., Striebel, M., Merder, J., Schnetger, B., Dittmar, T., et al., 2021. Biogeochemical cycling of molybdenum and thallium during a phytoplankton summer bloom: a mesocosm study. *Marine Chemistry* 229, 103910. <https://doi.org/10.1016/j.marchem.2020.103910>.
- Müller, M.N., Blanco-Ameijeiras, S., Stoll, H.M., Mendez-Vicente, A., Lebrato, M., 2021. Temperature induced physiological reaction norms of the coccolithophore *Gephyrocapsa oceanica* and resulting coccolith Sr/ca and mg/ca ratios. *Frontiers in Earth Science* 9. <https://doi.org/10.3389/feart.2021.582521>.
- Naselli-Flores, L., Padisák, J., 2023. Ecosystem services provided by marine and freshwater phytoplankton. *Hydrobiologia* 850 (12), 2691–2706. <https://doi.org/10.1007/s10750-022-04795-y>.
- Nejstgaard, J.C., Tang, K.W., Steinke, M., Dutz, J., Koski, M., Antajan, E., et al. van Leeuwe, M.A., Stefels, J., Belviso, S., Lancelot, C., Verity, P.G., Gieskes, W.W.C., 2007. Zooplankton grazing on *Phaeocystis*: a quantitative review and future challenges. In: *Phaeocystis*, Major Link in the Biogeochemical Cycling of Climate-Relevant Elements. Springer Netherlands, Dordrecht, pp. 147–172.
- Oliver, E.C.J., Burrows, M.T., Donat, M.G., Sen Gupta, A., Alexander, L.V., Perkins-Kirkpatrick, S.E., et al., 2019. Projected marine heatwaves in the 21st century and the potential for ecological impact. *Frontiers in Marine Science* 6. <https://doi.org/10.3389/fmars.2019.00734>.
- Ortiz-Burgos, S., 2016. Shannon-weaver diversity index. In: Kennish, M.J. (Ed.), *Encyclopedia of Estuaries*. Springer Netherlands, Dordrecht, pp. 572–573.
- Padfield, D., O'Sullivan, H., 2022. rTPC: functions for fitting thermal performance curves. R package version 1.0.2. <https://github.com/padpadpad/rTPC>.
- Pálffy, K., Kovács, A.W., Kardos, V., Hausz, I., Boros, G., 2021. Elevated temperature results in higher compositional variability of pioneer phytoplankton communities in a mesocosm system. *Journal of Plankton Research* 43 (2), 142–155. <https://doi.org/10.1093/plankt/fbab013>.
- Pielou, E.C., 1966. The measurement of diversity in different types of biological collections. *Journal of Theoretical Biology* 13, 131–144. [https://doi.org/10.1016/0022-5193\(66\)90013-0](https://doi.org/10.1016/0022-5193(66)90013-0).
- Pierrot, D., Wallace, D.W.R., Lewis, E.R., Pierrot, D., Wallace, R., Wallace, D.W.R., et al., 2011. MS excel program developed for CO2 system calculations.
- Quinn, T., Richardson, M.F., Lovell, D., Crowley, T., 2017. Propr: an R-package for identifying proportionally abundant features using compositional data analysis. *Scientific Reports* 7, 16252. <https://doi.org/10.1038/s41598-017-16520-0>.
- Ramond, P., Siano, R., Sourisseau, M., 2018. Functional Traits of Marine Protists. SEANO. <https://doi.org/10.17882/51662>.
- Ramond, P., Sourisseau, M., Simon, N., Romac, S., Schmitt, S., Rigaut-Jalabert, F., et al., 2019. Coupling between taxonomic and functional diversity in protistan coastal communities. *Environmental Microbiology* 21 (2), 730–749. <https://doi.org/10.1111/1462-2920.14537>.
- Raven, J.A., Geider, R.J., 1988. Temperature and algal growth. *The New Phytologist* 110 (4), 441–461. <https://doi.org/10.1111/j.1469-8137.1988.tb00282.x>.
- RCoreTeam, 2022. R: A Language and Environment for Statistical Computing. R Foundation for Statistical Computing, Vienna, Austria. <https://www.R-project.org/>.
- Rehder, L., Rost, B., Rokiitta, S.D., 2023. Abrupt and acclimation responses to changing temperature elicit divergent physiological effects in the diatom *Phaeodactylum tricornutum*. *The New Phytologist* 239 (3), 1005–1013. <https://doi.org/10.1111/nph.18982>.
- Robinson, K.L., Sponaugle, S., Luo, J.Y., Gleiber, M.R., Cowen, R.K., 2021. Big or small, patchy all: resolution of marine plankton patch structure at micro- to submesoscales for 36 taxa. *Science Advances* 7 (47), eabk2904. <https://doi.org/10.1126/sciadv.abk2904>.
- Rogers, T.L., Johnson, B.J., Munch, S.B., 2022. Chaos is not rare in natural ecosystems. *Nature Ecology & Evolution* 6 (8), 1105–1111. <https://doi.org/10.1038/s41559-022-01787-y>.
- Rönn, L., Antonucci di Carvalho, J., Blauw, A., Hillebrand, H., Kerimoglu, O., Lenhart, H., et al., 2023. Harmonisation of the phytoplankton assessment in the German and Dutch Wadden Sea. Interreg V A project “Wasserqualität-Waterkwaliteit” - Synthesis Report.
- RStudioTeam, 2022. RStudio: Integrated Development Environment for R. RStudio, PBC, Boston, MA. <http://www.rstudio.com/>.
- Sánchez-Benítez, A., Goessling, H., Pithan, F., Semmler, T., Jung, T., 2022. The July 2019 European heat wave in a warmer climate: storyline scenarios with a coupled model using spectral nudging. *Journal of Climate* 35 (8), 2373–2390. <https://doi.org/10.1175/JCLI-D-21-0573.1>.
- Sanz-Martín, M., Vernet, M., Cape, M.R., Mesa, E., Delgado-Huertas, A., Reigstad, M., et al., 2019. Relationship between carbon- and oxygen-based primary productivity in the Arctic Ocean, Svalbard archipelago. *Frontiers in Marine Science* 6. <https://doi.org/10.3389/fmars.2019.00468>.
- Sarker, S., Yadav, A.K., Akter, M., Shahadat Hossain, M., Chowdhury, S.R., Kabir, M.A., et al., 2020. Rising temperature and marine plankton community dynamics: is warming bad? *Ecological Complexity* 43, 100857. <https://doi.org/10.1016/j.ecocom.2020.100857>.
- Serra-Pompeí, C., Hagstrom, G.I., Visser, A.W., Andersen, K.H., 2019. Resource limitation determines temperature response of unicellular plankton communities. *Limnology and Oceanography* 64 (4), 1627–1640. <https://doi.org/10.1002/lno.11140>.
- Smith, W.O., Trimborn, S., 2024. *Phaeocystis*: a global enigma. *Annual Review of Marine Science* 16 (1), 417–441. <https://doi.org/10.1146/annurev-marine-022223-025031>.
- Staehr, P.A., Sand-Jensen, K., 2006. Seasonal changes in temperature and nutrient control of photosynthesis, respiration and growth of natural phytoplankton communities. *Freshwater Biology* 51 (2), 249–262. <https://doi.org/10.1111/j.1365-2427.2005.01490.x>.
- Stelfox-Widdicombe, C.E., Archer, S.D., Burkill, P.H., Stefels, J., 2004. Microzooplankton grazing in *Phaeocystis* and diatom-dominated waters in the southern North Sea in spring. *Journal of Sea Research* 51 (1), 37–51. <https://doi.org/10.1016/j.seares.2003.04.004>.
- Striebel, M., Schabhlütt, S., Hodapp, D., Hingsamer, P., Hillebrand, H., 2016. Phytoplankton responses to temperature increases are constrained by abiotic conditions and community composition. *Oecologia* 182 (3), 815–827. <https://doi.org/10.1007/s00442-016-3693-3>.
- Sunday, J.M., Bernhardt, J.R., Harley, C.D.G., O'Connor, M.I., 2023. Temperature dependence of competitive ability is cold-shifted compared to that of growth rate in marine phytoplankton. *Ecology Letters* n/a (n/a). <https://doi.org/10.1111/ele.14337>.
- Thomas, M.K., Kremer, C.T., Klausmeier, C.A., Litchman, E., 2012. A global pattern of thermal adaptation in marine phytoplankton. *Science* 338 (6110), 1085–1088. <https://doi.org/10.1126/science.1224836>.
- Thomas, M.K., Aranguren-Gassis, M., Kremer, C.T., Gould, M.R., Anderson, K., Klausmeier, C.A., et al., 2017. Temperature-nutrient interactions exacerbate sensitivity to warming in phytoplankton. *Global Change Biology* 23 (8), 3269–3280. <https://doi.org/10.1111/gcb.13641>.
- Thomas, P.K., Kunze, C., Van de Waal, D.B., Hillebrand, H., Striebel, M., 2022. Elemental and biochemical nutrient limitation of zooplankton: a meta-analysis. *Ecology Letters* 0 (0), 1–17. <https://doi.org/10.1111/ele.14125>.
- Thrane, J.-E., Kyle, M., Striebel, M., Haande, S., Grung, M., Rohrlack, T., et al., 2015. Spectro-photometric analysis of pigments: a critical assessment of a high-throughput

### 3 PUBLICATION II

A. Ahme et al.

*Science of the Total Environment* 926 (2024) 171971

- method for analysis of algal pigment mixtures by spectral deconvolution. *PLoS One* 10 (9), e0137645. <https://doi.org/10.1371/journal.pone.0137645>.
- de Vargas, C., Audic, S., Henry, N., Decelle, J., Mahé, F., Logares, R., et al., 2015. Eukaryotic plankton diversity in the sunlit ocean. *Science* 348 (6237), 1261605. <https://doi.org/10.1126/science.1261605>.
- Veldhuis, M.J.W., Colijn, F., Admiraal, W., 1991. Phosphate utilization in *Phaeocystis pouchetii* (haptophyceae). *Marine Ecology* 12 (1), 53–62. <https://doi.org/10.1111/j.1439-0485.1991.tb00083.x>.
- Verbeek, L., Gall, A., Hillebrand, H., Striebel, M., 2018. Warming and oligotrophication cause shifts in freshwater phytoplankton communities. *Global Change Biology* 24 (10), 4532–4543. <https://doi.org/10.1111/gcb.14337>.
- van de Waal, D.B., Verschoor, A.M., Verspagen, J.M., van Donk, E., Huisman, J., 2010. Climate-driven changes in the ecological stoichiometry of aquatic ecosystems. *Frontiers in Ecology and the Environment* 8 (3), 145–152. <https://doi.org/10.1890/080178>.
- Wang, J., Zeng, C., Feng, Y., 2024. Meta-analysis reveals responses of coccolithophores and diatoms to warming. *Marine Environmental Research* 193, 106275. <https://doi.org/10.1016/j.marenvres.2023.106275>.
- Wang, X., Tang, K.W., Wang, Y., Smith, W.O., 2010. Temperature effects on growth, colony development and carbon partitioning in three *Phaeocystis* species. *Aquatic Biology* 9 (3), 239–249. <https://doi.org/10.3354/ab00256>.
- Wetzel, R.G., Likens, G.E., 2003. *Limnological Analyses*. Springer-Verlag, New York.
- Wieczynski, D.J., Singla, P., Doan, A., Singleton, A., Han, Z.-Y., Votzke, S., et al., 2021. Linking species traits and demography to explain complex temperature responses across levels of organization. *Proceedings of the National Academy of Sciences* 118 (42), e2104863118. <https://doi.org/10.1073/pnas.2104863118>.
- Wiltshire, K.H., 2008. Hydrochemistry at time series station Helgoland roads, North Sea, in 2007. *PANGAEA*. <https://doi.org/10.1594/PANGAEA.683880>.
- Wiltshire, K.H., 2010. Hydrochemistry at time series station Helgoland roads, North Sea, in 2009. *PANGAEA*. <https://doi.org/10.1594/PANGAEA.737388>.
- Wiltshire, K.H., Manly, B.F.J., 2004. The warming trend at Helgoland roads, North Sea: phytoplankton response. *Helgoland Marine Research* 58 (4), 269–273. <https://doi.org/10.1007/s10152-004-0196-0>.
- Woods, H.A., Makino, W., Cotner, J.B., Hobbie, S.E., Harrison, J.F., Acharya, K., et al., 2003. Temperature and the chemical composition of poikilothermic organisms. *Functional Ecology* 17 (2), 237–245.
- Yvon-Durocher, G., Caffrey, J.M., Cescatti, A., Dossena, M., Giorgio, P.D., Gasol, J.M., et al., 2012. Reconciling the temperature dependence of respiration across timescales and ecosystem types. *Nature* 487 (7408), 472–476. <https://doi.org/10.1038/nature11205>.
- Yvon-Durocher, G., Schaum, C.E., Trimmer, M., 2017. The temperature dependence of phytoplankton stoichiometry: investigating the roles of species sorting and local adaptation. *Frontiers in Microbiology* 8 (OCT). <https://doi.org/10.3389/fmicb.2017.02003>.
- Zhang, Y., Chen, H.Y.H., Reich, P.B., 2012. Forest productivity increases with evenness, species richness and trait variation: a global meta-analysis. *Journal of Ecology* 100 (3), 742–749. <https://doi.org/10.1111/j.1365-2745.2011.01944.x>.
- Zhong, D., Listmann, L., Santelia, M.E., Schaum, C.E., 2020. Functional redundancy in natural pico-phytoplankton communities depends on temperature and biogeography. *Biology Letters* 16 (8), 20200330. <https://doi.org/10.1098/rsbl.2020.0330>.

### 3 PUBLICATION II

## 4 Publication III

The experimental implications of the rate of temperature change and timing of nutrient availability on growth and stoichiometry of a natural marine phytoplankton community

Published in *Limnology and Oceanography* (2024)





# The experimental implications of the rate of temperature change and timing of nutrient availability on growth and stoichiometry of a natural marine phytoplankton community

Anika Happe <sup>1,\*</sup> Antonia Ahme <sup>2</sup> Marco J. Cabrerizo <sup>3,4</sup> Miriam Gerhard <sup>5</sup> Uwe John <sup>2,6</sup>  
Maren Striebel <sup>1</sup>

<sup>1</sup>Institute for Chemistry and Biology of the Marine Environment (ICBM), University of Oldenburg, Wilhelmshaven, Germany

<sup>2</sup>Alfred Wegener Institute, Helmholtz Centre for Polar and Marine Research, Bremerhaven, Germany

<sup>3</sup>Department of Ecology, University of Granada, Granada, Spain

<sup>4</sup>Department of Ecology and Animal Biology, University of Vigo, Vigo, Spain

<sup>5</sup>Departamento de Ecología y Gestión Ambiental, Centro Universitario Regional del Este, Universidad de la República, Maldonado, Uruguay

<sup>6</sup>Helmholtz Institute for Functional Marine Biodiversity at the University of Oldenburg (HIFMB), Oldenburg, Germany

## Abstract

Climate change increases the need to understand the effect of predicted future temperature and nutrient scenarios on marine phytoplankton. However, experimental studies addressing the effects of both drivers use a variety of design approaches regarding their temperature change rate and nutrient supply regimes. This study combines a systematic literature map to identify the existing bias in the experimental design of studies evaluating the phytoplankton response to temperature change, with a laboratory experiment. The experiment was designed to quantify how different temperature levels (6°C, 12°C, and 18°C), temperature regimes (abrupt vs. gradual increase), timings of nutrient addition (before or after the temperature change) and nutrient regimes (limiting vs. balanced) alter the growth and stoichiometry of a natural marine phytoplankton community. The systematic map revealed three key biases in marine global change experiments: (1) 66% of the studies do not explicitly describe the experimental temperature change or nutrient regime, (2) 84% applied an abrupt temperature exposure, and (3) only 15% experimentally manipulated the nutrient regime. Our experiment demonstrated that the identified biases in experimental design toward abrupt temperature exposure induced a short-term growth overshoot compared to gradually increasing temperatures. Additionally, the timing of nutrient availability strongly modulated the direction of the temperature effect and strength of growth enhancement along balanced N : P supply ratios. Our study stresses that the rate of temperature change, the timing of nutrient addition and the N : P supply ratio should be considered in experimental planning to produce ecologically relevant results as different setups lead to contrasting directions of outcome.

\*Correspondence: [anika.happe@uni-oldenburg.de](mailto:anika.happe@uni-oldenburg.de)

Additional Supporting Information may be found in the online version of this article.

This is an open access article under the terms of the [Creative Commons Attribution](#) License, which permits use, distribution and reproduction in any medium, provided the original work is properly cited.

**Author Contribution Statement:** AH: Conceptualization (equal); Formal analysis (lead); Investigation (lead); Methodology (equal); Visualization (lead); Writing—original draft. AA: Formal analysis (supporting); Investigation (supporting); Validation, visualization (supporting); Writing—review and editing (equal). MJC: Funding acquisition; Investigation (supporting); Writing—review and editing (equal). MG: Conceptualization (equal); Methodology (equal); Writing—review and editing (equal). UJ: Funding acquisition; Resources; Writing—review and editing (equal). MS: Conceptualization (equal); Funding acquisition; Methodology (equal); Project administration; Supervision; Writing—review and editing (equal)

Increasing temperature and changes in nutrient regimes are among the most prevalent abiotic pressures of the last decades (Malone and Newton 2020; IPCC 2023). Both drivers exert a strong impact on phytoplankton growth (Thomas et al. 2017; Anderson et al. 2022) and stoichiometry (De Senerpont-Domis et al. 2014; Yvon-Durocher et al. 2017), which subsequently alter the nutritional quality and quantity for higher trophic levels (Sterner and Elser 2002; Hessen et al. 2013) and the carbon export out of the pelagic zone (Kwiatkowski et al. 2018). Future scenarios predict various possible combinations of temperature and nutrient availability, for example, that rising water temperatures increase stratification and thus reduce nutrient transport to surface waters (Steinacher et al. 2010), or that terrestrial run-off increases the nutrient input in coastal waters (Rabalais et al. 2009). These different scenarios stress the need to cover an extensive range of possible combinations



and underline the importance of gradient experiments, including extreme treatment levels (Collins et al. 2022). Moreover, the effects of temperature and nutrients on phytoplankton are often investigated independently (e.g., Pálffy et al. 2021; Soulié et al. 2022) or by using single species in laboratory experiments (e.g., Boyd et al. 2015; Bestion et al. 2018). However, to gain a comprehensive understanding of direct and indirect effects via species interactions (Boyd et al. 2018) and to draw conclusions on the ecosystem level, we need studies quantifying such responses at the community level.

Experimental studies have shown that the thermal dependence of phytoplankton metabolism accentuates with increasing nutrient concentration (and vice versa) (Thrane et al. 2017; Marañón et al. 2018), whereby nutrient availability changes the height and curvature of the thermal performance curve (Thomas et al. 2017). The combined effects of temperature and nutrients on the community level are expected to be more complex than patterns on single species level as phytoplankton taxa exhibit trade-offs in their ability to use resources and to outperform other taxa along their species-specific performance curves (Litchman and Klausmeier 2008). For a marine spring bloom community exposed to three temperatures and two different nutrient concentrations, Anderson et al. (2022) found higher temperatures (+3.4°C compared to ambient) to be beneficial for community growth rates under nutrient-replete conditions, but antagonistic under nutrient limitation. Applying a wide range of nutrient concentrations and ratios, Gerhard et al. (2019) found the temperature  $\times$  nutrient interaction effect on the growth rate of a freshwater community to be strongest under balanced N : P supply ratios (i.e., around the Redfield ratio) compared to extremely sub-optimal N : P supply ratios (N or P limitation). Additionally, under a balanced N : P supply ratio, nutrient concentration only slightly affected the sensitivity to temperature fluctuations (Gerhard et al. 2019). A recent analysis of long-term data showed that the North Sea is experiencing rising N : P supply ratios, potentially entailing an increasingly prevalent phosphorus limitation (Burson et al. 2016; Rönn et al. 2023) making the investigation of the interactive effects of nutrient conditions and temperature changes even more relevant in this system.

Considering phytoplankton stoichiometry (i.e., particulate N : P ratio), the *temperature-dependent physiology* hypothesis implies increasing particulate N : P ratios with higher temperatures due to a lower requirement for phosphorus-rich ribosomes relative to nitrogen-rich proteins to maintain an organism's performance (Woods et al. 2003). However, as phytoplankton taxa differ in their macronutrient requirements (Edwards et al. 2012) altering relative N and P supply may also reshape the phytoplankton community (Tilman et al. 1982). Although the phytoplankton community response to temperature increase (Striebel et al. 2016) and levels of nitrogen and phosphorus (Frost et al. 2023) was shown to be highly context-dependent, temperature change studies comprise very

heterogeneous approaches regarding their choice of experimental design.

To identify how temperature experiments with marine phytoplankton communities are designed, a systematic literature search has been conducted (see Methods; Supporting Information S1; Figs. S2.1, S2.2). It generally showed that an increase in temperature is performed either gradually (9 of 86 studies) with an applied rate of temperature change between 0.75°C d<sup>-1</sup> (Paul et al. 2021) and 2.5°C d<sup>-1</sup> (Soulié et al. 2023), but more often as an abrupt temperature exposure (72/86 studies), that is, directly placing the community on the experimental temperature below or above ambient conditions (e.g., Sommer and Lewandowska 2011; Moreau et al. 2014; Menden-Deuer et al. 2018). Even among the studies applying an abrupt temperature exposure, only half of the studies explicitly address this in the methods section (36/72), often it is not clearly stated but to be assumed from the experimental design (36/72). The abruptly applied temperature increases which were not defined as heat shock experiments were most often set to +3°C, +4°C, or +6°C, but also up to a temperature of +11.8°C compared to ambient conditions (Supporting Information Fig. S2.2). Furthermore, the literature search did not identify any study that tested the effect of different rates of temperature increase for a natural marine phytoplankton community. To our knowledge, this has only been tested for single species. In these studies, it was shown that populations abruptly exposed to temperatures above their acclimated condition achieved significantly higher growth rates than the population acclimated to this respective temperature (Kremer et al. 2018; Fey et al. 2021). This is referred to as gradual plasticity and describes phenotypic changes happening at a slower pace than the initiating environmental changes (Kremer et al. 2018). However, thermal acclimation can re-adjust the physiological processes that lead to the growth overshoot in monocultures in response to abrupt temperature exposure (Rehder et al. 2023).

Regarding the nutrient conditions during temperature change, the systematic literature map revealed that most studies use the ambient nutrient regime (46/86), but nutrient-enriched conditions are also common (19/86) to stimulate phytoplankton growth (Supporting Information Fig. S2.1). Few studies applied ambient-adapted nutrient conditions (6/86) which compensate for unusually low ambient concentrations of phosphorus or nitrogen at sampling time (Engel et al. 2011) or to achieve better comparability to a reference year or experiment (Sommer et al. 2007). Some studies (13/86) include at least two nutrient levels (also including studies using enriched treatments but with an ambient control), and only one of these also manipulated N : P supply ratios based on extended Representative Concentration Pathways scenarios (Moreno et al. 2022).

Overall, we lack studies testing if the species level response to different temperature change rates translates into natural communities or whether compensatory community dynamics may balance or outweigh the growth overshoot. Recently, it has also been shown that the temporal pattern of multiple

abiotic stressor occurrences (e.g., whether they are applied sequentially or simultaneously) defines the magnitude and direction of the combined effect, highlighting the importance but lack of consideration of timing in multi-stressor experiments (Gunderson et al. 2016; Brooks and Crowe 2019). More information is needed to compare temperature effects and their trade-offs between experimental designs in global change research and point toward the implications of choosing a certain rate of experimental temperature change, the nutrient regime, and timing of nutrient addition.

To fill the knowledge gaps outlined above, we experimentally addressed how the growth and stoichiometric responses were not only altered by the temperature level, but also their rate of temperature increase and the timing of nutrient addition. A microcosm study was conducted by exposing a natural phytoplankton spring community off the German coast at the Helgoland roads permanent sampling site to a nitrogen to phosphorus ratio gradient (from severe limitation to balanced ratios) across three temperature levels applied with either a gradual or abrupt temperature increase, and with nutrient addition during or after the temperature change (Fig. 1). Two consecutive microcosm experiments allowed for explicitly testing the following hypotheses:

(H1) The phytoplankton community growth rate and particulate N : P ratio depend on the rate of temperature change (abrupt vs. gradual) in interaction with nutrient supply ratios: precisely, (H1a) the growth performance of the abrupt exposure treatments is expected to show an overshoot compared to the gradually increasing temperature treatments (based on Anderson et al. 2022), with larger differences at higher temperatures (until the thermal optimum) under balanced nutrient conditions. (H1b) Limiting nutrient conditions lead to reduced growth rates which is strengthened at higher temperature levels (Thomas et al. 2017), and further decreased by abrupt temperature exposure.

By comparing the performance of communities that received the nutrient addition before vs. after the temperature increase, it is possible to disentangle whether (H2) the phytoplankton community growth rate and particulate N : P ratio depend on the timing of nutrient addition in interaction with the supplied nutrient ratios: Specifically, (H2a) when previously acclimated to an elevated temperature under ambient nutrient conditions, a nutrient addition after the temperature increase is expected to result in lower community growth rates and particulate N : P ratios compared to a community receiving the same nutrient additions before temperature increase. (H2b) This effect may also be strengthened under unbalanced or limiting nutrient conditions, as the community already used all remaining nutrients during thermal acclimation and drives into complete limitation.

## Methods

### Systematic literature map

A systematic literature search was performed, using the ISI Web of Knowledge as a search engine, to identify how experimental studies that investigate natural marine phytoplankton communities apply experimental temperature change treatments. The search and analysis followed the guideline of Preferred Reporting Item for Systematic Reviews and Meta-analysis in Ecology and Evolutionary biology (O'Dea et al. 2021) and matched 486 studies from which 83 papers and thus, 86 experimental designs remained after screening the full-texts. See Supporting Information S1 for details on the search string, inclusion criteria, categorization, the flow-chart of report screening, and a PRISMA-EcoEvo checklist. For extracting the information from the full-texts, only the method section and referred Supporting Information of each paper were considered.

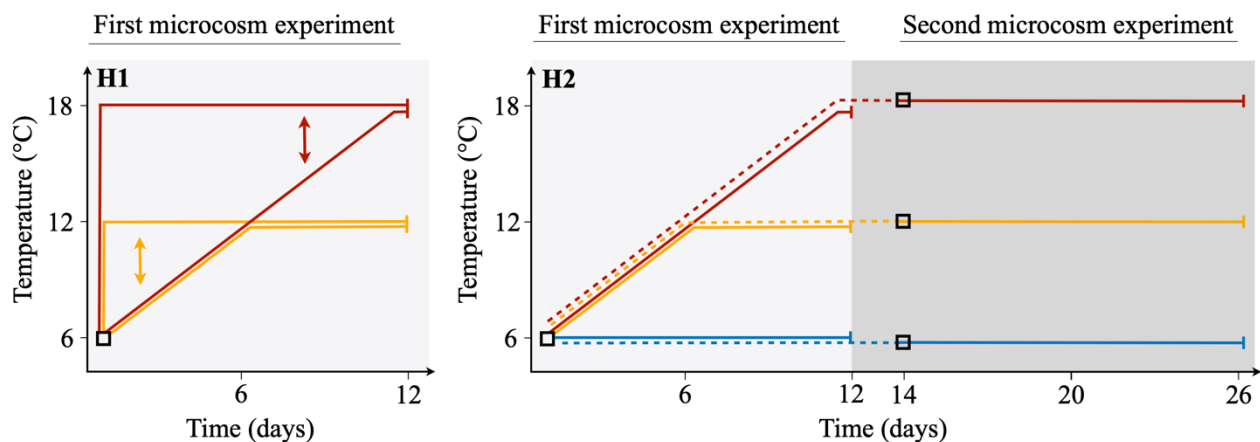


**Fig. 1.** Conceptual overview of experimental temperature treatments applied for testing the hypotheses (H1, H2). The line colors represent the final temperatures at 6 (blue), 12 (orange), and 18°C (red). For H1, an abrupt temperature exposure and a gradual temperature increase were applied. The black square represents the time point of nutrient addition to the microcosms. For H2, the dashed line indicates the thermal acclimation phase (under ambient nutrients) in indoor mesocosms before starting the microcosm experiment.

### Experimental design

The initial plankton community originated from surface seawater at a depth of 5 m collected off the coast of Helgoland Roads long-term time series site in the German part of the North Sea (54°11, 3'N, 7°54, 0'E) on 06 March 2022 at 05:00 h (UTC) using a diaphragm pump and filtered through a 200- $\mu$ m mesh to reduce mesozooplankton. The water was transported using eight 1000-liter polyethylene Intermediate Bulk Containers (IBC, AUER Packaging GmbH) onboard the German RV *Heincke*. A temperature of 5.4°C and a salinity of 30.7 PSU were recorded for the collection time and location. The phytoplankton community showed an initial concentration of  $0.44 \pm 0.13 \mu\text{g chlorophyll } a \text{ L}^{-1}$ .

The collected seawater was used to set up a mesocosm experiment in 600-liter stainless-steel tanks (analyzed in Ahme et al. 2024) and simultaneously run bottle incubations (microcosms) on the March 8, 2022. The effect of two gradual temperature increase scenarios (12°C and 18°C in steps of 1°C d<sup>-1</sup>) and an ambient temperature control (6°C) on phytoplankton functional responses was tested in the Planktotrons indoor mesocosm facility (Gall et al. 2017). In addition, two consecutive microcosm experiments using 160 mL cell culture bottles (SARSTEDT AG & Co. KG) with ventilated caps were conducted. The mesocosms and microcosms experienced identical light conditions set to 175  $\mu\text{mol photons s}^{-1} \text{ m}^{-2}$  from LED units (IT2040, Evergrow) and a day–night cycle of 12 h : 12 h chosen according to field conditions during that time of the year.

The first microcosm experiment started at the beginning of the mesocosm experiment using the initial phytoplankton community. In addition to the control (6°C), these microcosms were exposed to two temperature levels (12°C and 18°C) either as an abrupt exposure or as a gradual increase (1°C d<sup>-1</sup>) and supplied with a wide gradient of N : P supply ratios (Table 1) as a unique pulse at the start of the incubation.

The communities used in the second microcosm experiment acclimated to their experimental temperature under ambient nutrient conditions in the mesocosms. The water for setting up the microcosm experiments was pooled across the four replicated mesocosms after the 18°C temperature ramp was completed (Fig. 1). The acclimated phytoplankton communities were placed at the respective constant experimental temperatures which they originated from (6°C, 12°C, and 18°C). The communities were supplied with the same nutrient matrix as a unique pulse at the start of the microcosm incubation. Accordingly, these microcosms started the incubation with different community compositions due to temperature-dependent species sorting during the acclimation phase, while the community dynamics in the first experiment were simultaneously temperature- and nutrient-dependent. In total, both microcosm experiments ran in duplicated and summed up to 400 units (8 temperature change scenarios  $\times$  5 N levels  $\times$  5 P levels  $\times$  2 replicates). Both microcosm experiments were terminated after 12 d.

**Table 1.** Matrix of phosphorus (P) and nitrogen (N) concentrations and the resulting dissolved N : P ratios including the background concentration and the applied nutrient additions at the start of the first microcosm experiment. The ambient concentration (background concentration) refers to the lowest experimental level and is displayed in bold.

N ( $\mu\text{mol L}^{-1}$ )	P ( $\mu\text{mol L}^{-1}$ )				
	0.31	1.68	2.30	3.00	3.64
<b>18.07</b>	58	11	8	6	5
40.77	131	24	18	14	11
51.17	165	30	22	17	14
61.37	198	36	26	20	17
70.77	228	42	31	24	19

The nutrient treatments of both microcosm experiments were achieved by using five N and five P levels (similar to Gerhardt et al. 2019) creating a wide gradient of N : P molar supply ratios (Table 1). The addition of N ( $\text{NaNO}_3$ ) and P ( $\text{NaH}_2\text{PO}_4$ ) to the seawater was conducted as a unique pulse at the start of the respective microcosm experiment. Ultimately, the final nutrient supply (total dissolved nutrients) consisted of the concentration in seawater plus the added nutrients and ranged from 18.07 to 70.77  $\mu\text{mol N L}^{-1}$  and 0.31 to 3.64  $\mu\text{mol P L}^{-1}$ . The background concentration of dissolved nutrients was measured from the water samples before filling the bottles at the beginning of each microcosm experiment using a continuous flow auto-analyzer (Euro EA 3000; HEKAtech GmbH). The ambient nutrient conditions were 0.31  $\mu\text{mol P L}^{-1}$  and 18.07  $\mu\text{mol N L}^{-1}$  for the first microcosm experiment (Table 1), but differed between the temperature levels at 6°C (0.21  $\mu\text{mol P L}^{-1}$ , 16.78  $\mu\text{mol N L}^{-1}$ ), 12°C (0.20  $\mu\text{mol P L}^{-1}$ , 11.48  $\mu\text{mol N L}^{-1}$ ) and 18°C (0.20  $\mu\text{mol P L}^{-1}$ , 18.58  $\mu\text{mol N L}^{-1}$ ) at the start of the second microcosm run. In the following, a balanced nutrient supply refers to both N and P being equally abundant or equally rare (Cardinale et al. 2009) corresponding to an N : P supply ratio of  $\sim 16 : 1$  (Redfield 1958). Continuous data loggers (HOBO Pendant, Onset) monitored the temperature conditions during the experiment.

Every other day, 1 mL sample from each homogenized experimental unit was pipetted into a 48-well microplate (SARSTEDT AG & Co. KG) to measure in vivo autofluorescence of chlorophyll *a* (395/680 Ex./Em.) as a proxy for biomass using a SYNERGY H1 microplate reader (BioTek®). After 12 d, the experiments were terminated and one replicate was filtered onto precombusted acid-washed glass microfiber filters (Whatman® GF/C) to quantify their respective particulate carbon, nitrogen, and phosphorus content. This has also been done for the respective starting communities.

Filters for particulate organic carbon (POC) and nitrogen (PON) were dried at 60°C and measured using an elemental

auto-analyzer (Flash EA 1112, Thermo Scientific). The filters for particulate organic phosphorus (POP) were precombusted and analyzed by molybdate reaction after peroxydisulfate digestion (Wetzel and Likens 2003). The N : P ratio was calculated as the ratio between the molar masses of PON and POP.

The phytoplankton community composition throughout the mesocosm experiment and thus, the respective starting communities of the microcosm experiment (Supporting Information Fig. S2.3), were analyzed via V4 region of the 18S rRNA gene metabarcoding and is discussed in detail in Ahme et al. (2024). The thermal performance curve (TPC) of the start community showed a thermal optimum at 18°C (corresponding to the highest experimental temperature) and positive effect sizes of temperature on community growth were found between 7°C and 29°C (for details, see Ahme et al. 2024; Supporting Information Fig. S2.4).

### Statistical analyses

Linear growth rates  $\mu$  ( $\text{d}^{-1}$ ) were calculated manually as the slope of a linear regression based as  $(\ln(N_{t1}) - \ln(N_{t0})) / (t1 - t0)$ , with  $N$  as the autofluorescence at the chosen start ( $t0$ ) and endpoint ( $t1$ ) of the first experiment. The two points have been chosen as the exponential growth phase, that is, the time interval between the end of the lag phase and before the biomass of the first samples within a temperature treatment reached the decay phase (see times series; Supporting Information Figs. S2.5–S2.10). The majority of units that were gradually increased to 18°C went into their decay phase before reaching their final temperature (Supporting Information Fig. S2.6). This resulted in a calculation between days 2 and 8 for the abrupt temperature exposure treatments and control in the first experiment, between days 4 and 10 for the gradual temperature increase in the first experiment, and days 2–6 for the second experiment.

To test for the effect of the rate of temperature change on the response of phytoplankton growth and particulate N : P ratios to temperature and nutrient supply, log-response ratios (LRRt) were calculated as  $\log_{10}(\mu_1/\mu_2)$ , with  $\mu_1$  as the mean growth rate of the abrupt temperature exposure treatment, and  $\mu_2$  as the mean growth of the gradually increasing temperature treatments for each temperature. To test for the effect of timing of nutrient addition relative to temperature change, LRRn were calculated as  $\log_{10}(\mu_1/\mu_2)$ , with  $\mu_1$  as the mean community growth rate when nutrients were added during the gradual temperature change (experiment 1) and  $\mu_2$  as the mean community growth rate when nutrients were added after the gradual acclimation (experiment 2) to test for the effect of nutrient availability during temperature change.

For all following analyses, the applied nutrient ratios were categorized into nitrogen-limited (final N : P ratio  $\leq 11$ ), balanced (12–39), or phosphorus-limited ( $> 40$ ) nutrient conditions. This is based on Gerhard et al. (2019) who showed that the optimum N : P supply for a phytoplankton community

ranges between 13 and 40. This does not imply that all ratios in the assigned category were indeed limiting. For the statistical analyses of H1, generalized linear models (GLM) on the gradual and abrupt temperature increase treatments (12°C and 18°C) of the first experiment have been performed ( $\mu$ , particulate N : P ratio  $\sim$  temperature level \* N : P supply ratio \* rate of temperature change; and LRRt  $\sim$  N : P supply ratio \* temperature level). For the statistical analyses of H2, generalized linear models ( $\mu$ , particulate N : P ratio  $\sim$  temperature level \* N : P supply ratio \* nutrient availability during temperature change; and LRRn  $\sim$  temperature level \* N : P supply ratio) were conducted. Due to a right-shifted distribution of the growth data, a box-cox transformation with an exponent of three was used. The GLM for the particulate N : P ratio was run with log-transformed data. All GLMs were post-evaluated with a Tukey High Significant Differences post hoc test (Supporting Information Tables S2.1–S2.5).

All statistical results were interpreted as significant for a significance level of  $\alpha = 0.05$  and were performed using the R statistical environmental version 4.2.3 (R Core Team 2023). All plots were created using the “ggplot2” package (Wickham 2016).

## Results

### The type of temperature increase

Whether the temperature change has been experienced as an abrupt exposure or a gradual increase showed a significant main effect on community  $\mu$  (Table 2). An abrupt temperature exposure significantly increased overall  $\mu$  at 12°C (by 9%) and 18°C (by 11%) compared to a gradual temperature change (Fig. 2; Supporting Information Fig. S2.11). Additionally, phosphorus-limited growth conditions significantly decreased community  $\mu$  compared to both other nutrient conditions (Fig. 3; Supporting Information Table S2.1). When nutrients are limiting, especially in the gradual temperature increase treatments, community  $\mu$  is less dependent on temperature compared to balanced nutrient conditions (i.e., similar  $\mu$  over a 12°C thermal breadth) (Fig. 3). Although, no significant effect of the rate of temperature change on particulate N : P ratios has been found, significant differences between the three nutrient supply scenarios (N- or P-limited and balanced) were observed in which the N-limited nutrient conditions led to the lowest particulate N : P ratios, whereas P-limited conditions generated the highest particulate N : P ratios, mirroring the supplied ratios (Supporting Information Fig. S2.12; Table 2; Supporting Information Table S2.2). The LRRt was not significantly affected by temperature or nutrient conditions. Therefore, the general growth performance was affected by the rate of temperature change regardless of the final temperature level and nutrient conditions. Furthermore, no interactive effects of the rate of temperature change with the nutrient supply ratio or temperature level have been found for any response variable.



**Table 2.** GLMs of the rate of temperature change (rate), nitrogen to phosphorus (N : P) supply ratios (N-limited, P-limited, balanced), and temperature (T) on phytoplankton community growth rate ( $\mu$ ), particulate N : P ratios and log-response ratio between the abrupt and gradual temperature change treatment (LRRt).

Effect	df	$\mu$		LRRt		N : P ratio	
		F	P	F	P	F	P
T	1	0.22	0.638	0.18	0.676	1.78	0.186
Ratio	1	50.85	<0.001*	1.36	0.268	74.00	<0.001*
Rate	1	28.49	<0.001*	—	—	2.53	0.115
T * Ratio	1	0.69	0.501	—	—	1.05	0.355
T * Rate	1	0.01	0.937	1.08	0.348	2.09	0.152
Ratio * Rate	1	0.55	0.577	—	—	0.59	0.585
T * Ratio * Rate	1	0.30	0.742	—	—	0.41	0.663

### The timing of nutrient addition

The timing of nutrient availability showed significant main effects on community  $\mu$  and particulate N : P ratios as well as complex interactive patterns (Table 3). Adding nutrients before temperature change led to an overall positive effect on community  $\mu$  at 12°C and 18°C compared to 6°C, while adding nutrients after the temperature change reversed this effect (Fig. 2; Supporting Information Fig. S.2.11). This reversal was displayed in highest overall  $\mu$  at 6°C when P was limiting after the temperature acclimation (Fig. 2). The reversed temperature effect was accentuated at balanced N : P supply ratios in the lowest temperature treatment reflecting the significant three-way interaction between the timing of nutrient

addition, temperature level, and nutrient supply ratio (Table 2). Moreover, the LRRn showed that the effect size was significantly shaped by the interaction of temperature level and nutrient supply ratio as well as both main effects (Table 2), with positive overall effects of the availability of nutrients during temperature change in the warming treatments compared to ambient temperature, and a pronounced negative effect under balanced nutrient supply under ambient temperature. Furthermore, it is evident from the measured background concentrations of dissolved phosphorus at the respective start conditions (0.31  $\mu\text{mol L}^{-1}$  in the first experiment and 0.21  $\mu\text{mol L}^{-1}$  in the second experiment) and the growth response of the treatments without nutrient

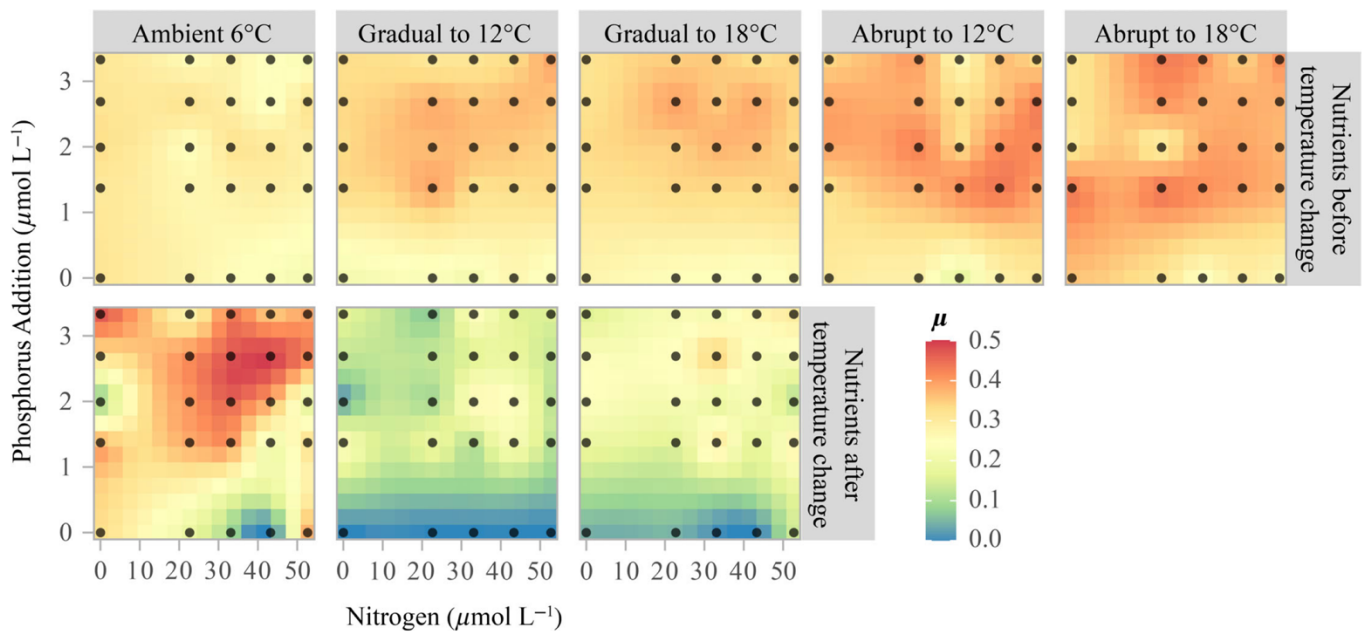


**Fig. 2.** Interpolated response surfaces of the growth rate ( $\mu$ ) over nitrogen and phosphorus supply ( $\mu\text{mol L}^{-1}$ ). All values below 0 have been set equal to 0. The points mark the tested experimental conditions. The rows represent the first experiment with nutrients added during the temperature change (upper) or the second experimental phase with nutrient additions after the temperature change (lower).

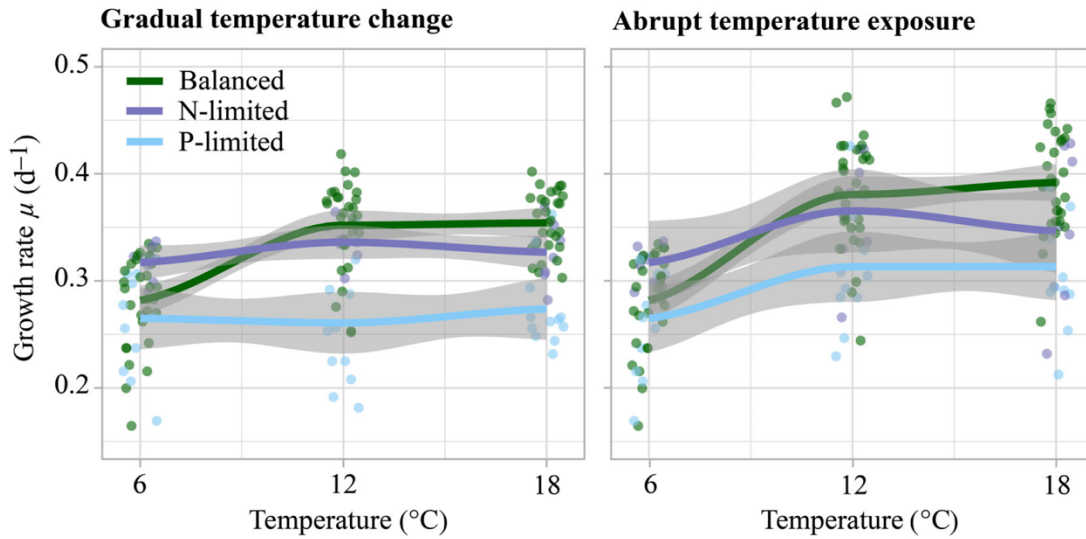


**Fig. 3.** Growth rate ( $\text{d}^{-1}$ ) of the phytoplankton community across experimental temperatures. Colors indicate the applied nutrient conditions. Each point represents an individual observation. The gray areas show smoothed conditional means with a sensitivity of 0.8 and a GAM fit.

addition within the nutrient supply matrix that the P-limitation strengthened during the course of the thermal acclimation.

Additionally, the acclimation under ambient nutrients (i.e., nutrients added after warming) led to lower particulate N : P ratios compared to communities with access to nutrients during temperature change, and thus an increasing divergence occurred between the treatments until an N : P supply ratio of  $\sim 40$  (Fig. 4). Beyond this threshold which also marks the P-limited scenario, the P-limitation led to a temperature-dependent increase in particulate N : P ratios. This increase was strongest at  $18^\circ\text{C}$ , whereby the communities that acclimated to temperature under nutrient depletion reached particulate N : P ratios 1.5-fold higher than communities with nutrients available during temperature change (Fig. 4). This reflects the highly significant three-way interactive effect of

timing of nutrient availability, temperature level, and ratio of supply nutrients (Table 3).

### Discussion

With the type of temperature change and the timing of nutrient availability relative to warming, this study covers two key aspects not considered before when we evaluate the interplay between temperature and nutrient supply in experimental approaches, and how it modulates the growth response and stoichiometry in marine phytoplankton. First, the rate of temperature change influences how phytoplankton respond to warming, that is, abrupt temperature exposure overestimates the phytoplankton growth rates when compared with those obtained under a gradual temperature increase. Second, the timing of nutrient availability (under a balanced N : P

**Table 3.** GLMs of the timing of nutrient availability (NutAv), N : P supply ratios as a categorical variable (N-limited, P-limited, balanced), and temperature (T) on phytoplankton community growth rate ( $\mu$ ), particulate N : P ratios and the log-response ratio between treatments with nutrients added during versus after the temperature change (LRRn).

Effect	df	$\mu$		LRRn		N : P ratio	
		F	P	F	P	F	P
T	2	36.30	<0.001*	115.92	<0.001*	2.34	0.101
Ratio	1	65.95	<0.001*	25.03	<0.001*	137.16	<0.001*
NutAv	1	93.54	<0.001*	—	—	38.27	<0.001*
T * Ratio	4	1.60	0.175	5.84	0.212	6.54	<0.001*
T * NutAv	2	90.25	<0.001*	—	—	0.01	0.988
Ratio * NutAv	1	13.81	0.005*	—	—	7.75	<0.001*
T * Ratio * NutAv	2	2.58	0.037*	—	—	6.75	<0.001*

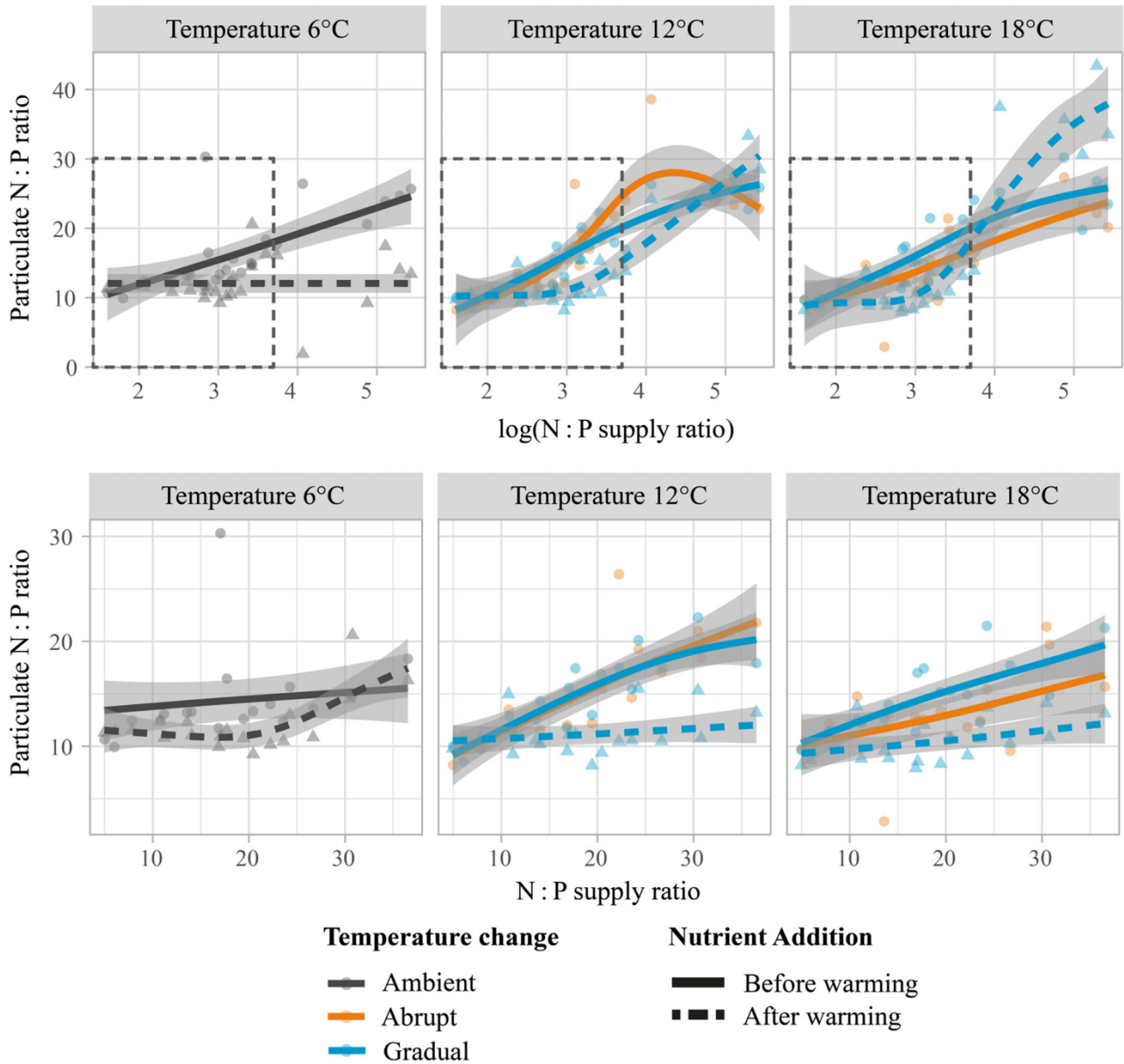


**Fig. 4.** Phytoplankton final particulate N : P ratios across N : P supply ratios (including background concentration) and experimental temperatures. The upper panels include all treatments on a logarithmic scale (to visualize the effects of very high N : P supply ratios), the lower panels focus on the low to intermediate N : P supply ratios ( $\leq 42$ ) by excluding the lowest phosphorus level. The rectangle in the upper panels represents the area shown in the lower panels. A GAM smoothing has been applied. The color indicates an abrupt (red) or gradual (blue) temperature change. The line type and shape of points represent ambient nutrient conditions during temperature change (dashed line and triangles) or nutrient additions before temperature change (solid line and circles).

supply) determines the magnitude and direction of the effects of temperature change on phytoplankton. On the one hand, some of the found patterns (e.g., the growth overshoot under abrupt temperature exposure) are in accordance with findings in monoculture studies (e.g., Kremer et al. 2018; Fey et al. 2021). Still, on the other hand, natural communities show more complex patterns and interactive effects with the

rate of temperature change and timing of nutrient availability driving their biological adjustments.

#### Abrupt vs. gradual temperature increase

Phytoplankton community growth rates generally increased with warming although depending on the rate of temperature change by overshooting in the abruptly exposed

temperature treatments compared to the gradual temperature increase treatments. The natural phytoplankton spring community used in our experiments was sampled at 5.4°C ambient temperature which is close to the identified thermal minimum in the community TPC. This suggests a community at the initiation of its spring bloom as thermal limitation was slowly alleviated in the field. With the thermal optimum of the community TPC at 18°C and being exposed to high temperature variability in the North Sea (Wiltshire and Manly 2004), the studied spring community naturally held a high potential for a positive response to higher temperatures. The broad thermal breadth displayed by the community TPC can potentially be explained by species in the community living below their temperature optimum to avoid detrimental effects of supra-optimal temperatures (Thomas et al. 2012) and/or (summer) species that were already present in low abundance ready to thrive at higher temperatures.

In species-specific studies, a higher performance under abrupt thermal changes in comparison with gradual changes has been attributed to gradual plasticity (Kremer et al. 2018). The growth rates of the community abruptly exposed to higher temperatures exceeded those of the gradually increasing temperature treatments, potentially due to a temporal delay in physiological acclimation such as regulations in respiration rate, photosynthetic machinery, and resource acquisition (Barton et al. 2020; Fey et al. 2021). However, in the long-term, a gradual abiotic change can lead to a higher end-point performance (Collins and de Meaux 2009). Thereby, surviving gradual warming on the species level is determined by acclimation and evolutionary processes, while surviving abruptly temperature exposure is based on resistance mechanisms (Peck et al. 2009). In natural phytoplankton assemblages, interspecific and intraspecific competition and selection can complement mechanisms based on physiological regulations (Bestion et al. 2018). For intraspecific population dynamics, sudden environmental changes may lead to the streamlining of a few well-adapted genotypes while gradual changes maintain higher genetic variability, thus buffering against additional perturbations (Hughes and Stachowicz 2004). Regarding interspecific competition, species that are more temperature-tolerant to high temperatures have a competitive advantage under abruptly temperature exposure that potentially results in an abrupt dominance shift toward more thermally resilient species. Contrarily, a gradual temperature increase provides more time for physiological adjustments within different species (Fey et al. 2021) alongside interspecific competitive interactions and with this reduces abrupt shifts in community composition and increases a potential proliferation of species with a more sustainable resource use. Overall, an abrupt temperature exposure may be predominantly driven by the species' physiological limits (Stefanidou et al. 2018) whereas, during a gradual change, competitive interactions gain importance.

Although we confirmed a short-term growth overshoot at both abruptly exposed temperature levels (in line with our

hypothesis H1), the difference in growth rate between the gradual and abrupt temperature exposures did not increase with increasing temperature, contradicting our hypothesis H1a. Furthermore, when nutrients were limiting (especially under gradual temperature increase), growth was completely independent of temperature resulting in similar growth rates over a 12°C thermal breadth. This reinforces the idea that nutrient limitation suppresses the thermal dependence of physiological processes which has been explicitly tested for single species (Marañón et al. 2018) and observed for a freshwater community (O'Connor et al. 2009).

Moreover, we found phosphorus-limited nutrient conditions to suppress community growth equally among the gradual temperature treatments (which partly rejects H1b). In line, Anderson et al. (2022) found (gradual) warming to be beneficial for community growth only under nutrient-amended conditions, whereas under nutrient limitation, warming acted as a second stressor and decreased community growth rates compared to those of the initial community. In our study, however, even with the second stressor of phosphorus limitation, abrupt temperature exposure still increased community growth for both higher temperatures compared to ambient temperature, underlining an increased phosphorus use efficiency (*temperature-dependent physiology* hypothesis). Despite lower relative phosphorus requirements with increased temperature, a phosphorus threshold concentration is likely a prerequisite for positive net community growth. Nevertheless, the results of our study suggest that the background concentration of nitrogen was not actually limiting community growth.

When applying a gradual increase in temperature, also the rate of environmental change determines which biological processes are important for the successful performance of an organism (Peck et al. 2009). Even among the studies inducing a gradual temperature increase, experimental warming applied within marine system studies is usually 10,000–100,000 times faster than predicted ocean warming (Peck et al. 2009). This has practical reasons and only this limitation makes laboratory experiments for global change research feasible. However, thermal responses determined by such relatively fast temperature change experiments should be used with care for predicting climate change effects on phytoplankton. Furthermore, it needs to be considered that the exponential growth phase during a gradual temperature increase may not cover the entire warming process and thus, affect the interpretation of calculated growth rates.

Thermal acclimation is a good way to let physiological processes adjust prior to experimental manipulation in monocultures (Rehder et al. 2023). However, acclimation such as the gradual increase in temperature conducted in this experiment changed the taxonomic composition during the acclimation period (i.e., period of gradual increase) (Ahme et al. 2024; Supporting Information Fig. S2.3). Consequently, communities arose with potentially different nutritional requirements, strategies, and limitations that may respond differently to



experimental treatments such as the later addition of nutrients.

#### The timing of nutrient addition: Growth

Our results further demonstrate that the community growth response depended on the timing of nutrient addition, the interaction with the nutrient supply ratio, and additionally the threefold interaction with both and the temperature level (which is in line with our hypothesis H2). The overall increase in phytoplankton community growth rate with warming (up to the optimum temperature) under nutrient-enriched conditions is an often-observed pattern in experimental studies (Bestion et al. 2018; Aranguren-Gassis et al. 2019; Fernández-González et al. 2020) and can be attributed to an increase in metabolic rates with higher temperatures under sufficiently available resources that support growth (Eppley 1972; Raven and Geider 1988). However, when the community was acclimated to its respective experimental temperature under ambient nutrient conditions and received a nutrient addition afterward, the ambient temperature treatment showed the highest growth performance (confirming our hypothesis H2a).

Although significant interactions of nutrient conditions and temperature have been demonstrated for the growth response in species-specific studies (Thomas et al. 2017; Aranguren-Gassis et al. 2019; Fernández-González et al. 2020), a temperature–nutrient interaction was not found in this experiment. This may be explained by the capability of a diverse community to buffer nutrient-dependent responses to temperature as long as minimum phosphorus requirements are covered. This potential minimum threshold was observed in the first experiment showing community growth despite phosphorus limitation, whereas in the second experiment, phosphorus was entirely depleted before the start of the experiment which led to the timing of nutrient availability to reverse the temperature effect. Therein, an increased metabolism could not be sustained under extreme phosphorus limitation and led to a collapse of the community (as predicted in hypothesis H2b). Similarly, Verbeek et al. (2018) found a relatively high phytoplankton community biomass under replete nutrients, but detrimental temperature effects under strengthening oligotrophication, highlighting that with a lack of available nutrients, the increased resource demand to maintain increased physiological processes cannot be satisfied.

#### The timing of nutrient addition: Stoichiometry

The type of nutrient limitation (P or N limitation) determined how the timing of nutrient addition (before vs. after temperature change) affected the particulate N : P ratios (which supports our hypothesis H2). While P-limitation exerted an interactive effect between nutrient supply, temperature level, and timing of nutrient addition, the N-limiting scenario did not show any significant differences in particulate N : P ratios compared to a balanced N : P supply.

In theory, higher temperatures increase the organismal N : P ratios due to a lower requirement in phosphorus-rich ribosomes relative to nitrogen-rich proteins to maintain growth as predicted by the *temperature-dependent physiology* hypothesis (Woods et al. 2003). Although we did not find a temperature main effect on phytoplankton N : P ratios, our study showed a divergence (i.e., increasing difference) in particulate N : P ratios in response to the timing of nutrient addition with increasing N : P supply ratios ( $\leq 40$ ) which was only found for the warming treatments.

The N : P supply ratio around 40 lies within a range shown for a transition into a complete phosphorus limitation (Geider and La Roche 2002). From this transition point onwards, the communities that received nutrients during warming already started to saturate at particulate N : P ratios of  $\sim 25$ , while only the communities that received the nutrient addition after thermal acclimation exceeded the others at 18°C with particulate N : P ratios of up to 40. The particulate ratio of 40 may reach physiological limits leading to a saturation with increasing N : P supply ratios which has also been shown for a freshwater phytoplankton community (Gerhard et al. 2019). In line, Klausmeier et al. (2004) also showed this particulate ratio to be at the upper end of structural N : P ratios of phytoplankton. The differences in phytoplankton community N : P ratios might be explained by two mechanisms: First, different phytoplankton species with specific particulate N : P ratios dominate under the respective experimental condition (Finkel et al. 2009), and second, the particulate N : P ratio of the present species change in response to the experimental condition (stoichiometric plasticity) (Yvon-Durocher et al. 2015). Due to the lack of community composition data at the end of the experiments, we are not able to determine the exact mechanism underpinning the response pattern observed here, however, it is likely that they act together in creating this complex interactive pattern as they are not mutually exclusive.

#### Implications for experimental design

The systematic literature map revealed an overrepresentation of abrupt temperature increase experiments and lack of clear reporting on the rate of temperature increase and experimental nutrient conditions, whereas our experimental results highlighted that an abrupt temperature exposure induces a short-term community growth overshoot compared to gradually increasing temperature, but without effects on the particulate N : P ratio. The addition of nutrients after (vs. before) thermal acclimation leads to a complex reversed temperature effect on growth and a response divergence with increasing N : P supply ratio in particulate N : P ratios.

These findings evidence that the selection of a combination of temperature change rate and timing of nutrient supply in future global change biology studies may not be trivial. If the study is conducted as a batch culture with one unique pulse, the rate of temperature change or even the decision of

whether the nutrients are applied during the acclimation phase (i.e., simultaneously with the temperature change) or at the beginning of the experiment (i.e., after the temperature change) can lead to significantly different outcomes in terms of community growth and stoichiometry.

Gunderson et al. (2016) already reported on the bias in experimental design toward simultaneously applied multiple stressors, rather than a range of different and potentially more realistic temporal patterns, with the consequence of predominantly finding synergistic effects of multiple stressors. In addition, the effects of several stressors were longer-lasting when the time lag between their occurrence was increased (Brooks and Crowe 2019). Therefore, the results of our study emphasize the need for considering the timing in multiple stressor studies (i.e., temperature increase and nutrient limitation level, in our case). Additionally, the results evidence the need for multi-level driver experiments to generate response surfaces that can contribute to the improvement of predictive models (Collins et al. 2022). Often, global change studies only consider two levels for a given driver (i.e., control vs. manipulated), while the results indicate complex interactive patterns when changes in the N : P supply ratio are considered among temperature scenarios.

To summarize, when designing a laboratory or mesocosm experiment aimed at testing the effect of temperature change on natural phytoplankton communities, we propose to carefully consider the rate of temperature change, the timing of nutrient addition and the N : P supply ratio to produce ecologically relevant results. Being aware of the implications of different rates of temperature change as well as nutrient additions and its timing, and clearly stating this and the reason for the decision in the methods section improves the interpretation of results, comparability across studies, and the transfer to natural systems.

### Data availability statement

The data that support the findings of this study are openly available in PANGAEA (<https://doi.org/10.1594/PANGAEA.963753>). The associated R scripts are provided in a public GitHub repository (<https://github.com/AnikaHappe/AQUACOSM2022>).

### References

- Ahme, A., and others. 2024. Warming increases the compositional and functional variability of temperate protist communities. *Sci. Total Environ.* **926**: 171971. doi:10.1016/j.scitotenv.2024.171971
- Anderson, S. I., and others. 2022. The interactive effects of temperature and nutrients on a spring phytoplankton community. *Limnol. Oceanogr.* **67**: 634–645.
- Aranguren-Gassis, M., C. T. Kremer, C. A. Klausmeier, and E. Litchman. 2019. Nitrogen limitation inhibits marine diatom adaptation to high temperatures. *Ecol. Lett.* **22**: 1860–1869.
- Barton, S., and others. 2020. Evolutionary temperature compensation of carbon fixation in marine phytoplankton. *Ecol. Lett.* **23**: 722–733.
- Bestion, E., B. Garcia-Carreras, C. E. Schaum, S. Pawar, and G. Yvon-Durocher. 2018. Metabolic traits predict the effects of warming on phytoplankton competition. *Ecol. Lett.* **21**: 655–664.
- Boyd, P. W., and others. 2015. Physiological responses of a Southern Ocean diatom to complex future ocean conditions. *Nat. Clim. Change* **6**: 207–213.
- Boyd, P. W., and others. 2018. Experimental strategies to assess the biological ramifications of multiple drivers of global ocean change—A review. *Glob. Change Biol.* **24**: 2239–2261.
- Brooks, P. R., and T. P. Crowe. 2019. Combined effects of multiple stressors: New insights into the influence of timing and sequence. *Front. Ecol. Evol.* **7**: 387.
- Burson, A., M. Stomp, L. Akil, C. P. D. Brussaard, and J. Huisman. 2016. Unbalanced reduction of nutrient loads has created an offshore gradient from phosphorus to nitrogen limitation in the North Sea. *Limnol. Oceanogr.* **61**: 869–888.
- Cardinale, B. J., H. Hillebrand, W. S. Harpole, K. Gross, and R. Ptacnik. 2009. Separating the influence of resource “availability” from resource “imbalance” on productivity–diversity relationships. *Ecol. Lett.* **12**: 475–487.
- Collins, S., and J. de Meaux. 2009. Adaptation to different rates of environmental change in *Chlamydomonas*. *Evolution* **63**: 2952–2965.
- Collins, S., H. Whittaker, and M. K. Thomas. 2022. The need for unrealistic experiments in global change biology. *Curr. Opin. Microbiol.* **68**: 102151.
- De Senerpont-Domis, L. N., D. B. Van de Waal, N. R. Helmsing, E. Van Donk, and W. M. Mooji. 2014. Community stoichiometry in a changing world: Combined effects of warming and eutrophication on phytoplankton dynamics. *Ecology* **95**: 1485–1495.
- Edwards, K. F., M. K. Thomas, C. A. Klausmeier, and E. Litchman. 2012. Allometric scaling and taxonomic variation in nutrient utilization traits and maximum growth rate of phytoplankton. *Limnol. Oceanogr.* **57**: 554–566.
- Engel, A., and others. 2011. Effects of sea surface warming on the production and composition of dissolved organic matter during phytoplankton blooms: Results from a mesocosm study. *J. Plankton Res.* **33**: 357–372.
- Eppley, R. W. 1972. Temperature and phytoplankton growth in the sea. *Fish. Bull.* **70**: 1063–1085.
- Fernández-González, C., M. Pérez-Lorenzo, N. Pratt, C. M. Moore, T. S. Bibby, and E. Marañón. 2020. Effects of temperature and nutrient supply on resource allocation, photosynthetic strategy, and metabolic rates of *Synechococcus* sp. *J. Phycol.* **56**: 818–829.

- Fey, S. B., C. T. Kremer, T. J. Layden, and D. A. Vasseur. 2021. Resolving the consequences of gradual phenotypic plasticity for populations in variable environments. *Ecol. Monogr.* **91**: e01478.
- Finkel, Z. V., J. Beardall, K. J. Flynn, A. Quigg, T. A. V. Rees, and J. A. Raven. 2009. Phytoplankton in a changing world: Cell size and elemental stoichiometry. *J. Plankton Res.* **32**: 119–137.
- Frost, P. C., and others. 2023. Interactive effects of nitrogen and phosphorus on growth and stoichiometry of lake phytoplankton. *Limnol. Oceanogr.* **68**: 1172–1184.
- Gall, A., and others. 2017. Planktotrons: A novel indoor mesocosm facility for aquatic biodiversity and food web research. *Limnol. Oceanogr. Methods* **15**: 663–677.
- Geider, R., and J. La Roche. 2002. Redfield revisited: Variability of C:N:P in marine microalgae and its biochemical basis. *Eur. J. Phycol.* **37**: 1–17.
- Gerhard, M., A. M. Koussoroplis, H. Hillebrand, and M. Striebel. 2019. Phytoplankton community responses to temperature fluctuations under different nutrient concentrations and stoichiometry. *Ecology* **100**: e02834.
- Gunderson, A. R., E. J. Armstrong, and J. H. Stillman. 2016. Multiple stressors in a changing world: The need for an improved perspective on physiological responses to the dynamic marine environment. *Annu. Rev. Mar. Sci.* **8**: 357–378.
- Hessen, D. O., J. J. Elser, R. W. Sterner, and J. Urabe. 2013. Ecological stoichiometry: An elementary approach using basic principles. *Limnol. Oceanogr.* **58**: 2219–2236.
- Hughes, A. R., and J. J. Stachowicz. 2004. Genetic diversity enhances the resistance of a seagrass ecosystem to disturbance. *Proc. Nat. Acad. Sci. USA* **101**: 8998–9002.
- IPCC, 2023. Summary for Policymakers, p. 1–34. *In* Core Writing Team, H. Lee and J. Romero [eds.], *Climate Change 2023: Synthesis Report. Contribution of Working Groups I, II and III to the Sixth Assessment Report of the Intergovernmental Panel on Climate Change*. IPCC. doi:10.59327/IPCC/AR6-9789291691647.001
- Klausmeier, C. A., E. Litchman, T. Daufrense, and S. A. Levin. 2004. Optimal nitrogen-to-phosphorus stoichiometry of phytoplankton. *Nature* **429**: 171–174.
- Kremer, C. T., S. B. Fey, A. A. Arellano, and D. A. Vasseur. 2018. Gradual plasticity alters population dynamics in variable environments: Thermal acclimation in the green alga *Chlamydomonas reinhardtii*. *Proc. R. Soc. B. Biol. Sci.* **285**: 20171942.
- Kwiatkowski, L., O. Aumont, L. Bopp, and P. Ciais. 2018. The impact of variable phytoplankton stoichiometry on projections of primary production, food quality, and carbon uptake in the global ocean. *Global Biogeochem. Cycles* **32**: 516–528.
- Litchman, E., and C. A. Klausmeier. 2008. Trait-based community ecology of phytoplankton. *Annu. Rev. Ecol. Evol. Syst.* **39**: 615–639.
- Malone, T. C., and A. Newton. 2020. The globalization of cultural eutrophication in the coastal ocean: Causes and consequences. *Front. Mar. Sci.* **7**: 670.
- Marañón, E., M. Pérez-Lorenzo, P. Cermeño, and B. Mourinho-Carballido. 2018. Nutrient limitation suppresses the temperature dependence of phytoplankton metabolic rates. *ISME J.* **12**: 1836–1845.
- Menden-Deuer, S., C. Lawrence, and G. Franze. 2018. Herbivorous protist growth and grazing rates at in situ and artificially elevated temperatures during an Arctic phytoplankton spring bloom. *PeerJ* **6**: e5264.
- Moreau, S., and others. 2014. Effects of enhanced temperature and ultraviolet B radiation on a natural plankton community of the Beagle Channel (southern Argentina): A mesocosm study. *Aquat. Microb. Ecol.* **72**: 155–173.
- Moreno, H. D., and others. 2022. An integrated multiple driver mesocosm experiment reveals the effect of global change on planktonic food web structure. *Commun. Biol.* **5**: 179.
- O'Connor, M. I., M. F. Piehler, D. M. Leech, A. Anton, and J. F. Bruno. 2009. Warming and resource availability shift food web structure and metabolism. *PLoS Biol.* **7**: e1000178.
- O'Dea, R. E., and others. 2021. Preferred reporting items for systematic reviews and meta-analyses in ecology and evolutionary biology: A PRISMA extension. *Biol. Rev. Camb. Philos. Soc.* **96**: 1695–1722.
- Pálffy, K., A. W. Kovács, V. Kardos, I. Hausz, and G. Boros. 2021. Elevated temperature results in higher compositional variability of pioneer phytoplankton communities in a mesocosm system. *J. Plankton Res.* **43**: 142–155.
- Paul, C., U. Sommer, and B. Matthiessen. 2021. Composition and dominance of edible and inedible phytoplankton predict responses of Baltic Sea summer communities to elevated temperature and CO<sub>2</sub>. *Microorganisms* **9**: 2294.
- Peck, L. S., M. S. Clark, S. A. Morley, A. Massey, and H. Rossetti. 2009. Animal temperature limits and ecological relevance: Effects of size, activity and rates of change. *Funct. Ecol.* **23**: 248–256.
- R Core Team. 2023. R: A language and environment for statistical computing. R Foundation for Statistical Computing, Available from <https://www.R-project.org/>
- Rabalais, N. N., R. E. Turner, R. J. Díaz, and R. D. Justić. 2009. Global change and eutrophication of coastal waters. *ICES J. Mar. Sci.* **66**: 1528–1537.
- Raven, J. A., and R. J. Geider. 1988. Temperature and algal growth. *New Phytol.* **110**: 441–461.
- Redfield, A. C. 1958. The biological control of chemical factors in the environment. *Am. Sci.* **46**: 205–221.
- Rehder, L., B. Rost, and S. D. Rokitta. 2023. Abrupt and acclimation responses to changing temperature elicit divergent physiological effects in the diatom *Phaeodactylum tricornutum*. *New Phytol.* **239**: 1005–1013.

- Rönn, L., and others. 2023. Harmonisation of the phytoplankton assessment in the German and Dutch Wadden Sea. Interreg V A project “Wasserqualität—Waterkwaliteit”—Synthesis report. Report prepared on behalf of NLWKN and Rijkswaterstaat, Oldenburg/Lelystad, 2023.
- Sommer, U., and others. 2007. An indoor mesocosm system to study the effect of climate change on the late winter and spring succession of Baltic Sea phyto- and zooplankton. *Oecologia* **150**: 655–667.
- Sommer, U., and A. Lewandowska. 2011. Climate change and the phytoplankton spring bloom: Warming and overwintering zooplankton have similar effects on phytoplankton. *Glob. Change Biol.* **17**: 154–162.
- Soulié, T., F. Vidussi, S. Mas, and B. Mostajir. 2022. Functional stability of a coastal Mediterranean plankton community during an experimental marine heatwave. *Front. Mar. Sci.* **9**: 831496.
- Soulié, T., F. Vidussi, S. Mas, and B. Mostajir. 2023. Functional and structural responses of plankton communities toward consecutive experimental heatwaves in Mediterranean coastal waters. *Sci. Rep.* **13**: 8050.
- Stefanidou, N., S. Genitsaris, J. Lopez-Bautista, U. Sommer, and M. Moustaka-Gouni. 2018. Effects of heat shock and salinity changes on coastal Mediterranean phytoplankton in a mesocosm experiment. *Mar. Biol.* **165**: 145.
- Steinacher, M., and others. 2010. Projected 21st century decrease in marine productivity: A multi-model analysis. *Biogeosciences* **7**: 979–1005.
- Sterner, R. W., and J. J. Elser. 2002. *Ecological stoichiometry: The biology of elements from molecules to the biosphere*. Princeton Univ. Press.
- Striebel, M., S. Schabhuettl, D. Hodapp, P. Hingsamer, and H. Hillebrand. 2016. Phytoplankton responses to temperature increases are constrained by abiotic conditions and community composition. *Oecologia* **182**: 815–827.
- Thomas, M. K., C. T. Kremer, C. A. Klausmeier, and E. Litchman. 2012. A global pattern of thermal adaptation in marine phytoplankton. *Science* **338**: 1085–1088.
- Thomas, M. K., and others. 2017. Temperature-nutrient interactions exacerbate sensitivity to warming in phytoplankton. *Glob. Change Biol.* **23**: 3269–3280.
- Thrane, J. E., D. O. Hessen, and T. Andersen. 2017. Plasticity in algal stoichiometry: Experimental evidence of a temperature-induced shift in optimal supply N:P ratio. *Limnol. Oceanogr.* **62**: 1346–1354.
- Tilman, D., S. S. Kilham, and P. Kilham. 1982. Phytoplankton community ecology: The role of limiting nutrients. *Annu. Rev. Ecol. Syst.* **13**: 349–372.
- Verbeek, L., A. Gall, H. Hillebrand, and M. Striebel. 2018. Warming and oligotrophication cause shifts in freshwater phytoplankton communities. *Glob. Change Biol.* **24**: 4532–4543.
- Wetzel, R. G., and G. E. Likens. 2003. *Limnological analyses*. Springer-Verlag.
- Wickham, H. 2016. *ggplot2: Elegant graphics for data analysis*. Springer-Verlag.
- Wiltshire, K. H., and B. F. J. Manly. 2004. The warming trend at Helgoland Roads, North Sea: phytoplankton response. *Helgol. Mar. Res.* **58**: 269–273.
- Woods, H. A., and others. 2003. Temperature and the chemical composition of poikilothermic organisms. *Funct. Ecol.* **17**: 237–245.
- Yvon-Durocher, G., M. Dossena, M. Trimmer, G. Woodward, and A. P. Allen. 2015. Temperature and the biogeography of algal stoichiometry. *Glob. Ecol. Biogeogr.* **24**: 562–570.
- Yvon-Durocher, G., C. E. Schaum, and M. Trimmer. 2017. The temperature dependence of phytoplankton stoichiometry: Investigating the roles of species sorting and local adaptation. *Front. Microbiol.* **8**: 2003.

#### Acknowledgments

We thank Jakob Giesler, Nancy Kühne, Simon Kline, Markus Olsson, Ruben Schulte-Hillen and Alexander Sentimenti for support during the accompanying mesocosm experiment. We thank Lutz Ter Hell, Sebastian Neun, Heike Rickels, Matthias Schröder and Lennart-Kilian Wenke for technical support. AQUACOSM-plus (Project No. 871081) is funded by the European Commission EU H2020-INFRAIA. “European Commission” via the Horizon 2020 funding programme from which the EU project “AQUACOSM-plus” was funded and by the Helmholtz Research Programme “Changing Earth, Sustaining our Future” (Theme 6 “Marine and Polar Life” in Subtheme 6.2 “Adaptation of marine life: from genes to ecosystems”) of the Alfred Wegener Institute Helmholtz Centre for Polar and Marine Research, Germany. Marco J. Cabrerizo was supported by a Juan de la Cierva-Incorporación (IJC2019-040850-I) contract and TITAN project (PID2022-136280NA-I00) funded by Spanish Ministry of Science and Innovation (MCIN/AEI/10.13039/501100011033/ and FEDER), by a Captación, Incorporación y Movilidad de Capital Humano de I+D+i contract funded by Junta de Andalucía (POSTDOC-21-00044), and programa de proyectos de investigación para la incorporación de jóvenes doctores a nuevas líneas de investigación at University of Granada (Ref. No. 15). Open Access funding enabled and organized by Projekt DEAL.

#### Conflict of Interest

None declared.

Submitted 08 December 2023

Revised 14 March 2024

Accepted 06 June 2024

Associate editor: Birte Matthiessen

## 5 Publication IV

Nutrient pulse scenarios drive contrasting patterns in the functional stability of freshwater phytoplankton

Published in *Limnology and Oceanography* (2025)





RESEARCH ARTICLE

# Nutrient pulse scenarios drive contrasting patterns in the functional stability of freshwater phytoplankton

Anika Happe <sup>1,\*</sup> Bence Buttyán <sup>2</sup> Bence Gergács <sup>2</sup> Silke Langenheder <sup>3</sup> Stella A. Berger <sup>4</sup>  
Jens C. Nejstgaard <sup>4</sup> Maren Striebel <sup>1</sup>

<sup>1</sup>School of Mathematics and Science, Institute for Chemistry and Biology of the Marine Environment (ICBM), Carl von Ossietzky Universität Oldenburg, Oldenburg, Germany; <sup>2</sup>Faculty of Science, Institute of Biology, Eötvös Loránd University, Budapest, Hungary; <sup>3</sup>Department of Ecology and Genetics/Limnology, Uppsala University, Uppsala, Sweden; <sup>4</sup>Department of Plankton and Microbial Ecology, Leibniz Institute of Freshwater Ecology and Inland Fisheries, Stechlin, Germany

## Abstract

Climate change is increasing the frequency, intensity, and stochasticity of extreme weather events such as heavy rainfall, storm-induced mixing, or prolonged drought periods. This results in more variable regimes of dissolved nutrients and carbon in lakes and induces temporal fluctuations in the resource availability for plankton communities, which can further lead to changes in growth and the cellular ratio of essential elements, such as carbon, nitrogen, and phosphorus. However, the current understanding of the effects of variations in regularity and frequency of precipitation events on both producer and consumer levels is limited by the lack of experimental studies examining processes at multiple trophic levels. In our mesocosm study, we added the same total amount of nitrate, phosphate, and colored dissolved organic matter (cDOM) to each mesocosm at pulses differing in frequency (daily, intermittent, or one extreme addition) and regularity (regular, irregular) over a simulated run-off period followed by a recovery period. Our results showed that phytoplankton biomass fully recovered to control conditions from one extreme nutrient and cDOM pulse, whereas pulses of higher frequency gradually increased the biomass. In terms of stoichiometry, the extreme pulse led to the lowest stability in particulate C : P and N : P ratios. At the zooplankton level, copepod biomass decreased across all nutrient and cDOM additions, but no effects between the treatments were found. Overall, our study demonstrates that phytoplankton stability depends on the regularity and frequency of nutrient additions and differs substantially between biomass and stoichiometry, but the effects may be buffered on zooplankton level.

\*Correspondence: [anika.happe@uni-oldenburg.de](mailto:anika.happe@uni-oldenburg.de)

This is an open access article under the terms of the [Creative Commons Attribution](#) License, which permits use, distribution and reproduction in any medium, provided the original work is properly cited.

**Associate editor:** C. Elisa Schaum

**Data Availability Statement:** The data that support the findings of this study are openly available in PANGAEA (<https://doi.org/10.1594/PANGAEA.968980>). Data on further environmental parameters measured during the experiment can be found in the SITES data portal (<https://data.fieldsites.se/portal/>). The associated R scripts are provided in a public GitHub repository ([https://github.com/AnikaHappe/RunOff\\_Erken\\_2022](https://github.com/AnikaHappe/RunOff_Erken_2022)).

**Special Issue:** Mesocosms: bridging the gap between in-situ and laboratory studies. Edited by: Christopher Cornwall, Christian Pansch-Hattich, Maren Striebel, Jens Nejstgaard and Deputy Editors Julia C. Mullarney, Steeve Comeau, and Elisa Schaum

Climate change is altering precipitation and run-off patterns by increasing the frequency and intensity of rainfall events (IPCC 2023). These stochastic occurrences induce high flushing rates and thus significantly decrease the light availability via colored dissolved organic matter (cDOM) (Roulet and Moore 2006) and modify the input of nutrients from terrestrial runoff into lakes and rivers (Hinton, Schiff, and English 1997; Jeppesen et al. 2009). This increased temporal heterogeneity of available resources and potential alteration of nutrient limitation patterns affect phytoplankton growth dynamics (Paerl et al. 1999) and their C : N : P elemental composition (Frost et al. 2023). Additionally, browning reduces the light availability and suppresses phytoplankton growth (Carpenter et al. 1998) which reflects in a reduced light : nutrient supply ratio yielding low phytoplankton cellular C : P ratios (Sterner et al. 1997; Striebel, Spörl, and Stibor 2008). By



determining the amount of carbon relative to nutrients that is bound into the phytoplankton cells, stoichiometry is an important regulator for primary production, nutrient cycling, and energy transfer through the aquatic food web. Therefore, changes in phytoplankton quantity and nutritional quality (e.g., cellular C : nutrient ratios) can have cascading effects up to the consumer level, potentially leading to producer–consumer mismatches, changes in ecological efficiency or restrictions in growth and survival (Dickman et al. 2008; Diehl et al. 2022).

Experimental studies have shown that phytoplankton growth and stoichiometry are highly influenced by the amount and ratio of available resources (Gerhard et al. 2019), but may also depend on the regularity (i.e., regular vs. irregular pulses) and frequency with which nutrients are introduced into the system. The competitive environment and thus, phytoplankton community composition is altered by fluctuating nutrient input compared to a steady state (Sommer 2003) and between fluctuation frequencies (Lagus et al. 2007). Based on the *intermediate disturbance hypothesis* (Connell 1978), the local species diversity may be maximized at an intermediate frequency of heavy rainfall events, which can also increase the overall productivity of the phytoplankton community due to complementary resource use (Gerhard et al. 2021). In a previous mesocosm experiment, marine plankton communities also showed different functional responses between low frequency nutrient pulses (i.e., once or twice over 19 d) and higher frequency nutrient pulses (i.e., every third day or continuously) (Svensen et al. 2002). While the high-frequency pulses resulted in low particulate organic carbon (POC) and chlorophyll *a* concentrations, low-frequency pulses produced higher values of chlorophyll *a*, POC and sedimentation rates. Moreover, phytoplankton was strongly affected, while zooplankton appeared less impacted by the nutrient pulse frequencies (Svensen et al. 2002). Using an artificial freshwater community, Weisse, Gröschl, and Bergkemper (2016) showed that a heavy rainfall scenario, in this case a temperature reduction and increase in nutrients, induces an increase in the total biomass and autotroph : heterotroph biomass ratio. An increase in the autotroph : heterotroph biomass ratio may suggest enhanced primary production and improved energy transfer efficiency within the food web, potentially leading to higher stability and productivity in lake ecosystems. Their study also supported the finding that nutrients are generally more important than temperature for phytoplankton dynamics in lake ecosystems (Salmaso 2010; Weisse, Gröschl, and Bergkemper 2016). This suggests a primary role of nutrient dynamics in shaping phytoplankton responses in lake ecosystems, a key aspect we explore in our study.

On the consumer level, zooplankton are more homeostatic in their stoichiometry compared to phytoplankton (Sterner and Elser 2002). There are differences in nutritional strategies between the selectively feeding copepods with higher nitrogen

requirements (Cowles, Olson, and Chisholm 1988; Walve and Larsson 1999) and the unselectively feeding cladocerans, which prefer P-rich phytoplankton (Andersen and Hessen 2003; Schatz and McCauley 2007). Additionally, larger grazers like *Daphnia* spp. were shown to attenuate the effects of nutrient fluctuations on freshwater phytoplankton communities likely due to their high clearance rates and consumption of broad algal size ranges (Cottingham and Schindler 2000; Koussoroplis, Kainz, and Striebel 2012). Thus, by regulating phytoplankton biomass, these larger grazers can stabilize community dynamics in the face of varying nutrient levels. In turn, functional and compositional changes in phytoplankton communities in response to alterations in the nutrient regime, and thus nutritional quality as prey, can also affect the performance and reproduction of zooplankton (Sterner and Hessen 1994).

Although heavy rainfall events typically occur over very short durations, their intensity can provoke both immediate and lasting impact on the ecosystem which makes them suitable examples for understanding extreme events in a general sense. The urgency to study extreme events (Jentsch, Kreyling, and Beierkuhnlein 2007) and the findings that the effects of nutrient pulse experiments cascade up the food web due to changes in the quantity and quality of the primary producers (Lagus et al. 2007) were already proposed almost two decades ago. Despite this, we still lack studies testing the effect of heavy rainfall events with different chronologies and frequencies for freshwater systems and especially with a focus on phytoplankton stoichiometry.

Therefore, we conducted a mesocosm experiment in which we manipulated the intensity, regularity, and frequency of nutrient and cDOM pulses applied as small daily pulses, intermittent irregular pulses, or one extreme pulse, but kept the total amount of added nutrients and cDOM constant. The applied treatments mimicked natural precipitation and run-off scenarios for which the amount of nutrient input was extracted from long-term monitoring data available from Lake Erken. We simulated a rainfall period lasting for 20 d, followed by a 17-d recovery period to identify whether the effects persist beyond the simulated rainfall period or experience recovery. To quantify the stoichiometric response in two size fractions, POC, particulate organic nitrogen (PON), and particulate organic phosphorus (POP) were analyzed. This experimental design allows for explicitly testing the following hypotheses: (H1) the stability of phytoplankton stoichiometry differs between run-off scenarios with different chronologies and amplitudes of nutrient and cDOM input. Precisely, we expect the extreme event to show the highest overall ecological vulnerability (OEV, as an integrated stability measure) in phytoplankton stoichiometry with long-lasting effects. (H2) Moreover, we expect the treatment effects on phytoplankton stoichiometry to be transferred to the zooplankton level with differences between the zooplankton groups with differing foraging strategies and nutritional demands.

## Methods

### In situ mesocosm experiment

The mesocosm experiment was conducted at Lake Erken in Sweden (59°50'N, 18°38'E) which is part of the Swedish Infrastructure for Ecosystem Science AquaNet mesocosm and monitoring network (Urrutia-Cordero, Langvall et al. 2021).

Lake Erken is a large mesotrophic to eutrophic lake with a mean depth of 9 m (Urrutia-Cordero, Langvall et al. 2021) and initial concentrations of  $141.64 \mu\text{g L}^{-1}$   $\text{NO}_3\text{-N}$ ,  $1.3 \mu\text{g L}^{-1}$   $\text{PO}_4\text{-P}$ , and  $10.3 \text{ mg L}^{-1}$  DOC. At the beginning of the experiment on July 7, 2022, unfiltered lake water was carefully pumped into 16 polyethylene in situ mesocosms (550 L). Three different nutrient and cDOM pulse scenarios were applied with the same total amount of nitrate, phosphate, and cDOM to each mesocosm with pulses in different frequencies (from one extreme to daily pulses) and chronologies (regular/irregular) over a simulated 20-d run-off period followed by a 17-d recovery period (Fig. 1). The pulses of each treatment summed up to a total addition of  $50 \mu\text{g L}^{-1}$  phosphorus (primarily  $\text{KH}_2\text{PO}_4$ ) and  $500 \mu\text{g L}^{-1}$  nitrogen (primarily  $\text{NaNO}_3$ ) and  $2 \text{ mg L}^{-1}$  cDOM (with additional low concentrations of  $\text{NO}_3\text{-N}$  and  $\text{PO}_4\text{-P}$  from the peat extractions; see Langenheder, Kothawala et al. 2024). The chosen  $\text{NO}_3\text{-N}$  and  $\text{PO}_4\text{-P}$  concentrations approximately correspond to the 95<sup>th</sup> percentile across a 30-yr time series from Lake Erken and represent maximum concentrations observed in the epilimnion during summer stratification. The DOC concentration marks the difference between the 95<sup>th</sup> and 5<sup>th</sup> percentiles measured since the beginning of monitoring in Lake Erken in 2016 (Langenheder, Kothawala et al. 2024). Details about the peat

extraction for the cDOM additions can be found in Kreuter et al. (2024). The treatments included multiple small and regular daily pulses (daily), multiple variable and irregular pulses (intermittent), one extreme pulse (extreme), and a control without additions (control). Each treatment was replicated by 4 which added up to 16 experimental units.

While the present study focuses on the size-fractionated stoichiometry (see below), additional sensor installations monitored the water temperature and dissolved oxygen concentration (oxygen optode 4531 sensor, Aanderaa Data instruments AS, Bergen, Norway) as well as photosynthetic active radiation (Apogee SQ-500 sensor, Apogee Instruments Inc.) in high frequency throughout the mesocosm experiment. Samples for dissolved nutrients were taken every fourth day. Dissolved nitrogen and phosphorus were measured as described in (Langenheder, Bergvall, et al. 2024). Dissolved silicate was measured photometrically after the addition of reagents (hydrochloric acid, ammonium molybdate, disodium ethylenediaminetetraacetic acid, and sodium sulfite) using a microplate plate reader (SYNERGY H1, BioTek, Bad Friedrichshall) at 700 nm with 48-well plates after 30 min of reaction time (Wetzel and Likens 2000). For further details on the experimental set-up and in situ measurements, see Langenheder, Kreuter et al. (2024).

### Stoichiometric analyses

For the study of size-fractionated stoichiometry, we separated between seston larger than  $105 \mu\text{m}$  and seston smaller than  $105 \mu\text{m}$ . This mesh size has been chosen to largely separate between medium-sized phytoplankton and large zooplankton. Water samples were taken every fourth day, which resulted in

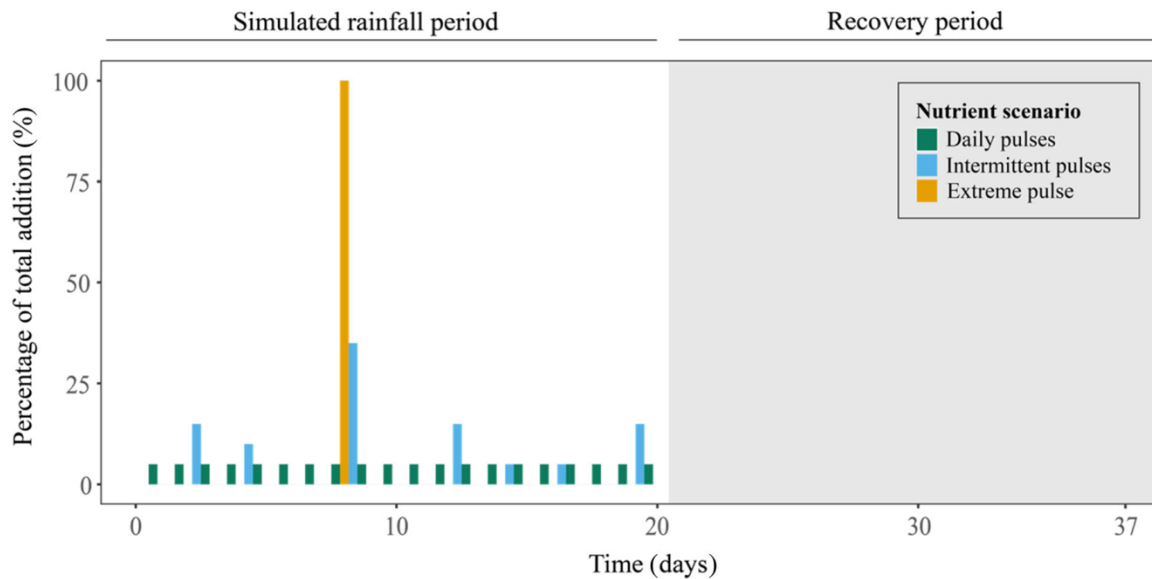


**Fig. 1.** Experimental nutrient and cDOM additions and timeline of the experiment. The total additions (100%) refer to  $2 \text{ mg L}^{-1}$  colored dissolved organic matter (cDOM),  $50 \mu\text{g L}^{-1}$  phosphorus primarily added as  $\text{KH}_2\text{PO}_4$  and  $500 \mu\text{g L}^{-1}$  primarily added as nitrogen  $\text{NaNO}_3$ . The experiment ended after 37 d. Time series of the dissolved nutrients can be found in Supporting Information Fig. S1.

10 data points (6 within the simulated rainfall period and 4 in the recovery period).

Water samples were filtered over a 105- $\mu\text{m}$  mesh from which the filtrate was caught in a separate plastic sampling bottle. The particles on the mesh were back-rinsed into a plastic measuring cylinder (large seston, > 105  $\mu\text{m}$ ) and half of the homogenized volume was tipped onto a pre-combusted and acid-washed glass microfiber filter (WHATMAN, GF/C filter) for POC/PON and the other half for POP. In the second step, the caught filtrate was filtered for biogenic silicate (Whatman NC45 membrane filters, cellulose nitrate, 0.45  $\mu\text{m}$ , 25 mm diameter; CAT no 10401106), POC/PON, and POP (same WHATMAN GF/C filter as above) for the small seston size fraction (105–0.45  $\mu\text{m}$ ). All filters were frozen at  $-20^\circ\text{C}$ .

Since a massive bloom of the giant cyanobacterium *Gloeotrichia echinulata* occurred in Lake Erken at the start of the experiment and dominated the large size fraction (Supporting Information Fig. S6), individual *Cladocera* and *Copepoda* were picked at three time points (start, mid and end) using a stereomicroscope (STEMI II, Zeiss) in order to separate between mesozooplankton and the remaining large seston size fraction. Depending on the availability of individuals over time 5–10 *Cladocera* and 10 *Copepoda* each were placed in pre-weighed tin capsules for POC/PON or POP analysis and frozen at  $-20^\circ\text{C}$ . Additionally, the abundances of *Cladocera* and *Copepoda* were quantified for the same time points by counting concentrated (sub-)samples under a stereo microscope using a counting chamber.

POP samples were quantified by molybdate reaction after potassium peroxydisulfate digestion (Wetzel and Likens 2000) and POC/PON was measured using a CHN analyzer (Flash EA 1112, Thermo Fisher Scientific) in the laboratory at ICBM in Wilhelmshaven, Germany. The POP analysis of individually picked zooplankton was unsuccessful due to methodological failure; therefore, these data are missing in the following analyses. Additionally, due to a wrong nutrient addition at the beginning of the experiment in one replicate of the daily-pulsed mesocosms, the community developed differently compared to the respective replicates. Therefore, this replicate has been excluded from all analyses. The filters for biogenic silicate were oxidized and autoclaved for 30 min using plastic tubes (Sarstedt). After cooling down to room temperature, reagents (molybdate reagent, oxalic acid, and ascorbic acid) were added, and then the samples were photometrically measured in a plate reader (as above) at 810 nm using 48-well plates after 1.5 h of reaction time (Grasshoff, Kremling, and Ehrhardt 1999). The absorption of each sample was converted into silicate concentrations via a silicon standard curve (based on 1.09947.0001, 1000 mg Si/ampoule, SiCl<sub>4</sub> in 14% NaOH, Merck) which was treated similarly to the samples.

#### Nutrient limitation bioassay

The nutrient limitation bioassay was performed 2 d after the last experimental nutrient addition on July 28, 2022. Lake

water and a pooled sample from all four mesocosms with daily pulses were filtered over a 105- $\mu\text{m}$  gaze (to exclude large grazers) and exposed to four nutrient treatments in cell culture bottles (SARSTEDT AG & Co. KG). This exposure consisted of an addition of phosphate ( $\text{KH}_2\text{PO}_4$ , 2.463  $\mu\text{g mL}^{-1}$  final concentration in the bottle), an addition of nitrogen ( $\text{NaNO}_3$ , 24.617  $\mu\text{g mL}^{-1}$  final concentration in the bottle), and an addition of the combination (N + P) in the same concentration as well as a control treatment without any nutrient addition. The used nutrients were the same as during the nutrient additions in the mesocosms and were added as one unique pulse at the beginning of the bioassay. This set-up thus consisted of 2 origins of water (lake and daily pulse treatment)  $\times$  4 nutrient treatments (N, P, N + P, control)  $\times$  3 replicates and summed up to 24 units. The bottles were incubated by hanging in the lake at a depth of 20 cm to experience the same temperature and light conditions. Fluorescence (as raw fluorescence units) from each unit was measured daily using a hand-held fluorometer (Turner Designs). The bioassay was ended after 5 d.

#### Calculation of stability measures

Zooplankton abundances were used to upscale the POC, PON, and POP content of the picked zooplankton and subtract the nutrient content attributable to zooplankton from the large size fraction. For each time point, the stoichiometric ratios of C : N, C : P, N : P, Si : C, Si : N, Si : P were calculated as the molar ratios between the particulate nutrient concentrations for the small seston, as well as the C : N ratio for the large seston, total zooplankton as well as cladocerans and copepods separately. To relate the treatment effects to the control, log response ratios (LRRs) for the stoichiometric ratios were calculated for each mesocosm as follows:

$$\text{LRR} = \ln \left( \frac{F_{\text{treat}}}{\text{mean}(F_{\text{con}})} \right) \quad (1)$$

as the natural logarithm of each treatment unit ( $F_{\text{treat}}$ ) divided by the mean of the control mesocosms ( $F_{\text{con}}$ ). The variability within the control was calculated by dividing each control unit from the control mean (Urrutia-Cordero, Langenheder, Striebel, Angeler et al. 2021). To explicitly quantify the vulnerability of plankton stoichiometry to the pulse treatments, the functional OEV framework (Urrutia-Cordero, Langenheder, Striebel, Angeler et al. 2021) was used. This assessment captures multiple stability components in one metric and thus, enables to quantify the overall vulnerability of an ecosystem to disturbances in its environment. The OEV is composed of the area under the curve of the LRR and therefore represents the destabilization over the entire time series for all stoichiometric ratios and was calculated using the *pk.calc.auc* function of the PKNCA package (Denney, Duvvuri, and Buckeridge 2015). The larger the OEV value, the higher the

vulnerability (and instability) of the measured variable to the pulse treatments.

To compare long-lasting effects of the treatments, final recovery (Hillebrand et al. 2018; Urrutia-Cordero, Langenheder, Striebel, Angeler et al. 2021) was calculated as the LRR of the last sampling point for respective stoichiometric ratios and for small seston, total zooplankton, large seston as well as cladocerans and copepods separately. A value of 0 can be interpreted as a full recovery.

### Statistical analyses

To identify the limiting nutrient, differences between the treatments in the nutrient limitation bioassay were assessed. Since the data were not normally distributed, nonparametric Kruskal–Wallis one-way ANOVAs using the “kruskal\_test” function in the “rstatix” package (Kassambara 2023) were conducted for each origin of water separately with the final fluorescence measurements as the response variable and the nutrient treatments as a predictor. To determine which treatments differed from each other, Conover–Iman multiple comparisons tests using the function “ConoverTest” in the package “DescTools” (Signorell 2022) followed the ANOVAs.

To identify significant effects of the run-off scenarios, functional stability (i.e., AUC and recovery) of small seston biomass and stoichiometry as well as recovery of C and C : N ratios in large seston and total zooplankton as response variables were individually tested against the run-off scenarios as predictor variables using Kruskal–Wallis one-way ANOVAs with Conover–Iman multiple comparisons tests (using the same functions and packages as above). To test for the differences in the C and C : N ratio recovery of the different zooplankton groups, nonparametric two-way analyses of variance (the Scheirer–Ray–Hare extension of the Kruskal–Wallis test) were conducted with recovery as individually tested response variables and both the zooplankton group and the run-off scenarios as predictor variables using the “scheirerRayHare” function in the “rcompanion” package (Mangiafico 2023). Recovery was standardized to absolute values prior to all statistical analyses (Hillebrand et al. 2018).

All statistical results were interpreted as significant for a significance level of  $\alpha = 0.05$  and were performed using the R statistical environmental version 4.2.3 (R Core Team 2023). All plots were created using the “ggplot2” package (Wickham 2016).

## Results

### Environmental conditions

The nutrient limitation bioassay indicated a clear phosphorus limitation in Lake Erken and a nitrogen–phosphorus co-limitation in the mesocosms after the simulated rainfall period (Supporting Information Fig. S2; Table S1). Photosynthetic active radiation decreased with the addition of cDOM into the mesocosms. This decrease proceeded drastically in the extreme scenario from  $\sim 110$  to  $35 \text{ W m}^{-2}$  and was more gradual in

the smaller-pulse scenarios (Fig. 2). Dissolved silicate strongly decreased until complete depletion in all treatments, with a 1-week time lag in the extreme treatment and an even slower decrease under control conditions (Supporting Information Fig. S1E). The water temperature ranged between  $18.5^\circ\text{C}$  and  $21.5^\circ\text{C}$  throughout the experiment (Supporting Information Fig. S1D).

### Small seston biomass

Generally, dissolved oxygen (DO) concentration and POC differ in their response time to environmental changes. Overall, both parameters showed similar response patterns in which the daily- and intermittent-pulsed treatments gradually shifted toward higher values that were maintained until the end of the experiment (Fig. 2). On average, the daily pulses resulted in 49% and the intermittent pulses in 89% higher carbon-based biomass compared to the control treatment at the end of the experiment. The extreme and control treatments initially showed a similar development in DO. The extreme nutrient and cDOM addition induced an increase in DO that exceeded all other treatments in magnitude and a smaller increase in cellular C to the same level as the daily and intermittent treatments. This short-term stimulation fully aligned back to control conditions after 8 d and showed no deviation from the control at the end of the experiment (Fig. 2).

### Stability of small seston biomass and stoichiometry

Small seston biomass ( $< 105 \mu\text{m}$ ) showed the lowest OEV and highest recovery when nutrients were applied as one extreme pulse compared to both multiple smaller pulse scenarios (i.e., daily and intermittent pulse scenarios) (Fig. 3; Table 1).

A similar pattern was found in the cellular C : N ratio, in which the extreme pulse also showed the lowest OEV and (although not significant) most complete recovery (Table 1). The daily and intermittent pulse scenarios initially followed a similar course during the simulated rainfall period with a shift toward lower C : N ratios compared to the control (Fig. 2). In the recovery phase, however, the daily-pulsed treatments maintained the shift toward lower C : N ratios longer (Fig. 2), leading to a significant difference in OEV also between the daily and intermittent pulse scenarios (Table 1). The extreme treatment shows a deviation shortly after the extreme nutrient addition but aligned back with the control in the later course of the experiment (Fig. 2).

For the C : P and N : P ratios, this pattern was reversed and the extreme treatment significantly deviated from both the daily and intermittent pulse scenarios and was thus, furthest from a full recovery (Figs. 2, 3; Table 1). Simultaneously, the daily-pulsed treatment achieved the fullest (nonsignificant) recovery and significantly lowest OEV for C : P and N : P ratios (Fig. 3, Table 1).



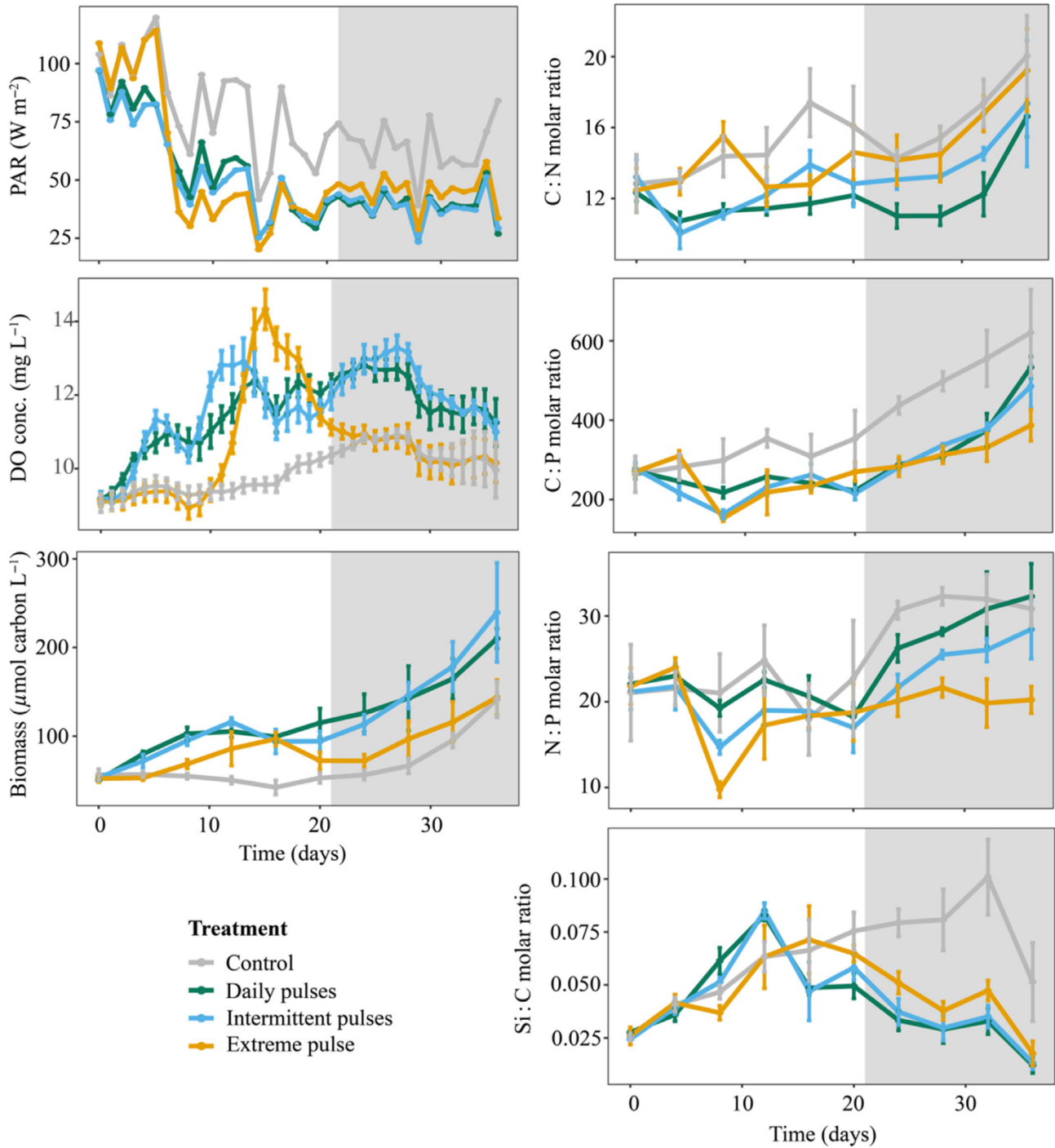


**Fig. 2.** Time series of photosynthetic active radiation (PAR), dissolved oxygen (DO) concentration, and particulate carbon concentration (biomass), and the particulate molar ratios of C : N, C : P, N : P, and Si : C of seston < 105  $\mu\text{m}$ . The time series of Si : nutrients can be found in Supporting Information Fig. S3. The gray background represents the recovery period. The error bars represent standard deviations.

The Si : C and both Si : nutrient ratios showed a similar development throughout the experiment but with a time delay in the extreme pulse scenario. This time-lag led to a

significantly lower OEV in the Si : C and Si : N ratios (Table 1). All three ratios decreased from the mid of the simulated rain-fall period in all nutrient pulse scenarios, while the control

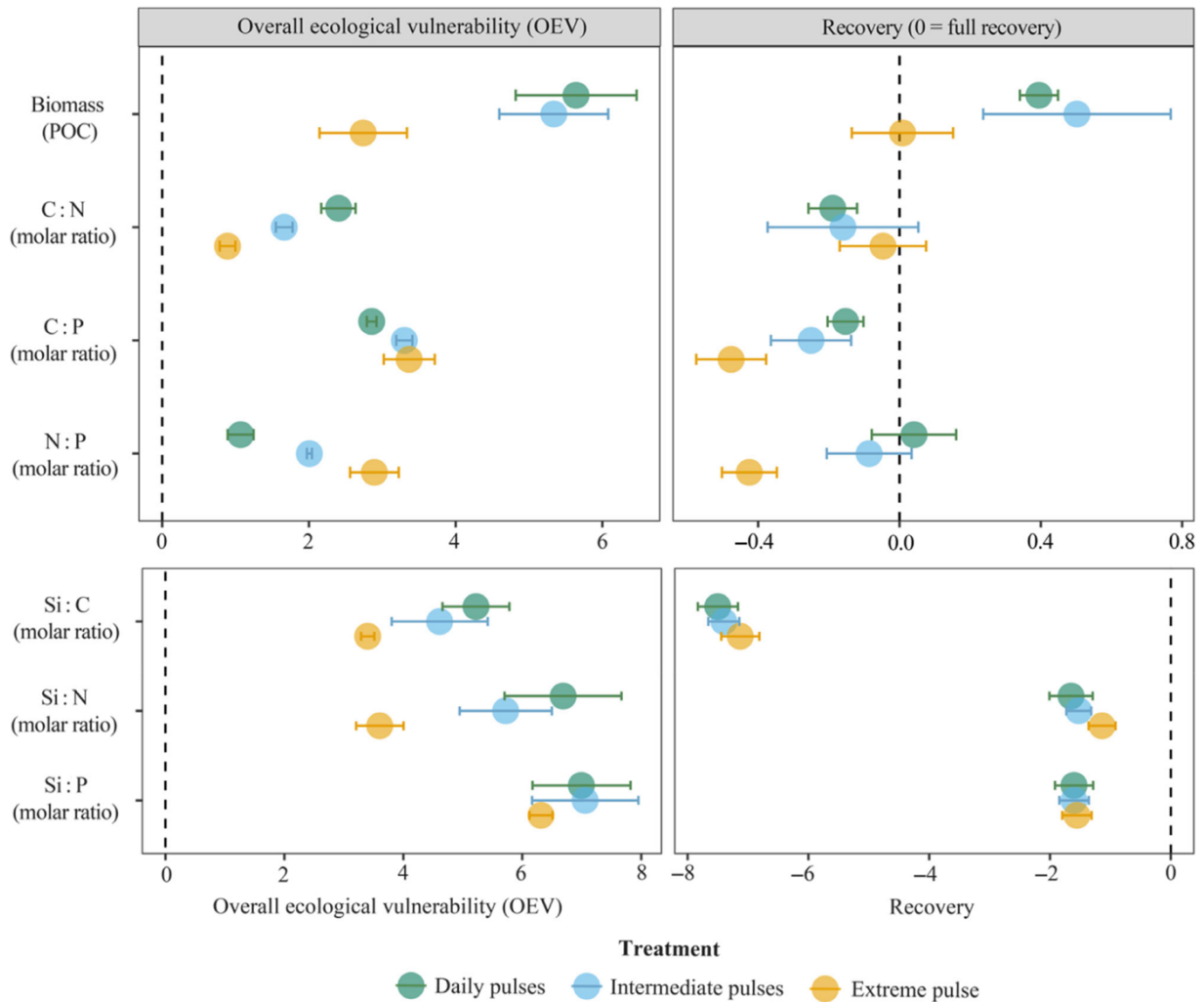


**Fig. 3.** Overall ecological vulnerability (OEV) and final recovery as functional stability measures of small seston biomass and all stoichiometric ratios (as molar ratios). High OEV values represent a larger destabilization over the entire time series. A recovery value of 0 indicates full recovery. The error bars represent standard deviations. The time series of log response ratios (LRRs) can be found in Supporting Information Fig. S4.

**Table 1.** Results of the Kruskal–Wallis and Conover’s multiple comparisons test for overall ecological vulnerability and recovery of small seston cellular carbon concentration (C) as a proxy for biomass, and as well as particulate C : N, C : P, N : P, Si : C, Si : N, and Si : P ratios. D, I, and E indicate the nutrient treatments of daily, intermittent and extreme pulses. Significant  $p$ -values are indicated by an asterisk (\*) for  $p < 0.05$  for  $p < 0.1$ . Mean rank differences (MRD) are reported.

	C		C : N		C : P		N : P		Si : C		Si : N		Si : P	
	MRD	$p$	MRD	$p$	MRD	$p$	MRD	$p$	MRD	$p$	MRD	$p$	MRD	$p$
Overall ecological vulnerability (OEV)														
E–D	–6.17	0.01*	–7.50	<0.01*	5.50	0.05*	7.50	<0.01*	–6.25	0.02*	–6.83	<0.01*	–3.92	0.41
I–D	–1.17	0.46	–3.50	<0.01*	5.50	0.05*	3.50	<0.01*	–2.00	0.26	–2.33	0.11	–0.67	0.79
I–E	5.00	0.01*	4.00	<0.01*	0.00	1.00	–4.00	<0.01*	4.25	0.05*	4.50	0.01*	3.25	0.41
Recovery														
E–D	–4.00	0.14	–2.67	1.00	6.25	0.02*	6.17	0.01*	–3.17	0.77	–4.75	0.17	–0.25	1.00
I–D	1.25	0.53	–1.92	1.00	2.00	0.26	1.17	0.46	–1.42	0.97	–0.75	0.73	0.25	1.00
I–E	5.25	0.06	0.75	1.00	–4.25	0.05*	–5.00	0.01*	1.75	0.97	4.00	0.17	0.50	1.00



**Table 2.** Results of the Kruskal–Wallis and Conover’s multiple comparisons test for the recovery of the cellular carbon concentration (C), carbon : nitrogen ratio (C : N) in large seston and total zooplankton (zoopl.). D, I, and E indicate the nutrient treatments of daily, intermittent and extreme pulses. Significant  $p$ -values are indicated by an asterisk (\*) for  $p < 0.05$ . Mean rank differences (MRD) are reported.

	Seston > 105 $\mu\text{m}$ POC		Seston > 105 $\mu\text{m}$ C : N		Zoopl. C		Zoopl. C : N	
	MRD	$p$ -value	MRD	$p$ -value	MRD	$p$ -value	MRD	$p$ -value
E–D	–3.58	0.0908†	7.5	0.0001*	0.8257	0.58	–4.42	0.1908
I–D	2.67	0.1161	3.5	0.0057*	0.7470	–2.42	–0.17	0.9396
I–E	6.25	0.0063*	–4.0	0.0034*	0.7257	–3.00	4.25	0.1908

continued to increase (Fig. 2; Supporting Information Fig. S3) which is also reflected in the large deviation from recovery with no differences between the nutrient-addition treatments (Fig. 3; Table 1).

#### Recovery in cellular carbon and C : N ratios across plankton size classes

Large seston biomass (C) showed a similar pattern as phytoplankton with a full recovery in the extreme treatment which differed significantly from the non-recovered intermittent pulse treatment (Table 2). While both large and small seston generally overperformed (recovery > 0), mesozooplankton generally underperformed compared to the control. This shift is mainly

driven by an overall biomass decrease in *Copepoda* which differed significantly from the only slightly overperforming *Cladocera* (Fig. 4). However, no effect of the nutrient addition scenarios was found for total mesozooplankton, nor the different groups of mesozooplankton (Table 3).

In the cellular C : N ratio, large seston fully recovered in the daily and intermittent pulse scenarios, and shifted slightly but significantly toward higher C : N ratios in the extreme treatment (Table 2). Mesozooplankton strongly underperformed without differences between the treatments. Although both mesozooplankton groups showed a strong shift toward lower C : N ratios, *Copepoda* expressed significantly lower C : N ratios than *Cladocera* (Fig. 3; Table 3).

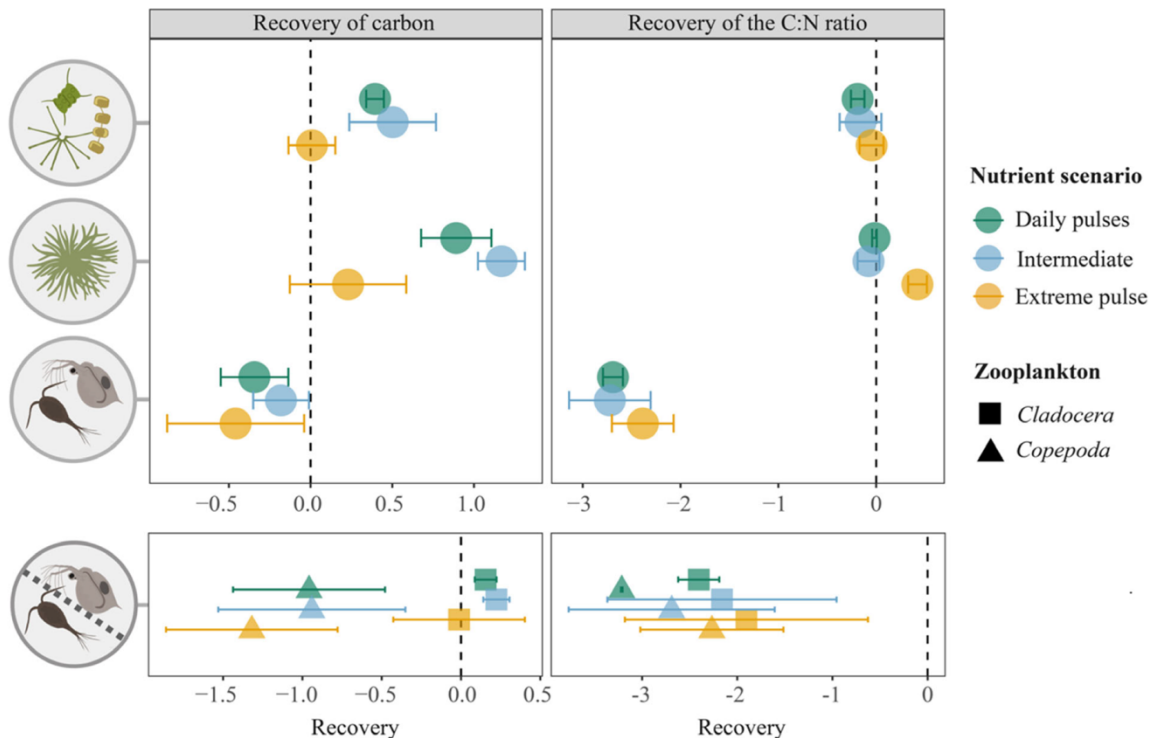


**Fig. 4.** Recovery of cellular carbon and C : N ratios across small seston, large seston, total zooplankton (from top to bottom), *Copepoda*, and *Cladocera* over time. The bottom panels represent the recovery per major mesozooplankton group. A recovery value of 0 indicates full recovery. The error bars represent standard deviations.

**Table 3.** Results of the Scheirer–Ray–Hare test for the recovery of the particulate organic carbon (POC), carbon : nitrogen ratio (C : N) across the different nutrient pulse scenarios and mesozooplankton groups. D, I, and E indicate the nutrient treatments of daily, intermittent and extreme pulses. Significant *p*-values are indicated by an asterisk (\*) for  $p < 0.05$ . Mean rank differences (MRD) are reported.

	df	POC		C : N	
		<i>H</i>	<i>p</i> -value	<i>H</i>	<i>p</i> -value
Treatment	2	0.28	0.8688	2.56	0.2782
Group	1	14.95	0.0001*	3.86	0.0494*
Treatment × group	2	0.19	0.9101	1.59	0.4509

## Discussion

### Phytoplankton biomass and stoichiometry

The small size fraction was composed of phytoplankton as well as microzooplankton, for example, ciliates, rotifers, and copepod nauplii with low relative abundances, but treatment-dependent differences over time (Supporting Information Fig. S7). However, with phytoplankton as the dominant organism group, the small size fraction will be discussed as phytoplankton in the following.

The presented results show that the functional stability of phytoplankton stoichiometry differed between the applied run-off scenarios. Considering the phytoplankton biomass proxy (POC), the extreme pulse induced a short-term growth stimulation, but fully recovered to control conditions in the long-term. However, cellular C : P and N : P ratios were still substantially disrupted even a month after the extreme pulse, which suggests that stoichiometric recovery did not occur to the same extent (Fig. 2). Thus, the intensity and frequency (i.e., one extreme pulse vs. multiple smaller pulses) of nutrient input determined the phytoplankton stoichiometry, whereas the regularity (i.e., regular vs. irregular smaller pulses) only played a minor role.

Generally, changes in phytoplankton community stoichiometry can be explained by plastic changes in the stoichiometry of the present species in response to environmental changes (Yvon-Durocher et al. 2015) or compositional shifts in a community consisting of species with taxon-specific elemental ratios (Finkel et al. 2009). The extreme nutrient pulse most strikingly triggered phytoplankton growth and with this potentially increased the phosphorus demand connected to higher growth rates (Elser et al. 2003) leading to a decrease in cellular N : P ratios shortly after the addition. However, since the decrease in N : P and C : P ratios was maintained until the end of the experiment, even after the biomass fully recovered, phosphorus-driven luxury consumption and nutrient storage (Stern and Elser 2002) may complement the reasoning. This would be in line with Graham and Vinebrooke (2009) who

found a single nutrient pulse (i.e., heavy rainfall scenario) to be favorable for large species (colonial chrysophytes and filamentous chlorophytes) and proposed their capability to store and exploit the available nutrients (Reynolds 1984) and DOC (Weyhenmeyer, Willén, and Sonesten 2004) to be advantageous. Phosphorus storages can support more than five generations (Barnes and Hughes 1988), which might explain why the decreased C : P and N : P ratios were maintained throughout the recovery period so that the cells could benefit from the stored nutrients even after dissolved nutrients had been depleted. Additionally, the storage capacity of N is much lower than the one of P which is reflected in the minimum and maximum cell quota of phytoplankton (Edwards et al. 2012) and explains the faster recovery of the C : N ratio compared to the C : P and N : P ratio after the extreme nutrient pulse. Moreover, the cDOM additions increase turbidity and create an environment with a reduced light : nutrient supply ratio (Stern et al. 1997) which thus, potentially evoked the overall decrease in phytoplankton C : P ratios with decreasing light intensity, as also shown in Striebel, Spörl, and Stibor (2008).

In the gleaner-opportunist framework (Grover 1990), gleaners represent specialists that utilize less accessible and residual resources, while opportunists express a more generalist approach by quickly exploiting favorable resource conditions. Based on this, one extreme nutrient pulse may favor opportunistic species with a high minimum resource requirement  $R^*$  and high maximum growth rates in the short term, while the fast depletion of nutrients after the pulse creates conditions advantageous for gleaner species with a low  $R^*$  and low maximum growth rate during the recovery period. The scenarios with multiple smaller pulses (i.e., daily and intermittent pulse scenarios) and therefore higher resource fluctuations may provide an advantage for opportunistic species that generally cope better with variable environments (Yamamichi and Letten 2022) which may explain the biomass shift toward higher values in the daily and intermittent pulse scenarios.

Another explanation is that the communities in the daily and intermittent pulse scenarios experienced a rather stable and gradual increase in nutrients and thus, potentially had more time to select for species with higher phosphorus use efficiencies (i.e., produced biomass per unit of limiting nutrient) (Hodapp, Hillebrand, and Striebel 2019) as reflected in the increase in C : P ratios in combination with an overall higher biomass build-up after the recovery period. Based on our findings, we propose that a sudden, extreme increase in nutrients to the water (i.e., a heavy rainfall event) may favor nutrient-storage specialists or opportunist species, while multiple smaller pulses bring forward a community with higher nutrient use efficiencies or gleaner species.

Previous studies testing the effect of the nutrient addition frequency show opposing results in terms of biomass: Svensen

et al. (2002) found a higher mean phytoplankton biomass after an extreme pulse for a Baltic community, whereas Estrada et al. (2003) did not observe any effects for a Mediterranean community. Lagus et al. (2007) suggested that these different results may arise from the preceding limitation patterns and nutrient levels since the composition and biomass of their Baltic phytoplankton community depended not only on the fluctuation frequencies but even more on the supplied nutrient ratio. However, due to a difference in limitation patterns between freshwater and marine systems (Elser et al. 2007), the findings may only be partly comparable to our study.

The decrease in the Si : C and Si : nutrient ratios and thus, the arising deviance from the control (reflected in high OEI and very low recovery) is likely explained by a decrease in silicate-embedding phytoplankton species (i.e., diatoms) due to altered competitive dynamics under nutrient addition. The addition of nutrients potentially favored species that were able to use the supplied resources irrespective of the silicate concentration which might have limited diatom growth due to a progressing dissolved silicate depletion in these treatments.

Further aspects that may shape the response to different precipitation scenarios are temperature and light. Graham and Vinebrooke (2009) evidenced that the positive effect of nutrient increase on phytoplankton biomass (driven by large species) is amplified by warming. Our experiment was interfered with by a summer heat wave and therefore, the effects of the nutrient treatments may have been amplified. Furthermore, the addition of DOC including humic substances reduced the light availability in the water which has for example been shown to induce shifts in the phytoplankton community composition toward mobile cryptophytes in two Swedish lakes (Weyhenmeyer, Willén, and Sonesten 2004).

#### *Gloeotrichia echinulata* colonies

The effects within the large seston size class were not exclusively driven by *G. echinulata* but included other large phytoplankton species (like *Ceratium* sp., and *Fragilaria* sp.) and rotifers. However, the biomass effects can mainly be attributed to the giant cyanobacterium *G. echinulata* which dominated this size class (see Supporting Information Fig. S5, S6).

It has been proposed that with proceeding climate change and input of phosphorus into lakes, cyanobacteria will increase in importance (Jeppesen et al. 2009). In terms of carbon-based biomass, colonies of the giant cyanobacterium *G. echinulata* were still elevated at the final sampling in the daily and intermittent pulse scenarios, while they fully recovered after the extreme pulse. Due to their ability to fix nitrogen (Cottingham et al. 2015), as well as their high internal supply of phosphorus brought along from their resting stage phase (Pettersson, Herlitz, and Istánovics 1993), and a concurrent heat wave, it is likely neither nutrients nor temperature limiting their growth in the extreme treatment. However, the reduction in light availability due to the sudden and complete

addition of nutrients and cDOM (Fig. 2) may have disrupted the ongoing recruitment phase (Barbiero 1993) and pelagic division. A recent study by Lyche Solheim et al. (2024) found a similar pattern with a declining biomass of a nitrogen-fixing cyanobacterium species under browning-induced light limitation which could potentially be linked to higher energy demands for nitrogen fixation (Reynolds et al. 2002).

Additionally, the treatments with high *G. echinulata* carbon-based biomass showed a decreased C : N ratio which may be explained by their ability to fix nitrogen (Cottingham et al. 2015). However, due to their high internal supply of phosphorus and thus, high C : P ratio (Pettersson, Herlitz, and Istánovics 1993), differences in the overall C : P and N : P ratio between the treatments can be expected to be more pronounced.

#### Mesozooplankton

The results of this study did not find that the effects of the different run-off scenarios on phytoplankton stoichiometry were transferred to the zooplankton level. Yet, we lack data on the zooplankton C : P and N : P ratios (see “Methods” section) to make a conclusive statement. However, we found a strong difference between the nutrient treatments and the control regarding the biomass performance of the mesozooplankton groups.

Throughout the course of the experiment, a dominance shift in abundance from *Copepoda* to *Cladocera* across all treatments (including the control) was observed (Supporting Information Fig. S8). However, *Cladocera* showed a stable carbon-based biomass (POC), whereas *Copepoda* decreased their carbon-based biomass under nutrient addition. The competitive advantage of *Cladocera* with generally lower body N : P ratios (Andersen and Hessen 2003; Schatz and McCauley 2007) can be explained by the change from phosphorus to nitrogen-phosphorus co-limitation in the water which induced an overall decrease in phytoplankton C : P and N : P ratios and thus, relatively phosphorus-rich phytoplankton cells were available which are required for a high *Cladocera* performance (Andersen and Hessen 2003; Schatz and McCauley 2007). These findings are in line with Hassett et al. (2003), and highlight the general importance of nutritional quality in shaping the community composition and dominance of mesozooplankton.

Since an unselective filter feeder dominated during the course of the experiment, we can exclude top-down selection processes as a dominant driver in shaping the changes in phytoplankton community stoichiometry in our study. However, *Ceriodaphnia* spp. which dominated the group have a food niche of 2–8  $\mu\text{m}$  (Geller and Müller 1981) and therefore may have influenced the size distribution within the phytoplankton community. Since we found no difference between the nutrient addition scenarios on *Cladocera* and *Copepoda* biomass, we can also exclude that mesozooplankton caused differences in phytoplankton functional and compositional responses to the nutrient scenarios, which is in agreement

with a previous marine study (Svensen et al. 2002). Contrarily, Lagus et al. (2007) found a response of mesozooplankton total biomass and community composition to different nutrient pulse frequencies (i.e., daily vs. weekly) in a Baltic Sea community. In their study, the weekly additions favored larger zooplankton, whereas the daily nutrient additions increased the biomass of small rotifers which the authors relate to changes in the phytoplankton community composition (Lagus et al. 2007).

However, the reorganization of the zooplankton community may also partly be explained by the release from predation pressure and thus, the effects of a transient phase in the mesocosm system.

## Conclusion

In this study, we investigated the size-fractionated stoichiometric response of a plankton community to different run-off scenarios. We found contrasting patterns between the functional stability of phytoplankton biomass and stoichiometry: While the simulated extreme rainfall event (one strong pulse of nutrients and cDOM) led to a low vulnerability and full recovery for phytoplankton biomass, the stoichiometry (specially the particulate C : P and N : P ratio) was still substantially disrupted 1 month after the pulse. Overall, the intensity and frequency (i.e., one extreme pulse vs. multiple smaller pulses) of the nutrient and cDOM inputs determined the phytoplankton responses, whereas the regularity (i.e., regular vs. irregular smaller pulses) only played an underlying role.

From an ecological perspective, lower-intensity but high-frequency rainfall events inducing substantially increased phytoplankton biomass may hold the risk of algal blooms and prolonged episodes of critically low dissolved oxygen concentrations in lake bottom water due to continuous biomass decomposition by heterotrophic bacteria which negatively affects benthic communities. Moreover, the increased turbidity following rapid phytoplankton bloom developments could result in a lowered abundance of macrophytes which serve as important refuge for zooplankton (Celewicz-Goldyn and Kuczynska-Kippen 2017).

As a consequence of the nutrient additions, a shift from a phosphorus-limitation to a nitrogen-phosphorus co-limitation induced an overall increase in nutritional quality for *Cladocera* in the form of P-rich phytoplankton cells. Therefore, *Cladocera* carbon-based biomass remained stable (as opposed to *Copepoda*) independent of the frequency, intensity or regularity of the nutrient pulses. This implies that various patterns of increased precipitation and terrestrial runoff as predicted for the future can lead to a shift in the mesozooplankton community dominance and therefore decrease selective top-down control in a fish-excluded setting, or may have cascading effects onto higher trophic levels. In a natural setting, prolonged dry periods (control) may alternate with extended wet phases (daily, intermittent) or disruptions by extreme events

(extreme pulse). Low-intensity multi-pulse events increase biomass instability and are potentially disrupted by extreme rainfall events that, in turn, destabilize phytoplankton stoichiometry. The alternation of scenarios may drive either a self-reinforcing destabilization or a return to stability for both phytoplankton stoichiometry and biomass. However, this alternation of precipitation patterns as well as the response to reoccurring extreme events needs further investigation.

To summarize, our study shows that phytoplankton stoichiometry (i.e., nutritional quality) responds to the variability in nutrient and carbon availability and is important to understand the effects on the consumer level. The direction of observed effects on functionality is expected to be consistent across lake ecosystems, whereas the magnitude of these effects may be largely driven by seasonality and specific lake characteristics (Urrutia-Cordero, Langenheder, Striebel, Eklöv et al. 2021). However, research on phytoplankton community stoichiometry is still lacking from experimental nutrient pulse studies. This becomes even more pressing when taking into account that proceeding climate warming will shift trophic dynamics to a point where even small increases in nutrient concentrations or temperature can trigger large disruptions across the aquatic network (Merz et al. 2023). Thus, understanding these dynamics could inform management strategies aimed at mitigating negative impacts on water quality and ecosystem health.

## Author Contributions

A.H.: Conceptualization of the study (equal); Conceptualization and coordination of the mesocosm study (supporting); coordination of the specific study (lead); implementation of the mesocosm study (equal); sample analysis and data generation (lead); data analysis, interpretation of results (lead); writing – original draft. B.B.: Implementation of the mesocosm study (equal); sample analysis and data generation (supporting); interpretation of results (supporting); writing – review and editing (equal). B.G.: Implementation of the mesocosm study (equal); sample analysis and data generation (supporting); interpretation of results (supporting), writing – review and editing (equal). S.L.: Conceptualization of the study (equal); conceptualization and coordination of the mesocosm study (lead); coordination of the specific study (equal); implementation of the mesocosm study (equal); sample analysis and data generation (supporting); interpretation of results (supporting); writing – review and editing (equal). S.B.: Conceptualization and coordination of the mesocosm study (supporting); implementation of the mesocosm study (equal); interpretation of results (supporting); writing – review and editing (equal). J.N.: Conceptualization and coordination of the mesocosm study (supporting); implementation of the mesocosm study (equal); interpretation of results (supporting); writing – review and editing (equal). M.S.: Conceptualization of the specific study

(equal); conceptualization and coordination of the mesocosm study (supporting); coordination of the specific study (lead); interpretation of results (supporting); writing – review and editing (equal).

### Acknowledgments

We would like to thank everyone who participated in the mesocosm experiment at Lake Erken: Nils Kreuter, William Colom, Dolly Kothawala, Berenike Bick, Congcong Jiao, Gabriela Agreda López, Don Pierson, Jorrit Mesman, Katerina Symiakaki, Jimmy Clifford Oppong, Nusret Karakaya, Pelin Ertürk Ari, and Akif Ari. This study has been made possible by the Swedish Infrastructure for Ecosystem Science, in this case at the Erken Laboratory, and the EU H2020-INFRAIA project (No. 871081) AQUACOSM-plus Network of Leading Ecosystem Scale Experimental AQUATIC MesoCOSM Facilities Connecting Rivers, Lakes, Estuaries, and Oceans in Europe and beyond—funded by the European Commission. The Swedish Infrastructure for Ecosystem Science receives funding through the Swedish Research Council under Grant No. 2017-00635. A.H. was supported by a DAAD (German Academic Exchange Service) research grant for doctoral candidates (No. 57556281). B.G. and B.B. were supported by the Transnational Access Program of the EU H2020-INFRAIA project (No. 871081) AQUACOSM-plus.

### References

- Andersen, T., and D. O. Hessen. 2003. "Carbon, Nitrogen, and Phosphorus Content of Freshwater Zooplankton." *Limnology and Oceanography* 36: 807–814. <https://doi.org/10.4319/lo.1991.36.4.0807>
- Barbiero, R. P. 1993. "A Contribution to the Life History of the Planktonic Cyanophyte *Gloeotrichia echinulata*." *Archiv für Hydrobiologie* 127: 87–100. <https://doi.org/10.1127/archiv-hydrobiol/127/1993/87>
- Barnes, R. S. K., and R. N. Hughes. 1988. *An Introduction to Marine Ecology*. 2nd ed. London, UK: Oxford Blackwell Scientific Publications.
- Carpenter, S. R., J. J. Cole, J. F. Kitchell, and M. L. Pace. 1988. "Impact of Dissolved Organic Carbon, Phosphorus, and Grazing on Phytoplankton Biomass and Production in Experimental Lakes." *Limnology and Oceanography* 43: 73–80. <https://doi.org/10.4319/lo.1998.43.1.0073>
- Celewicz-Goldyn, S., and N. Kuczynska-Kippen. 2017. "Ecological Value of Macrophyte Cover in Creating Habitat for Microalgae (Diatoms) and Zooplankton (Rotifers and Crustaceans) in Small Field and Forest Water Bodies." *PLoS One* 12: e0177317. <https://doi.org/10.1371/journal.pone.0177317>
- Connell, J. H. 1978. "Diversity in Tropical Rain Forests and Coral Reefs." *Science* 199, no. 4335: 1302–1310. <https://doi.org/10.1126/science.199.4335.1302>
- Cottingham, K. L., and D. E. Schindler. 2000. "Effects of Grazer Community Structure on Phytoplankton Response to Nutrient Pulses." *Ecology* 81: 183–200. [https://doi.org/10.1890/0012-9658\(2000\)081\[0183:EOGCSO\]2.0.CO;2](https://doi.org/10.1890/0012-9658(2000)081[0183:EOGCSO]2.0.CO;2)
- Cottingham, K. L., H. A. Ewing, M. L. Greer, C. C. Carey, and K. C. Weathers. 2015. "Cyanobacteria as Biological Drivers of Lake Nitrogen and Phosphorus Cycling." *Ecosphere* 6: 1–19. <https://doi.org/10.1890/ES14-00174.1>
- Cowles, T. J., R. J. Olson, and S. W. Chisholm. 1988. "Food Selection by Copepods: Discrimination on the Basis of Food Quality." *Marine Biology* 100: 41–49. <https://doi.org/10.1007/BF00392953>
- Denney, W., S. Duvvuri, and C. Buckeridge. 2015. "Simple, Automatic Noncompartmental Analysis: The PKNCA R Package." *Journal of Pharmacokinetics and Pharmacodynamics* 42: 11–107. <https://doi.org/10.1007/s10928-015-9432-2>
- Dickman, E. M., J. M. Newell, M. J. González, and M. J. Vanni. 2008. "Light, Nutrients, and Food-Chain Length Constrain Planktonic Energy Transfer Efficiency across Multiple Trophic Levels." *Proceedings of the National Academy of Sciences of the United States of America* 105: 18408–18412. <https://doi.org/10.1073/pnas.0805566105>
- Diehl, S., S. A. Berger, W. Uszko, and H. Stibor. 2022. "Stoichiometric Mismatch Causes a Warming-Induced Regime Shift in Experimental Plankton Communities." *Ecology* 103: e3674. <https://doi.org/10.1002/ecy.3674>
- Edwards, K. F., M. K. Thomas, C. A. Klausmeier, and E. Litchman. 2012. "Allometric Scaling and Taxonomic Variation in Nutrient Utilization Traits and Maximum Growth Rate of Phytoplankton." *Limnology and Oceanography* 57: 554–566. <https://doi.org/10.4319/lo.2012.57.2.0554>
- Elser, J. J., K. Acharya, M. Kyle, et al. 2003. "Growth Rate–Stoichiometry Couplings in Diverse Biota." *Ecology Letters* 6: 936–943. <https://doi.org/10.1046/j.1461-0248.2003.00518.x>
- Elser, J. J., M. E. S. Bracken, E. E. Cleland, et al. 2007. "Global Analysis of Nitrogen and Phosphorus Limitation of Primary Producers in Freshwater, Marine and Terrestrial Ecosystems." *Ecology Letters* 10: 1135–1142. <https://doi.org/10.1111/j.1461-0248.2007.01113.x>
- Estrada, M., E. Berdalet, M. Vila, and C. Marrasé. 2003. "Effects of Pulsed Nutrient Enrichment on Enclosed Phytoplankton: Ecophysiological and Successional Responses." *Aquatic Microbial Ecology* 32: 61–71. <https://doi.org/10.3354/ame032061>
- Finkel, Z. V., J. Beardall, K. J. Flynn, A. Quigg, T. A. V. Rees, and J. A. Raven. 2009. "Phytoplankton in a Changing World: Cell Size and Elemental Stoichiometry." *Journal of Plankton Research* 32: 119–137. <https://doi.org/10.1093/plankt/fbp098>
- Frost, P. C., N. J. T. Pearce, S. A. Berger, et al. 2023. "Interactive Effects of Nitrogen and Phosphorus on Growth and Stoichiometry of Lake Phytoplankton." *Limnology and Oceanography* 9999: 1–13. <https://doi.org/10.1002/lno.12337>



- Different Nitrogen Sources and Co-Limiting Nutrients.” *Marine Ecology Progress Series* 176: 205–214. <https://doi.org/10.3354/meps176205>.
- Pettersson, K., E. Herlitz, and V. Istánovics. 1993. “The Role of *Gloeotrichia echinulata* in the Transfer of Phosphorus From Sediments to Water in Lake Erken.” *Hydrobiologia* 253: 123–129. <https://doi.org/10.1007/BF00050732>.
- R Core Team. 2023. R: A Language and Environment for Statistical Computing. Vienna, Austria: R Foundation for Statistical Computing. <https://www.R-project.org/>.
- Reynolds, C. S. 1984. *The Ecology of Freshwater Phytoplankton*. Cambridge, UK: Cambridge University Press.
- Reynolds, C. S., V. Huszar, C. Kruk, L. Nasellini-Flores, and S. Melo. 2002. “Towards a Functional Classification of the Freshwater Phytoplankton.” *Journal of Plankton Research* 24: 417–428. <https://doi.org/10.1093/plankt/24.5.417>.
- Roulet, N., and T. R. Moore. 2006. “Browning the Waters.” *Nature* 444: 283–284. <https://doi.org/10.1038/444283a>.
- Salmaso, N. 2010. “Long-Term Phytoplankton Community Changes in a Deep Subalpine Lake: Responses to Nutrient Availability and Climatic Fluctuations.” *Freshwater Biology* 55: 825–846. <https://doi.org/10.1111/j.1365-2427.2009.02325.x>.
- Schatz, G. S., and E. McCauley. 2007. “Foraging Behavior by *Daphnia* in Stoichiometric Gradients of Food Quality.” *Oecologia* 153: 1021–1030. <https://doi.org/10.1007/s00442-007-0793-0>.
- Signorell, A. 2022. DescTools: Tools for Descriptive Statistics. R Package Version 0.99.47 <https://CRAN.R-project.org/package=DescTools>.
- Sommer, U. 2003. “Comparison Between Steady State and Non-steady State Competition: Experiments With Natural Phytoplankton.” *Limnology and Oceanography* 30: 335–346. <https://doi.org/10.4319/lo.1985.30.2.0335>.
- Sterner, R. W., and J. J. Elser. 2002. *Ecological Stoichiometry: The Biology of Elements From Molecules to the Biosphere*. Princeton, NJ: Princeton University Press.
- Sterner, R. W., J. J. Elser, J. F. Everett, S. J. Guildford, and T. H. Chrzanowski. 1997. “The Light:Nutrient Ratio in Lakes: The Balance of Energy and Materials Affects Ecosystem Structure and Process.” *American Naturalist* 150: 663–684. <https://doi.org/10.1086/286088>.
- Sterner, R. W., and D. O. Hessen. 1994. “Algal Nutrient Limitation and the Nutrition of Aquatic Herbivores.” *Annual Review of Ecology and Systematics* 25: 1–29. <https://doi.org/10.1146/annurev.es.25.110194.000245>.
- Striebel, M., G. Spörl, and H. Stibor. 2008. “Light-Induced Changes of Plankton Growth and Stoichiometry: Experiments With Natural Phytoplankton Communities.” *Limnology and Oceanography* 53: 513–522. <https://doi.org/10.4319/lo.2008.53.2.0513>.
- Svensen, C., J. C. Nejstgaard, J. K. Egge, and P. Wassmann. 2002. “Pulsing Versus Constant Supply of Nutrients (N, P and Si): Effect on Phytoplankton, Mesozooplankton and Vertical Flux of Biogenic Matter.” *Scientia Marina* 66: 189–203. <https://doi.org/10.3989/scimar.2002.66n3189>.
- Urrutia-Cordero, P., S. Langenheder, M. Striebel, et al. 2021. “Integrating Multiple Dimensions of Ecological Stability Into a Vulnerability Framework.” *Journal of Ecology*: 1–13. <https://doi.org/10.1111/1365-2745.13804>.
- Urrutia-Cordero, P., S. Langenheder, M. Striebel, et al. 2021. “Functionally Reversible Impacts of Disturbances on Lake Food Webs Linked to Spatial and Seasonal Dependencies.” *Ecology* 102: e03283. <https://doi.org/10.1002/ecy.3283>.
- Urrutia-Cordero, P., O. Langvall, P. Blomkvist, et al. 2021. “SITES AquaNet: An Open Infrastructure for Mesocosm Experiments With High Frequency Sensor Monitoring across Lakes.” *Limnology and Oceanography: Methods* 19: 385–400. <https://doi.org/10.1002/lom3.10432>.
- Walve, J., and U. Larsson. 1999. “Carbon, Nitrogen and Phosphorus Stoichiometry of Crustacean Zooplankton in the Baltic Sea: Implications for Nutrient Recycling.” *Journal of Plankton Research* 21: 2309–2321. <https://doi.org/10.1093/plankt/21.12.2309>.
- Weisse, T., B. Gröschl, and V. Bergkemper. 2016. “Phytoplankton Response to Short-Term Temperature and Nutrient Changes.” *Limnologica* 59: 78–89. <https://doi.org/10.1016/j.limno.2016.05.002>.
- Wetzel, R. G., and G. E. Likens. 2000. *Limnological Analyses*. New York, NY: Springer-Verlag.
- Weyhenmeyer, G. A., E. Willén, and L. Sonesten. 2004. “Effects of an Extreme Precipitation Event on Water Chemistry and Phytoplankton in the Swedish Lake Mälaren.” *Boreal Environment Research* 9: 409–420.
- Wickham, H. 2016. *ggplot2: Elegant Graphics for Data Analysis*. New York, NY: Springer-Verlag.
- Yamamichi, M., and A. D. Letten. 2022. “Extending the Gleaner-Opportunist Trade-off.” *Journal of Animal Ecology* 91: 2163–2170. <https://doi.org/10.1111/1365-2656.13813>.
- Yvon-Durocher, G., M. Dossena, M. Trimmer, G. Woodward, and A. P. Allen. 2015. “Temperature and the Biogeography of Algal Stoichiometry.” *Global Ecology and Biogeography* 24: 562–570. <https://doi.org/10.1111/geb.12280>.

### Supporting Information

Additional Supporting Information may be found in the online version of this article.

Submitted 09 July 2024  
Revised 12 November 2024  
Accepted 14 December 2024



## **6 Publication V**

The effects of nutrient pulse scenarios on the  
stoichiometry of a freshwater plankton community  
across sites and seasons

Submitted to *Ecology*

## **The effects of nutrient pulse scenarios on the stoichiometry of a freshwater plankton community across sites and seasons**

Anika Happe<sup>1\*</sup>, Johanna Exner<sup>2</sup>, Bence Buttyán<sup>3,4</sup>, Eleni A. Charmpila<sup>5</sup>, Bence Gergác<sup>3,4</sup>, Clara Mangold<sup>6</sup>, Sebastian Neun<sup>1</sup>, Jimmy Clifford Oppong<sup>7</sup>, Majd Muwafaq Yaqoob<sup>8</sup>, Jens C. Nejstgaard<sup>9</sup>, Stella A. Berger<sup>9</sup>, Silke Langenheder<sup>10‡</sup>, Maren Striebel<sup>1‡</sup>

‡ S. Langenheder and M. Striebel share senior authorship.

<sup>1)</sup> *Institute for Chemistry and Biology of the Marine Environment (ICBM), School of Mathematics and Science, Carl von Ossietzky Universität Oldenburg, Ammerländer Heerstraße 114-118, 26129 Oldenburg, Germany*

<sup>2)</sup> *Department of Biology and Environmental Science, Centre for Ecology and Evolution in Microbial Model Systems (EEMiS), Linnaeus University, Kalmar, Sweden*

<sup>3)</sup> *Eötvös Loránd University, Faculty of Science, Institute of Biology, Egyetem tér 1-3, 1053 Budapest, Hungary*

<sup>4)</sup> *Lund University, Faculty of Science, Department of Biology, Kontaktvägen 10, 223 62 Lund, Sweden*

<sup>5)</sup> *Charles University, Faculty of Science, Department of Ecology, Vinicna 7, 128 00, Prague, Czechia*

<sup>6)</sup> *University of Innsbruck, Department of Ecology, Technikerstraße 25, 6020, Innsbruck, Austria*

<sup>7)</sup> *Charles University, Faculty of Science, Institute for Environmental Studies, Benatska 2, 128 00, Prague, Czechia*

<sup>8)</sup> *University of Debrecen, Faculty of Science and Technology, Institute of Biology and Ecology, Department of Hydrobiology, Debrecen, Hungary*

<sup>9)</sup> *Leibniz Institute of Freshwater Ecology and Inland Fisheries, Department of Plankton and Microbial Ecology, Zur alten Fischerhütte 2, 16775 Stechlin, Germany*

<sup>10)</sup> *Uppsala University, Evolutionsbiologiskt centrum (EBC), Uppsala, Sweden*

## Abstract

Extreme weather events, including heavy rainfalls, are predicted to further increase in frequency and intensity in the coming decades. The associated flushing of colored and non-colored organic matter from terrestrial systems via run-off into lakes contributes to increasingly fluctuating aquatic nutrient and modified light regime with potential impacts for plankton growth and stoichiometry. Lake characteristics, such as the trophic status and level of browning, and seasonality add complexity to the plankton response to run-off events. Therefore, we conducted three identical mesocosm experiments across two sites (that differed in nutrient concentration and watercolor) and seasons during which we added the same total concentration of nitrate, phosphate and colored dissolved organic matter (cDOM) to each mesocosm in pulses of different frequencies (daily, intermittent or one extreme addition) over a simulated run-off period followed by a recovery period. Our results showed a consistent direction of C:nutrient responses in the small seston ( $< 105\mu\text{m}$ ) with increased biomass, lowered C:N and C:P, but increased C:Si ratios across all run-off scenarios and experimental settings. However, seasonal and spatial differences determined the magnitude of responses with the eutrophic lake and spring conditions exhibiting less vulnerability compared to the oligotrophic lake and summer conditions, respectively, in various response variables. Our findings highlight the critical role of trophic status and seasonal dynamics in shaping ecosystem responses to run-off scenarios and thus, the need for multi-site and multi-seasonal approaches to capture the complexity and context-dependency of freshwater ecosystem dynamics.

## Introduction

The impacts of climate change are increasingly evident, with shifts in precipitation and runoff patterns, such as an increase in more frequent and heavy rainfalls, potentially reshaping freshwater ecosystems (IPCC 2023). Although these pulse disturbances are usually of short duration, they often provoke intense short and long-term impacts on the ecosystem (Jentsch et al. 2007; Urrutia-Cordero et al. 2021b; Urrutia-Cordero et al. 2020). For example, extreme precipitation events cause high flushing rates, which diminish light availability through the influx of colored dissolved organic matter (cDOM) (Lyche Solheim et al. 2024; Roulet and Moore 2006) and modify the timing and concentration of essential nutrient and cDOM inputs from terrestrial sources via run-off into aquatic systems (Jeppesen et al. 2009). Such alterations in nutrient availability influence the growth and stoichiometry of primary producers such as phytoplankton (Frost et al. 2023; Sterner and Elser 2002). Phytoplankton stoichiometry i.e., the elemental ratio of carbon (C), nitrogen (N) and phosphorus (P), is an important determinant in

nutrient cycling and energy transfer within aquatic food webs. For higher trophic levels, phytoplankton stoichiometry determines the nutritional quality with low seston C:nutrient ratios usually representing higher-quality prey for zooplankton (De Senerpont-Domis et al. 2014), but too low C:nutrient ratios potentially inducing energy-limitation for consumers (Urabe and Sterner 1996). Increased nutrient input typically decreases seston C:nutrient ratios due to increased nutrient uptake (Elser et al. 2001), whereas species-specific responses and effects of preceding limitation patterns can be expected. Lake characteristics, such as the identity of the limiting nutrient, trophic status and level of browning influence the expected response to perturbations (Burns and Schallenberg 2001; Lyche Solheim et al. 2024). For example, light limitation due to browning can counteract the stimulatory effects of increased nutrient input on phytoplankton growth (Lyche Solheim et al. 2024) and thus, phytoplankton cells shift toward lower cellular C and higher P content (Sterner et al. 1997; Striebel et al. 2008). These stoichiometric shifts cascade through the ecosystem, causing mismatches between producers and consumers, affecting ecological efficiency and the survival of higher trophic levels (Diehl et al. 2022; Hessen et al. 2013). In natural systems, seasonality also adds complexity to the effects as biological and chemical processes can vary significantly between summer and spring due to temperature changes, shifts in light exposure, and alterations in biological activity (Woolway 2023).

Previous experimental studies compared the effects of pulse disturbances across sites (Cottingham and Schindler 2000; Hillebrand et al. 2018) or both seasons and sites (Urrutia-Cordero et al. 2021b; Urrutia-Cordero et al. 2020). In response to disturbances across sites and seasons, functional variables (e.g. biomass and chlorophyll-*a*) showed the same direction, but differences in the magnitude of effects. In contrast, the compositional response was subject to a high context-dependency even in terms of direction of the effect (Urrutia-Cordero et al. 2021b). Furthermore, Cottingham and Schindler (2000) showed a site-dependent resistance of the phytoplankton biomass response to small nutrient and cDOM pulses in systems dominated by large-bodied grazers, such as *Daphnia*, compared to systems with smaller grazers. However, a large nutrient and cDOM pulse led to an inconsistent response pattern in phytoplankton biomass and thus, a lack of buffering, potentially driven by compositional differences of the phytoplankton and grazer community (Cottingham and Schindler 2000).

Whilst the impact of resource availability on phytoplankton community stoichiometry is broadly investigated (e.g., De Senerpont-Domis et al. 2014; Frost et al. 2023), the impacts of fluctuating nutrient inputs, particularly in timing and frequency, are less understood. In a single-site study, Happe et al. (2025b) showed a high vulnerability and long-lasting effects of seston

C:P and N:P ratios but a high stability of seston biomass in response to an extreme nutrient and cDOM pulse compared to multiple smaller pulses. However, the identification of general patterns requires a multi-site and multi-seasonal approach that accounts for context-dependency (Urrutia-Cordero et al. 2021b). Revisiting the response of plankton stoichiometry to different run-off scenarios with a more extensive data set is critical to fundamentally understand how phytoplankton communities respond to specific facets of environmental change, specifically altered rainfall patterns.

To address this research gap and generalize results, we conducted three mesocosm experiments with identical set-ups, spanning two seasons and sites with different trophic states. By manipulating the intensity, chronology and frequency of nutrient and cDOM pulses (i.e., small daily pulses, intermediate irregular pulses, one extreme pulse), but keeping the total amount constant, we mimic potential future run-off scenarios. To assess the recovery and overall ecological vulnerability of plankton stoichiometry, a 20-day simulated run-off period was followed by a 17-day recovery period. This comparative approach across temporal and spatial scales is the first to examine the stoichiometric responses of different seston size classes to variable and cDOM pulses. It explicitly tests the hypothesis that the magnitude, but not the direction (i.e., sign of the mean in the same direction), of effects on seston stoichiometry to the run-off scenarios differs between the seasons and sites. Based on the findings of Happe et al. (2025b), we expect that an extreme run-off event causes long-term disruptions to phytoplankton stoichiometry but only short-term biomass effects, while multiple smaller pulses show a contrasting response with a long-term biomass accumulation and only short-term stoichiometric shifts. For the seasonal and spatial comparisons, we expect seston stoichiometry to be more vulnerable to nutrient and cDOM pulses in an oligotrophic compared to a mesotrophic lake, and in summer compared to spring due to lower nutrient concentrations.

## Methods

### *Description of the study sites*

In this study, three identical mesocosm experiments were conducted across two seasons and sites using the SITES AquaNet infrastructure (Urrutia-Cordero et al. 2021). Lake Erken (59.835 N, 18.632 E) located in Eastern Central Sweden is a mesotrophic clearwater lake with a mean depth of 9 m and a total area of 23 km<sup>3</sup>. About 500 km away, Lake Bolmen (56.9418 N, 13.6409 E) is located in the Southwest of Sweden and represents a humic and oligotrophic lake with a mean depth of 5 m and an area of 173 km<sup>3</sup>. The summer experiments at Lake Bolmen and Erken

lasted from 7th of July to 11th of August 2022, followed by the spring experiment at Lake Erken from 2nd of May to 8th of June 2023.

### *Mesocosm set-up*

At the beginning of each experiment, 16 in-situ polyethylene mesocosms (550 L) were filled with unfiltered lake water. The experimental duration covered a 20-day simulated run-off period and a subsequent 17-day recovery period. By this, we mimic the run-off of water and the contained substances from land surfaces via rivers into lakes following different rainfall patterns. The run-off scenarios were applied as three different nutrient and cDOM pulse treatments with the same total amount of nitrate, phosphate and cDOM: i) multiple small daily pulses (5% of the total amount added in 20 pulses), ii) multiple pulses with irregular frequencies and amounts (5-30% of the total amount added in 7 pulses), iii) one extreme pulse (100% of the total amount added once on day 7), iv) as well as a control without additions (Fig. S1). The pulses of each treatment summed up to an addition of 2 mg L<sup>-1</sup> cDOM, 50 µg L<sup>-1</sup> phosphorus (mainly as KH<sub>2</sub>PO<sub>4</sub>) and 500 µg L<sup>-1</sup> nitrogen (mainly as NaNO<sub>3</sub>). With this, the scenarios differed in their frequency, from one extreme pulse to daily pulses, and in their chronology, covering regular (deterministic) and irregular (stochastic) additions. Each treatment was replicated by 4 which summed up to 16 experimental units per mesocosm experiment.

Sensors were installed to monitor the water temperature and dissolved oxygen concentration (oxygen optode 4531 sensor, Aanderaa Data instruments AS, Bergen, Norway), and turbidity (TriLux sensor, Chelsea Technologies Group, UK) during the experiments. Data on the development of pH was obtained from handheld multiprobe measurements (YSI Exo Sonde, 13M100983) and on photosynthetic photon flux density (PPFD) using a handheld Apogee PAR SQ-500 sensor (389 to 692 nm ± 5 nm, Apogee Instruments Inc., USA). Samples were taken every fourth day to determine dissolved nutrients and stoichiometry. Dissolved phosphorus (as PO<sub>4</sub>-P) was measured using a Metrohm Ion Chromatography system (883 Basic IC Plus), while dissolved nitrogen and dissolved organic carbon (DOC) were measured on a Shimadzu TOC-L TNM-L at 6 selected time points as described in Langenheder et al. (2024). Dissolved silicate was measured photometrically at a wavelength of 810 nm using a microplate reader (SYNERGY H1, BioTek, Bad Friedrichshall, Germany) after the addition of hydrochloric acid, ammonium molybdate, disodium EDTA and sodium sulfite as reagents following Wetzel and Likens (2003). Further details on the experimental design and *in-situ* measurements can be found in Langenheder et al. (2024).



*Stoichiometric analyses*

Water samples for size-fractionated stoichiometry analyses were taken every fourth day resulting in 10 data points. In the first step, the water sample was separated into a small and large size fraction using a 105  $\mu\text{m}$  mesh. Then, the small ( $< 105 \mu\text{m}$ ) and large ( $> 105 \mu\text{m}$ ) size fractions were filtered onto pre-combusted and acid-washed glass microfiber filters (WHATMAN, GF/C filter) for subsequent particulate organic carbon (POC) and nitrogen (PON), and phosphorus (POP) analyses. Additionally, the small size fraction was filtered onto membrane filters (Whatman NC45 membrane filters, cellulose nitrate, 0.45  $\mu\text{m}$ , 25mm diameter; CAT no 10401106) for determining the biogenic silicate (BSi) content. All filters were frozen at  $-20^\circ\text{C}$ .

The POP content collected on the filters was quantified by molybdate reaction after potassium peroxydisulfate digestion (Wetzel and Likens 2003) and measured photometrically at 880 nm (SYNERGY H1, BioTek®). Samples for POC/PON samples were measured using a CHN analyzer (Flash EA 1112, Thermo Fisher Scientific, Waltham, USA). The filters for BSi were oxidised and reagents (molybdate reagent, oxalic acid and ascorbic acid) were added before photometrically measuring the samples in a plate reader (SYNERGY H1, BioTek®) at 810nm (Grasshoff et al. 1999; Happe et al. 2025b).

For the experiment at Lake Erken in summer, one replicate of the daily-pulsed treatment (#2) was excluded from all analyses due to an early wrong addition of nutrients and cDOM, and a subsequent functional deviation from the remaining replicates.

*Nutrient limitation bioassay*

Nutrient limitation bioassays were performed two days after the last experimental nutrient and cDOM addition (day 21) in each mesocosm experiment. Due to personnel limitations at Lake Bolmen, the bioassay with mesocosm water was started after the bioassay with lake water was finished (day 25). For the bioassays, water from the lake and a pooled sample from all four daily-pulsed replicates was filtered over a 105  $\mu\text{m}$  gauze to reduce large grazers and exposed to four nutrient treatments in cell culture bottles (SARSTEDT AG & Co. KG). Treatments comprised an addition of phosphate ( $\text{KH}_2\text{PO}_4$ , 2.46  $\mu\text{g ml}^{-1}$  final concentration), an addition of nitrogen ( $\text{NaNO}_3$ , 24.62  $\mu\text{g ml}^{-1}$  final concentration), an addition of the combination (N+P) in the same concentration and a control treatment without any nutrient addition. The nutrients originated from the same stock that has been used for the mesocosm experiments and were added as a unique pulse at the start of each bioassay. In summary, each set-up consisted of 2 origins of water (lake and daily-pulsed treatment)  $\times$  4 nutrient treatments (N, P, N+P, control)

× 3 replicates and added up to 24 experimental units. The bottles were incubated under natural temperature and light conditions by hanging in the lake at a depth of 20 cm. Each bioassay was terminated after 4 days. During both experiments at Lake Erken, fluorescence was measured daily from each unit using a handheld fluorometer (Turner Designs). For all experiments, particulate carbon (as a proxy for biomass) was measured by filtering a start sample and the whole volume of each bottle at the end onto pre-combusted and acid-washed glass microfiber filters (WHATMAN, GF/C filter). The filters were analyzed as described above. To test for significant differences between the run-off treatments for each water origin and experiment separately, non-parametric Kruskal-Wallis one-way ANOVAs were used due to the violation of the homogeneity of variances in several cases and thus, to use a consistent method across the experiments.

### *Stability calculations*

To follow the patterns of biomass-nutrient ratios and ensure independence of response variables, all stoichiometric C:nutrient ratios (i.e., C:N, C:P for both size fractions, and C:Si for the small size fraction) were calculated as the molar ratios between the particulate nutrient concentrations. For experimental units in the large size fraction where PON concentrations were below detection limit, a value of half of the lowest measured value was assumed for further analyses (Clarke 1998).

To assess the vulnerability of the size fractions to the run-off scenarios, the overall ecological vulnerability (OEV) framework proposed by Urrutia-Cordero et al. (2021a) was used. The OEV indicates the destabilization across the duration of the experiment, which allows us to quantify the ecosystem vulnerability to disturbance by integrating multiple dimensions of stability into one metric (Urrutia-Cordero et al. 2021a). The area under the curve was calculated using the “*pk.calc.au*” function in the PKNCA package (Denney et al. 2015) based on the time series of the log-response ratios (LRR) of the stoichiometric ratios. The LRRs were calculated for each mesocosm as the natural logarithm of the quotient between the treatment unit divided by the mean of the control mesocosms. To test the persistence of the treatment effects, recovery (Hillebrand et al. 2018; Urrutia-Cordero et al. 2021a) was calculated as the LRR of the final sampling point. A value of 0 indicates a full recovery. Recovery was standardized to absolute values prior to all statistical analyses (Hillebrand et al. 2018). To visualize the magnitude of the difference between the sites and seasons,  $\Delta\text{OEV}$  and  $\Delta\text{Recovery}$  were calculated as the absolute difference between the mean value of the respective stoichiometric ratio at Lake Erken in

summer and either Lake Erken in spring (for season) or Lake Bolmen (for site) for each treatment.

### *Statistical analyses*

To assess whether the stoichiometric stability differed significantly between (a) the run-off scenarios and (b) the seasons (or sites), two-way multivariate analyses of variance (MANOVAs) were conducted to analyze the carbon-based response variables for the small (C, C:N ratio, C:P ratio, C:Si ratio) and large size fraction (C, C:N ratio, C:P ratio). Overall, four MANOVAs were performed for each size fraction to account for non-independent response variables: (i) with the OEV for each response variable predicted by the applied run-off scenarios, the season and their interaction using only the two Erken experiments, (ii) the same analysis but based on the recovery for each response variable, (iii) with the OEV for each response variable predicted by the run-off-scenarios, sites and their interaction using only the two summer experiments, and (iv) the same analysis but based on recovery for each response variable. The model assumptions of multivariate normality of data and residuals were evaluated with Mardia's skewness and kurtosis analysis using the “*mvn*” function in the MVN package (Korkmaz et al. 2014) and homoscedasticity was assessed using Levene's tests using the “*leveneTest*” function in the car package (Fox and Weisberg 2019). For significant site-treatment or season-treatment effects, two-way ANOVAs and subsequent post-hoc comparisons were performed to identify pairwise differences between levels of treatments and sites or seasons. For this, the “*emmeans*” package (Lenth 2023) was used to estimate marginal means and pairwise comparisons were conducted using Tukey's Honest Significant Difference (HSD) test, adjusted for multiple comparisons using the Bonferroni correction.

To assess the effects of different nutrient use of phytoplankton between the treatment, the resource efficiency (RUE) across treatments and experiments for nitrogen and phosphorus was calculated based on Hodapp et al. (2019) (see Fig. S. 26-29 for more details).

To estimate the factors driving the effects between sites and seasons, a principal component analysis (PCA) on the environmental parameters measured in the mesocosms throughout the experiment was performed using the packages *factoextra* (Kassambara and Mundt 2020) and *FactoMineR* (Le et al. 2008). The PCA was performed based on time, temperature, photosynthetic photon flux density (PPFD) on the water surface (-5 cm), turbidity, pH, DOC, dissolved nitrogen, dissolved phosphorus (PO<sub>4</sub>-P) and dissolved silicate. The eigenvalues were obtained and their contribution to the principal components was analyzed.

All statistical results were interpreted as significant for a significance level of  $\alpha = 0.05$  and performed using the R statistical environmental version 4.2.3 (R Core Team 2023).

## Results

### *Abiotic conditions during experiments*

The PCA shows a high overlap between sites but a clear distinction between seasons indicating that environmental conditions were more similar between sites at the same season than between seasons at the same site (Fig. 1). Seasonal differences were mostly driven by temperature and dissolved nutrients (N and P). This arises from a mean seasonal temperature difference of  $7.7^{\circ}\text{C}$  (Fig. S2) and substantially lower dissolved nitrogen but higher phosphorus mean concentrations in during the summer experiment ( $0.6 \text{ mg N L}^{-1}$  and  $6.6 \mu\text{g PO}_4 \text{ L}^{-1}$ ) than in the spring experiment ( $630.6 \text{ mg N L}^{-1}$  and  $3.0 \mu\text{g PO}_4 \text{ L}^{-1}$ ) (Fig. S3-4). The spatial differences were largely driven by PPFD, DOC and pH, where Erken is characterized by a lower mean PPFD ( $177 \mu\text{mol m}^{-2}$ ), but higher pH (8.7) and DOC concentration ( $11.6 \text{ mg C L}^{-1}$ ) compared to Bolmen ( $414 \mu\text{mol m}^{-2}$ , pH of 7.8,  $10.7 \text{ mg C L}^{-1}$ ) (Fig. S5-7). However, Bolmen showed a 63 % larger light attenuation coefficient ( $0.0181 \text{ m}^{-2}$ ) compared to Erken ( $0.0111 \text{ m}^{-2}$ ) in summer. The dispersion within experiments was driven by treatment differences i.e., the addition of nutrients and cDOM, and time effects (Fig. S10).

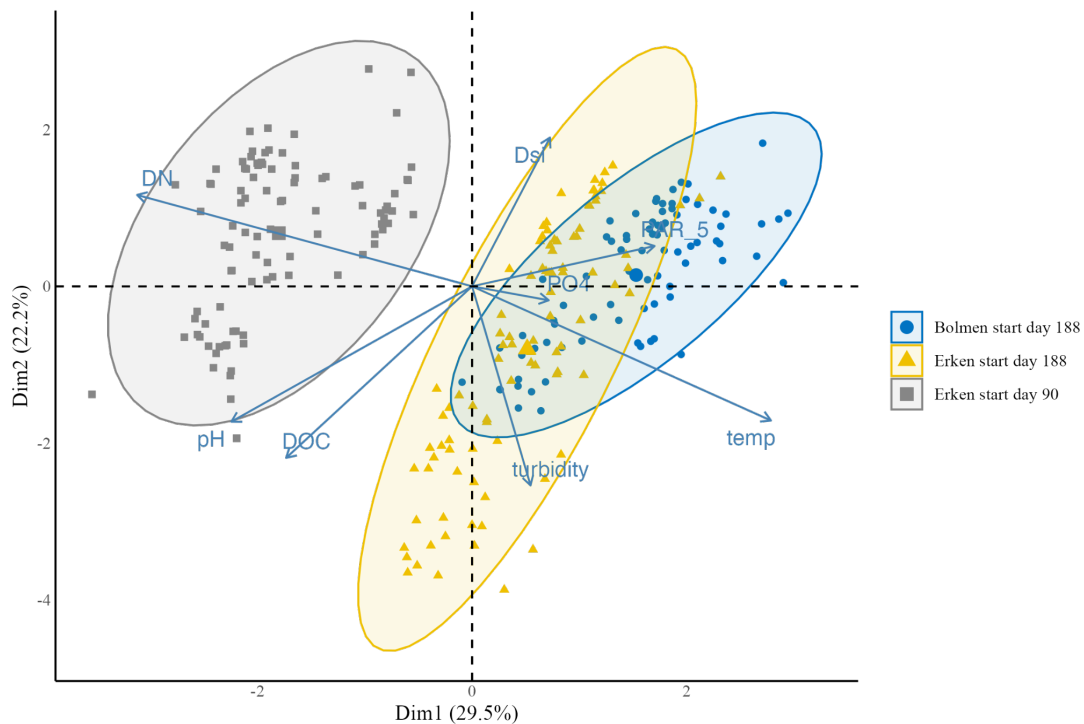


**Figure 1:** Environmental principal component analysis (PCA) of the abiotic conditions during the experiments at Lake Erken and Bolmen in summer (julian day 188) and Lake Erken in spring (julian day 90). Concentration ellipses are given in respective colors (Bolmen summer in blue, Erken in spring grey, Erken in summer yellow).

*Small seston (< 105 µm)*

The small size fraction showed significant main effects for the spatial and seasonal difference of OEV across biomass and all stoichiometric ratios (Table 1). Additionally, for many OEV responses significant interactive effects between the treatments and seasons were found. For recovery, significant main effects of the season were found for C, the C:N ratio and C:Si ratio as well as between-sites effects for the C:P and C:Si ratio (Table 1).

In all experiments (i.e., all sites and seasons), POC fully recovered after the extreme pulse and showed a lower or similar OEV compared to multiple smaller pulses (Fig. 2). Only the Erken summer experiment showed a higher OEV in both multi-pulsed scenarios compared to the extreme pulse, but also compared to Bolmen and the spring experiment. This is also reflected in an overall shift towards higher biomass throughout the course of the experiment (Fig. S12). Hence, the multi-pulse scenarios induced a significantly different response between sites and seasons, with a higher vulnerability in summer compared to spring (Table S2,  $p < 0.001$  for both treatments) and in Erken versus Bolmen (Table S3,  $p = 0.005$  for both treatments).

**Table 1:** MANOVA results for overall ecological vulnerability and recovery of stoichiometric ratios for the **small size fraction (< 105 µm)**.

Overall Ecological Vulnerability (OEV)									
		C		C:N		C:P		C:Si	
	Df	F-value	p-value	F-value	p-value	F-value	p-value	F-value	p-value
Treatment	2	15.027	<0.001 *	42.989	<0.001 *	3.848	0.042 *	2.938	0.080
Season	1	95.661	<0.001 *	58.302	<0.001 *	12.454	0.003 *	142.668	<0.001 *
Interaction	2	19.894	<0.001 *	9.334	0.002 *	0.539	0.593	5.874	0.012 *
Treatment	2	6.052	0.010 *	19.397	<0.001 *	1.252	0.311	1.521	0.247
Site	1	25.150	<0.001 *	6.265	0.023 *	23.237	<0.001 *	56.965	<0.001 *
Interaction	2	4.274	0.031 *	11.263	<0.001 *	0.200	0.821	2.061	0.158
Recovery									
		C		C:N		C:P		C:Si	
	Df	F-value	p-value	F-value	p-value	F-value	p-value	F-value	p-value
Treatment	2	157.248	<0.001 *	7.482	0.005 *	0.393	0.681	4.031	0.037 *
Season	1	6.795	0.018 *	17.963	<0.001 *	0.061	0.808	129.481	<0.001 *
Interaction	2	1.393	0.275	0.937	0.411	13.479	<0.001 *	0.141	0.870
Treatment	2	9.931	0.001 *	0.048	0.954	2.890	0.083	1.458	0.260
Site	1	2.569	0.127	0.013	0.909	14.418	0.001 *	66.866	<0.001 *
Interaction	2	0.968	0.400	0.912	0.421	1.523	0.246	0.132	0.877

The OEV of the particulate C:N ratio depended on season and site, whereas for recovery only seasonal differences were found (Table 1). Summer conditions induced a lower OEV to the extreme (Table S4,  $p < 0.001$ ) and intermittent (Table S4,  $p = 0.003$ ) pulses compared to spring conditions. On the contrary daily pulses showed significant differences between the sites with Bolmen being less vulnerable compared to Erken (Table S5,  $p = 0.003$ ). The  $\Delta$ OEV of the particulate C:P ratio showed a consistent pattern with larger magnitudes of differences between sites compared to seasons across all run-off scenarios (Fig. 2). Within this, Bolmen showed the

highest vulnerability and weakest recovery across all run-off scenarios (Fig. 2) and thus, induced significant site and season effects on OEV and a site effect on recovery (Table 1). For the C:Si ratio, significant spatial and seasonal effects were found for both OEV and recovery (Table 1). This arose from a consistent pattern across all treatments with a significantly lower recovery and higher OEV ( $p < 0.01$  for all combinations, except for the site-dependent OEV to the extreme pulse) in Erken in summer compared with both other settings (Fig. 2, Table S8-9, Table S14-15).

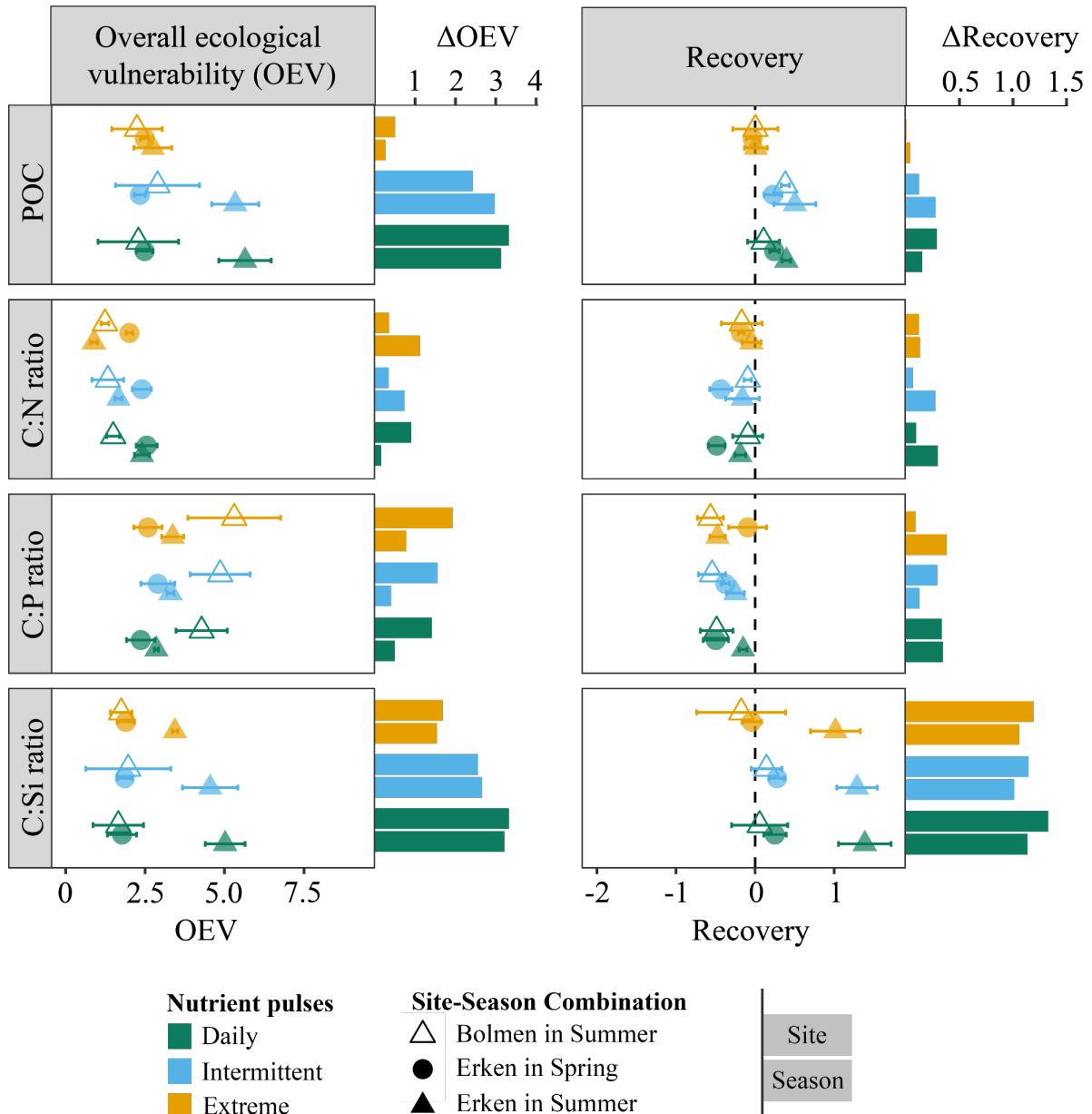


**Figure 2:** Overall ecological vulnerability (OEV) and recovery as functional stability measures of biomass in particulate organic carbon (POC) and molar stoichiometric ratios (C:N ratio, C:P ratio, C:Si ratio) of the **small seston size class** (< 105  $\mu\text{m}$ ). Higher OEV values represent a larger destabilisation over the entire time of the experiments. A recovery value of 0 indicates full recovery. The horizontal bars represent the  $\Delta$ OEV and  $\Delta$ Recovery (absolute difference between the mean value of the respective stoichiometric ratio) as the visualized magnitude of difference between the sites (shapes) and seasons (filled shapes). Colors represent the run-off scenarios. The results for N:P ratios, Si:N ratios and Si:P ratios are presented in Fig. S3.



Overall, a consistent direction of recovery effects (i.e., sign of the mean in the same direction) was found in all but two (out of 39) cases of site and season comparisons. Both exceptions were related to the recovery of the C:Si ratios to the extreme pulse, which was strongly deflected in the Erken summer experiment, whereas the two other experiments showed the opposite sign, but were close to a full recovery (Fig. 2).

#### *Large seston (> 105 $\mu\text{m}$ )*

The large seston showed a less consistent pattern compared to the small size fraction. Whereas Erken showed a significantly higher OEV and lower recovery in response to the multi-pulse scenarios in summer than in spring ( $p < 0.05$  for all combinations, Table S16, Table S18), the extreme pulse led to a consistently low OEV and almost complete recovery during both seasons (Fig. 3). The differences in OEV between the sites followed the same pattern ( $p < 0.02$  for both multi-pulse scenarios, Table S17), but no differences were found after the extreme pulse. The  $\Delta\text{OEV}$  of the C:N ratio showed consistently larger differences between seasons than sites. This mainly arose from a low instability in Erken during summer and a particularly high instability during spring across all treatments (Fig. 3). Despite this, there was full recovery in all treatments in the Erken spring experiment. Both multi-pulse treatments showed significant between-site effects ( $p \leq 0.001$  for both scenarios, Table S24) with opposing directions i.e., Lake Bolmen was deflected towards higher C:N ratios and Lake Erken towards lower C:N ratios compared to control conditions. The OEV of the C:P ratio in response to the extreme pulse was significantly lower in spring than in summer ( $p = <0.001$ , Table S24). This pattern was reversed in both multi-pulse scenarios but only significantly in case of the daily pulses ( $p = <0.001$ , Table S24). No significant differences between sites and seasons were found for the recovery of C:P ratios. However,  $\Delta\text{recovery}$  and  $\Delta\text{OEV}$  point towards a consistently larger difference between seasons than sites.

Overall, the direction of effects on recovery was not consistent in 44% (8 of 18) of site and season comparisons. Most of the different directions of effects are either attributed to insignificant differences close to 0 (4 cases) or to one season being fully recovered, while the other one is deflected (2 cases). However, in the recovery of the C:N ratio to intermittent and daily pulses between sites, a significant difference was found with response in opposing directions (Fig. 3).

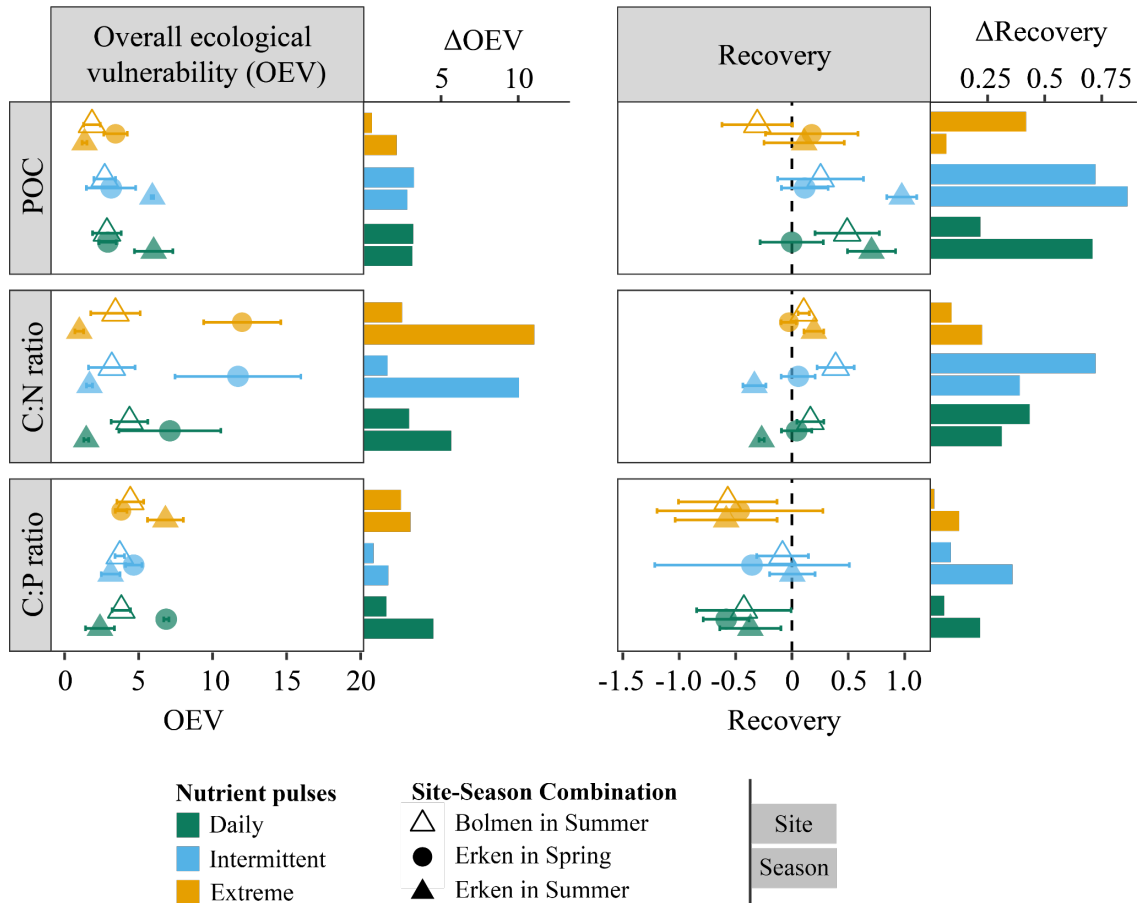
## 6 PUBLICATION V

**Table 2:** MANOVA results for overall ecological vulnerability and recovery of stoichiometric ratios for the large size fraction ( $> 105 \mu\text{m}$ ). The C:N ratio for OEV was log-transformed due to a violation of homoscedasticity.

Overall Ecological Vulnerability (OEV)							
		POC		C:N		C:P	
	Df	F-value	p-value	F-value	p-value	F-value	p-value
Treatment	2	12.262	<0.001 *	1.433	0.266	8.232	0.003 *
Season	1	9.160	0.008 *	222.959	<0.001 *	7.708	0.013 *
Interaction	2	19.056	<0.001 *	4.822	0.022 *	50.355	<0.001 *
Treatment	2	35.795	<0.001 *	2.531	0.109	20.711	<0.001 *
Site	1	39.628	<0.001 *	30.522	<0.001 *	0.286	0.600
Interaction	2	17.044	<0.001 *	1.352	0.285	11.486	<0.001 *

Recovery							
		POC		C:N		C:P	
	Df	F-value	p-value	F-value	p-value	F-value	p-value
Treatment	2	3.995	0.038 *	9.620	0.002 *	1.015	0.383
Season	1	16.768	<0.001 *	11.566	0.003 *	0.429	0.521
Interaction	2	5.966	0.011 *	19.342	<0.001 *	0.422	0.662
Treatment	2	11.562	<0.001 *	13.439	<0.001 *	2.791	0.093
Site	1	5.357	0.035 *	45.008	<0.001 *	0.658	0.430
Interaction	2	0.762	0.484	16.263	<0.001 *	0.413	0.669



**Figure 3:** Overall ecological vulnerability (OEV) and recovery as functional stability measures of biomass in particulate organic carbon (POC) and molar stoichiometric ratios (C:N ratio, C:P ratio) of the **large seston size class** ( $> 105 \mu\text{m}$ ). Higher OEV values represent a larger destabilisation over the entire time of the experiments. A recovery value of 0 indicates full recovery. The horizontal bars represent the  $\Delta\text{OEV}$  and  $\Delta\text{Recovery}$  (absolute difference between the mean value of the respective stoichiometric ratio) as the visualized magnitude of difference between the sites (shapes) and seasons (filled shapes). Colors represent the run-off scenarios. The results for N:P ratios are presented in Fig. S4.

*Nutrient limitation bioassay*

The nutrient limitation bioassay indicates a shift from a tendency towards a nitrogen-phosphorus co-limitation in the lake water to non-limiting nutrient conditions after the simulated run-off scenarios during spring for the mesocosm experiment in Lake Erken (Fig. S11, Table S1). In the Erken summer experiment, the run-off treatments shifted the nutrient conditions from non-limiting for POC towards co-limitation of nitrogen and phosphorus (Fig. S11, Table S1). The Bolmen experiment showed a tendency towards a nitrogen-phosphorus co-limitation in the lake water and phosphorus limitation after the run-off scenarios (Fig. S11, Table S1).

**Discussion***Consistent direction of stoichiometric response to run-off scenarios*

The response direction to the nutrient and cDOM pulses was largely consistent across seasons and sites for the phytoplankton-dominated small seston size class. As hypothesized, a persistent overperformance of biomass (POC) was observed in the multi-pulse scenarios, however, following the extreme pulse, the biomass fully recovered after a short-term peak. Regarding stoichiometry, a tendency for persistently decreased C:N and C:P ratios was found while the C:Si ratios recovered or increased across all run-off scenarios.

The contrasting biomass response between the multi-pulse and the extreme scenarios may be explained by phytoplankton utilizing the supplied resources more efficiently under multiple smaller pulses (Fig. S12), by aligning their nutrient uptake machinery or selecting for species that are most competitive under the given nutrient scenario (Hodapp et al. 2019). As shown for the Erken summer experiment, biomass differences between the nutrient pulse scenarios and the control indicate effects of nutrient availability, while differences between the scenarios were largest between the multi-pulse (i.e., daily and intermittent) and the extreme treatments (Ágreda López 2023). In theory, especially the daily-pulsed scenario may select for species with high maximum uptake rates throughout the simulated run-off period. During the extreme pulse, in turn, species with higher nutrient uptake affinities (i.e., efficiency of nutrient uptake at low concentrations) may prevail after the prolonged pre-pulse phase (Tilman 1982), eventually preventing the community from translating the pulse into proportional biomass increases. Moreover, the extreme pulse likely promoted luxury consumption, as indicated by sharp declines of dissolved phosphorus alongside moderate biomass peaks and decreased C:P ratios after the pulse. Simultaneously, the sudden decrease in light availability after the extreme

cDOM pulse likely counteracted the expected stimulatory effects of nutrient inputs on biomass (Heinrichs et al. 2025; Sterner et al. 1997).

Regarding particulate stoichiometry, the nutrient and cDOM pulses induced the expected reduction in seston C:N and C:P ratios due to the assimilation of nutrients (Tanioka and Matsumoto 2020; Verbeek et al. 2018). Additionally, despite not being tested in the nutrient limitation bioassay (due to logistical limitations), the strong drawdown of dissolved silicate throughout the experiment (Fig. S9) may point towards an emerging silicate limitation. This would explain the increased and non-recovered C:Si ratios, especially during the spring experiment in Erken, as diatoms may have been outcompeted by non-siliceous phytoplankton groups such as chlorophytes or dinoflagellates.

The large size fraction, comprising zooplankton and large phytoplankton or cyanobacteria colonies (e.g., *Gloeotrichia echinulata* during summer in Erken), displayed less consistent responses in POC and C:N ratios, but showed a tendency towards a persistent decrease in C:P ratios in response to the daily and extreme pulses, whereas the recovery to intermittent pulses was more complete. Overall, the large seston size fraction demonstrated higher within-treatment variability of POC and C:P ratios during the recovery in all experiments. This could be explained by the complexity of this size fraction due to the coexistence of multiple trophic levels within the same size class and differences in the community composition between sites and seasons.

Overall, biomass and stoichiometry of the small seston follow the same response direction, independent of seasonal or spatial settings. In contrast, the large seston size fraction displayed less consistent and less unidirectional responses. Even for unidirectional responses across experiments, the magnitudes of the effects often differ and likely depend on seasonal and spatial differences in environmental and biotic conditions.

#### *Seasonal differences moderated by temperature, photoperiod and species succession*

The expected pattern of a higher vulnerability to the nutrient and cDOM pulses in summer compared to spring (based on the Erken experiments) was only confirmed for specific responses to the multi-pulse scenarios. These include a stronger biomass response in both seston size classes, and a gradual shift towards elevated C:Si ratios. Furthermore, both seston size classes showed a higher vulnerability of C:N ratios in spring, whereas a contrasting and treatment-dependent response pattern was found for the C:P ratios of the large size fraction.

The environmental conditions between seasons most strongly differed due to seasonal temperature changes i.e., a steady increase from 4 to 15 °C in spring and a rather constant temperature around 19 °C in summer, the baseline availability of dissolved nutrients and the photoperiod. Higher temperatures not only increase phytoplankton metabolic rates and thus increase the nutrient demand, which amplifies rapid nutrient uptake (Pomati et al. 2017), but also modulate the co-limitation of light and nutrients (Heinrichs et al. 2025). In line, the nutrient and cDOM pulses in summer could only be translated into relatively higher biomass for both seston size classes in the multi-pulse scenarios, as the extreme pulse likely induces a strong light limitation (as discussed above). Interestingly, the multi-pulse scenarios (i.e., daily and intermittent) in summer behaved similarly to each other but contrasted to the extreme pulse regarding effects on phytoplankton biomass as well as diversity and community composition (Ágreda López 2023), highlighting the importance of frequency of run-off events (multiple smaller pulses versus one extreme pulse) against regularity.

Ultimately, the dominant species and their succession may also determine the community response to the nutrient pulses. The typical phytoplankton spring community in Lake Erken is dominated by larger ( $>15\mu\text{m}$ ) and fast-growing diatom species with a highly efficient nutrient use (Ahlgren et al. 1997; Yang et al. 2016). The high nutrient use efficiency of the spring community may be mirrored in the more vulnerable and decreased small seston C:N ratios during spring. Furthermore, the nutrient and cDOM pulses induced a shift in nutrient and light conditions away from those typical for a spring bloom, for example, by preventing the plankton community from developing a typical nutrient limitation. Thus, the phytoplankton species likely optimized their nutrient uptake which can be amplified under gradually increasing temperatures in spring (Anderson et al. 2022) and thus, showed a more pronounced relative decrease in C:N ratios.

The initial summer conditions, in contrast, were dominated by 50% of cryptophytes, followed by around 25% of diatoms (Ágreda López 2023). Over the course of the summer experiment, the cyanobacterium *Gloeotrichia echinulata* bloomed in the large size fraction across all but the extreme treatment (Happe et al. 2025a) due to a preference for high temperatures as reported for previous years (Pettersson et al. 1993; Yang et al. 2016). Simultaneously, *Bacillariophyta* decreased and *Chlorophyta* increased until a strong dominance at the end of the experiment (Ágreda López 2023) in response to the nutrient scenarios (but not in the control) indicating a response to altered resource conditions. This is in line with the shift in C:Si ratios towards the end of the summer experiment, which led to both spatial and seasonal differences.

In the large seston, higher OEV towards lowered C:N ratios in response to intermittent and extreme pulses was found in spring but not in summer. This mirrors the decreased C:N ratios of the small seston during the spring experiment and the differences in nutritional strategies between copepods with higher nitrogen requirements typically dominating in spring (Cowles et al. 1988) and mesozooplankton typically dominating in summer, like cladocerans that prefer P-rich phytoplankton (Andersen and Hessen 1991). However, in spring, the C:N ratios were recovered at the end of the experiment, whereas the summer experiment showed pronounced deflections. The cyanobacterium *G. echinulata* that dominated the large size fraction in the multi-pulse scenarios during the summer experiment is a nitrogen fixer (Cottingham et al. 2015), in line with persistently decreased C:N ratios coupled with a strong large seston biomass increase opposing fully recovered conditions of the same metrics in spring.

*Spatial differences: Lake characteristics may suppress responses*

As hypothesized, oligotrophic Bolmen showed a consistently higher vulnerability of small seston C:P ratios following the run-off scenarios. Contrary to our hypothesis, however, mesotrophic Erken showed a higher vulnerability of C:Si ratios, and more strongly increased biomass of both size classes in the multi-pulse scenarios. Generally, the site with the highest OEV to the pulses in a given response variable was also further deflected from a full recovery.

Above all, previous studies identified the trophic status and turbidity as the largest difference in lake characteristics between Bolmen and Erken (Urrutia-Cordero et al. 2021), whereas the differences in the summer experiments mainly arose from light intensity, DOC concentration and pH. Importantly, the concentration of dissolved nutrients between lakes at the time of the experiment did not strongly differ. Additionally, differences in baseline community composition shaped the response with the largest difference between Erken and Bolmen being the typical *Gloeotrichia* bloom in Erken during summer (Pettersson 1990). Oligotrophic lakes, like Bolmen, are expected to be more vulnerable to nutrient inputs than mesotrophic or eutrophic lakes since even small nutrient pulses represent proportionally large changes under low baseline conditions (Reinl et al. 2021). In contrast, the small seston biomass only showed a moderate response to the run-off scenarios in Bolmen, while the biomass in Erken strongly responded to the multi-pulse scenarios in summer. This suggests that a second environmental parameter, likely the high level of browning and the associated shift in the light intensity and spectrum suppressed the stimulatory effect of nutrient inputs on seston biomass in Bolmen in summer. The extreme nutrient and cDOM pulse induced a sudden decrease in light availability which likely induced a shift towards light-limitation (Deininger et al. 2017; Seekell et al. 2015)



and suppressed the phytoplankton biomass equally across both lakes. In Bolmen, however, the combination of a high light attenuation coefficient alongside spectral limitation due to its high level of browning (Klante et al. 2021) likely functioned as a physiological bottleneck which prevented phytoplankton from utilizing multiple smaller nutrient inputs to increase biomass. This is in line with a Swedish multi-lake experiment showing that the positive effects of nitrogen are weaker or neutralized with increased level of browning (Deininger et al. 2017). Generally, spectral selectivity for the absorption of blue light by cDOM (Thrane et al. 2014) directly overlaps with peak absorption capabilities of many phytoplankton species (Clementson and Wojtasiewicz 2019) with blue light typically leading to highest community growth rates (Hintz et al. 2021). Thus, the high degree of browning in Bolmen (Klante et al. 2021) created a spectral environment forcing phytoplankton to utilize energetically less efficient red-green wavelengths (Hintz et al. 2021). This spectral mismatch and reduction in light availability likely limited carbon assimilation, and the prevailing nitrogen-phosphorus co-limitation potentially pushed phytoplankton to rapidly assimilate phosphorus (proportionally more than carbon) following the pulses which is reflected in more vulnerable and strongly lowered C:P ratios in the small seston in Bolmen. The higher importance of phosphorus (relative to nitrogen) in the system is also evidenced by a phosphorus limitation after the run-off scenarios (Fig. S11) which explains the smaller response magnitude of C:N ratios.

Overall, the community in oligotrophic but browning-influenced Bolmen was more vulnerable to nutrient pulses than mesotrophic and clear Erken regarding C:P ratios, but not in terms of the C:N ratio, C:Si ratio and biomass. This highlights that despite its relatively low nutrient concentrations, the plankton response underlies a high context-dependency involving the interaction of further lake characteristics, such as the level of browning or prevailing limitation patterns, and biotic dynamics in Bolmen. Additionally, cDOM pulses naturally impose complex responses by causing light limitation while increasing the nutrient availability.

## Conclusion

Our findings emphasize the critical role of lake characteristics, seasonal dynamics and biotic dynamics in shaping ecosystem responses to nutrient pulses. We show that biomass and stoichiometric responses in small seston follow the same direction, independent of seasonal or spatial settings, whereas the large seston size fraction displayed a less consistent response pattern. Generally, the environmental conditions differed more strongly between seasons than between lakes, but still differences in response magnitudes were revealed on both scales.

Although oligotrophic systems, such as Lake Bolmen, with their limited nutrient reserves, may be particularly vulnerable to such perturbations, an overlying browning-induced light limitation can act as a natural buffer against increased run-off from heavy rainfall events. Seasonal differences are likely driven by species succession, differences in temperature and photoperiod or seasonal nutrient limitation patterns which may be delayed due to run-off events during a spring bloom or alleviated early-on in summer. Further environmental parameters, such as temperature or PAR, can intensify plankton responses to changed nutrient dynamics.

Our results can help to predict ecosystem stability under future scenarios of increased precipitation, extreme events and nutrient run-off driven by climate change. By demonstrating the context-dependency of stoichiometric responses, this study also underscores the need for multi-site and multi-seasonal approaches to capture the complexity of freshwater ecosystem dynamics. Investigating these effects across temporal and spatial scales is essential for the development of dynamic and effective restoration strategies adapted to specific ecosystems and seasonal conditions, therefore maintaining the functional stability of lake ecosystems in the face of environmental change.

### **Acknowledgements**

We would like to thank everyone who participated in the mesocosm experiments at Lake Erken and Bolmen. This study has been made possible by the Swedish Infrastructure for Ecosystem Science (SITES), in this case at the Erken Laboratory and the Bolmen Research Station, and the EU H2020-INFRAIA project (No. 871081) AQUACOSM-plus Network of Leading Ecosystem Scale Experimental AQUatic MesoCOSM Facilities Connecting Rivers, Lakes, Estuaries and Oceans in Europe and beyond - awarded by the European Commission to JCN, SAB, SL and MS. SITES receives funding through the Swedish Research Council under grant no 2017-00635. AH, SAB and JCN were directly supported by AQUACOSM-plus, while BG, BB, JCO, MM and EC were supported by the Transnational Access program of the EU H2020-INFRAIA project (No. 871081) AQUACOSM-plus. AH was supported by a DAAD (German Academic Exchange Service) research grant for doctoral candidates (No. 57556281).

**Open research statement:** All data used in this study is openly available on PANGAEA as Happe et al. (2024), Happe et al. (2025a) and in the SITES AquaNet data portal (<https://data.fieldsites.se/portal/>). The R scripts to analyze the data are openly available on GitHub ([https://github.com/AnikaHappe/SITES\\_RunOff\\_Comparison](https://github.com/AnikaHappe/SITES_RunOff_Comparison)).

## References

- Ágreda López, G. 2023. Are legacy effects important for the response of phytoplankton communities to nutrient and dissolved organic matter pulses? Uppsala Universiteit.
- Ahlgren, G., W. Goedkoop, H. Markensten, L. Sonesten, and M. Boberg. 1997. Seasonal variations in food quality for pelagic and benthic invertebrates in Lake Erken - the role of fatty acids. *Freshwater Biol* **38**: 555-570.
- Andersen, T., and D. O. Hessen. 1991. Carbon, nitrogen, and phosphorus content of freshwater zooplankton. *Limnology and Oceanography* **36**: 807-814.
- Anderson, S. I. and others 2022. The interactive effects of temperature and nutrients on a spring phytoplankton community. *Limnol. Oceanogr.* **67**: 634-645.
- Burns, C. W., and M. Schallenberg. 2001. Short-term impacts of nutrients, *Daphnia*, and copepods on microbial food-webs of an oligotrophic and eutrophic lake. *New Zealand Journal of Marine and Freshwater Research* **35**: 695-710.
- Clarke, J. U. 1998. Evaluation of censored data methods to allow statistical comparisons among very small samples with below detection limit observations. *Environ Sci Technol* **32**: 177-183.
- Clementson, L. A., and B. Wojtasiewicz. 2019. Dataset on the absorption characteristics of extracted phytoplankton pigments. Data in Brief **24**: 103875.
- Cottingham, K., and D. E. Schindler. 2000. Effects of grazer community structure on phytoplankton response to nutrient pulses. *Ecology* **81**: 183-200.
- Cottingham, K. L., H. A. Ewing, M. L. Greer, C. C. Carey, and K. C. Weathers. 2015. Cyanobacteria as biological drivers of lake nitrogen and phosphorus cycling. *Ecosphere* **6**: 1-19.
- Cowles, T. J., R. J. Olson, and S. W. Chisholm. 1988. Food selection by copepods: discrimination on the basis of food quality. *Marine Biology* **100**: 41-49.
- De Senerpont-Domis, L. N., D. B. Van de Waal, N. R. Helmsing, E. Van Donk, and W. M. Mooji. 2014. Community stoichiometry in a changing world: combined effects of warming and eutrophication on phytoplankton dynamics. *Ecology* **95**(6): 1485-1495.
- Deininger, A., C. L. Faithfull, and A. K. Bergström. 2017. Phytoplankton response to whole lake inorganic N fertilization along a gradient in dissolved organic carbon. *Ecology* **98**: 982-994.
- Denney, W., S. Duvvuri, and C. Buckeridge. 2015. Simple, Automatic Noncompartmental Analysis: The PKNCA R Package. *Journal of Pharmacokinetics and Pharmacodynamics*.
- Diehl, S., S. A. Berger, W. Uszko, and H. Stibor. 2022. Stoichiometric mismatch causes a warming-induced regime shift in experimental plankton communities. *Ecology* **103**: e3674.
- Elser, J. J., K. Hayakawa, and J. Urabe. 2001. Nutrient limitation reduces food quality for zooplankton: *Daphnia* response to seston phosphorus enrichment. *Ecology* **82**: 898-903.
- Fox, J., and S. Weisberg. 2019. *An R Companion to Applied Regression*, 3rd Edition. Thousand Oaks CA: Sage.
- Frost, P. C. and others 2023. Interactive effects of nitrogen and phosphorus on growth and stoichiometry of lake phytoplankton. *Limnol. Oceanogr.* **9999**: 1-13.
- Grasshoff, K., K. Kremling, and M. Ehrhardt. 1999. *Methods of Seawater Analysis*.
- Happe, A. and others 2025a. The stoichiometric response of a freshwater plankton community to different nutrient pulse scenarios: A comparison across sites and seasons [dataset]. *In* PANGAEA [ed.].
- Happe, A. and others 2025b. Nutrient pulse scenarios drive contrasting patterns in the functional stability of freshwater phytoplankton. *Limnology and Oceanography*.

- Happe, A., B. Gergácz, B. Buttyán, S. Neun, and M. Striebel. 2024. The stoichiometric response of a freshwater plankton community to different rainfall scenarios.
- Heinrichs, A. L., A. Happe, A. M. Koussoroplis, H. Hillebrand, J. Merder, and M. Striebel. 2025. Temperature-dependent responses to light and nutrients in phytoplankton. *Ecology* **106**: e70027.
- Hessen, D. O., J. J. Elser, R. W. Sterner, and J. Urabe. 2013. Ecological stoichiometry: An elementary approach using basic principles. *Limnol. Oceanogr.* **58**: 2219-2236.
- Hillebrand, H., S. Langenheder, K. Lebet, E. Lindstrom, O. Ostman, and M. Striebel. 2018. Decomposing multiple dimensions of stability in global change experiments. *Ecol Lett* **21**: 21-30.
- Hintz, N. H., M. Zeising, and M. Striebel. 2021. Changes in spectral quality of underwater light alter phytoplankton community composition. *Limnology and Oceanography* **66**: 3327-3337.
- Hodapp, D., H. Hillebrand, and M. Striebel. 2019. “Unifying” the concept of resource use efficiency in ecology. *Frontiers in Ecology and Evolution* **6**.
- IPCC. 2023. Climate change 2023. Synthesis report. Summary for policymakers.
- Jentsch, A., J. Kreyling, and C. Beierkuhnlein. 2007. A new generation of climate change experiments: events, not trends. *Front. Ecol. Environ.* **5**: 315-324.
- Jeppesen, E. and others 2009. Climate change effects on runoff, catchment phosphorus loading and lake ecological state, and potential adaptations. *J Environ Qual* **38**: 1930-1941.
- Kassambara, A., and F. Mundt. 2020. factoextra: Extract and Visualize the Results of Multivariate Data Analyses. R package version 1.0.7, <https://CRAN.R-project.org/package=factoextra>.
- Klante, C., M. Larson, and K. M. Persson. 2021. Brownification in Lake Bolmen, Sweden, and its relationship to natural and human-induced changes. *J Hydrol-Reg Stud* **36**.
- Korkmaz, S., D. Goksuluk, and G. Zararsiz. 2014. MVN: An R Package for Assessing Multivariate Normality. *The R Journal* **6**: 151-162.
- Langenheder, S. and others 2024. SITES AquaNet - AQUACOSM-plus run off variability experiment. <https://doi.org/10.23700/KKFA-HY54>.
- Le, S., J. Josse, and F. Husson. 2008. FactoMineR: An R Package for Multivariate Analysis. *Journal of Statistical Software* **25**: 1-18.
- Lenth, R. 2023. emmeans: Estimated Marginal Means, aka Least-Squares Means. R package version 1.8.4-1, <https://CRAN.R-project.org/package=emmeans>.
- Lyche Solheim, A. and others 2024. Lake browning counteracts cyanobacteria responses to nutrients: Evidence from phytoplankton dynamics in large enclosure experiments and comprehensive observational data. *Glob Chang Biol* **30**: e17013.
- Pettersson, K. 1990. The Spring Development of Phytoplankton in Lake Erken - Species Composition, Biomass, Primary Production and Nutrient Conditions - a Review. *Hydrobiologia* **191**: 9-14.
- Pettersson, K., E. Herlitz, and V. Istánovics. 1993. The role of *Gloeotrichia echinulata* in the transfer of phosphorus from sediments to water in Lake Erken. *Hydrobiologia* **253**: 123-129.
- Pomati, F., B. Matthews, O. Seehausen, and B. W. Ibelings. 2017. Eutrophication and climate warming alter spatial (depth) co-occurrence patterns of lake phytoplankton assemblages. *Hydrobiologia* **787**: 375-385.
- R Core Team. 2023. R: A language and environment for statistical computing. R Foundation for Statistical Computing, Vienna, Austria. URL <https://www.R-project.org/>.
- Reinl, K. L. and others 2021. Cyanobacterial blooms in oligotrophic lakes: Shifting the high-nutrient paradigm. *Freshwater Biol* **66**: 1846-1859.
- Roulet, N., and T. R. Moore. 2006. Browning the waters. *Nature* **444**: 283-284.

- Seekell, D. A. and others 2015. The influence of dissolved organic carbon on primary production in northern lakes. *Limnology and Oceanography* **60**: 1276-1285.
- Sterner, R. W., and J. J. Elser. 2002. *Ecological stoichiometry: The biology of elements from molecules to the biosphere*. Princeton University Press.
- Sterner, R. W., J. J. Elser, J. F. Everett, S. J. Guildford, and T. H. Chrzanowski. 1997. The light:nutrient ratio in lakes: the balance of energy and materials affects ecosystem structure and process. *The American Naturalist* **150**: 663-684.
- Striebel, M., G. Spörl, and H. Stibor. 2008. Light-induced changes of plankton growth and stoichiometry: Experiments with natural phytoplankton communities. *Limnology and Oceanography* **53**: 513-522.
- Tanioka, T., and K. Matsumoto. 2020. A meta-analysis on environmental drivers of marine phytoplankton C : N : P. *Biogeosciences* **17**: 2939-2954.
- Thrane, J. E., D. O. Hessen, and T. Andersen. 2014. The Absorption of Light in Lakes: Negative Impact of Dissolved Organic Carbon on Primary Productivity. *Ecosystems* **17**: 1040-1052.
- Tilman, D. 1982. Resource competition and community structure. *Monogr. Pop. Biol.* **17**.
- Urabe, J., and R. W. Sterner. 1996. Regulation of herbivore growth by the balance of light and nutrients. *Proc. Natl. Acad. Sci.* **93**: 9465-8469.
- Urrutia-Cordero, P. and others 2021a. Integrating multiple dimensions of ecological stability into a vulnerability framework. *Journal of Ecology* **00**: 1-13.
- Urrutia-Cordero, P. and others 2021b. Functionally reversible impacts of disturbances on lake food webs linked to spatial and seasonal dependencies. *Ecology* **102**: e03283.
- Urrutia-Cordero, P., H. Zhang, F. Chaguaceda, H. Geng, and L. A. Hansson. 2020. Climate warming and heat waves alter harmful cyanobacterial blooms along the benthic-pelagic interface. *Ecology* **101**.
- Urrutia-Cordero, P. and others 2021. SITES AquaNet: An open infrastructure for mesocosm experiments with high frequency sensor monitoring across lakes. *Limnology and Oceanography: Methods* **19**: 385-400.
- Verbeek, L., A. Gall, H. Hillebrand, and M. Striebel. 2018. Warming and oligotrophication cause shifts in freshwater phytoplankton communities. *Glob. Change Biol.* **24**: 4532-4543.
- Wetzel, R. G., and G. E. Likens. 2003. *Limnological analyses*. Springer-Verlag, New York, New York, USA.
- Woolway, R. I. 2023. The pace of shifting seasons in lakes. *Nature Communications* **14**.
- Yang, Y., K. Pettersson, and J. Padisák. 2016. Repetitive baselines of phytoplankton succession in an unstably stratified temperate lake (Lake Erken, Sweden): a long-term analysis. *Hydrobiologica*: 211-227.





## **7 Synthesis**

## 7 SYNTHESIS

By integrating long-term monitoring data with targeted experiments, this thesis aimed to unravel the effects of a wide range of facets of climate change on phytoplankton community functioning (Fig. 7.1). After assessing phytoplankton long-term trends within a whole-ecosystem perspective (*publication I*), experimentally derived mechanistic insights into the impact of relevant environmental drivers on phytoplankton performance (*publication II-V*) form the basis to explain causes and consequences of these long-term trends.

Overall, *publication I* highlighted the current status of phytoplankton relative to other ecosystem components in the natural environment. Whereas fish and zooplankton demonstrated overall decreasing population trends, phytoplankton showed as many positive as negative population trends but dominated the significantly decreasing classes. Overall, this clearly showed a drastic reorganization of coastal communities, including phytoplankton, which supports previous findings of a massive restructuring of phytoplankton biodiversity (van Beusekom et al. 2019, Di Cavalho et al. 2023) and traits (Hillebrand et al. 2022). These alterations are strongly linked to a multitude of changing abiotic parameters. By mimicking and manipulating various factors of environmental change, such as the temperature level (*publication II*), the rate of temperature change, the temporal sequence of stressors, the ratio of dissolved nitrogen to phosphorus (*publication III*), or the amplitude and frequency of nutrient and cDOM inputs (*publication II and IV*), this thesis encompasses often overlooked facets of environmental change.

The following synthesis will integrate the results derived from the previous chapters by highlighting overarching patterns of climate change effects on phytoplankton biomass and growth (*chapter 7.1*), and stoichiometry (*chapter 7.2*), transferring the mechanistic insights to observational findings on the ecosystem scale (*chapter 7.3*) and linking the results to food-web implications (*chapter 7.4*). Finally, methodological potentials for monitoring and experimental studies will be outlined to manage phytoplankton changes caused by climate change more efficiently (*chapter 7.5*). Throughout the synthesis sub-chapters, particular emphasis will be placed on highlighting the key outcomes relevant to the thesis objectives: to (1) mechanistically address the effects of various facets of future temperature and nutrient changes in moderating phytoplankton community biomass and stoichiometry; (2) map phytoplankton change in a whole-ecosystem perspective and identify potential effect on trophic dynamics; (3) and address methodological issues in observational and experimental studies focusing on phytoplankton responses to climate change.

## 7 SYNTHESIS

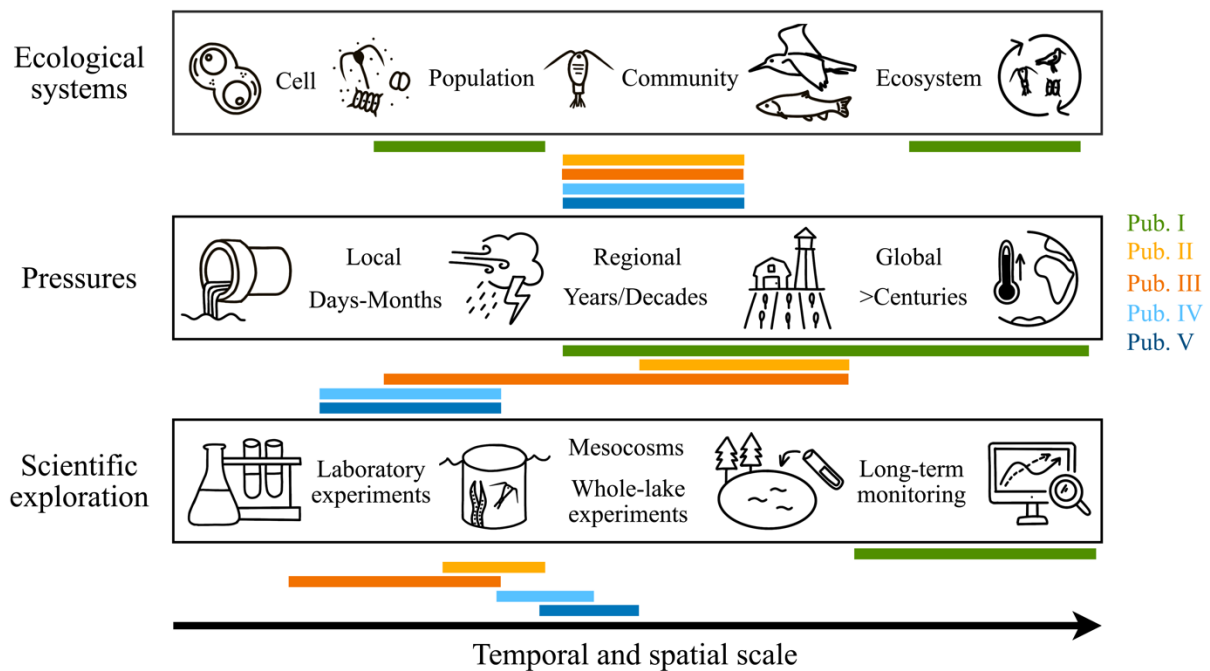


**Fig. 7.1:** Scales of ecological systems, pressures and scientific exploration addressed in this thesis. Ecological systems range from biochemical reactions on cell-level over populations of small, short-lived organisms to communities and larger organisms (such as birds and fish) to the entire ecosystem perspective. Pressures act on local scales (such as wastewater outlets), on regional scale (such as extreme events and agricultural use of fertilizers) and with climate change on the global scale. Scientific studies explore the responses of ecological systems to these pressures, for example, in laboratory experiments, mesocosm studies, whole-lake experiments or via long-term monitoring and time series analyses. Along these scales, the complexity and realism that these scientific approaches address increases. The scales covered by each publication are highlighted by color. Modified after Petersen et al. (2009).

### 7.1 Mechanistic effects on phytoplankton biomass and growth across studies

*Publications II-V* provide mechanistic insights into the phytoplankton community biomass and growth performance across various facets of temperature and nutrient change (Table 7.1). Warming increased community biomass (*publication II*) and community-averaged growth rates if the experimental temperature was manipulated abruptly (*publication III*). In contrast, if the temperature was gradually increased, warming did not enhance community-averaged growth rates (*publication III*). Kremer et al. (2018) proposed that a temperature increase can lead to a temporary growth overshoot at organismal scales, and here I confirmed the same mechanism for communities, likely complemented by shifts in community composition. Further, a balanced macronutrient supply ratio (N:P) enhanced community growth rates, which decreased with nutrient limitation (*publication III*). Adding nutrients before warming increased the community growth rate, whereas adding nutrients after warming reversed this effect to decreasing community growth rates (*publication III*). In line with the findings of temperature-oligotrophication experiments by Verbeek et al. (2018), this is likely attributed to the generally low phosphorus concentration in this experiment prior to warming, which subsequently was

fully depleted after the temperature change, pushing the community towards a collapse in which the increased metabolic rates could not be sustained. Regarding the frequency and intensity of nutrient input into aquatic systems (*publication IV*), an extreme nutrient pulse (contrary to multiple smaller pulses) revealed a short, unsustainable biomass increase which may be explained by lower resource use efficiency in this extreme scenario.

The drivers manipulated in *publication II-IV* – temperature and nutrients – are also the strongest moderators of seasonal changes at the spring-summer transition assessed in *publication V*, aligning with studies in freshwater (Zhang et al. 2021, Hung et al. 2024) and marine environments (Wiltshire et al. 2015). However, the dominance of temperature and nutrients as drivers of phytoplankton performance is only applicable from spring to summer when the photoperiod is not suppressing growth (Wiltshire et al. 2015), suggesting that the winter-spring and autumn-winter transitions are predominantly governed by light availability. In *publication V*, the elevated temperature and low nitrogen concentrations in summer led to a higher biomass vulnerability, manifested as a stronger increase, in response to the run-off scenarios (applied as nutrient and cDOM pulses) than in spring. Higher water temperatures in summer stimulate phytoplankton metabolism and nutrient demand (Marañón et al. 2018), leading to nutrient depletion that makes summer communities highly responsive in terms of growth and biomass to nutrient pulses from run-off (Fernández-González et al. 2022).































## 7.2 Mechanistic effects on phytoplankton community stoichiometry across studies

Beyond phytoplankton as food quantity (biomass), *publications II-V* provide mechanistic insights into its nutritional quality for higher trophic levels. To link the responses of phytoplankton community stoichiometry to environmental change (objective 1), it is featured throughout all experimental studies in this thesis (*publication II-V*) summarized in Table 7.1. By subsequently associating the mechanistic responses to those drivers as a moderator of seasonal differences (*chapter 7.3*, based on *publication V*) and as long-term climate change drivers (*chapter 7.3*, based on *publication I*), I demonstrate the diverse effects of warming and nutrient dynamics on phytoplankton community stoichiometry.

The identified effects on phytoplankton community stoichiometry comprise stoichiometric plasticity on the cellular level (Yvon-Durocher et al. 2015) and changes in community composition with associated phylogenetic differences in macromolecular composition (Rhee and Gotham 1980, Finkel et al. 2009, Finkel et al. 2016).

## 7 SYNTHESIS

**Table 7.1:** Overview of the phytoplankton stoichiometric (carbon:nitrogen ratios, carbon:phosphorus ratios and nitrogen:phosphorus ratios) and growth ( $\mu$ ) response to various driver facets of temperature and nutrients based on the publications presented in this thesis. A positive effect is represented by a green circle (+), a negative effect is shown by an orange circle (-), a grey circle indicates no effect, and an empty space represents that the respective combination has not been tested or is too highly interactive to be displayed here.

Driver	C:N	C:P	N:P	$\mu$
Warming	 <i>Pub. II-III</i>	 <i>Pub. II-III</i>	 <i>Pub. III</i>	 <i>Pub. III</i> (at abrupt exposure at nutrient repletion)  <i>Pub. III</i> (at gradual exposure at nutrient repletion)
Rate of warming	 <i>Pub. III</i>	 <i>Pub. III</i>	 <i>Pub. III</i>	 <i>Pub. III</i> (at abrupt exposure)
N:P supply ratio		 <i>Pub. III</i> (Saturation func.)	 <i>Pub. III</i>	 <i>Pub. III</i> (at balanced ratios and no limitation)
N limitation	 <i>Pub. III</i> (if nutrients added before warming)	 <i>Pub. III</i>	 <i>Pub. III</i>	 <i>Pub. III</i>
P limitation	 <i>Pub. III</i> (if nutrients added before warming)	 <i>Pub. III</i>	 <i>Pub. III</i>	 <i>Pub. III</i>
Nutrient addition before (versus after) temperature change	 <i>Pub. III</i>	 <i>Pub. III</i>	 <i>Pub. III</i> N limitation  <i>Pub. III</i> P limitation, 18°C  <i>Pub. III</i> P limitation, 6°C Balanced supply	 <i>Pub. III</i>
Extreme nutrient and cDOM pulse (versus multiple pulses)	 <i>Pub. IV</i>  <i>Pub. V</i> (Lake Bolmen)	 <i>Pub. IV-V</i>	 <i>Pub. IV</i>	

In *publication II and III*, I showed that phytoplankton stoichiometry remained generally stable in response to warming. For C:N ratios, this is in line with previous studies on phytoplankton populations (Tanioka and Matsumoto 2020, and references therein) and communities (Yvon-Durocher et al. 2017, Verbeek et al. 2018) which can be attributed to the close correlation between carbon assimilation and nitrogen uptake in addition to the relatively limited capacity of many phytoplankton species to store excess nitrogen (Frost et al. 2023). For the C:P ratio, however, previous studies showed an increase (Toseland et al. 2013, Yvon-Durocher et al. 2017, Tanioka and Matsumoto 2020) in response to warming, thus contrasting the here found stable C:P ratios in *publication II and III*. As these stable C:P ratios in response to warming occurred across diverse nutrient scenarios (*publication III*), the prevailing phosphorus limitation in *publication II* can be excluded as a reason for this discrepancy, fostering further investigation towards possible explanations based on the growth phase or community shifts. In accordance with the absence of a temperature effect on stoichiometry, the rate of temperature change did not affect phytoplankton stoichiometry either (*publication III*). However, in natural systems, warming induces an additional indirect effect on phytoplankton stoichiometry by increasing

## 7 SYNTHESIS

stratification and thus, reducing nutrient transport to surface waters (Bopp et al. 2013, Boyd et al. 2015).

In terms of nutrients as a driver, I tested the effects of N:P supply ratios and associated limitation patterns (*publication III*), the timing of nutrient input relative to warming (*publication III*) and the effect of different nutrient pulse scenarios (*publication IV-V*) on phytoplankton community performance. The stoichiometric responses induced by nitrogen and phosphorus limitation are in line with a meta-analysis on population level by Tanioka and Matsumoto (2020) finding a general increase in C:N ratios and no effect on C:P ratios under nitrogen limitation, but an increase in both C:nutrient ratios under phosphorus limitation (*publication III*). Under reduced phosphorus concentrations, both cellular macronutrient pools decrease (Tanioka and Matsumoto 2020) suggesting an impaired protein synthesis due to its dependency on ribosomes. Vice versa, under nitrogen limitation, cellular P concentration is unaffected as only downstream protein synthesis (high N demand) is impaired, resulting in stable C:P ratios but increasing C:N ratios. Similarly, the correlation of macronutrient availability and its respective intracellular pool is reflected in a decreased N:P ratio under N limitation and vice-versa as well as in increased phytoplankton C:P and N:P ratios with increasing N:P supply ratios (*publication III*). Moreover, making nutrients available before warming (versus after) results in lower phytoplankton C:N and C:P ratios (*publication III*) arising from a more balanced uptake of nutrients in relation to carbon if nutrients are available during a temperature increase (Armin and Inomura 2021). In contrast, phytoplankton experiencing warming without sufficient nutrients may continue to fix carbon, resulting in unbalanced cellular C:nutrient pools. For the phytoplankton N:P ratio, however, complex interactions with nutrient levels and temperature were found in response to the timing of nutrient input (*publication III*). When nutrients were applied as pulses, an extreme pulse triggered fast phytoplankton growth which increases the demands for carbon and phosphorus (Elser et al. 2003), whereas cellular nitrogen concentrations remained constant, leading to higher C:N ratios, no effect on C:P ratios and lower N:P ratios in Lake Erken (*publication IV-V*).

Generally, the various tested dimensions of nutrient dynamics impacted phytoplankton community stoichiometry more broadly than temperature. However, beyond the single-driver responses displayed in Table 7.1, multiple two-fold and three-fold interactions between the different facets of temperature and nutrient manipulations exist. For example, the addition of nutrients before (versus after) temperature change only lowered phytoplankton N:P ratios under phosphorus-limited conditions at ambient temperature but reversed this effect under high temperatures (*publication III*, Table 7.1). Overall, these mechanistic insights into phytoplankton



community stoichiometry underline the manifold facets of temperature and nutrient dynamics beyond classically tested single drivers, such as temperature level and nutrient concentrations, and highlight the complexity of how environmental drivers affect the functioning of natural communities.

### 7.3 Transferring mechanistic effects to the ecosystem scale

In *publication II-V*, I investigated natural phytoplankton communities in controlled laboratory and mesocosm systems and thereby covered broad experimental and ecological scales towards more realism (Fig. 7.1). Further, I experimentally simulated naturally possible environmental scenarios that despite seeming abstract if applied in controlled systems, are already observed and relevant in nature by exerting multifactorial pressures that are restructuring phytoplankton communities and food webs. A suitable case study can be found in the Wadden Sea which is currently experiencing multifactorial changes in the afore studied drivers, namely long-term trends of warming at a rate of 0.4°C per decade (Rönn et al. 2023), increased episodes of extreme warming (Philippart et al. 2024), increasing N:P ratios and decreasing total macronutrient loading (van Beusekom et al. 2019, Rönn et al. 2023).

These shifts in nutrient regimes can be attributed to the implementation of effective management strategies. Following a peak of eutrophication in the 1980s, successful efforts to reduce eutrophication resulted in historically low nutrient levels (Grizzetti et al. 2012, van Beusekom et al. 2019, Rönn et al. 2023). However, since phosphorus is decreasing by about 5% per year and thus proportionally faster than nitrogen with about 2.5% per year, the N:P ratio increased across the North Sea (Box 1, Rönn et al. 2023, Brandenburg et al. 2025). This results in a long-term shift towards coastal phosphorus limitation (Burson et al. 2016) and thus favors certain phytoplankton species and functional groups (Philippart et al. 2007).

In *publication I*, I have shown structural changes among the phytoplankton community, specifically with many phytoplankton classes being identified as losers including Bacillariophyceae and Coscinodiscophyceae (diatoms), whereas Mamiellophyceae (*Micromonas pusilla*) and Coccolithophyceae (the harmful algae-bloom (HAB) species *Phaeocystis globosa*) were the only winners among phytoplankton classes. This increase of HAB-forming species in the North Sea has been previously reported (Edwards et al. 2006, Bresnan et al. 2013) and specifically, the increase in *Phaeocystis* species abundances was observed for different parts of the Southern North Sea (e.g., Cadée and Hegeman 1986, Beukema and Cadée 1991, Rönn et al. 2023, Brandenburg et al. 2025). As *Phaeocystis* is known

to be a strong competitor under low phosphorus concentrations (*publication 2*, Hegarty and Villareal 1998, Schoemann et al. 2005) and increasing N:P ratios (Brandenburg et al. 2025), the current nutrient shifts in the Wadden Sea create an optimal competitive environment for them to thrive.

### | Box 1: Stoichiometry in observational Wadden Sea data

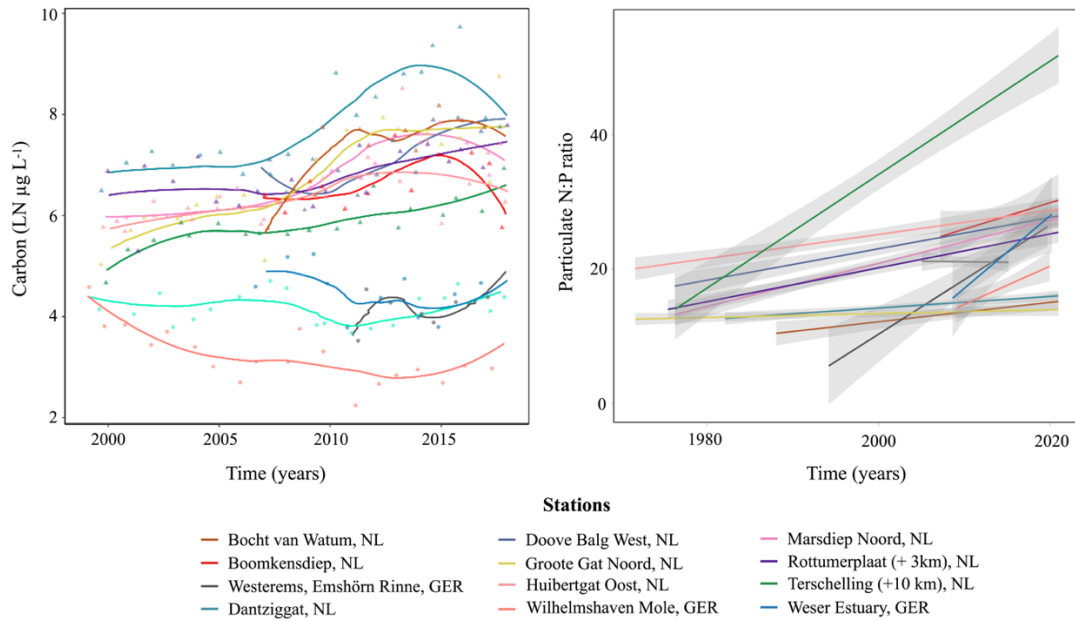


**Figure 7.2:** Time series of carbon and the particulate N:P ratio at the Wadden Sea stations used in *publication I*. The lengths of the time series differ between carbon and the N:P ratio. Grey shaded areas represent 95% confidence intervals. The left figure (carbon) was created by Rönn et al. (2023). The right figure (N:P ratios) is based on data from Rönn et al. (2023) collected alongside the phytoplankton data used in *publication I*. For this, the difference between total and dissolved nutrients for nitrogen and phosphorus was calculated before creating the ratio between both nutrients.

While particulate carbon increased by an order of magnitude between 1999 and 2014 in the Netherlands with a subsequent decrease in recent years, the German stations show slightly negative or neutral trends (Rönn et al. 2023). Both particulate nutrients show a decrease over time with a 0.93% decrease per year in particulate organic nitrogen (PON) and a 1.31% decrease per year in particulate organic phosphorus (POP) averaged across the whole Wadden Sea. Since POP is decreasing proportionally faster than PON, corresponding to the faster decrease in dissolved phosphorus observed in Rönn et al. (2023), the particulate N:P ratio increases by 1.46% per year. Simultaneously to an increase in the dissolved N:P ratios from 14 to 35 (Rönn et al. 2023), this means an increase of the mean particulate N:P ratios from 16 to 26 since the 1970s (Fig. 7.2). With particulate carbon increasing or staying neutral and particulate nutrient concentrations decreasing at the same stations, this points towards a general increase in C:P and C:N ratios in the Wadden Sea.

Moreover, the trend towards small cell sizes within and across species in the Wadden Sea (Hillebrand et al. 2022) is in line with the increases in small flagellates such as *Micromonas pusilla* at the expense of larger groups such as diatoms found in *publication I*. However, population trends of diatoms show mixed directions across the Wadden Sea and higher variability between years (Beukema and Cadée 1991). Despite increasing trends of diatoms in the Dutch Wadden Sea (Alvarez-Fernandez and Riegman 2014, Rönn et al. 2023), decreasing trends in line with our findings were also observed in the Central North Sea (Edwards et al. 2006) and in the German Bight (Radach et al. 1990). In response to nutrient shifts, diatoms were also observed to show contrasting patterns with certain species increasing and decreasing in response to increasing N:P ratios (Rönn et al. 2023). Additionally, the temperature response of diatoms in *publication II* indicated diatom-dominated communities at 6 and 18 °C and thus, a high thermal niche diversity or wider thermal breadth (Chen 2015, Anderson et al. 2021) compared to haptophytes dominating the community at intermediate temperatures (12 °C).

To extend this to a functional perspective on the effects of global change on aquatic ecosystems, phytoplankton responses beyond changes in quantity need to be considered. Precisely, the afore described changes in community composition are accompanied by changes in net cellular stoichiometry of the phytoplankton community with important implications for food quality. As shown for monocultures (Tanioka and Matsumoto 2020) and confirmed for communities (*publication III*, Table 7.1), phosphorus limitation not only leads to increasing C:P ratios but also increases C:N ratios based on the intracellular coupling of ribosomes and protein synthesis (*see chapter 7.2*). This pattern is also reflected in increasing C:P and C:N ratios in the Wadden Sea (*Box I*), although the decreasing nitrogen loading is likely the predominant reason for increasing C:N ratios. In *publication II*, a correlation between the dominance of *Phaeocystis* and an increase in C:P ratios was shown. Thus, a dominance shift from diatoms towards *Phaeocystis* as identified in *publication I* would strengthen or be accompanied by an increase in C:P ratios, as previously demonstrated for polar communities (Arrigo et al. 1999, Arrigo et al. 2002, Zhu et al. 2016). The higher *Phaeocystis*-specific C:P ratios are likely based on their carbon- and nitrogen-rich extracellular matrix (Solomon et al. 2003) or comparably low phosphorus demand due to lower regulatory costs (McCain et al. 2022). Furthermore, the increasing coastal phosphorus limitation of the Wadden Sea might also intensify the vulnerability of phytoplankton biomass to nutrient disturbances such as run-off events following extreme precipitation (*publication IV*). These nutrient pulse disturbances are especially relevant at the aquatic-terrestrial interface and thus occur in both freshwater (Roulet and Moore 2006) and coastal marine environments (Nunes et al. 2009, Mustaffa et al. 2020).

## 7 SYNTHESIS

Overall, all chapters (*publication I-V*) have shown that changes in response to environmental drivers not only occur on the biomass or community composition level, but also in terms of community stoichiometry. Together, they set the quantity and quality of food available to consumers at higher trophic levels and thus, determine their performance, survival and reproduction.

### 7.4 Implications for the food-web and ecosystem

Scaled up, these mechanistic insights into phytoplankton responses to different facets of warming and macronutrient availability (*publication 2-5*) allow to construct general trophic consequences for a simplified future scenario in aquatic ecosystems. Findings generated throughout this thesis aid in estimating the effect of scenario-based changes in food quantity (biomass) and quality (stoichiometry), while knowledge from the literature complements this by delivering insights into how these effects transfer to higher trophic levels.

In recent decades, warming and re-oligotrophication due to successful management strategies are increasingly occurring together in lake systems (Jeppesen et al. 2005, Verbeek et al. 2018). The same pattern is found in marine systems, for which global climate models predict an increase in water temperature alongside decreasing macronutrient concentrations resulting from increased water column stratification (Bopp et al. 2013, Boyd et al. 2015). In line with current environmental trajectories for the Wadden Sea (Box 1, Rönn et al. 2023), phosphorus decreases proportionally faster than nitrogen, also on the global scale (Tanioka and Matsumoto 2020). Despite different responsible mechanisms acting on unequal spatial scales, the outcome of increased C:nutrient and N:P ratios is consistent (Box 1, Tanioka and Matsumoto 2020) and points towards drastic changes in food quality for higher trophic levels. These shifts towards high C:nutrient ratios potentially induce nutrient limitation (i.e., quality starvation) for consumers as nutrients may become too dilute in their prey (Urabe and Sterner 1996, Sterner and Elser 2002, Hodapp et al. 2019) and thus, constrain the carbon transfer efficiency between phytoplankton and zooplankton (Hessen 2008). This, in turn, affects nutrient recycling as grazers retain the limiting resource (nitrogen or phosphorus in this case) to actively maintain their homeostasis (Andersen and Hessen 1991) and release excess dissolved organic carbon via respiration or excretion (Hessen et al. 2004) which is associated with additional metabolic costs for consumers reflected in suppressed growth, reproduction or survival (Boersma and Elser 2006). Beyond deleterious effects on zooplankton growth (Boersma and Kreutzer 2002), high C:P ratios of algae were, for example, also shown to decrease the growth of herbivorous snails (Stelzer and Lamberti 2002). Despite stoichiometric imbalances often being buffered on the

zooplankton level (*publication IV*, Cottingham and Schindler 2000), it is rather the effects on performance and associated shifts in community composition that propagate through the food-web. In freshwater systems, increased phytoplankton C:P ratios induce a shift from phosphorus-rich *Daphnia* to low-phosphorus copepods (Laspoumaderes et al. 2013, Diehl et al. 2022), in support of the mechanisms identified in *publication IV*. This is not only based on the lower phosphorus demand of copepods compared to cladocerans (Andersen and Hessen 1991, Elser et al. 2001), but also on the advantage of copepod selective feeding which is likely energetically more effective during periods of low food quality than non-selective feeding by cladocerans. In marine systems, zooplankton communities are typically dominated by copepods which show impaired feeding and reproductive rates under phosphorus limitation (Saiz et al. 2023). In line, the increasing phosphorus limitation in marine systems is also reflected in the population decline of many copepod families in the Wadden Sea (*publication I*, Fig. S6). In turn, the zooplankton community composition affects the nutritional quality for fish (Heneghan et al. 2023) and with decreasing prey quality and quantity, food webs might switch from a top-down controlled system, characterized by the efficient transport of energy and maintenance of enhanced production in higher trophic levels to a trophic decoupling with bottom-up control and inefficient energy transfer (Danielsdottir et al. 2007). Alternatively, decreasing prey quality and quantity may enhance the significance of the microbial loop, where bacteria and associated micrograzers (e.g., nanoflagellates and ciliates) process dissolved organic matter, potentially offering an alternative, but less efficient, pathway for energy to reach higher trophic levels, thereby altering food-web dynamics and energy transfer efficiencies (Azam et al. 1983, Jiao et al. 2010).

These gradual long-term trends of warming and re-oligotrophication are increasingly disrupted by extreme events (IPCC 2023), such as heatwaves or heavy rainfall with associated run-off into lakes and coastal systems (Jeppesen et al. 2009, Donat et al. 2017). Depending on the local characteristics (*publication V*), an extreme nutrient pulse would temporally stimulate phytoplankton growth and enhance their food quality for consumers, but significantly less compared to low-intensity rainfall events with a higher frequency of occurrence (*publication IV*). However, the chronology of stressors strongly modulates the response of phytoplankton biomass and stoichiometry and thus, heavy rainfall with associated run-off before or after a heatwave leads to significantly different outcomes (*publication III*). Overall, these changes suggest that the total energy flux through the food web will be subject to higher degrees of fluctuation (*publication II*), particularly in the summer months with lower baseline nutrient conditions and higher temperatures (*publication V*). This could have consequences for

the life cycles of other organisms that depend on phytoplankton phenology which would be negatively affected by an attenuation of clear seasonal bloom patterns or the switch of energy fluxes to alternative but less effective trophic pathways such as the microbial loop.

### 7.5 Future perspectives

The results of this thesis improved our understanding of the effects of climate change on natural plankton communities by integrating observational population trends and experimental findings from multiple environmental settings. However, further research potential has emerged and general methodological constraints regarding the design of climate change experiments and on how phytoplankton is included in monitoring and assessment strategies were identified. This subchapter outlines promising avenues for future research to make the complex and multi-dimensional nature of climate change effects on aquatic communities more tangible, to design ecologically relevant experiments (*chapter 7.5.2*) and to increase the representation of phytoplankton in monitoring and assessment (*chapter 7.5.1*).

#### 7.5.1 Policy: Missing aspects in standard monitoring and assessment

Despite the multitude of political frameworks focusing on halting biodiversity loss and the legally binding commitment of EU countries, European marine conservation policies were shown to not effectively address conservation needs (Fraschetti et al. 2018, Katsanevakis et al. 2020). The heterogeneity of implementation efforts and strategies (e.g., in monitoring programs, selection of protected sites) between EU countries (Fraschetti et al. 2018, Di Cavalho et al. 2023) and the high complexity of the policy landscape, which may fuel ambiguity over requirements of biodiversity assessment and monitoring (Greathead et al. 2020), dampens the success of biodiversity conservation in European waters.

On the European scale, the Water Framework Directive (WFD, EU 2000) for the protection of groundwaters, inland, transitional, and coastal surface waters, which encompasses all systems discussed in this thesis, aims to reach good environmental status (GES) and regularly assess biological quality elements for associated water bodies. Despite including parameters like phytoplankton community, abundance and biomass, and frequency and intensity of blooms (European Union 2000, Heiskanen et al. 2016), only chlorophyll-a as a proxy for phytoplankton biomass is widely applied by European member states (Rönn et al. 2023). On a regional scale, The Trilateral Wadden Sea Cooperation (TWSC) is in practice lacking indicators for assessing

diversity in pelagic habitats beyond phytoplankton chlorophyll-a as an indicator of eutrophication (Kloepper et al. 2017, Kloepper et al. 2022) and the extent of *Phaeocystis* blooms (Baretta-Bekker and Prins 2013), even though the handbook for the Wadden Sea assessment strategy (CWSS 2008) mentions the assessment of temporal trends, species richness and dominance structure of phytoplankton. Even if the proposed diversity metrics were implemented in the assessment strategy, important aspects that determine the functioning of the food-web, with phytoplankton at the base of it, were still neglected and overlooked. Thus, the question remains on what we are missing by lacking information on functional and compositional changes of phytoplankton in a system of interest.

This thesis has highlighted the complex effects that compositional shifts and cellular changes in the macronutrient elemental composition of phytoplankton under climate change have on the food quality for grazers and thus, higher trophic levels. As a less charismatic group that is mostly invisible to the bare human eye, the base of the food-web is underrepresented and undervalued in quality status reports despite its crucial functions. Only considering phytoplankton as an indicator for eutrophication provides a too simplistic view of its role in the ecosystem. Rönn et al. (2023) even raised the question of the usefulness of selected species (specifically *Phaeocystis globosa* and *Pseudo-nitzschia complex* in the Wadden Sea) as indicators for eutrophication as the response of phytoplankton to nutrient changes is rarely so consistent that they reliably qualify as indicator species.

Therefore, I propose to assess phytoplankton community stoichiometry – as simplistically but easily calculated from already monitored parameters (Box 1) – and regularly identify winners and losers across the phytoplankton classes to obtain a generalized overview of how the phytoplankton community is restructuring (*publication I*). Ideally, the assessment of phytoplankton community composition would be complemented by a multi-metric approach to calculate diversity, going beyond population trends and including Hill-number based alpha-diversity metrics and temporal dissimilarity of communities, thus capturing indicators on each dimension in which human impacts alter biodiversity (Hillebrand et al. *in prep*).

### 7.5.2 Experimental gaps and biases

This thesis highlighted the importance of designing ecologically relevant experiments to transfer laboratory findings to natural ecosystems. As such, the studies included in this thesis are rooted in the increasing pressure on aquatic ecosystems from multiple facets of human-



induced environmental change (IPBES 2019, IPCC 2023) that do not act in isolation in nature, but rather occur simultaneously. Due to the complex interactions between pressures that shape the response of phytoplankton to environmental change (Fig. 7.3), predicting and estimating the consequences for aquatic ecosystems remains a pressing topic.

By now, multiple stressor research receives the attention it deserves (Jackson et al. 2016, Jackson et al. 2021, Kremer et al. 2024, Orr et al. 2024) and has been established as a major future direction in aquatic ecology. This thesis has contributed to this emergent field by studying the effects of multiple environmental drivers, e.g., temperature and nutrients (*publication III*, Thomas et al. 2017, Thrane et al. 2017, Verbeek et al. 2018), and nutrients and light (*publication IV-V*, Dickman et al. 2006, Dickman et al. 2008) on phytoplankton performance. Despite answering open research questions and closing gaps in this thesis, new potentials for further research emerge. For example, building on the idea of sequentially versus simultaneously applied stressors (*publication III*), only a handful of studies experimentally tested realistic temporal patterns of stressors (Gunderson et al. 2016). Such underrepresented but naturally occurring patterns include studies in which the second stressor directly follows the first stressor, the stressors have a short or long time lag (Gunderson et al. 2016) or testing different orders of stressors (*publication III*). Thus, to attenuate climate change effects on phytoplankton (and cascading effects up the food web), it is crucial to understand the interactions among drivers and based on this, create scenarios that more accurately represent the natural aquatic ecosystems and the multi-faceted changes they experience.

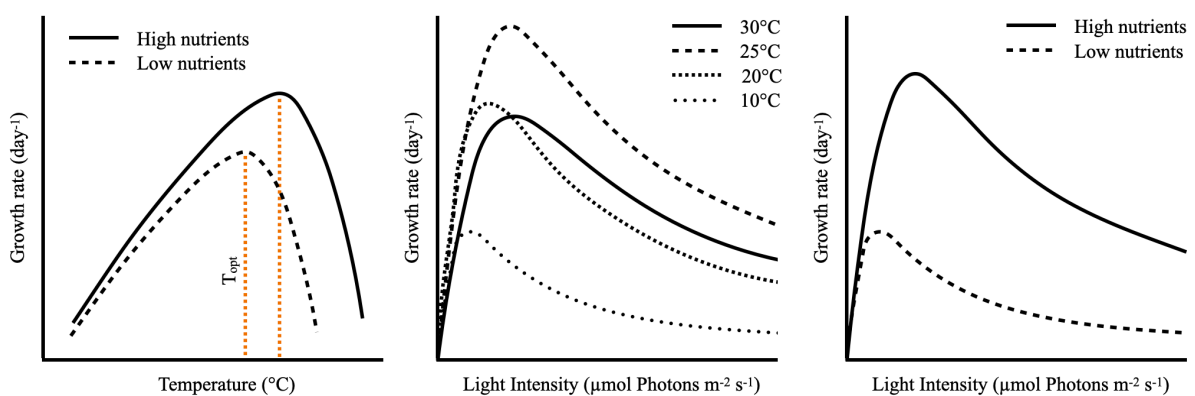


**Fig. 7.3:** (a) Interactive effect of nutrients and temperature on the growth rate following Thomas et al. (2017), Bestion et al. (2018). The temperature optimum  $T_{opt}$  is highlighted by an orange dashed line. (b) Interactive effect of light and temperature on the growth rate following Dauta et al. (1990). (c) Expected interactive effect of light and nutrients on the growth rate based on data of Heinrichs et al. (2025) for *Coelastrum* sp. in a monoculture).

Based on the findings from my thesis, I am advocating for (1) testing established understanding of single and multi-drivers on natural communities to expand the knowledge gained from

population studies to a more transferable system which includes biotic interactions, and (2) experimental designs that are strongly based on current and future abiotic conditions and do not represent natural conditions and processes too simplistically. This means to mimic the natural world more closely in terms of ecological systems and pressures, for example, by including multiple drivers (*publication III-V*), testing different temporal patterns of stressors (*publication III-V*) applying ecologically relevant rates of temperature (*publication III*) or nutrient conditions (*publication III*). By this, we increase the biotic and abiotic relevance of our research and ultimately, tackle climate change more effectively by providing more accurate recommendations.

### 7.5.3 Concluding remarks

In the context of accelerating climate change and increasing overuse of aquatic systems, research on how phytoplankton and their important functions are affected by these stressors is one of the most pressing topics in the present and future. Both by experimentally mimicking future scenarios and thus, estimating effects of climate change in the coming years and decades, as well as monitoring how phytoplankton is changing in the natural system, provide crucial tools to mitigate ecosystem-scale effects.

In this thesis, I demonstrated that phytoplankton communities are strongly restructuring. Despite not showing a unified response direction for all phytoplankton species populations (i.e., balancing positive and negative trends), phytoplankton highly dominate the classes with negative trends in a whole-ecosystem perspective. This is most strongly modulated by changing temperature and nutrient conditions and is accompanied by a decrease in food quality for their consumers. To mechanistically understand the effects of various facets of temperature and nutrient change in aquatic systems, a range of laboratory and mesocosm experiments was conducted. In summary, the experiments showed that phytoplankton stoichiometry is most strongly influenced by nutrient dynamics. However, this response goes beyond prevailing nutrient conditions and associated limitation patterns, but also includes the temporal pattern of nutrient input, the nutrient supply ratio as well as its relative timing and interaction with other stressors, as exemplified with temperature. In turn, long-term climate change-driven alterations of phytoplankton food quantity and quality, as well as disruptions by extreme events impact higher trophic levels, for example, by inducing quality starvation, constraining the energy transfer efficiency and promoting shifts in grazer community composition which eventually impact fish and bird populations and communities.

## 7 SYNTHESIS

Ultimately, I advocate for including phytoplankton stoichiometry (as a community response to nutrient conditions and an indicator for food quality) in environmental assessments to record changes at the base of the food-web and be aware of potential critical thresholds that induce food quality limitation for higher trophic levels. Additionally, I propose unifying and synthesizing multiple stressor responses of experiments to generalize overarching phytoplankton response patterns. Further, conducting ecologically relevant, informative and transferable experiments using a multi-driver and scenario-based approach with natural communities helps to increase our understanding of the fate of aquatic systems and the ecosystem services they provide.

## REFERENCES

### References

- Aebischer, N. J., J. C. Coulson, and J. M. Colebrook. 1990. Parallel long-term trends across four marine trophic levels and weather. *Nature* **347**:753-755.
- Alvarez-Fernandez, S., and R. Riegman. 2014. Chlorophyll in North Sea coastal and offshore waters does not reflect long term trends of phytoplankton biomass. *Journal of Sea Research* **91**:35-44.
- Andersen, T., and D. O. Hessen. 1991. Carbon, nitrogen, and phosphorus content of freshwater zooplankton. *Limnology and Oceanography* **36**:807-814.
- Anderson, S. I., A. D. Barton, S. Clayton, S. Dutkiewicz, and T. A. Ryneerson. 2021. Marine phytoplankton functional types exhibit diverse responses to thermal change. *Nature Communications* **12**:6413.
- Anderson, S. I., G. Franze, J. D. Kling, P. Wilburn, C. T. Kremer, S. Menden-Deuer, E. Litchman, D. A. Hutchins, and T. A. Ryneerson. 2022. The interactive effects of temperature and nutrients on a spring phytoplankton community. *Limnol. Oceanogr.* **67**:634-645.
- Armin, G., and K. Inomura. 2021. Modeled temperature dependencies of macromolecular allocation and elemental stoichiometry in phytoplankton. *Computational and Structural Biotechnology Journal* **19**:5421-5427.
- Arrigo, K. R., R. B. Dunbar, M. P. Lizotte, and D. H. Robinson. 2002. Taxon-specific differences in C/P and N/P drawdown for phytoplankton in the Ross Sea, Antarctica. *Geophysical Research Letters* **29**.
- Arrigo, K. R., D. H. Robinson, D. L. Worthen, R. B. Dunbar, G. R. DiTullio, M. VanWoert, and M. P. Lizotte. 1999. Phytoplankton community structure and the drawdown of nutrients and CO in the Southern Ocean. *Science* **283**:365-367.
- Azam, F., T. Fenchel, J. G. Field, J. S. Gray, L. A. Meyerreil, and F. Thingstad. 1983. The Ecological Role of Water-Column Microbes in the Sea. *Marine Ecology Progress Series* **10**:257-263.
- Baretta-Bekker, J. G., and T. C. Prins. 2013. Assessment of phytoplankton in the Netherlands and neighbouring countries according to OSPAR and WFD. *Deltares*, [https://publications.deltares.nl/1207005\\_000.pdf](https://publications.deltares.nl/1207005_000.pdf).
- Beaugrand, G., K. M. Brander, J. A. Lindley, S. Souissi, and P. C. Reid. 2003. Plankton effect on cod recruitment in the North Sea. *Nature* **426**:661-664.
- Berman-Frank, I., and Z. Dubinsky. 1999. Balanced growth in aquatic plants: Myth or reality? Phytoplankton use the imbalance between carbon assimilation and biomass production to their strategic advantage. *BioScience* **49**:29-37.
- Bestion, E., C. E. Schaum, and G. Yvon-Durocher. 2018. Nutrient limitation constrains thermal tolerance in freshwater phytoplankton. *Limnology and Oceanography Letters* **3**:436-443.
- Beukema, J. J., and G. C. Cadée. 1991. Growth-Rates of the Bivalve *Macoma-Balthica* in the Wadden Sea during a Period of Eutrophication - Relationships with Concentrations of Pelagic Diatoms and Flagellates. *Marine Ecology Progress Series* **68**:249-256.
- Boersma, M., and J. J. Elser. 2006. Too much of a good thing: On stoichiometrically balanced diets and maximal growth. *Ecology* **87**:1325-1330.
- Boersma, M., and C. Kreutzer. 2002. Life at the Edge: Is Food Quality Really of Minor Importance at Low Quantities? *Ecology* **83**:2552-2561.
- Bopp, L., L. Resplandy, J. C. Orr, S. C. Doney, J. P. Dunne, M. Gehlen, P. Halloran, C. Heinze, T. Ilyina, R. Séférian, J. Tjiputra, and M. Vichi. 2013. Multiple stressors of ocean ecosystems in the 21st century: projections with CMIP5 models. *Biogeosciences* **10**:6225-6245.

## REFERENCES

- Boyd, P. W., S. T. Lennartz, D. M. Glover, and S. C. Doney. 2015. Biological ramifications of climate-change-mediated oceanic multi-stressors. *Nature Climate Change* **5**:71-79.
- Brandenburg, K. M., J. Merder, A. Budiša, A. M. Power, C. J. M. Philippart, A. M. Michalak, T. J. van den Broek, and D. B. Van de Waal. 2025. Multiple global change factors and the long-term dynamics of harmful algal blooms in the North Sea. *Limnology and Oceanography*.
- Bresnan, E., K. Davidson, M. Edwards, L. Fernand, R. Gowen, A. Hall, K. Kennington, A. McKinney, S. Milligan, R. Raine, and J. Silke. 2013. Impacts of Climate Change on Harmful Algal Blooms. *MCCIP Science Review*:236-243.
- Breton, E., E. Goberville, B. Sautour, A. Ouadi, D. I. Skouroliakou, L. Seuront, G. Beaugrand, L. Kléparski, M. Crouvoisier, D. Pecqueur, C. Salmeron, A. Cauvin, A. Poquet, N. Garcia, F. Gohin, and U. Christaki. 2022. Multiple phytoplankton community responses to environmental change in a temperate coastal system: A trait-based approach. *Frontiers in Marine Science* **9**.
- Burson, A., M. Stomp, L. Akil, C. P. D. Brussaard, and J. Huisman. 2016. Unbalanced reduction of nutrient loads has created an offshore gradient from phosphorus to nitrogen limitation in the North Sea. *Limnol. Oceanogr.* **61**:869-888.
- Cadée, G. C., and J. Hegeman. 1986. Seasonal and Annual Variation in *Phaeocystis-Pouchetii* (Haptophyceae) in the Westernmost Inlet of the Wadden Sea during the 1973 to 1985 Period. *Netherlands Journal of Sea Research* **20**:29-36.
- Chen, B. Z. 2015. Patterns of thermal limits of phytoplankton. *Journal of Plankton Research* **37**:285-292.
- Cottingham, K., and D. E. Schindler. 2000. Effects of grazer community structure on phytoplankton response to nutrient pulses. *Ecology* **81**:183-200.
- Cowles, T. J., R. J. Olson, and S. W. Chisholm. 1988. Food selection by copepods: discrimination on the basis of food quality. *Marine Biology* **100**:41-49.
- CWSS. 2008. TMAP Handbook. TMAP guidelines for an integrated Wadden Sea monitoring. Version 0.9. Common Wadden Sea Secretariat, Wilhelmshaven, Germany.
- Danielsdottir, M. G., M. T. Brett, and G. B. Arhonditsis. 2007. Phytoplankton food quality control of planktonic food web processes. *Hydrobiologia* **589**:29-41.
- Dauta, A., J. Devaux, F. Piquemal, and L. Boumnick. 1990. Growth rate of four freshwater algae in relation to light and temperature. *Hydrobiologia* **207**:221-226.
- Di Cavalho, J. A., L. Rönn, T. C. Prins, and H. Hillebrand. 2023. Temporal change in phytoplankton diversity and functional group composition. *Marine Biodiversity* **53**.
- Di Pane, J., K. H. Wiltshire, M. McLean, M. Boersma, and C. L. Meunier. 2022. Environmentally induced functional shifts in phytoplankton and their potential consequences for ecosystem functioning. *Global Change Biology* **28**:2804-2819.
- Dickman, E. M., J. M. Newell, M. J. González, and M. J. Vanni. 2008. Light, nutrients, and food-chain length constrain planktonic energy transfer efficiency across multiple trophic levels. *PNAS* **105**.
- Dickman, E. M., M. J. Vanni, and M. J. Horgan. 2006. Interactive effects of light and nutrients on phytoplankton stoichiometry. *Oecologia* **149**:676-689.
- Diehl, S., S. A. Berger, W. Uszko, and H. Stibor. 2022. Stoichiometric mismatch causes a warming-induced regime shift in experimental plankton communities. *Ecology* **103**:e3674.
- Donat, M. G., A. L. Lowry, L. V. Alexander, P. A. O'Gorman, and N. Maher. 2017. More extreme precipitation in the world's dry and wet regions (vol 6, pg 508, 2016). *Nature Climate Change* **7**:154-158.
- Edwards, K. F., M. K. Thomas, C. A. Klausmeier, and E. Litchman. 2012. Allometric scaling and taxonomic variation in nutrient utilization traits and maximum growth rate of phytoplankton. *Limnol. Oceanogr.* **57**:554-566.

## REFERENCES

- Edwards, K. F., M. K. Thomas, C. A. Klausmeier, and E. Litchman. 2016. Phytoplankton growth and the interaction of light and temperature: A synthesis at the species and community level. *Limnology and Oceanography* **61**:1232-1244.
- Edwards, M., D. G. Johns, S. C. Leterme, E. Svendsen, and A. J. Richardson. 2006. Regional climate change and harmful algal blooms in the northeast Atlantic. *Limnology and Oceanography* **51**:820-829.
- Elser, J. J., W. F. Fagan, R. F. Denno, D. R. Dobberfuhl, A. Folarin, A. Huberty, S. Interlandi, S. S. Kilham, E. McCauley, K. L. Schulz, E. H. Siemann, and R. W. Sterner. 2000. Nutritional constraints in terrestrial and freshwater food webs. *Nature* **408**:578-580.
- Elser, J. J., K. Hayakawa, and J. Urabe. 2001. Nutrient limitation reduces food quality for zooplankton: *Daphnia* response to seston phosphorus enrichment. *Ecology* **82**:898-903.
- Eppley, R. W. 1972. Temperature and phytoplankton growth in the sea. *Fish. Bull.* **70**:1063-1085.
- Eppley, R. W., J. N. Rogers, and J. J. McCarthy. 1969. Half-Saturation Constants for Uptake of Nitrate and Ammonium by Marine Phytoplankton. *Limnology and Oceanography* **14**:912-&.
- EU. 2000. Directive 2000/60/EC of the European Parliament and of the Council of 23 October 2000 establishing a framework for community action in the field of water policy, OJ L 327, 22.12.2000, p. 1-73.
- Falkowski, P. G. 1994. The Role of Phytoplankton Photosynthesis in Global Biogeochemical Cycles. *Photosynthesis Research* **39**:235-258.
- Falkowski, P. G., T. Fenchel, and E. F. Delong. 2008. The microbial engines that drive Earth's biogeochemical cycles. *Science* **320**:1034-1039.
- Fernández-González, C., G. A. Tarran, N. Schuback, E. M. S. Woodward, J. Arístegui, and E. Marañón. 2022. Phytoplankton responses to changing temperature and nutrient availability are consistent across the tropical and subtropical Atlantic. *Communications Biology* **5**.
- Field, C. B., M. J. Behrenfeld, J. T. Randerson, and P. Falkowski. 1998. Primary production of the biosphere: Integrating terrestrial and oceanic components. *Science* **281**:237-240.
- Filippelli, G. M. 2008. The global phosphorus cycle: Past, present, and future. *Elements* **4**:89-95.
- Finkel, Z. V., J. Beardall, K. J. Flynn, A. Quigg, T. A. V. Rees, and J. A. Raven. 2009. Phytoplankton in a changing world: cell size and elemental stoichiometry. *J. Plankton Res.* **32**:119-137.
- Finkel, Z. V., M. J. Follows, J. D. Liefer, C. M. Brown, I. Benner, and A. J. Irwin. 2016. Phylogenetic Diversity in the Macromolecular Composition of Microalgae. *PLoS One* **11**:e0155977.
- Fraschetti, S., C. Pipitone, A. D. Mazaris, G. Rilov, F. Badalamenti, S. Bevilacqua, J. Claudet, H. Caric, K. Dahl, G. D'Anna, D. Daunys, M. Frost, E. Gissi, C. Göke, P. Goriup, G. Guarnieri, D. Holcer, B. Lazar, P. Mackelworth, S. Manzo, G. Martin, A. Palialexis, M. Panayotova, D. Petza, B. Rumes, V. Todorova, and S. Katsanevakis. 2018. Light and Shade in Marine Conservation Across European and Contiguous Seas. *Frontiers in Marine Science* **5**.
- Frederiksen, M., M. Edwards, A. J. Richardson, N. C. Halliday, and S. Wanless. 2006. From plankton to top predators: bottom-up control of a marine food web across four trophic levels. *Journal of Animal Ecology* **75**:1259-1268.
- Frost, P. C., N. J. T. Pearce, S. A. Berger, M. O. Gessner, A. K. Makower, V. Marzetz, J. C. Nejstgaard, A. Pralle, S. Schällicke, A. Wacker, N. D. Wagner, and M. A. Xenopoulos. 2023. Interactive effects of nitrogen and phosphorus on growth and stoichiometry of lake phytoplankton. *Limnol. Oceanogr.* **9999**:1-13.

## REFERENCES

- Geider, R., and J. La Roche. 2002. Redfield revisited: variability of C:N:P in marine microalgae and its biochemical basis. *Eur. J. Phycol.* **37**:1-17.
- Gerhard, M., A. M. Koussoroplis, H. Hillebrand, and M. Striebel. 2019. Phytoplankton community responses to temperature fluctuations under different nutrient concentrations and stoichiometry. *Ecology* **100**(11):e02834.
- Gerhard, M., A. M. Koussoroplis, M. Raatz, C. Pansch, S. B. Fey, J. Vajedsamiei, M. Calderó-Pascual, D. Cunillera-Montcusí, N. P. D. Juvigny-Khenafou, F. Polazzo, P. K. Thomas, C. C. Symons, M. Beklioglu, S. A. Berger, R. M. Chefaoui, K. A. Ger, S. Langenheder, J. C. Nejstgaard, R. Ptacnik, and M. Striebel. 2023. Environmental variability in aquatic ecosystems: Avenues for future multifactorial experiments. *Limnology and Oceanography Letters* **8**:247-266.
- Greathead, C., P. Magni, J. Vanaverbeke, L. Buhl-Mortensen, U. Janas, M. Blomqvist, J. A. Craeymeersch, J. Dannheim, A. Darr, S. Degraer, N. Desroy, A. Donnay, Y. Griffiths, I. Guala, L. Guerin, H. Hinchén, C. Labrune, H. Reiss, G. Van Hoey, and S. N. R. Birchenough. 2020. A generic framework to assess the representation and protection of benthic ecosystems in European marine protected areas. *Aquatic Conservation: Marine and Freshwater Ecosystems* **30**:1253-1275.
- Grizzetti, B., F. Bouraoui, and A. Aloe. 2012. Changes of nitrogen and phosphorus loads to European seas. *Global Change Biology* **18**:769-782.
- Gunderson, A. R., E. J. Armstrong, and J. H. Stillman. 2016. Multiple stressors in a changing world: the need for an improved perspective on physiological responses to the dynamic marine environment. *Ann. Rev. Mar. Sci.* **8**:357-378.
- Hegarty, S. G., and T. A. Villareal. 1998. Effects of light level and N:P supply ratio on the competition between *Phaeocystis* cf. *pouchetii* (Hariot) Lagerheim (Prymnesiophyceae) and five diatom species. *Journal of Experimental Marine Biology and Ecology* **226**:241-258.
- Heinrichs, A. L., A. Happe, A. M. Koussoroplis, H. Hillebrand, J. Merder, and M. Striebel. 2025. Temperature-dependent responses to light and nutrients in phytoplankton. *Ecology* **106**:e70027.
- Heinrichs, A. L., O. J. Hardorp, H. Hillebrand, T. Schott, and M. Striebel. 2024. Direct and indirect cumulative effects of temperature, nutrients, and light on phytoplankton growth. *Ecol Evol* **14**:e70073.
- Heiskanen, A.-S., T. Berg, L. Uusitalo, H. Teixeira, A. Bruhn, D. Krause-Jensen, C. P. Lynam, A. G. Rossberg, S. Korpinen, M. C. Uyarra, and A. Borja. 2016. Biodiversity in Marine Ecosystems—European Developments toward Robust Assessments. *Frontiers in Marine Science* **3**.
- Heneghan, R. F., J. D. Everett, J. L. Blanchard, P. Sykes, and A. J. Richardson. 2023. Climate-driven zooplankton shifts cause large-scale declines in food quality for fish. *Nature Climate Change* **13**:470-+.
- Hessen, D. O. 2008. Efficiency, Energy and Stoichiometry in Pelagic Food Webs; Reciprocal Roles of Food Quality and Food Quantity. *Freshwater Reviews* **1**:43-57.
- Hessen, D. O., G. I. Agren, T. R. Anderson, J. J. Elser, and P. C. De Ruiter. 2004. Carbon sequestration in ecosystems: The role of stoichiometry. *Ecology* **85**:1179-1192.
- Hessen, D. O., P. J. Færevig, and T. Andersen. 2002. Light, nutrients, and P:C ratios in algae:: Grazer performance related to food quality and quantity. *Ecology* **83**:1886-1898.
- Hessen, D. O., E. Leu, P. J. Faerovig, and S. F. Petersen. 2008. Light and spectral properties as determinants of C:N:P-ratios in phytoplankton. *Deep-Sea Research Part II-Topical Studies in Oceanography* **55**:2169-2175.
- Hillebrand, H., J. A. Di Carvalho, J. C. Dajka, C. D. Dürselen, O. Kerimoglu, L. Kuczynski, L. Rönn, and A. Ryabov. 2022. Temporal declines in Wadden Sea phytoplankton cell



## REFERENCES

- volumes observed within and across species. *Limnology and Oceanography* **67**:468-481.
- Hillebrand, H., W. Armonies, C. Buschbaum, B. K. Eriksson, A. Happe, H. Haslob, I. Kirstein, M. Kleyer, L. Kuczynski, K. Löhmus, K. J. Meijer, L. Rönn, G. Scheiffarth, A. F. Sell, D. W. Thieltges (*in prep*). Systematic assessemnt of biodiversity change in the Wadden Sea.
- Hodapp, D., H. Hillebrand, and M. Striebel. 2019. “Unifying” the concept of resource use efficiency in ecology. *Frontiers in Ecology and Evolution* **6**.
- Hung, C. R. L. E., C. Diamond, R. Sinclair, M. C. Lee, M. Stenstrom, M. A. Freilich, Q. Montgomery, C. Marquez, and T. W. Lyons. 2024. Nutrient loading as a key cause of short- and long-term anthropogenic ecological degradation of the Salton Sea. *Scientific Reports* **14**.
- IPBES. 2019. Global assessment report on biodiversity and ecosystem services of the Intergovernmental Science-Policy Platform on Biodiversity and Ecosystem Services. IPBES secretariat, Bonn, Germany. 1148 pages. <https://doi.org/10.5281/zenodo.3831673>.
- IPCC. 2023. Climate change 2023. Synthesis report. Summary for policymakers.
- Jackson, M. C., C. J. G. Loewen, R. D. Vinebrooke, and C. T. Chimimba. 2016. Net effects of multiple stressors in freshwater ecosystems: a meta-analysis. *Global Change Biology* **22**:180-189.
- Jackson, M. C., S. Pawar, and G. Woodward. 2021. The Temporal Dynamics of Multiple Stressor Effects: From Individuals to Ecosystems. *Trends in Ecology & Evolution* **36**:402-410.
- Jak, R. G., and D. M. E. Slijkerman. 2023. Short review on zooplankton in the Dutch Wadden Sea. Considerations for zooplankton monitoring. Wageningen University and Research Report.
- Jeppesen, E., B. Kronvang, M. Meerhoff, M. Sondergaard, K. M. Hansen, H. E. Andersen, T. L. Lauridsen, L. Liboriussen, M. Beklioglu, A. Ozen, and J. E. Olesen. 2009. Climate change effects on runoff, catchment phosphorus loading and lake ecological state, and potential adaptations. *J Environ Qual* **38**:1930-1941.
- Jeppesen, E., M. Sondergaard, J. P. Jensen, K. E. Havens, O. Anneville, L. Carvalho, M. F. Coveney, R. Deneke, M. T. Dokulil, B. Foy, D. Gerdeaux, S. E. Hampton, S. Hilt, K. Kangur, J. Köhler, E. H. H. R. Lammens, T. L. Lauridsen, M. Manca, M. R. Miracle, B. Moss, P. Noges, G. Persson, G. Phillips, R. Portielje, C. L. Schelske, D. Straile, I. Tatrai, E. Willén, and M. Winder. 2005. Lake responses to reduced nutrient loading -: an analysis of contemporary long-term data from 35 case studies. *Freshwater Biology* **50**:1747-1771.
- Jiao, N., G. J. Herndl, D. A. Hansell, R. Benner, G. Kattner, S. W. Wilhelm, D. L. Kirchman, M. G. Weinbauer, T. W. Luo, F. Chen, and F. Azam. 2010. Microbial production of recalcitrant dissolved organic matter: long-term carbon storage in the global ocean. *Nature Reviews Microbiology* **8**:593-599.
- Katsanevakis, S., M. Coll, S. Fraschetti, S. Giakoumi, D. Goldsborough, V. Mačić, P. Mackelworth, G. Rilov, V. Stelzenmüller, P. G. Albano, A. E. Bates, S. Bevilacqua, E. Gissi, V. Hermoso, A. D. Mazaris, C. Pita, V. Rossi, Y. Teff-Seker, and K. Yates. 2020. Twelve Recommendations for Advancing Marine Conservation in European and Contiguous Seas. *Frontiers in Marine Science* **7**.
- Klausmeier, C. A., and E. Litchman. 2004. Phytoplankton growth and stoichiometry under multiple nutrient limitation.
- Klausmeier, C. A., E. Litchman, T. Daufrense, and S. A. Levin. 2004. Optimal nitrogen-to-phosphorus stoichiometry of phytoplankton. *Nature* **429**:171-174.

## REFERENCES

- Kloepper, S., M. J. Baptist, A. Bostelmann, J. A. Busch, C. Buschbaum, L. Gutow, G. Janssen, K. Jensen, H. P. Jørgensen, F. de Jong, G. Lüerßen, K. Schwarzer, R. Stempel, and D. Thielges. 2017. Wadden Sea Quality Status Report. Common Wadden Sea Secretariat, Wilhelmshaven, Germany.
- Kloepper, S., A. Bostelmann, T. Bregnballe, J. A. Busch, C. Buschbaum, K. Deen, A. Domnick, L. Gutow, K. Jensen, N. Jepsen, S. Luna, K. Meise, J. Teilmann, and A. van Wezel. 2022. Wadden Sea Quality Status Report. Common Wadden Sea Secretariat, Wilhelmshaven, Germany.
- Kontopoulou, D. G., A. Sentis, M. Daufresne, N. Glazman, A. I. Dell, and S. Pawar. 2024. No universal mathematical model for thermal performance curves across traits and taxonomic groups. *Nature Communications* **15**.
- Kooijman, S. A. L. M., T. Andersen, and B. W. Kooi. 2004. Dynamic energy budget representations of stoichiometric constraints on population dynamics. *Ecology* **85**:1230-1243.
- Koussoroplis, A. M., M. J. Kainz, and M. Striebel. 2012. Fatty acid retention under temporally heterogeneous dietary intake in a cladoceran. *OIKOS* **122**:1017-1026.
- Kremer, C. T., S. B. Fey, A. A. Arellano, and D. A. Vasseur. 2018. Gradual plasticity alters population dynamics in variable environments: thermal acclimation in the green alga *Chlamydomonas reinhardtii*. *Proc. Royal Soc. B.* **285**:20171942.
- Kremer, C. T., M. K. Thomas, C. A. Klausmeier, and E. Litchman. 2024. How interactions between temperature and resources scale from populations to communities. *bioRxiv* 2024.09.19.613936; doi: <https://doi.org/10.1101/2024.09.19.613936>.
- Kunze, C., M. Gerhard, M. Jacob, N. A. Franke, M. Schroeder, and M. Striebel. 2022. Phytoplankton Community Performance Depends on the Frequency of Temperature Fluctuations. *Frontiers in Marine Science* **8**.
- Langdon, C. 1988. On the Causes of Interspecific Differences in the Growth Irradiance Relationship for Phytoplankton .2. A General-Review. *Journal of Plankton Research* **10**:1291-1312.
- Laspoumaderes, C., B. Modenutti, M. S. Souza, M. Bastidas Navarro, F. Cuassolo, and E. Balseiro. 2013. Glacier melting and stoichiometric implications for lake community structure: zooplankton species distributions across a natural light gradient. *Glob Chang Biol* **19**:316-326.
- Li, F. Y., A. Burger, J. M. Eppley, K. E. Poff, D. M. Karl, and E. F. Delong. 2023. Planktonic microbial signatures of sinking particle export in the open ocean's interior. *Nature Communications* **14**.
- Li, G. C., L. J. Cheng, J. Zhu, K. E. Trenberth, M. E. Mann, and J. P. Abraham. 2020. Increasing ocean stratification over the past half-century. *Nature Climate Change* **10**:1116-U1176.
- Liefer, J. D., A. Garg, M. H. Fyfe, A. J. Irwin, I. Benner, C. M. Brown, M. J. Follows, A. W. Omta, and Z. V. Finkel. 2019. The Macromolecular Basis of Phytoplankton C:N:P Under Nitrogen Starvation. *Frontiers in Microbiology* **10**.
- Litchman, E., and C. A. Klausmeier. 2008. Trait-based community ecology of phytoplankton. *Annu. Rev. Ecol. Evol. Syst.* **39**:615-639.
- Mandal, S., R. Abbott Wilkins, and J. B. Shurin. 2018. Compensatory grazing by *Daphnia* generates a trade-off between top-down and bottom-up effects across phytoplankton taxa. *Ecosphere* **9**.
- Marañón, E., P. Cermeno, D. C. Lopez-Sandoval, T. Rodriguez-Ramos, C. Sobrino, M. Huete-Ortega, J. M. Blanco, and J. Rodriguez. 2013. Unimodal size scaling of phytoplankton growth and the size dependence of nutrient uptake and use. *Ecol. Lett.* **16**:371-379.
- Marañón, E., M. P. Lorenzo, P. Cermeno, and B. Mourino-Carballido. 2018. Nutrient limitation suppresses the temperature dependence of phytoplankton metabolic rates. *ISME Journal* **12**:1836-1845.

## REFERENCES

- Martin, J. H., S. E. Fitzwater, and R. M. Gordon. 1990. Iron Deficiency Limits Phytoplankton Growth in Antarctic Waters. *Global Biogeochemical Cycles* **4**:5-12.
- Martiny, A. C., C. T. A. Pham, F. W. Primeau, J. A. Vrugt, J. K. Moore, S. A. Levin, and M. W. Lomas. 2013. Strong latitudinal patterns in the elemental ratios of marine plankton and organic matter. *Nature Geoscience* **6**:279-283.
- Mazaris, A. D., A. Kallimanis, E. Gissi, C. Pipitone, R. Danovaro, J. Claudet, G. Rilov, F. Badalamenti, V. Stelzenmüller, L. Thiault, L. Benedetti-Cecchi, P. Goriup, S. Katsanevakis, and S. Fraschetti. 2019. Threats to marine biodiversity in European protected areas. *Science of the Total Environment* **677**:418-426.
- McCain, J. S. P., A. E. Allen, and E. M. Bertrand. 2022. Proteomic traits vary across taxa in a coastal Antarctic phytoplankton bloom. *ISME Journal* **16**:569-579.
- Meunier, C., M. Boersma, K. H. Wiltshire, and A. M. Malzahn. 2015. Zooplankton eat what they need: copepod selective feeding and potential consequences for marine systems. *OIKOS* **000**:001–009.
- Mustaffa, N. I. H., L. Kallajoki, J. Biederbick, F. I. Binder, A. Schlenker, and M. Striebel. 2020. Coastal Ocean Darkening Effects via Terrigenous DOM Addition on Plankton: An Indoor Mesocosm Experiment. *Frontiers in Marine Science* **7**.
- Noy-Meir, I. 1973. Desert Ecosystems: Environment and Producers. *Annu. Rev. Ecol. Syst.* **4**:25-51.
- Nunes, J. P., J. Seixas, J. J. Keizer, and A. J. D. Ferreira. 2009. Sensitivity of runoff and soil erosion to climate change in two Mediterranean watersheds. Part II: assessing impacts from changes in storm rainfall, soil moisture and vegetation cover. *Hydrological Processes* **23**:1212-1220.
- O'Reilly, C. M., S. Sharma, D. K. Gray, S. E. Hampton, J. S. Read, R. J. Rowley, P. Schneider, J. D. Lenters, P. B. McIntyre, B. M. Kraemer, G. A. Weyhenmeyer, D. Straile, B. Dong, R. Adrian, M. G. Allan, O. Anneville, L. Arvola, J. Austin, J. L. Bailey, J. S. Baron, J. D. Brookes, E. de Eyto, M. T. Dokulil, D. P. Hamilton, K. Havens, A. L. Hetherington, S. N. Higgins, S. Hook, L. R. Izmet'eva, K. D. Joehnk, K. Kangur, P. Kasprzak, M. Kumagai, E. Kuusisto, G. Leshkevich, D. M. Livingstone, S. MacIntyre, L. May, J. M. Melack, D. C. Mueller-Navarra, M. Naumenko, P. Noges, T. Noges, R. P. North, P. D. Plisnier, A. Rigosi, A. Rimmer, M. Rogora, L. G. Rudstam, J. A. Rusak, N. Salmaso, N. R. Samal, D. E. Schindler, S. G. Schladow, M. Schmid, S. R. Schmidt, E. Silow, M. E. Soylu, K. Teubner, P. Verburg, A. Voutilainen, A. Watkinson, C. E. Williamson, and G. Q. Zhang. 2015. Rapid and highly variable warming of lake surface waters around the globe. *Geophysical Research Letters* **42**:10773-10781.
- Orr, J. A., S. J. Macaulay, A. Mordente, B. Burgess, D. Albini, J. G. Hunn, K. Restrepo-Sulez, R. Wilson, A. Schechner, A. M. Robertson, B. Lee, B. R. Stuparyk, D. Singh, I. O'Loughlin, J. J. Piggott, J. Zhu, K. V. Dinh, L. C. Archer, M. Penk, M. T. T. Vu, N. P. D. Juvigny-Khenafou, P. Zhang, P. Sanders, R. B. Schafer, R. D. Vinebrooke, S. Hilt, T. Reed, and M. C. Jackson. 2024. Studying interactions among anthropogenic stressors in freshwater ecosystems: A systematic review of 2396 multiple-stressor experiments. *Ecology Letters* **27**:e14463.
- Padfield, D., G. Yvon-Durocher, A. Buckling, S. Jennings, and G. Yvon-Durocher. 2016. Rapid evolution of metabolic traits explains thermal adaptation in phytoplankton. *Ecology Letters* **19**:133-142.
- Paul, C., B. Matthiessen, and U. Sommer. 2015. Warming, but not enhanced CO<sub>2</sub> concentration, quantitatively and qualitatively affects phytoplankton biomass. *Marine Ecology Progress Series* **528**:39-51.
- Peck, L. S., M. S. Clark, S. A. Morley, A. Massey, and H. Rossetti. 2009. Animal temperature limits and ecological relevance: effects of size, activity and rates of change. *Funct. Ecol.* **23**:248-256.

## REFERENCES

- Peñuelas, J., B. Poulter, J. Sardans, P. Ciais, M. van der Velde, L. Bopp, O. Boucher, Y. Godderis, P. Hinsinger, J. Llusia, E. Nardin, S. Vicca, M. Obersteiner, and I. A. Janssens. 2013. Human-induced nitrogen-phosphorus imbalances alter natural and managed ecosystems across the globe. *Nature Communications* **4**.
- Petersen, J. E., V. S. Kennedy, W. C. Dennison, and W. M. e. Kemp. 2009. *Enclosed Experimental Ecosystems and Scale: Tools for Understanding and Managing Coastal Ecosystems*. Springer, New York, USA.
- Philippart, C., M. Baptist, M. Bastmeijer, T. Bregnballe, C. Buschbaum, P. Hoekstra, K. Laursen, S. M. van Leeuwen, A. P. Oost, M. Wegner, and R. Zijlstra. 2024. Wadden Sea Quality Status Report: Climate Change. Common Wadden Sea Secretariat. <https://doi.org/10.5281/zenodo.15111640>.
- Philippart, C. J. M., J. J. Beukema, G. C. Cadee, R. Dekker, P. W. Goedhart, J. M. van Iperen, M. F. Leopold, and P. M. J. Herman. 2007. Impacts of nutrient reduction on coastal communities. *Ecosystems* **10**:95-118.
- Quigg, A., Z. V. Finkel, A. J. Irwin, Y. Rosenthal, T.-Y. Ho, J. R. Reinfelder, O. Schofield, F. M. M. Morel, and P. G. Falkowski. 2003. The evolutionary inheritance of elemental stoichiometry in marine phytoplankton. *Nature* **425**:291-294.
- Radach, G., J. Berg, and E. Hagmeier. 1990. Long-Term Changes of the Annual Cycles of Meteorological, Hydrographic, Nutrient and Phytoplankton Time-Series at Helgoland and at Lv Elbe 1 in the German Bight. *Continental Shelf Research* **10**:305-328.
- Ramírez, F., M. Coll, J. Navarro, J. Bustamante, and A. J. Green. 2018. Spatial congruence between multiple stressors in the Mediterranean Sea may reduce its resilience to climate impacts. *Scientific Reports* **8**.
- Redfield, A. C. 1958. The biological control of chemical factors in the environment. *Am. Sci.* **46**:205-221.
- Rhee, G. Y., and I. J. Gotham. 1980. Optimum N:P Ratios and Coexistence of Planktonic Algae. *Journal of Phycology* **16**:486-489.
- Richardson, A. J., E. H. John, X. Irigoien, R. P. Harris, and G. C. Hays. 2004. How well does the continuous plankton recorder (CPR) sample zooplankton? A comparison with the Longhurst Hardy Plankton Recorder (LHPR) in the northeast Atlantic. *Deep-Sea Research Part I-Oceanographic Research Papers* **51**:1283-1294.
- Rönn, L., J. Antonucci di Carvalho, A. Blauw, H. Hillebrand, O. Kerimoglu, H. Lenhart, S. Gholamreza, L. Tack, D. Thewes, and T. Troost. 2023. Harmonisation of the phytoplankton assessment in the German and Dutch Wadden Sea. Interreg V A project “Wasserqualität - Waterkwaliteit” - synthesis report. Report prepared on behalf of NLWKN and Rijkswaterstaat, Oldenburg/Lelystad, 2023.
- Roulet, N., and T. R. Moore. 2006. Browning the waters. *Nature* **444**:283-284.
- Saiz, E., K. Griffell, S. Isari, and A. Calbet. 2023. Ecophysiological response of marine copepods to dietary elemental imbalances. *Marine Environmental Research* **186**.
- Schoemann, V., S. Becquevort, J. Stefels, W. Rousseau, and C. Lancelot. 2005. blooms in the global ocean and their controlling mechanisms:: a review. *Journal of Sea Research* **53**:43-66.
- Schwinning, S., and O. E. Sala. 2004. Hierarchy of responses to resource pulses in and semi-arid ecosystems. *Oecologia* **141**:211-220.
- Simon, F. W., and D. A. Vasseur. 2021. Variation cascades: resource pulses and top-down effects across time scales. *Ecology* **102**.
- Solomon, C. M., E. J. Lessard, R. G. Keil, and M. S. Foy. 2003. Characterization of extracellular polymers of *Phaeocystis globosa* and *P. antarctica*. *Marine Ecology Progress Series* **250**:81-89.

## REFERENCES

- Song, K., M. A. Xenopoulos, J. M. Buttle, J. Marsalek, N. D. Wagner, F. R. Pick, and P. C. Frost. 2013. Thermal stratification patterns in urban ponds and their relationships with vertical nutrient gradients. *Journal of Environmental Management* **127**:317-323.
- Spilling, K., P. Ylostalo, S. Simis, and J. Seppala. 2015. Interaction effects of light, temperature and nutrient limitations (N, P and Si) on growth, stoichiometry and photosynthetic parameters of the cold-water diatom *Chaetoceros wighamii*. *PLoS One* **10**:e0126308.
- Stelzer, R. S., and G. A. Lamberti. 2002. Ecological stoichiometry in running waters: Periphyton chemical composition and snail growth. *Ecology* **83**:1039-1051.
- Sterner, R. W., and J. J. Elser. 2002. *Ecological stoichiometry: The biology of elements from molecules to the biosphere*. Princeton University Press.
- Striebel, M., G. Singer, H. Stibor, and T. Andersen. 2012. "Trophic overyielding": Phytoplankton diversity promotes zooplankton productivity. *Ecology* **93**:2719-2727.
- Svensen, C., J. C. Nejstgaard, J. K. Egge, and P. Wassmann. 2002. Pulsing versus constant supply of nutrients (N, P and Si): effect on phytoplankton, mesozooplankton and vertical flux of biogenic matter. *Scientia Marina* **66**:189-203.
- Tanioka, T., and K. Matsumoto. 2020. A meta-analysis on environmental drivers of marine phytoplankton C : N : P. *Biogeosciences* **17**:2939-2954.
- Thomas, M. K., M. Aranguren-Gassis, C. T. Kremer, M. R. Gould, K. Anderson, C. A. Klausmeier, and E. Litchman. 2017. Temperature-nutrient interactions exacerbate sensitivity to warming in phytoplankton. *Glob. Change Biol.* **23**:3269-3280.
- Thomas, M. K., C. T. Kremer, C. A. Klausmeier, and E. Litchman. 2012. A global pattern of thermal adaptation in marine phytoplankton. *Science* **338**:1085-1088.
- Thrane, J. E., D. O. Hessen, and T. Andersen. 2017. Plasticity in algal stoichiometry: experimental evidence of a temperature-induced shift in optimal supply N:P ratio. *Limnol. Oceanogr.* **62**:1346–1354.
- Todgham, A. E., and J. H. Stillman. 2013. Physiological responses to shifts in multiple environmental stressors: relevance in a changing world. *Integr Comp Biol* **53**:539-544.
- Toseland, A., S. J. Daines, J. R. Clark, A. Kirkham, J. Strauss, C. Uhlig, T. M. Lenton, K. Valentin, G. A. Pearson, V. Moulton, and T. Mock. 2013. The impact of temperature on marine phytoplankton resource allocation and metabolism. *Nat. Clim. Change* **3**:979-984.
- Urabe, J., and R. W. Sterner. 1996. Regulation of herbivore growth by the balance of light and nutrients. *Proc. Natl. Acad. Sci.* **93**:9465-8469.
- Urabe, J., J. U. N. Togari, and J. J. Elser. 2003. Stoichiometric impacts of increased carbon dioxide on a planktonic herbivore. *Global Change Biology* **9**:818-825.
- van Beusekom, J. E. E., J. Carstensen, T. Dolch, A. Grage, R. Hofmeister, H. Lenhart, O. Kerimoglu, K. Kolbe, J. Pätsch, J. Rick, L. Rönn, and H. Ruiter. 2019. Wadden Sea Eutrophication: Long-Term Trends and Regional Differences. *Frontiers in Marine Science* **6**.
- van de Waal, D. B., A. M. Verschoor, J. M. H. Verspagen, E. van Donk, and J. Huisman. 2010. Climate-driven changes in the ecological stoichiometry of aquatic ecosystems. *Frontiers in Ecology and the Environment* **8**:145-152.
- Verbeek, L., A. Gall, H. Hillebrand, and M. Striebel. 2018. Warming and oligotrophication cause shifts in freshwater phytoplankton communities. *Glob. Change Biol.* **24**:4532-4543.
- Vitousek, P. M., J. D. Aber, R. W. Howarth, G. E. Likens, P. A. Matson, D. W. Schindler, W. H. Schlesinger, and D. Tilman. 1997. Human alteration of the global nitrogen cycle: Sources and consequences. *Ecological Applications* **7**:737-750.
- Weithoff, G., and B. E. Beisner. 2019. Measures and Approaches in Trait-Based Phytoplankton Community Ecology – From Freshwater to Marine Ecosystems. *Frontiers in Marine Science* **6**.

## REFERENCES

- Wilhelm, S., and R. Adrian. 2008. Impact of summer warming on the thermal characteristics of a polymictic lake and consequences for oxygen, nutrients and phytoplankton. *Freshwater Biology* **53**:226-237.
- Wiltshire, K. H., M. Boersma, K. Carstens, A. C. Kraberg, S. Peters, and M. Scharfe. 2015. Control of phytoplankton in a shelf sea: Determination of the main drivers based on the Helgoland Roads Time Series. *Journal of Sea Research* **105**:42-52.
- Wu, Z., J. C. Li, Y. X. Sun, J. Peñuelas, J. L. Huang, J. Sardans, Q. S. Jiang, J. C. Finlay, G. L. Britten, M. J. Follows, W. Gao, B. Q. Qin, J. R. Ni, S. L. Huo, and Y. Liu. 2022. Imbalance of global nutrient cycles exacerbated by the greater retention of phosphorus over nitrogen in lakes. *Nature Geoscience* **15**:464-+.
- Yvon-Durocher, G., C. E. Schaum, and M. Trimmer. 2017. The temperature dependence of phytoplankton stoichiometry: investigating the roles of species sorting and local adaptation. *Front. Microbiol.* **8**:2003.
- Yvon-Durocher, G., M. Dossena, M. Trimmer, G. Woodward, and A. P. Allen. 2015. Temperature and the biogeography of algal stoichiometry. *Glob. Ecol. Biogeogr.* **24**:562-570.
- Zhang, M., X. L. Shi, F. Z. Chen, Z. Yang, and Y. Yu. 2021. The underlying causes and effects of phytoplankton seasonal turnover on resource use efficiency in freshwater lakes. *Ecology and Evolution* **11**:8897-8909.
- Zhu, Z., K. Xu, F. X. Fu, J. L. Spackeen, D. A. Bronk, and D. A. Hutchins. 2016. A comparative study of iron and temperature interactive effects on diatoms and *Phaeocystis antarctica* from the Ross Sea, Antarctica. *Marine Ecology Progress Series* **550**:39-51.

## **Appendix Publication I**

Synthesis of population trends reveals seascape-wide reorganisation of biodiversity from microalgae to birds

*Shortened supplementary material*

*The full supplementary material can be found here:*  
<https://tinyurl.com/38jekbem>



# APPENDIX PUBLICATION I

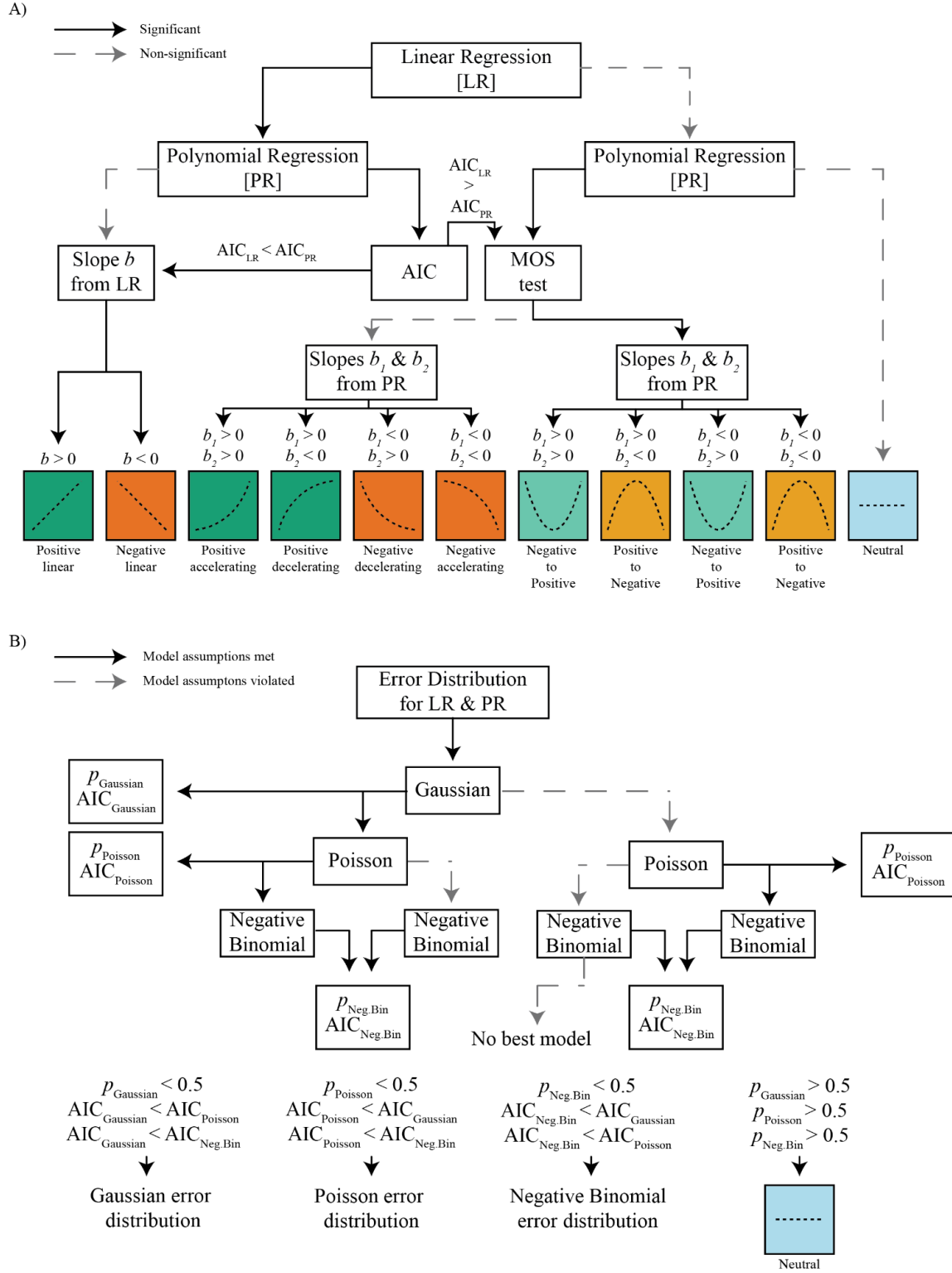


Figure S1: A) Schematic workflow for the vote count of the trends. B) Schematic workflow for the chosen error distribution for the models used in the vote count.

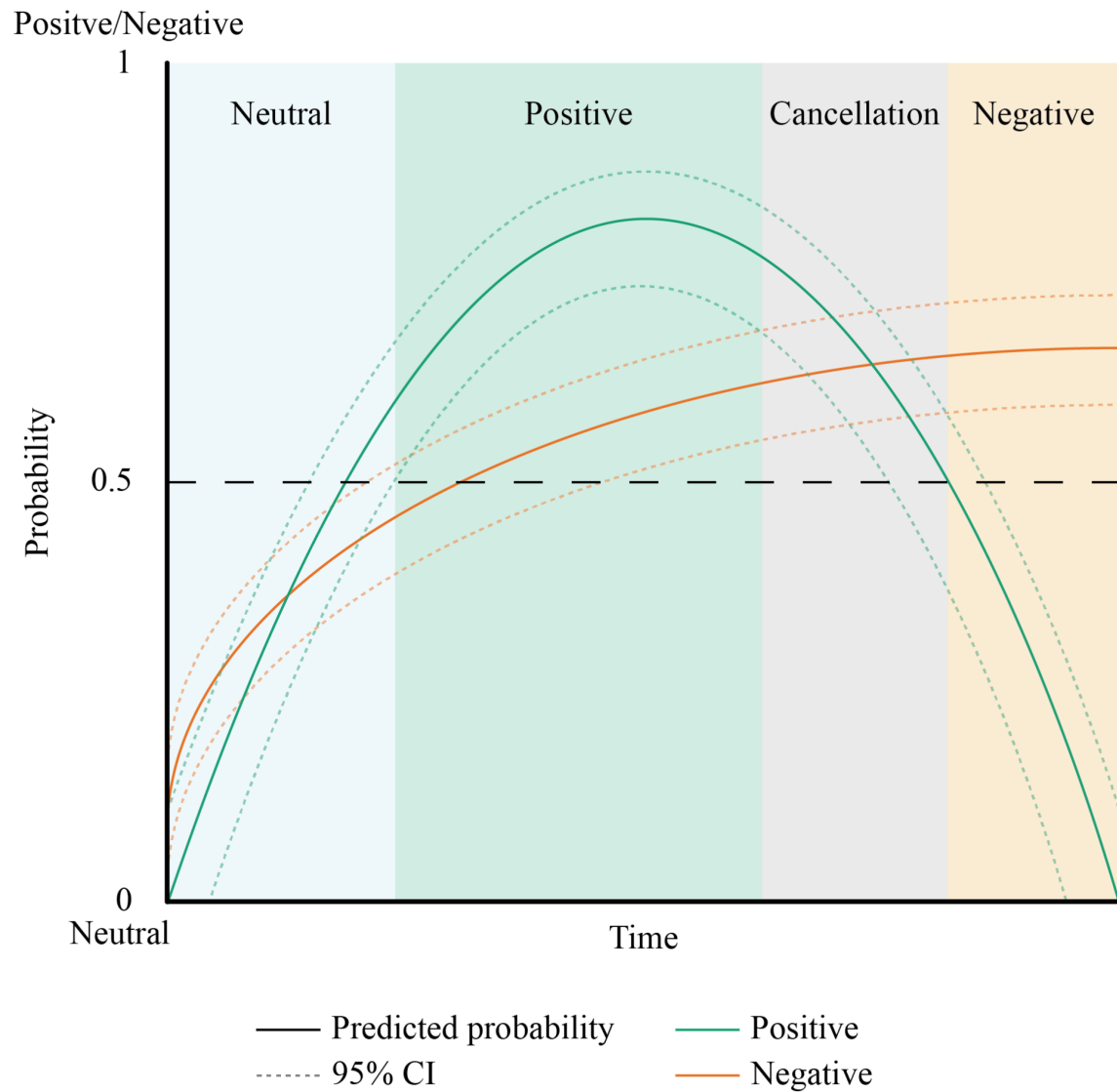


Figure S2: Schematic overview of the temporal trends classification. The probability of positive or negative trends is always considered against the probability of the trend being neutral. In case the probability of both a negative and positive trend is below 0.5, the overall trend is neutral. In case the probabilities are higher than 0.5, the overall trend is that with the highest probability. In case both trend probabilities overlap, there is an equal probability of positive and negative trends which cancel each other out.

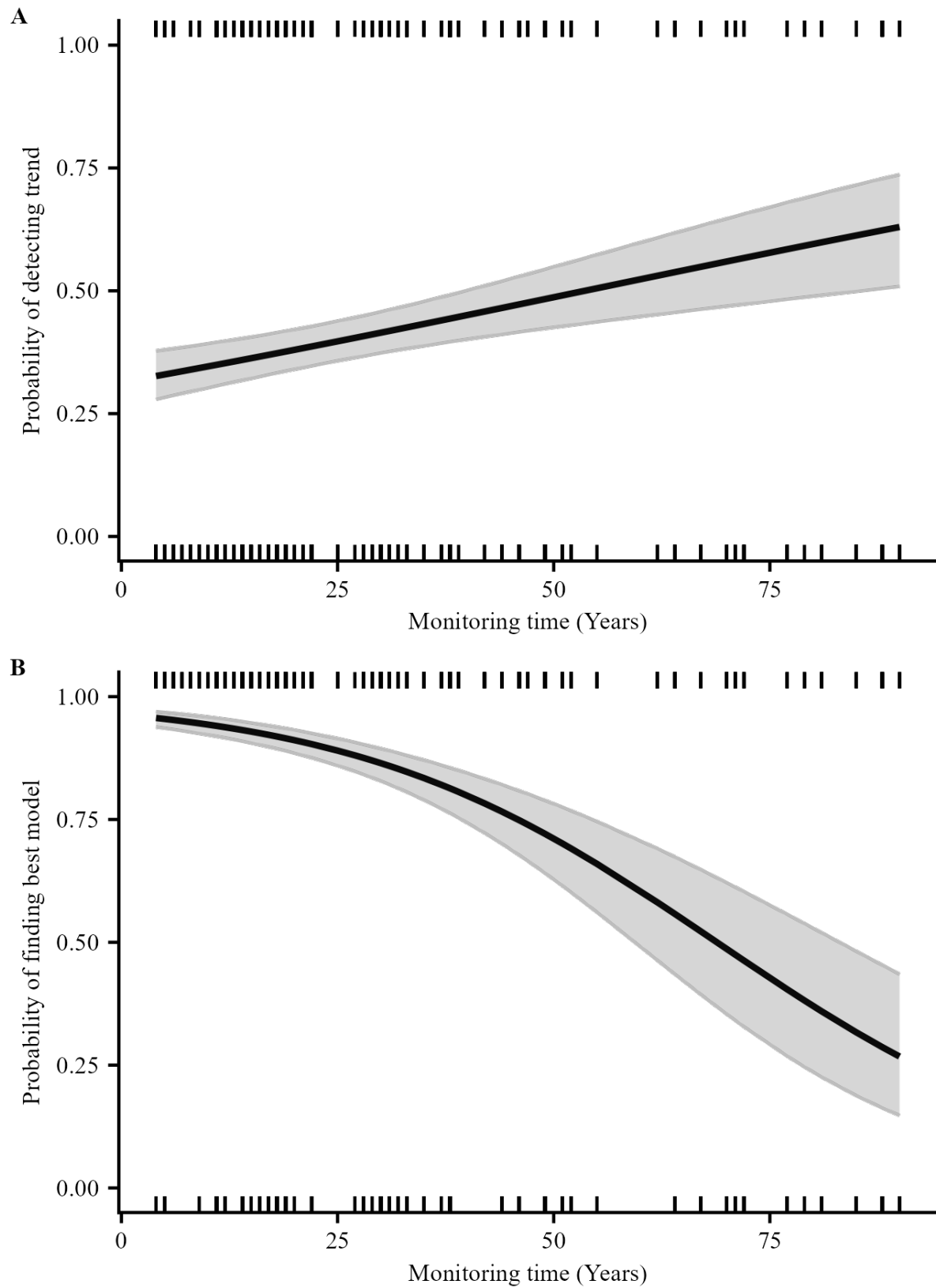


Figure S3: A) Probability of detecting a trend with increasing monitoring time; B) Probability of a model meeting assumptions of a Gaussian, Poisson or negative binomial error distribution using linear or polynomial regression with increasing monitoring time.

# APPENDIX PUBLICATION I

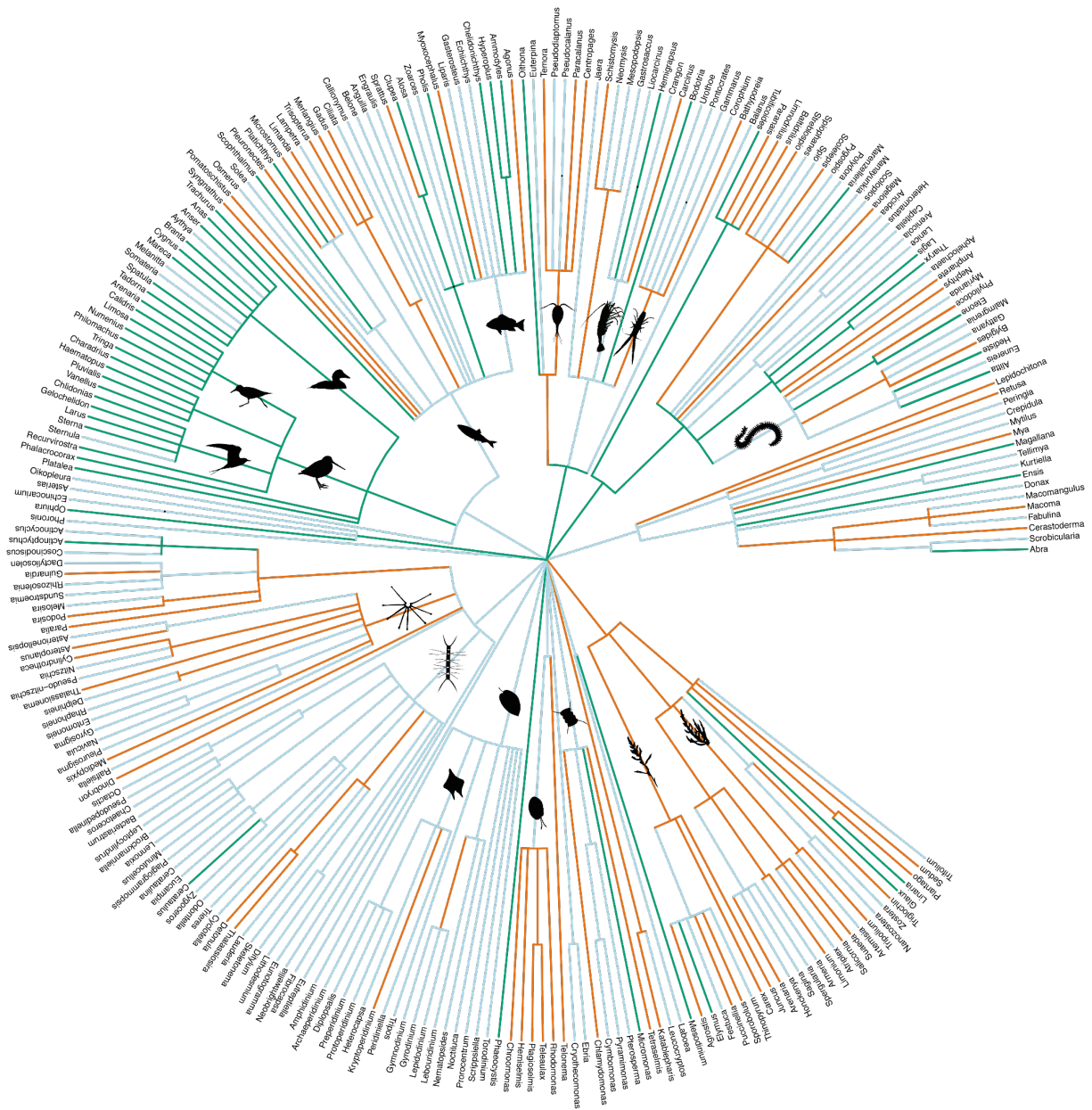


Figure S4: Dendrogram of the meta-analysis results (coloured branches). The colour indicates an overall significantly positive trend (green), negative trend (orange) or a non-significant overall trend (blue). The labels refer to the genus of the branch. The estimates and 95% confidence intervals for each taxonomic level are presented in Table S4-8.

## APPENDIX PUBLICATION I

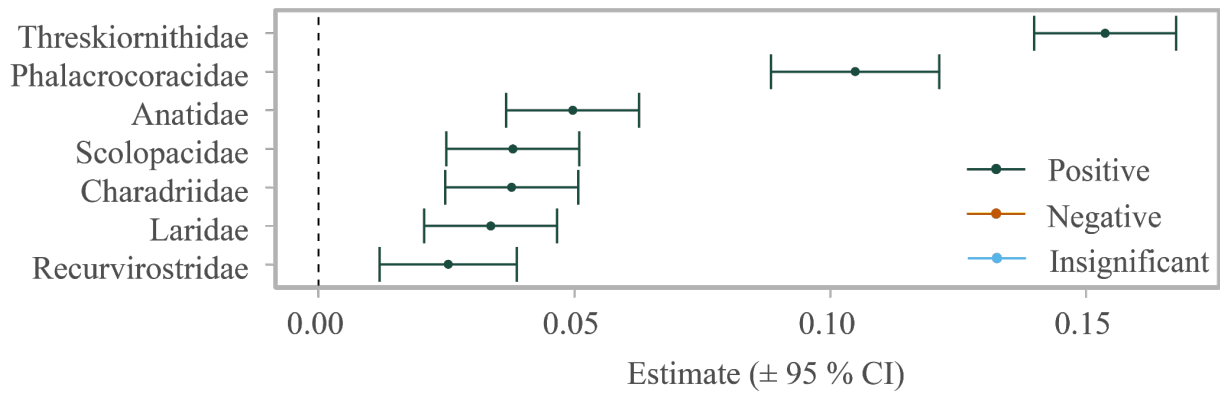


Figure S5: Winners and losers in the class of Aves (birds). Estimates and 95 % confidence intervals (CI) were derived from the meta-analysis to identify winners (green) and losers (orange) on the phylogenetic level of family. Significance ( $p < 0.05$ ) is indicated by CI not crossing the dashed line at 0.

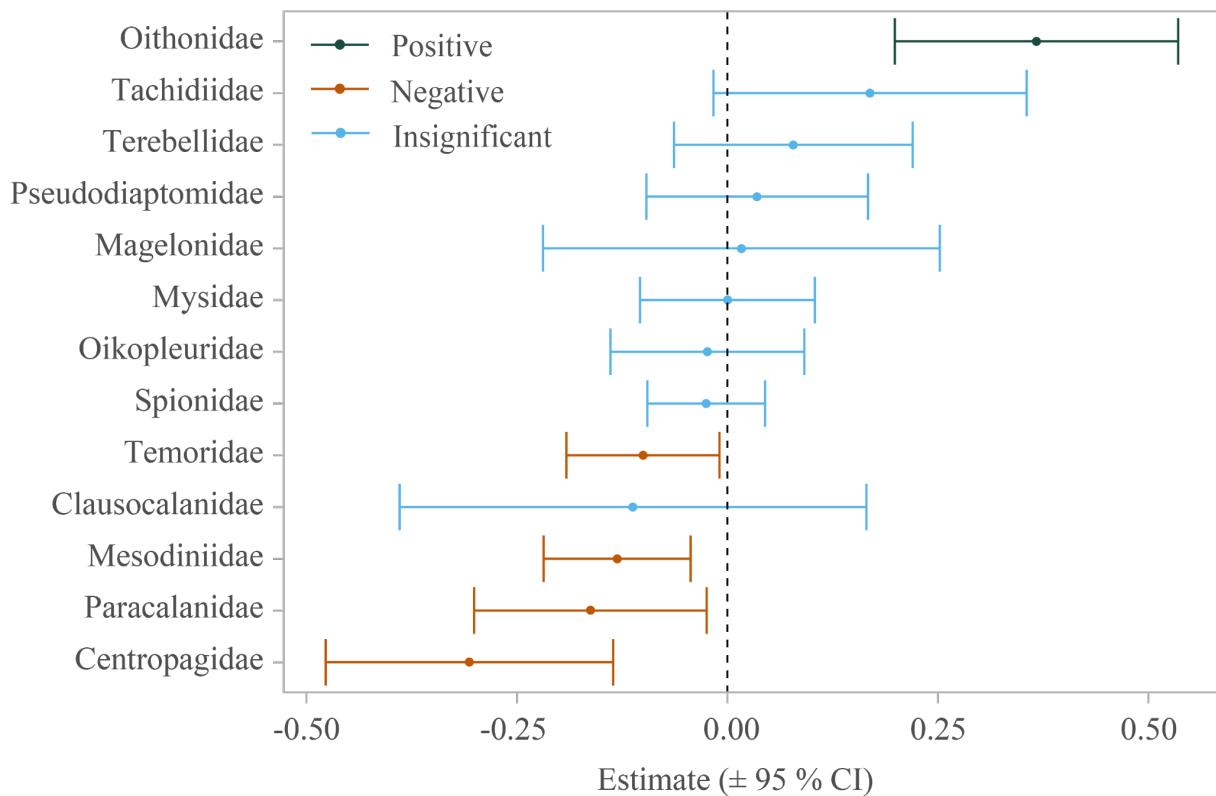


Figure S6: Winners and losers in the ecosystem component of zooplankton. Estimates and 95 % confidence intervals (CI) were derived from the meta-analysis to identify winners (green) and losers (orange) on the phylogenetic level of family. Significance ( $p < 0.05$ ) is indicated by CI not crossing the dashed line at 0.

# APPENDIX PUBLICATION I

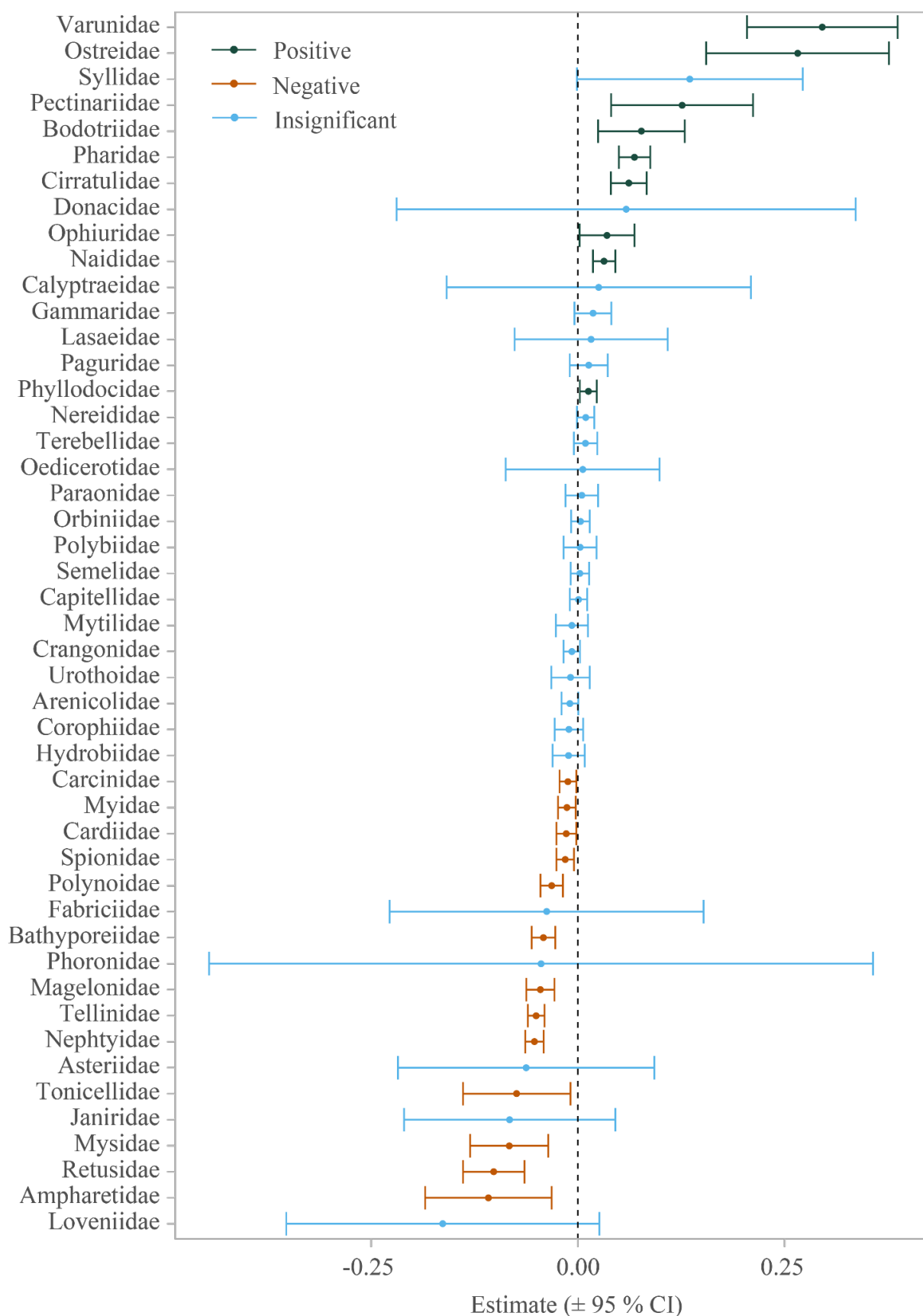


Figure S7: Winners and losers in the ecosystem component of macrozoobenthos. Estimates and 95 % confidence intervals (CI) were derived from the meta-analysis to identify winners (green) and losers (orange) on the phylogenetic level of family. Significance ( $p < 0.05$ ) is indicated by CI not crossing the dashed line at 0.

## APPENDIX PUBLICATION I

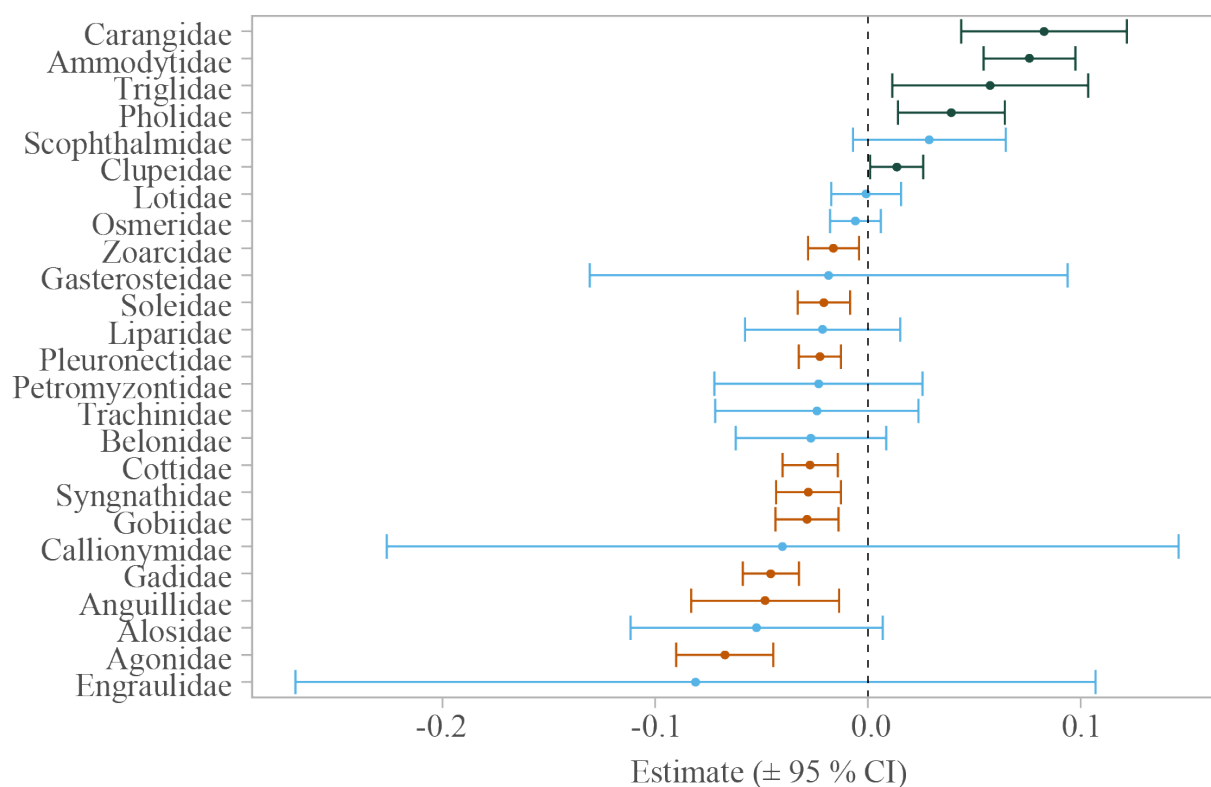


Figure S8: Winners and losers in the ecosystem component of fish. Estimates and 95 % confidence intervals (CI) were derived from the meta-analysis to identify winners (green) and losers (orange) on the phylogenetic level of family. Significance ( $p < 0.05$ ) is indicated by CI not crossing the dashed line at 0.

Table S2: Number of entries for each ecosystem component and phylogenetic level. Entries identified only to genus level were included as “Genera sp.” at species level. The ecosystem component of “Plants” includes both salt marsh plants and seagrasses. Macroinvertebrates show a lower number of genera than families as three genera could not be assigned. Abbreviations are as follows: Phytoplankton (Phytopl.), macrozoobenthos (MZB), zooplankton (Zoopl.).

	Phytopl.	MZB	Birds	Fish	Plants	Zoopl.
Phyla	10	7	1	1	1	4
Classes	19	11	1	1	3	5
Orders	48	27	6	12	9	8
Families	69	51	10	25	15	14
Genera	97	72	34	33	28	14
Species	161	96	57	40	33	14



## APPENDIX PUBLICATION I

Table S4: Meta-analysis results used to assign the winner and loser status on class level. The meta-analysis was run on the full dataset.

Class	Estimate	Std. Error	z-value	CI (lower)	CI (upper)	p-value
Appendicularia	-0.050	0.054	-0.913	-0.156	0.057	0.361
Asteroidea	-0.074	0.078	-0.953	-0.226	0.078	0.341
Aves	0.027	0.006	4.322	0.015	0.039	<0.001
Bacillariophyceae	-0.049	0.014	-3.599	-0.076	-0.022	<0.001
Bivalvia	-0.010	0.005	-1.931	-0.020	<0.001	0.054
Chlorodendrophyceae	-0.541	0.127	-4.255	-0.790	-0.292	<0.001
Chlorophyceae	-0.032	0.024	-1.337	-0.080	0.015	0.181
Chrysophyceae	-0.363	0.120	-3.035	-0.598	-0.129	0.002
Clitellata	0.040	0.007	6.045	0.027	0.053	<0.001
Coccolithophyceae	0.118	0.051	2.319	0.018	0.217	0.020
Copepoda	-0.058	0.030	-1.965	-0.117	<0.001	0.049
Coscinodiscophyceae	-0.035	0.013	-2.715	-0.061	-0.010	0.007
Cryptophyceae	-0.002	0.014	-0.144	-0.030	0.026	0.886
Cyanophyceae	-0.786	0.170	-4.613	-1.120	-0.452	<0.001
Dictyochophyceae	-0.075	0.058	-1.299	-0.189	0.038	0.194
Dinophyceae	-0.023	0.013	-1.818	-0.048	0.002	0.069
Echinoidea	-0.152	0.097	-1.570	-0.341	0.038	0.117
Equisetopsida	-0.159	0.011	-14.803	-0.180	-0.138	<0.001
Euglenophyceae	-0.014	0.017	-0.858	-0.047	0.019	0.391
Gastropoda	-0.010	0.009	-1.039	-0.028	0.009	0.299
Hexacorallia	0.105	0.080	1.318	-0.051	0.262	0.187
Katablepharidophyceae	-0.177	0.046	-3.828	-0.268	-0.086	<0.001
Liliopsida	-0.039	0.006	-6.529	-0.050	-0.027	<0.001
Litostomatea	-0.098	0.041	-2.376	-0.178	-0.017	0.018
Magnoliopsida	-0.053	0.006	-8.338	-0.065	-0.041	<0.001
Malacostraca	0.008	0.005	1.653	-0.002	0.018	0.098
Mamiellophyceae	0.270	0.087	3.100	0.099	0.441	0.002
Mediophyceae	-0.021	0.012	-1.717	-0.045	0.003	0.086
Oligotrichea	-0.026	0.025	-1.039	-0.074	0.023	0.299
Ophiuroidea	0.058	0.014	4.102	0.030	0.085	<0.001
Polychaeta	0.013	0.005	2.564	0.003	0.022	0.010
Polyplacophora	-0.093	0.033	-2.831	-0.157	-0.029	0.005
Pyramimonadophyceae	-0.026	0.018	-1.455	-0.061	0.009	0.146
Raphidophyceae	0.006	0.027	0.206	-0.048	0.059	0.837
Teleostei	-0.010	0.005	-1.836	-0.020	0.001	0.066
Telonemea	-0.367	0.122	-3.002	-0.606	-0.127	0.003
Thecofilosea	0.010	0.030	0.332	-0.049	0.069	0.740
Thecostraca	0.020	0.022	0.898	-0.023	0.062	0.369



## **Appendix Publication II**

Warming increases the compositional and functional  
variability of a temperate protist community

*Supplementary material*

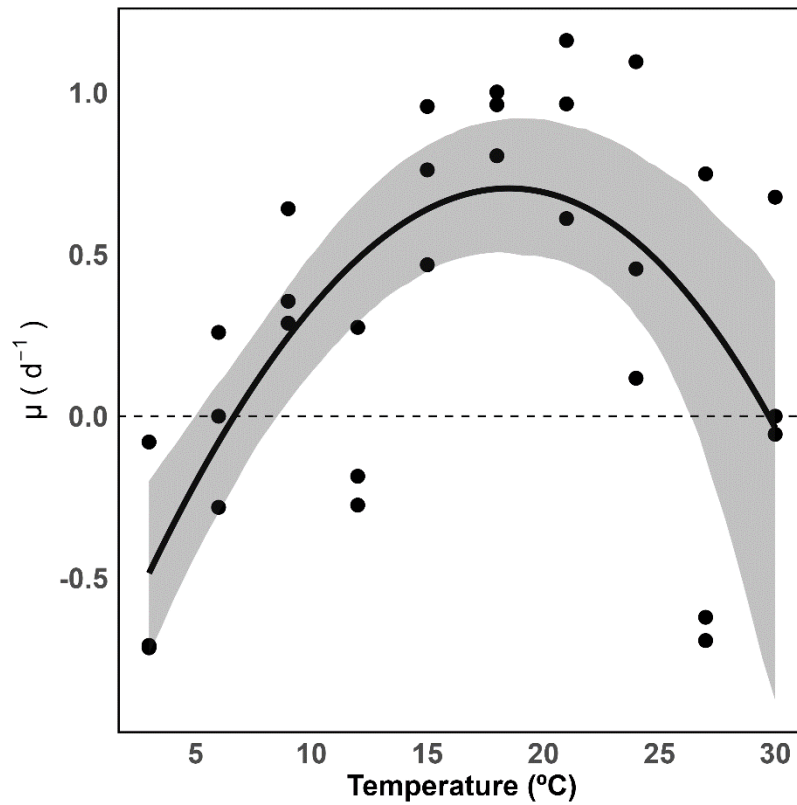


**Figure S1:** Thermal performance curve of the starting community with the growth rate ( $\mu$ ) across experimental temperatures. The line represents the fit by Thomas et al. (2017) and the grey shaded areas the 95% confidence interval predicted through bootstrapping.

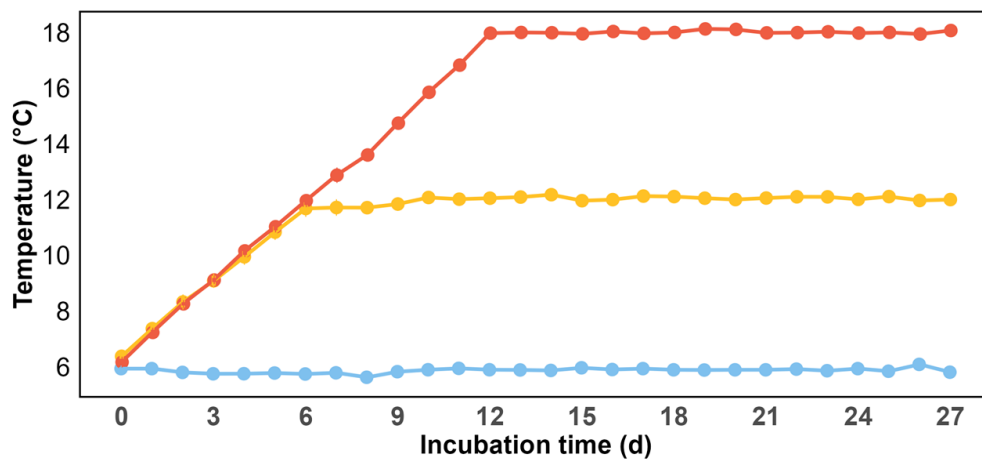


**Figure S2:** Daily measured temperature over time. Dots represent the arithmetic mean of the temperatures (6 °C: blue, 12 °C: yellow, 18 °C: red) and error bars the standard deviation.

## APPENDIX PUBLICATION II

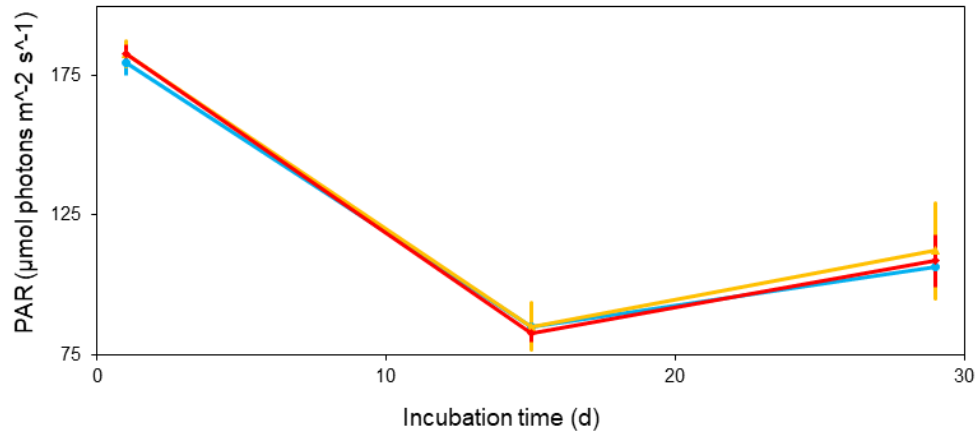


**Figure S3:** Photosynthetic active radiation (PAR) at 10 cm below the surface over time. Dots represent the arithmetic mean of the temperatures (6 °C: blue, 12 °C: yellow, 18 °C: red) and error bars the standard deviation.

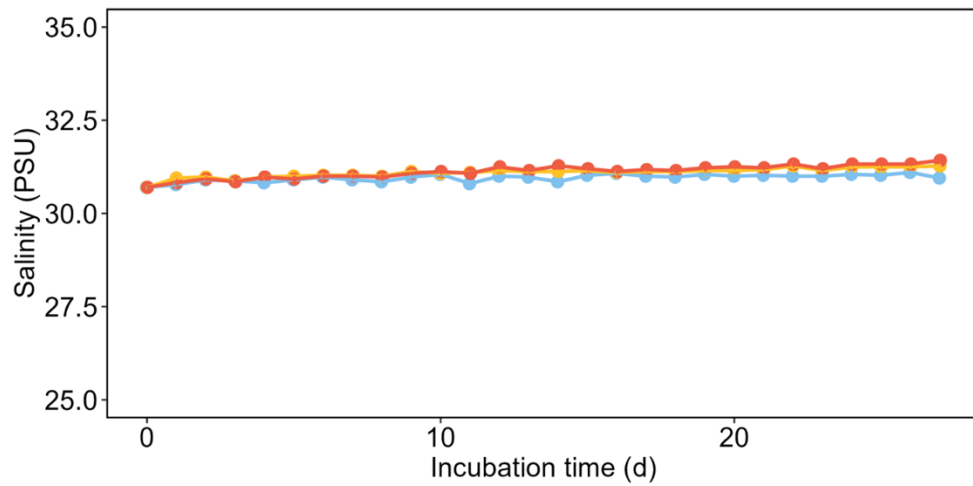


**Figure S4:** Daily measured salinity over time. Dots represent the arithmetic mean of the temperatures (6 °C: blue, 12 °C: yellow, 18 °C: red) and error bars the standard deviation.

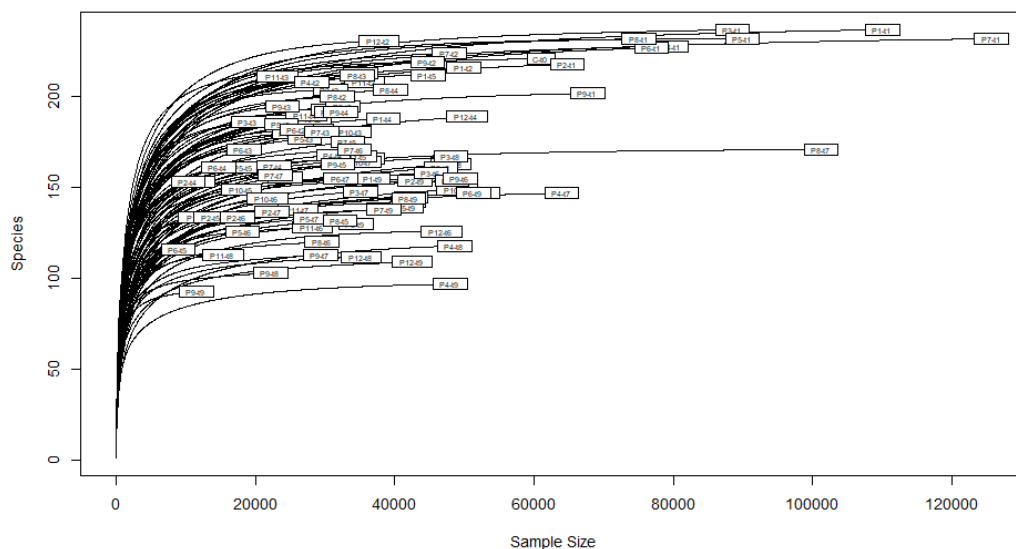


**Figure S5:** Rarefaction curves of the raw read counts for all samples.

## APPENDIX PUBLICATION II

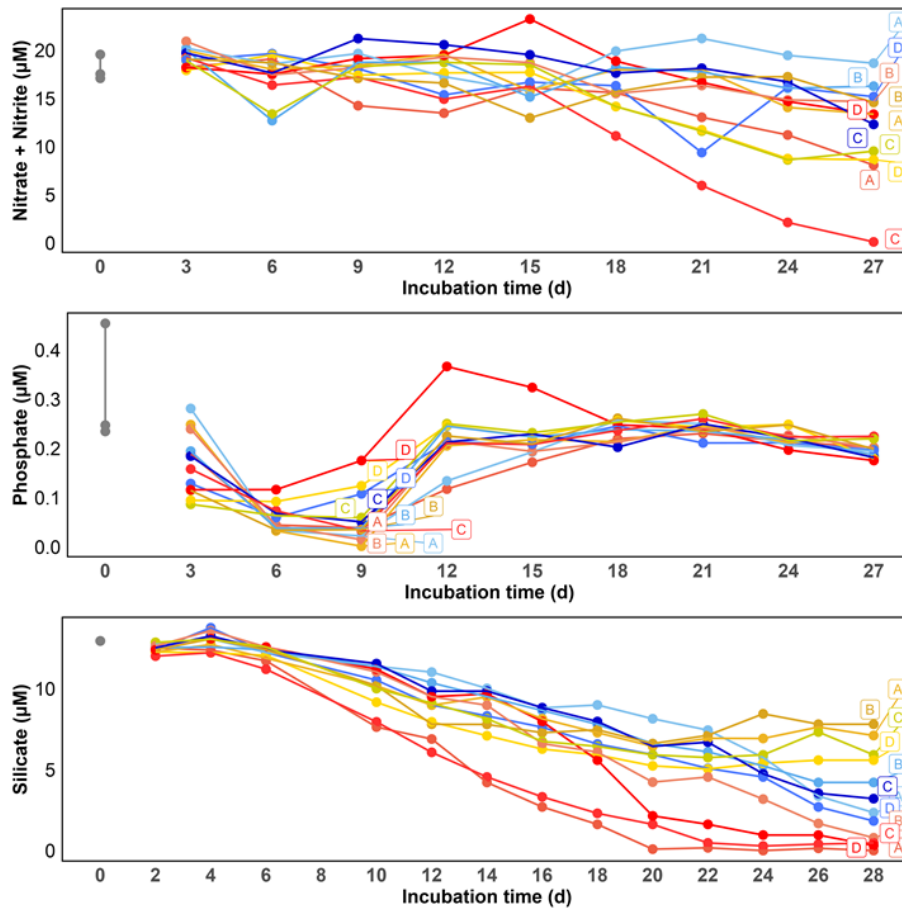


**Figure S6:** Development of each replicate mesocosm (A-D) over time for (a) nitrate + nitrite, (b) phosphate, (c) silicate. Colours denote the temperature treatments (6 °C: blue, 12 °C: yellow, 18 °C: red).

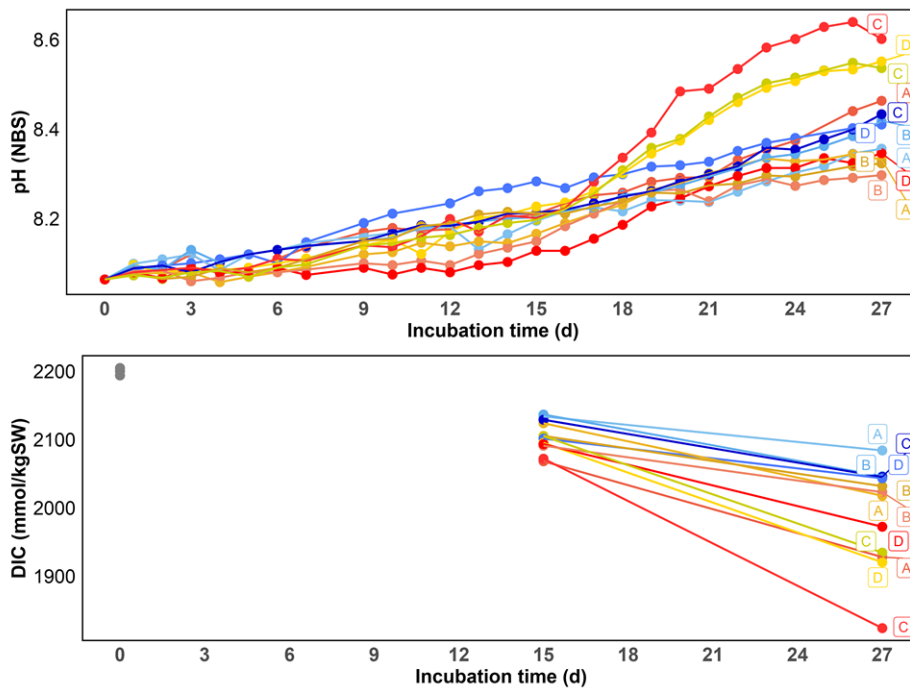


**Figure S7:** Development of each replicate mesocosm (A-D) over time for (a) the pH and (b) dissolved inorganic carbon (DIC). Colours denote the temperature treatments (6 °C: blue, 12 °C: yellow, 18 °C: red, t0: grey).

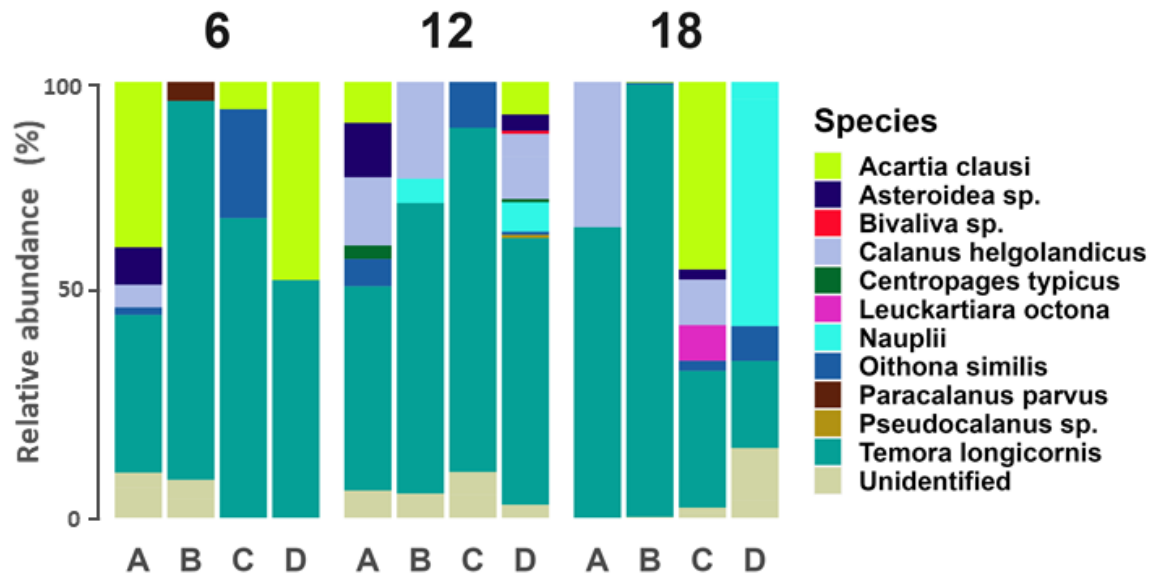


**Figure S8:** Microscopy-based mesozooplankton community composition and total mesozooplankton abundance L-1 (numbers on bar graphs) on species level at day 27 for all replicate mesocosms (A-D) of the temperature treatments (6, 12 and 18 °C).

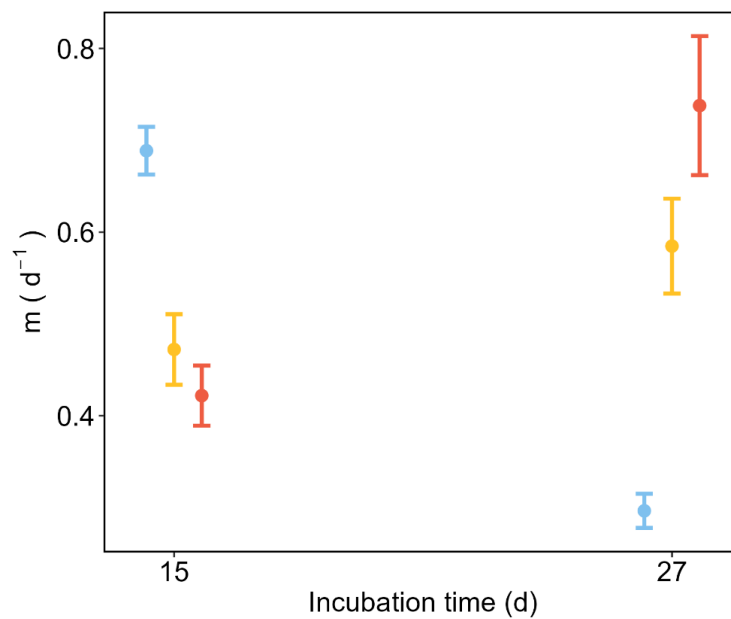


**Figure S9:** Pooled micro-grazing rates ( $m$ ) per day at the start (incubation day 15) and the end (incubation day 27) of the experiment for the three treatment temperatures (blue = 6 °C, yellow = 12 °C, red = 18 °C). Dots represent the mean and error bars the standard deviation of the replicates.



## APPENDIX PUBLICATION II

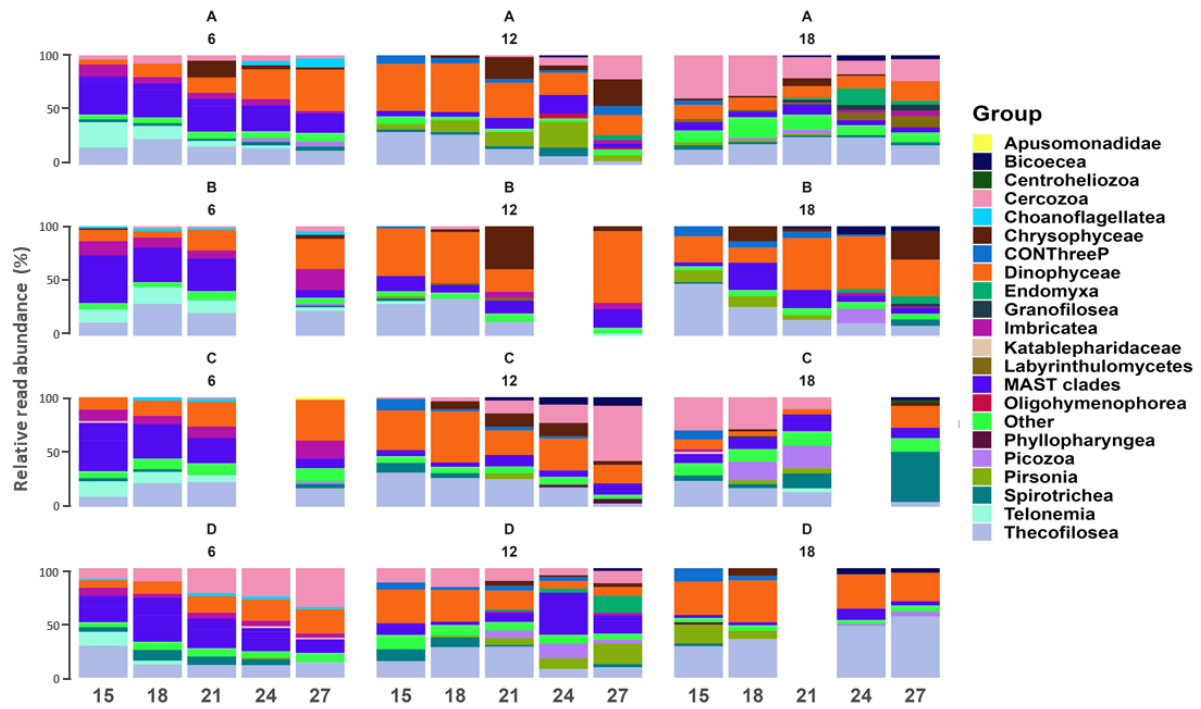


**Figure S10:** Metabarcoding-based heterotrophic protist community composition on phylum level over time for all replicates (horizontal alignment) and temperatures (vertical alignment). ASVs which could not be annotated were categorized as “other”.

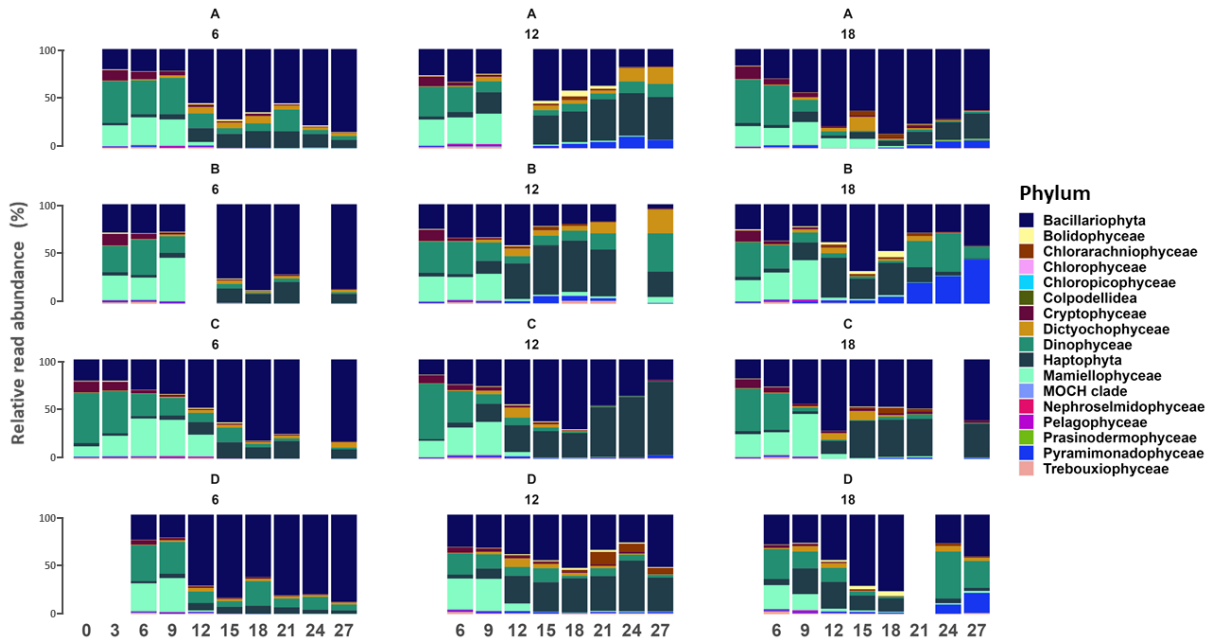


**Figure S11:** Metabarcoding-based phytoplankton community composition on phylum level over time for all replicates (horizontal alignment) and temperatures (vertical alignment). ASVs which could not be annotated were categorized as “other”.

## APPENDIX PUBLICATION II

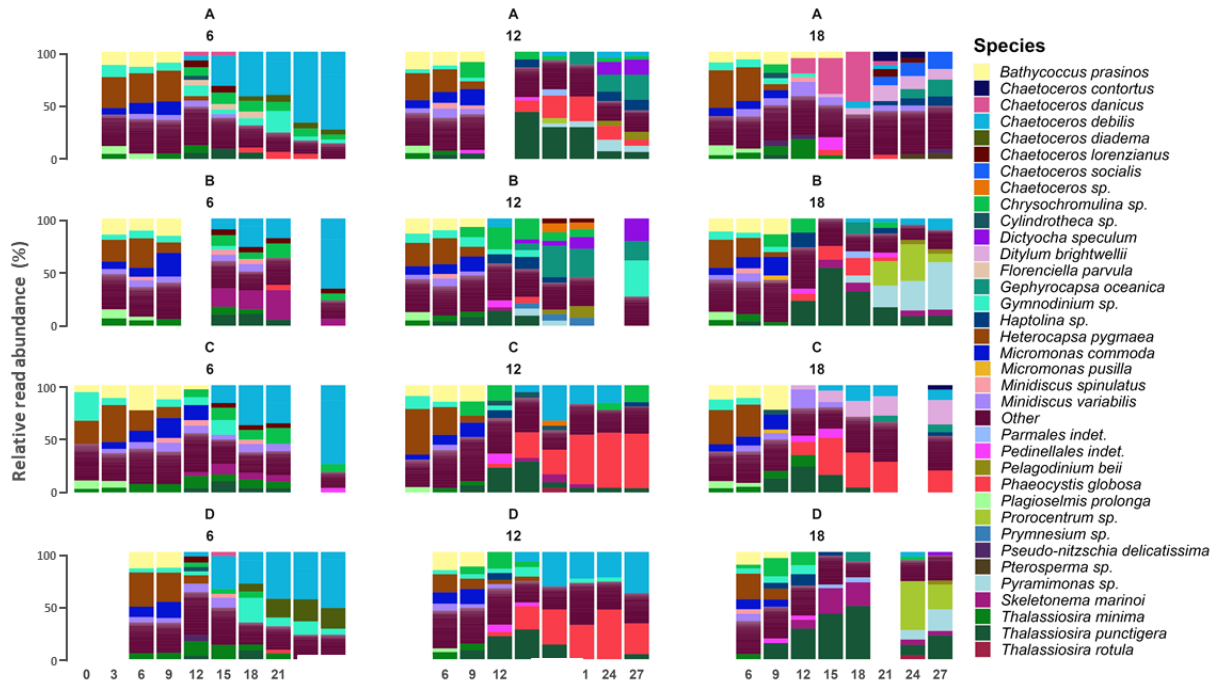


**Figure S12:** Metabarcoding-based phytoplankton community composition on species level over time for all replicates (horizontal alignment) and temperatures (vertical alignment). ASVs with an abundance of fewer than 200 reads among temperatures were categorized as “other”.

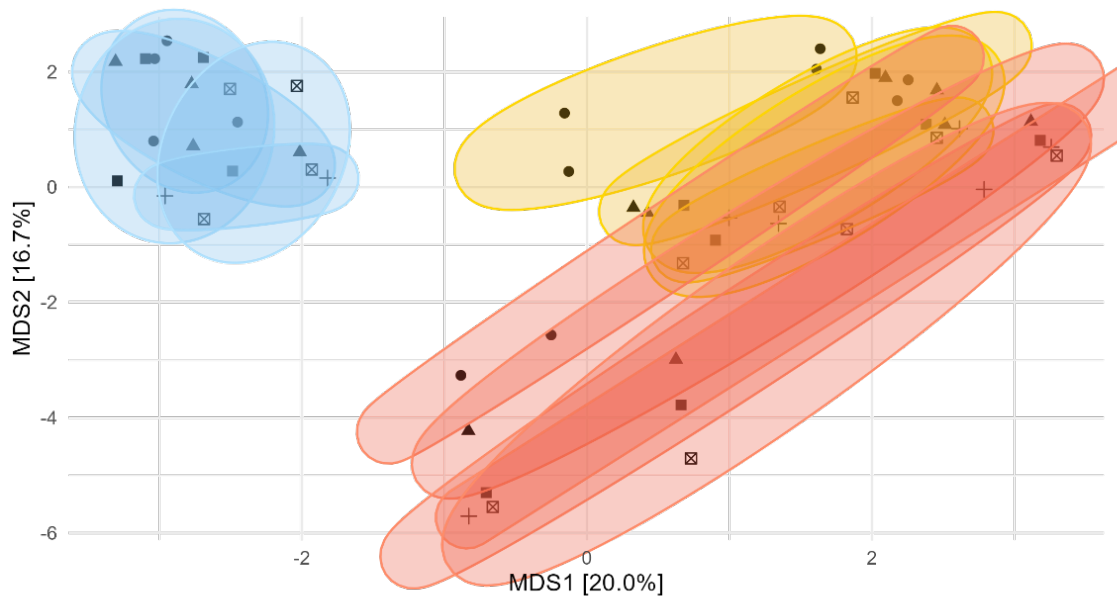


**Figure S13:** Principal component analysis (PCoA) using euclidean distances of the CLR-transformed ASV-based species composition at the different temperatures (blue = 6 °C; yellow = 12 °C; red = 18 °C) on all sampling days (circle = day 15; triangle = day 18; square = day 21; cross = day 24; cross in square = day 27) of the experiment, including 55 samples and 379 taxa. Ellipsoids are grouped per temperature and day.

## APPENDIX PUBLICATION II

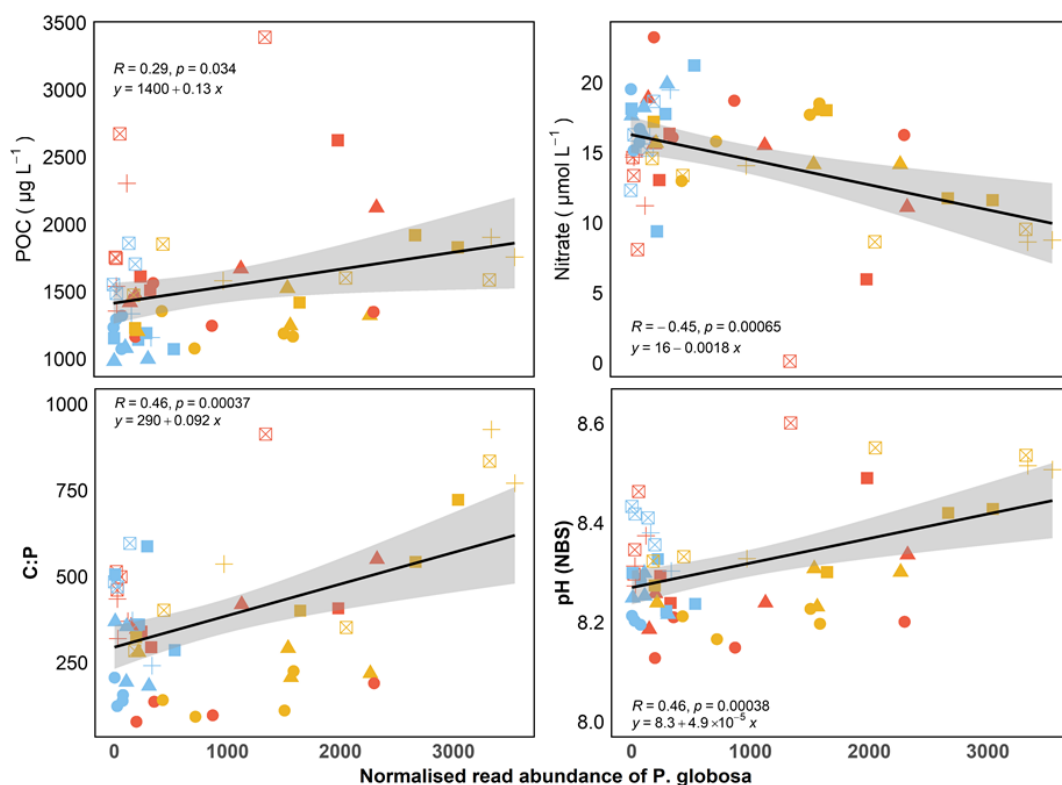


**Figure S14:** POC (a), nitrate (b), the C:P ratio (c) and pH (d) per normalised read abundance of *Phaeocystis globosa* of the different temperatures (blue = 6 °C; yellow = 12 °C; red = 18 °C) on all sampling days (circle = day 15; triangle = day 18; square = day 21; cross = day 24; cross in square = day 27) of the experiment. Fitted linear regressions with approximate 95% point-wise confidence intervals (grey-shaded areas).

**Table S1:** Sequencing statistics from the DADA2 pipeline for all samples after each filtering step and the ratio of final reads to raw reads.

Sample	Raw	Primer/Quality-filtered	Denoised	Merged	Chimera-filtered
6°C C Day 0	425746	265061	264737	262032	259640
18°C A Day 3	405838	247022	246447	243937	239755
18°C A Day 6	160562	95963	95600	93431	90872
18°C A Day 9	102683	61644	61380	59906	58866
18°C A Day 12	142835	88403	87965	86194	84454
18°C A Day 15	134250	80175	79835	77258	75657
18°C A Day 18	86662	52945	52687	50639	49745
18°C A Day 21	93995	57148	56883	54475	54031
18°C A Day 24	139649	77712	77384	73608	72909
18°C A Day 27	115802	67453	67170	65011	64191
6°C D Day 6	101620	60386	60120	59052	57085
6°C D Day 9	131791	76415	76166	74695	72979
6°C D Day 12	99537	58427	58246	57235	56491
6°C D Day 15	169255	86546	86244	84321	82773
6°C D Day 18	117443	69041	68767	67349	66007
6°C D Day 21	155635	88882	88597	86654	84566
6°C D Day 24	147561	89048	88665	86671	84107

## APPENDIX PUBLICATION II

6°C D Day 27	145536	83179	82951	81274	78878
12°C D Day 6	138838	86583	86261	84553	82168
12°C D Day 9	122961	75312	74992	73469	71506
12°C D Day 12	133665	78459	78153	76698	75177
12°C D Day 15	118082	69209	68992	67710	66242
12°C D Day 18	116100	68284	68096	66863	64969
12°C D Day 21	102708	59095	58966	58024	57635
12°C D Day 24	120073	70615	70520	70004	68694
12°C D Day 27	111097	63771	63557	62116	60521
18°C D Day 6	135631	82357	82013	80353	78369
18°C D Day 9	135503	81081	80822	79305	77787
18°C D Day 12	157516	98183	97866	96133	93736
18°C D Day 15	125748	75330	75072	73541	71081
18°C D Day 18	106690	64888	64757	63904	62449
18°C D Day 24	115471	66265	65982	63528	62098
18°C D Day 27	148832	85134	84803	75721	73806
6°C A Day 3	307239	187409	187098	185232	183159
6°C A Day 6	119999	69097	68830	67706	66348
6°C A Day 9	141878	80111	79864	78415	76727
6°C A Day 12	106713	63144	62784	61476	60243
6°C A Day 15	186801	107411	106967	104628	100223
6°C A Day 18	111252	65288	65054	63802	62354
6°C A Day 21	98008	54593	54445	53537	52516
6°C A Day 24	152000	81374	81188	79932	77887
6°C A Day 27	116779	66817	66579	65365	63090
12°C A Day 3	456422	259825	259475	257458	253694
12°C A Day 6	100454	62083	61836	60783	59778
12°C A Day 9	110346	64363	64158	63359	62536
12°C A Day 15	126387	70925	70710	69692	67818
12°C A Day 18	115119	69438	69174	67733	65884
12°C A Day 21	103373	60236	60090	59018	57568
12°C A Day 24	156179	92955	92613	90401	88178
12°C A Day 27	104101	59451	59320	58509	57845
18°C B Day 3	376605	225059	224694	222779	219061
18°C B Day 6	122624	71025	70789	69781	68614
18°C B Day 9	159773	94340	93957	91774	89681
18°C B Day 12	110663	66770	66562	65450	64396
18°C B Day 15	127156	69998	69789	67099	65132
18°C B Day 18	121547	69327	69106	67571	65841
18°C B Day 21	175716	100953	100453	97120	91833
18°C B Day 24	135735	75061	74814	70642	69142
18°C B Day 27	125271	70848	70573	62528	60871
6°C B Day 3	414007	247889	247522	245381	242480
6°C B Day 6	114226	63945	63703	62569	61082
6°C B Day 9	96637	59888	59766	59115	58696
6°C B Day 15	136918	82285	82071	80276	78129
6°C B Day 18	105543	61796	61611	60337	59372
6°C B Day 21	125533	71498	71173	69487	67191

## APPENDIX PUBLICATION II

6°C B Day 27	142827	88894	88515	86203	82380
6°C C Day 3	317774	188965	188607	186618	182933
6°C C Day 6	108781	52841	52655	51625	50526
6°C C Day 9	90464	55488	55272	54388	53490
6°C C Day 12	99031	55578	55403	54537	53826
6°C C Day 15	62634	35897	35751	35010	34240
6°C C Day 18	133589	72373	72089	70545	68635
6°C C Day 21	149600	87522	87202	85243	82898
6°C C Day 27	146385	89992	89741	87675	84056
18°C C Day 3	368426	207634	207140	204327	201073
18°C C Day 6	180547	106326	105862	103219	98931
18°C C Day 9	103966	64664	64453	63314	62486
18°C C Day 12	95492	56775	56560	55639	54900
18°C C Day 15	115196	69015	68777	65616	64504
18°C C Day 18	150658	87754	87431	84225	82856
18°C C Day 21	133553	81400	81119	79673	78389
18°C C Day 27	110909	67327	67175	66370	65749
12°C B Day 3	366019	217754	217210	214702	209318
12°C B Day 6	129842	77721	77469	76263	74475
12°C B Day 9	129893	79099	78821	77230	75547
12°C B Day 12	194761	113334	112911	110306	106205
12°C B Day 15	126304	74598	74408	73478	71909
12°C B Day 18	99809	56551	56407	55862	55280
12°C B Day 21	394299	225346	224989	222553	218581
12°C B Day 27	141807	82718	82459	80410	78029
12°C C Day 3	434730	257556	257130	244469	236088
12°C C Day 6	144605	88861	88487	86557	84177
12°C C Day 9	108637	66463	66159	64564	63030
12°C C Day 12	126494	78525	78203	76641	74575
12°C C Day 15	100736	59221	59027	58098	56771
12°C C Day 18	115039	66469	66276	64998	63174
12°C C Day 21	79631	45682	45605	43922	43655
12°C C Day 24	93860	52975	52868	48776	48304
12°C C Day 27	86529	47376	47280	38509	38064

**Table S2:** Results of the two-way rmANOVA regarding the effect of temperature, time, and their interactive effects on the mean beta-dispersions of the Aitchinson distances during the experiment phase. Dfn is the degree of freedom for the numerator of the F ratio, and DFd is for the denominator. Significant effects are highlighted in bold.

Parameter	Effect	DFn	DFd	<i>F</i>	<i>p</i>
6 °C – 12 °C	Temperature	1	6	3.466	.112
	Time	3	18	1.752	.192
	Temperature:Time	3	18	0.432	.733
6 °C – 18 °C	Temperature	1	5	12.241	<b>0.017</b>
	Time	1.21	6.04	0.004	0.969
	Temperature:Time	1.21	6.04	0.150	0.754

## **Appendix Publication III**

The experimental implications of the rate of temperature change and timing of nutrient availability on growth and stoichiometry of a natural marine phytoplankton community

*Shortened supplementary material*

*The full supplementary material can be found here:*  
<https://tinyurl.com/ebdpz8yc>

## APPENDIX PUBLICATION III

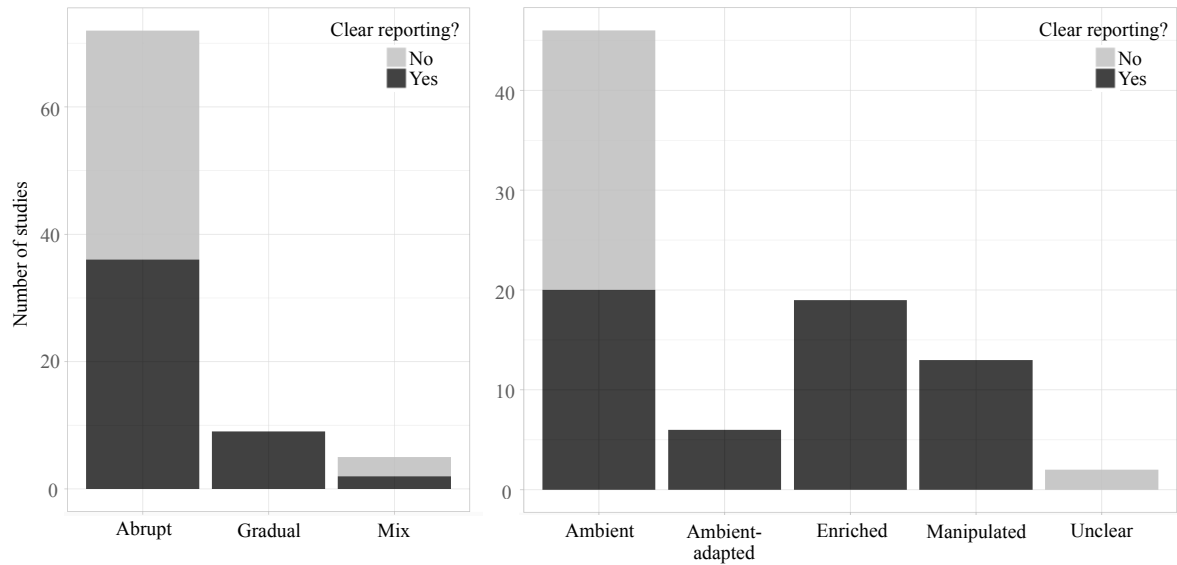


**Figure S2.1:** Overview of the systematic literature map. The left side shows the type of temperature change (abrupt, gradual, mix) that experimental studies applied. The right side indicates the type of nutrient conditions that were applied. More details about the criteria for the categories can be found in Supplement 1. The colors indicate whether the respective conditions were clearly reported (dark grey) or only to be assumed from the experimental design (light grey).

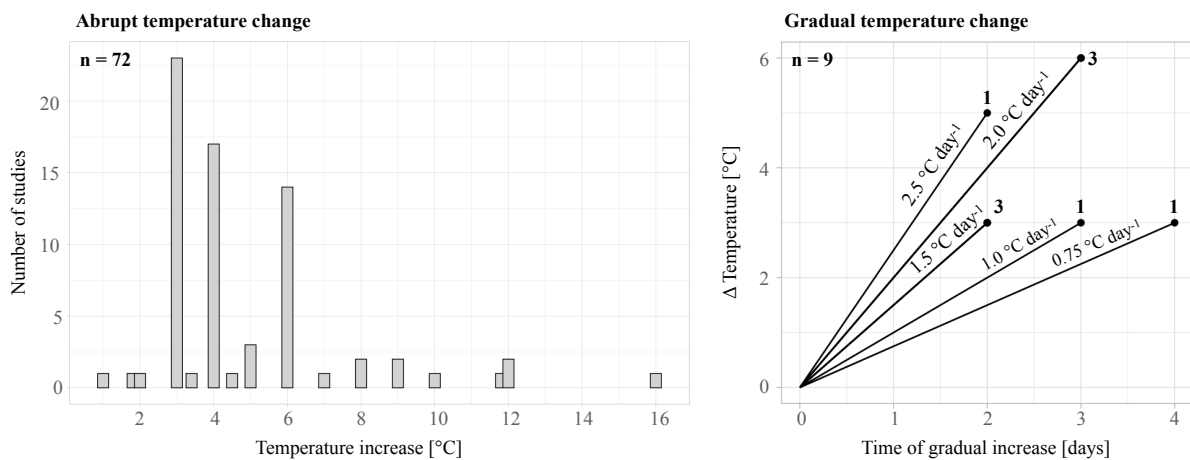


**Figure S2.2:** Types of temperature increase in experimental studies separated into abrupt (left side) and gradual temperature increases (right side). The temperature increase in the left figure and  $\Delta$  Temperature in the right figure refer to the highest applied increase (compared to ambient conditions) of the respective study. For gradual temperature increase, the bold values indicate the number of studies that applied the respective gradual increase.



## APPENDIX PUBLICATION III

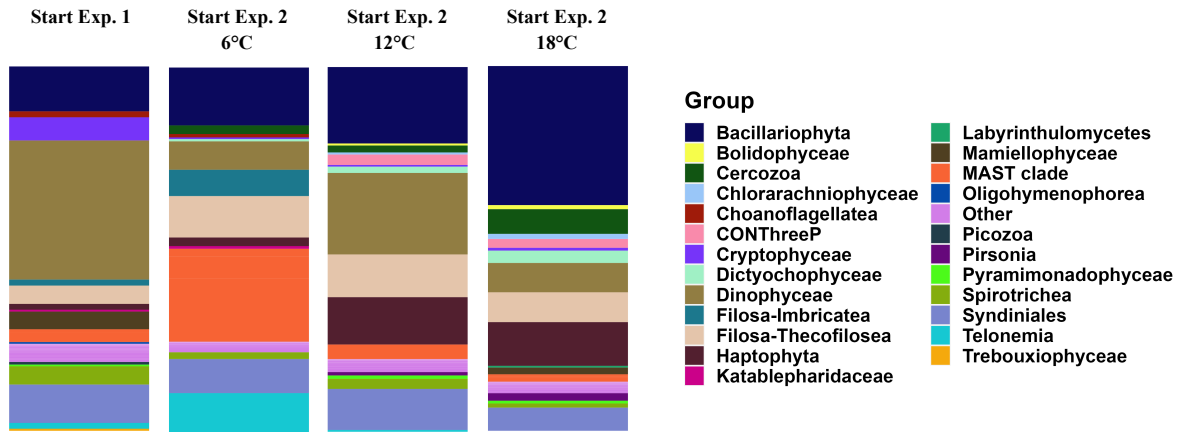


**Figure S2.3:** Community composition of the start community of both microcosm experiments based on DNA data (18S rRNA sequencing). Experiment 2 is separated into three different temperature treatments: ambient 6 °C, an increase by 1 °C day<sup>-1</sup> to 12 °C and 18 °C. For readability, ASVs with an abundance of fewer than 100 reads among replicates were categorized as “other”. The data are based on ASV reads counts and therefore do not represent biomass contributions. For detailed figures on species level and more information about changes in community composition in the accompanying mesocosm experiment see Ahme et al. (2024). The sample water was filtered onto 0.8 µm polycarbonate filters (Nucleopore, Whatman, Maidstone, UK) and DNA was extracted using the NucleoSpin Soil extraction Kit (Macherey-Nagel GmbH, Düren, Germany). Using primers targeting the variable region 4 of the 18S rRNA gene (Bradley et al. 2016), amplicons were generated and sequenced on a MiSeq sequencer following the standard protocol for library preparation and sequencing (Illumina, San Diego, CA, USA). After primer removal, quality-trimming, denoising, and chimera removal, amplicon sequence variants (ASVs) were taxonomically annotated using the protist reference database v4.12.0 PR2 (Guillou et al. 2013). The validity of the 18S rRNA metabarcoding was qualitatively post-evaluated via light microscopy screening using the method by Utermöhl (1958).

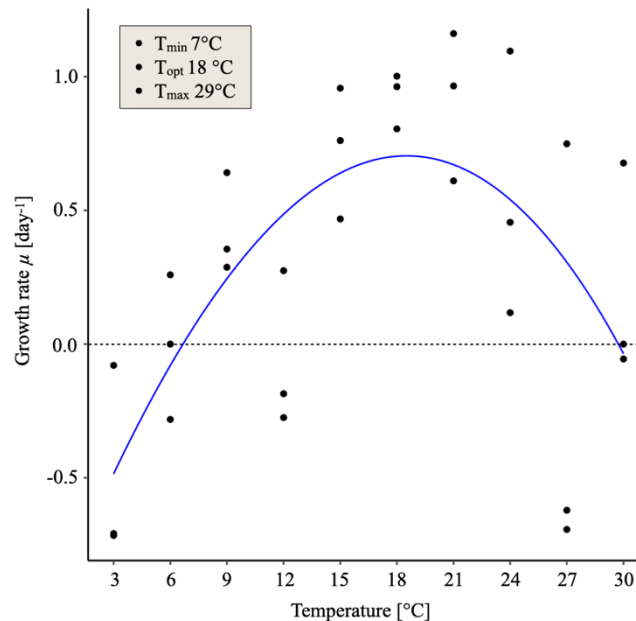


**Figure S2.4:** Thermal performance curve (TPC) of the phytoplankton community directly after sampling it from the North Sea. The nutrient conditions were kept at ambient. The temperature exposure was done abruptly to temperatures between 3 and 30 °C in steps of 3 °C. The methods for the TPC are described in detail in Ahme et al. (2024).

## APPENDIX PUBLICATION III

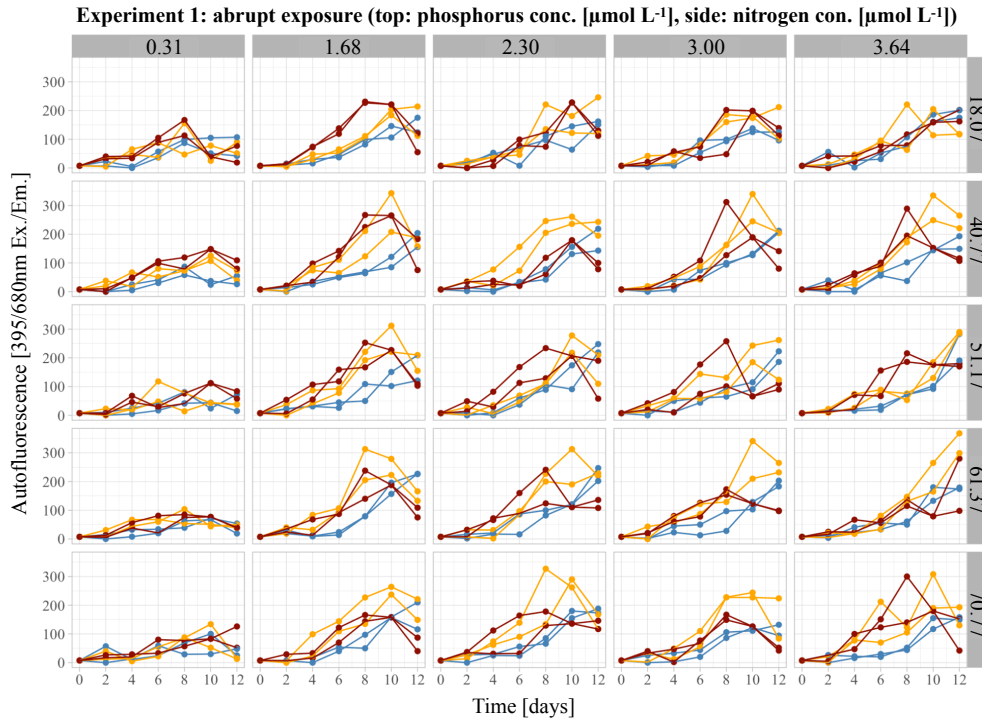


**Figure S2.5:** Time series of phytoplankton growth as autofluorescence at 395/680nm Ex./Em. in the ambient temperature treatment ( $6^{\circ}\text{C}$ , blue) and the abruptly exposed temperature treatments ( $12^{\circ}\text{C}$  in orange and  $18^{\circ}\text{C}$  in red) over a nitrogen ( $18.07\text{--}70.77 \mu\text{mol L}^{-1}$ ) and phosphorus ( $0.31\text{--}3.64 \mu\text{mol L}^{-1}$ ) gradient in the first run of the experiment. The stated values on the facet axes correspond to the final concentrations including background concentration.

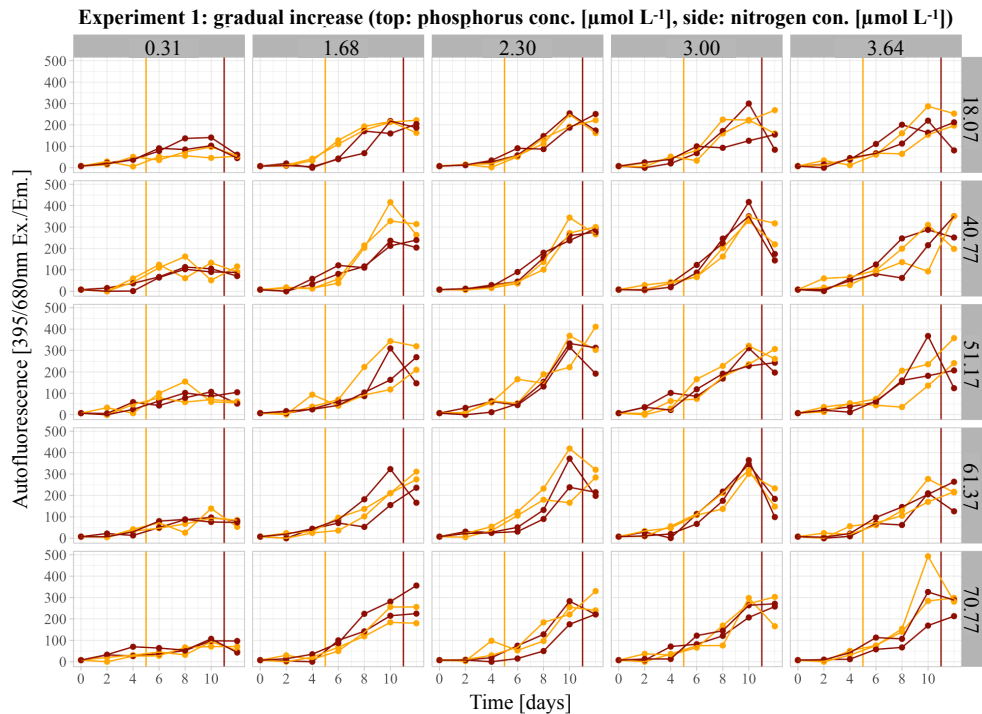


**Figure S2.6:** Time series of phytoplankton growth as autofluorescence at 395/680nm Ex./Em. in the gradually increased temperature treatments of  $12^{\circ}\text{C}$  (orange) and  $18^{\circ}\text{C}$  (red) over a nitrogen ( $18.07\text{--}70.77 \mu\text{mol L}^{-1}$ ) and phosphorus ( $0.31\text{--}3.64 \mu\text{mol L}^{-1}$ ) gradient in the first microcosm experiment. The vertical lines indicate the time point at which the respective final experimental has been reached. The stated values on the facet axes correspond to the final concentrations including background concentration.

## APPENDIX PUBLICATION III

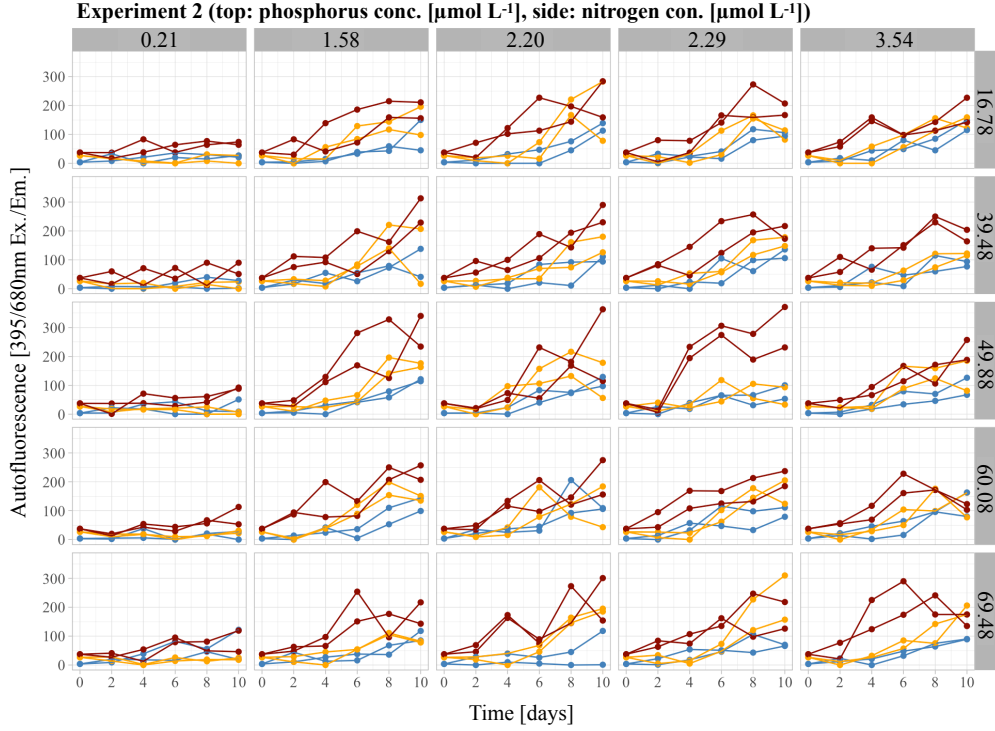


**Figure S2.7:** Time series of phytoplankton growth at the three temperatures 6 °C (blue), 12 °C (orange) and 18 °C (red) in the second experiment over a nitrogen ( $\mu\text{mol L}^{-1}$ ) and phosphorus ( $\mu\text{mol L}^{-1}$ ) gradient. This run received the addition of nutrients after thermal acclimation. The stated values on the facet axes correspond to the final concentrations including background concentration for 6 °C (for 12 °C add  $-5.3 \mu\text{mol L}^{-1}$  N and  $0.0075 \mu\text{mol L}^{-1}$  P to the shown values, and for 18 °C add  $1.80 \mu\text{mol L}^{-1}$  N and  $-0.01 \mu\text{mol L}^{-1}$  P to the values).

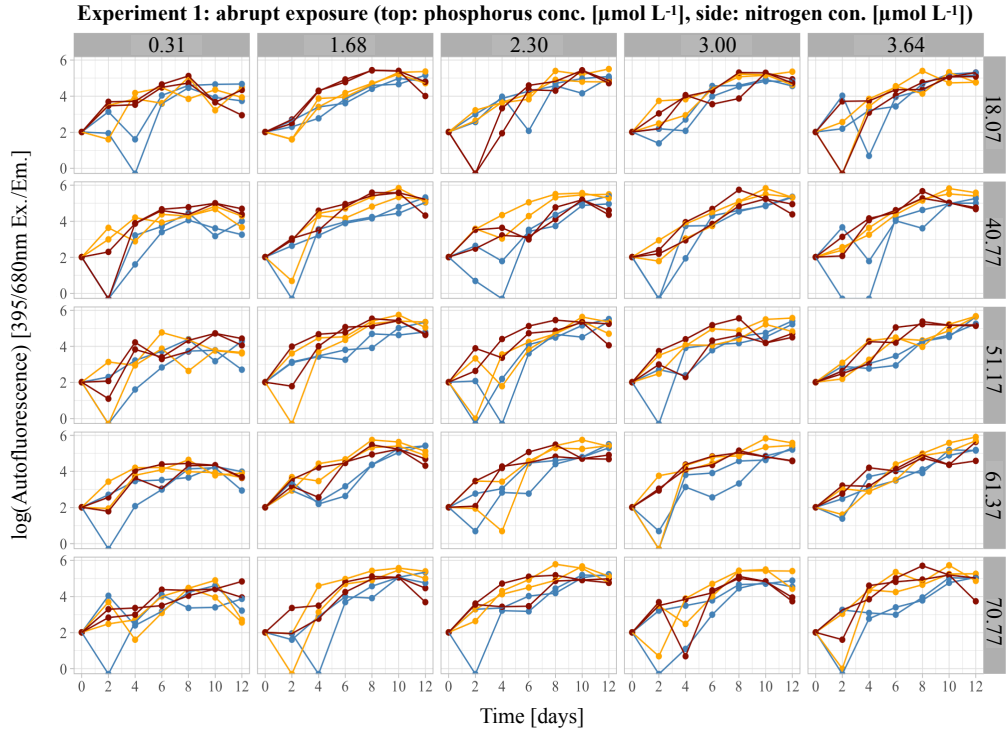


**Figure S2.8:** Time series of phytoplankton growth as the logarithm of autofluorescence at 395/680nm Ex./Em. in the ambient temperature treatment (6°C, blue) and the abruptly exposed temperature treatments (12 °C in orange and 18 °C in red) over a nitrogen (18.07-70.77  $\mu\text{mol L}^{-1}$ ) and phosphorus (0.31-3.64  $\mu\text{mol L}^{-1}$ ) gradient in the first run of the experiment. The stated values on the facet axes correspond to the final concentrations including background concentration.

## APPENDIX PUBLICATION III

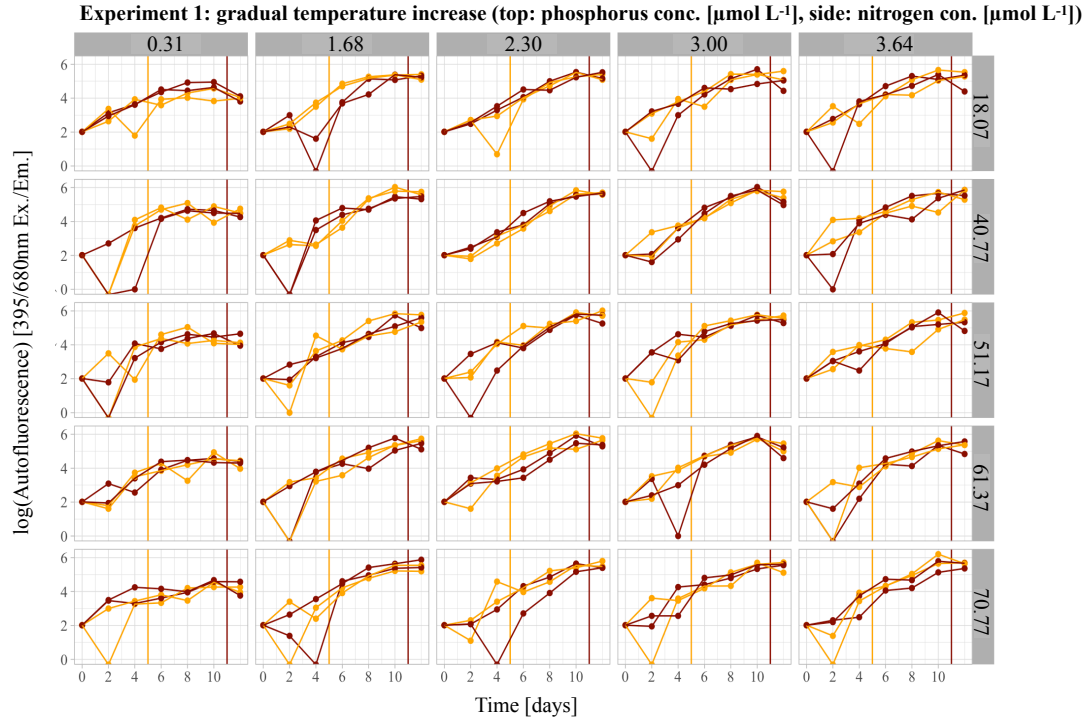


**Figure S2.9:** Time series of phytoplankton growth as the logarithm of autofluorescence at 395/680nm Ex./Em. in the gradually increased temperature treatments of 12 °C (orange) and 18 °C (red) over a nitrogen (18.07-70.77  $\mu\text{mol L}^{-1}$ ) and phosphorus (0.31-3.64  $\mu\text{mol L}^{-1}$ ) gradient in the first microcosm experiment. The vertical lines indicate the time point at which the respective final experimental temperature has been reached. The stated values on the facet axes correspond to the final concentrations including background concentration.

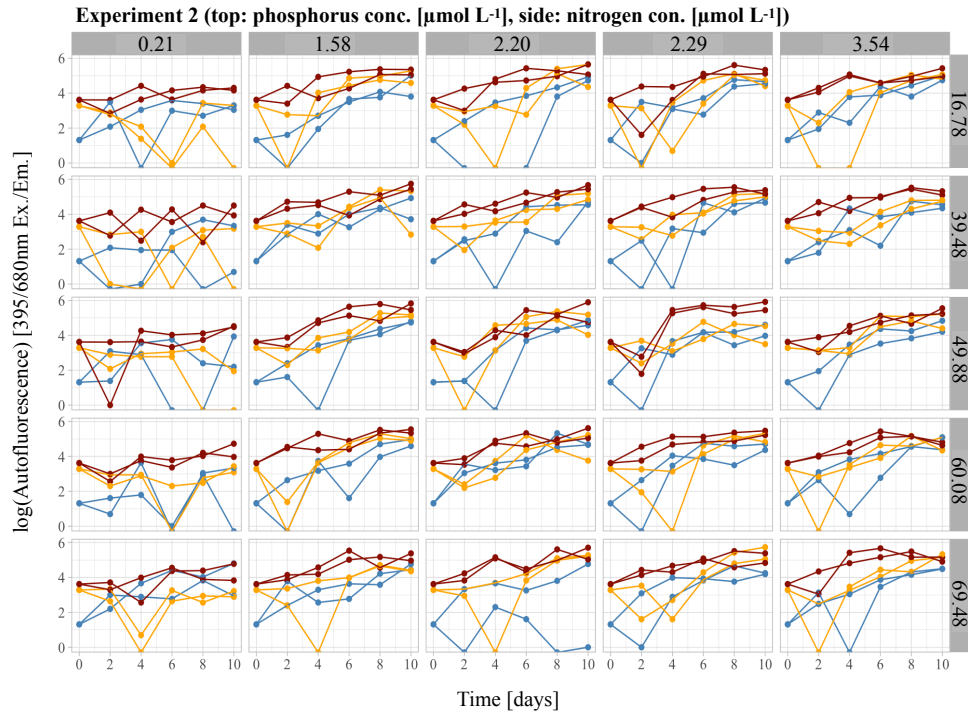


**Figure S2.10:** Time series of phytoplankton growth as the logarithm of autofluorescence at 395/680nm Ex./Em. At the three temperatures 6 °C (blue), 12 °C (orange) and 18 °C (red) in the second experiment over a nitrogen ( $\mu\text{mol L}^{-1}$ ) and phosphorus ( $\mu\text{mol L}^{-1}$ ) gradient. This run received the addition of nutrients after thermal acclimation. The stated values on the facet axes correspond to the final concentrations including background concentration for 6 °C (for 12 °C add  $-5.3 \mu\text{mol L}^{-1}$  N and  $0.0075 \mu\text{mol L}^{-1}$  P to the shown values, and for 18 °C add  $1.80 \mu\text{mol L}^{-1}$  N and  $-0.01 \mu\text{mol L}^{-1}$  P to the values).

## APPENDIX PUBLICATION III

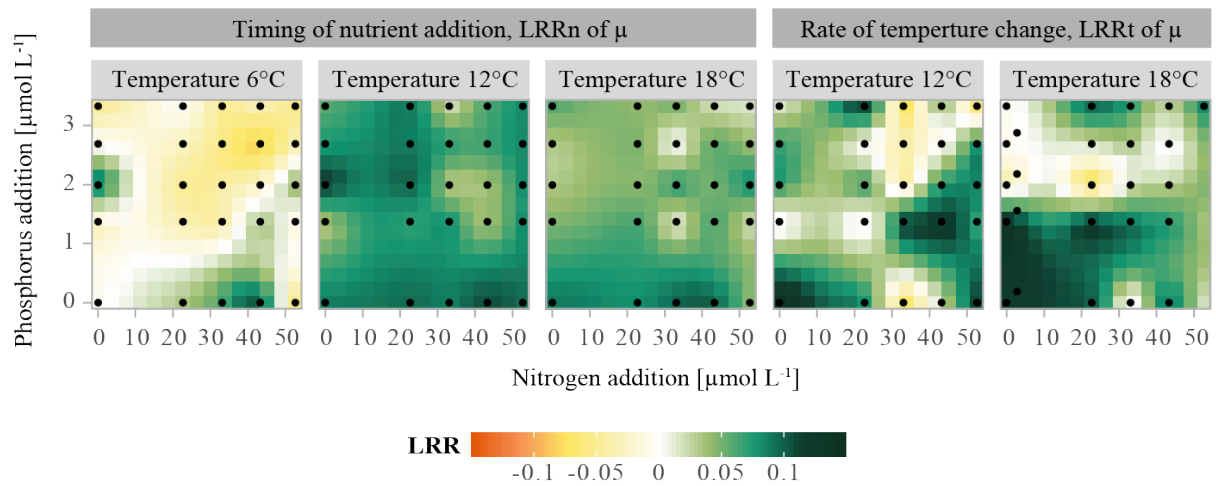


**Figure S2.11:** Interpolated response surfaces of the LRR for nutrient addition (LRRn: community  $\mu$  for nutrients added before temperature change divided by community  $\mu$  for nutrients added after the temperature change) and rate of temperature change (LRRt: community  $\mu$  for abrupt temperature increase divided by community  $\mu$  in a gradual temperature change) across nitrogen and phosphorus supply (in  $\mu\text{mol L}^{-1}$ ). Positive values in the left panels indicate that nutrient availability during temperature change led to higher growth rates. Positive values in the right panels mean that an abrupt temperature exposure led to higher growth rates compared to a gradual temperature increase.

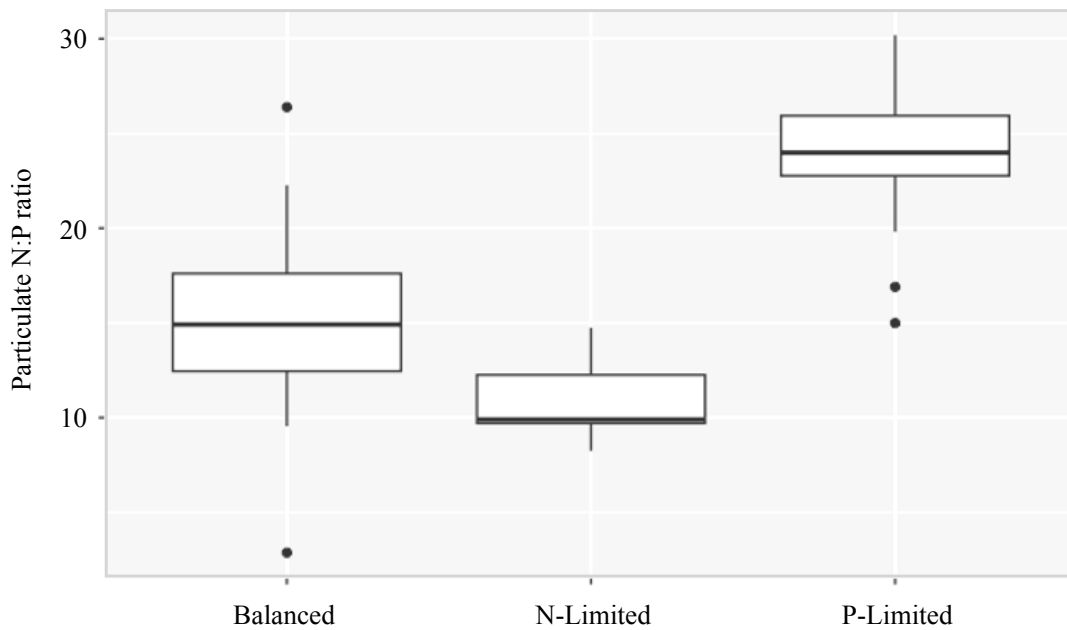


**Figure S2.12:** The effect of nitrogen:phosphorus (N:P) supply conditions (balanced, nitrogen-limited, phosphorus-limited) on particulate N:P ratios for all abrupt and gradual temperature increase treatments together (since no effect of the rate of temperature increase on particulate N:P ratios has been found). See statistical results in Table S2.2.

## APPENDIX PUBLICATION III

**Table S2.1:** *Post-hoc test for Generalized Linear Model ( $\mu \sim$  temperature level \* final N:P supply ratio \* rate of temperature change). Asterisks indicate significance ( $p > 0.05$ ).*

Term	Group 1	Group 2	Estimate	Conf. Low	Conf. High	P (adjusted)	Significance
Temp	12	18	3.08e-3	-0.00981	0.0160	6.38e-1	
Ratio	Balanced	N-Limited	-2.60e-2	-0.0476	-0.00431	1.41e-2	*
Ratio	Balanced	P-Limited	-7.99e-2	-0.0986	-0.0612	0	****
Ratio	N-Limited	P-Limited	-5.39e-2	-0.0789	-0.0290	2.40e-6	****
Temp. Rate	Abrupt	Gradual	-3.49e-2	-0.0478	-0.0220	2.71e-7	****

**Table S2.2:** *Post-hoc test for Generalized Linear Model (particulate N:P ratio  $\sim$  temperature level \* final N:P supply ratio \* rate of temperature change). Asterisks indicate significance ( $p > 0.05$ ).*

Term	Group 1	Group 2	Estimate	Conf. Low	Conf. High	P (adjusted)	Significance
Temp	12	18	-0.938	-2.34	0.459	1.86e-1	
Ratio	Balanced	N-Limited	-4.55	-6.90	-2.20	3.88e-5	****
Ratio	Balanced	P-Limited	8.41	6.36	10.5	3.09e-10	****
Ratio	N-Limited	P-Limited	13.0	10.2	15.7	3.09e-10	****
Temp. Rate	Abrupt	Gradual	1.12	-0.279	2.52	1.15e-1	

**Table S2.3:** *Post-hoc test for Generalized Linear Model ( $\mu \sim$  temperature level \* final N:P supply ratio \* nutrient availability during temperature change). Asterisks indicate significance ( $p > 0.05$ ).*

Term	Group 1	Group 2	Estimate	Conf. Low	Conf. High	P (adjusted)	Significance
Temp	6	12	-0.450	-0.575	-0.325	4.50e-13	****
Temp	6	18	-0.264	-0.389	-0.139	3.22e-6	****
Temp	12	18	0.186	0.0620	0.310	1.39e-3	**
Ratio	Balanced	N-Limited	-0.0686	-0.212	0.0749	4.99e-1	
Ratio	Balanced	P-Limited	-0.592	-0.715	-0.469	4.25e-13	****
Ratio	N-Limited	P-Limited	-0.523	-0.688	-0.359	3.09e-12	****
Nut. Av.	Before	After	-0.417	-0.502	-0.332	4.35e-13	****

**Table S2.4:** *Post-hoc test for Generalized Linear Model (LRRn  $\sim$  final N:P supply ratio \* nutrient availability during temperature change). Asterisks indicate significance ( $p > 0.05$ ).*

Term	Group 1	Group 2	Estimate	Conf. Low	Conf. High	P (adjusted)	Significance
Temp	6	12	0.0890	0.0709	0.107	1.89e-11	****
Temp	6	18	0.0664	0.0481	0.0847	2.55e-11	****
Temp	12	18	-0.0226	-0.0403	-0.00488	8.94e-3	**
Ratio	Balanced	N-Limited	0.00106	-0.0215	0.0236	9.93e-1	
Ratio	Balanced	P-Limited	0.0404	0.0224	0.0583	3.37e-6	****
Ratio	N-Limited	P-Limited	0.0393	0.0135	0.0651	1.5e-3	**

**Table S2.5:** *Post-hoc test for Generalized Linear Model (particulate N:P ratio  $\sim$  temperature level \* final N:P supply ratio \* nutrient availability during temperature change). Asterisks indicate significance ( $p > 0.05$ ).*

Term	Group 1	Group 2	Estimate	Conf. Low	Conf. High	P (adjusted)	Significance
Temp	6	12	0.0747	-0.0207	0.170	1.56e-1	
Temp	6	18	0.0764	-0.0190	0.172	1.43e-1	
Temp	12	18	0.00172	-0.0927	0.0961	9.99e-1	
Ratio	Balanced	N-Limited	-0.188	-0.296	-0.0790	2.15e-4	***
Ratio	Balanced	P-Limited	0.578	0.484	0.672	3.55e-15	****
Ratio	N-Limited	P-Limited	0.766	0.641	0.891	3.55e-15	****
Nut. Av.	Before	After	-0.202	-0.267	-0.138	7.47e-9	****

## **Appendix Publication IV**

Nutrient pulse scenarios drive contrasting patterns in the  
functional stability of freshwater phytoplankton

*Supplementary material*



## APPENDIX PUBLICATION IV

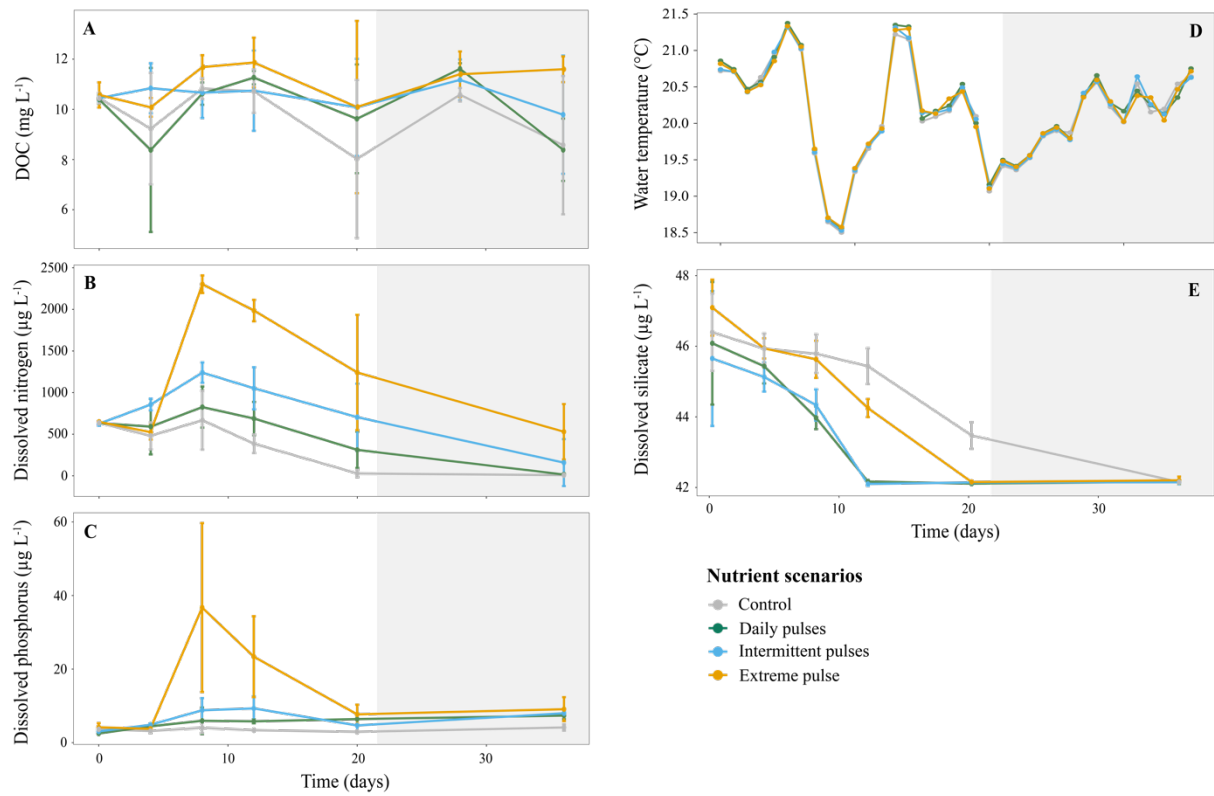


**Figure S1:** Timeseries of dissolved organic carbon (DOC), nitrogen, phosphorus and silicate as well as temperature for the control (C), the daily pulses (D), intermittent pulses (I) and the extreme pulse (E). The grey area represents the recovery period.

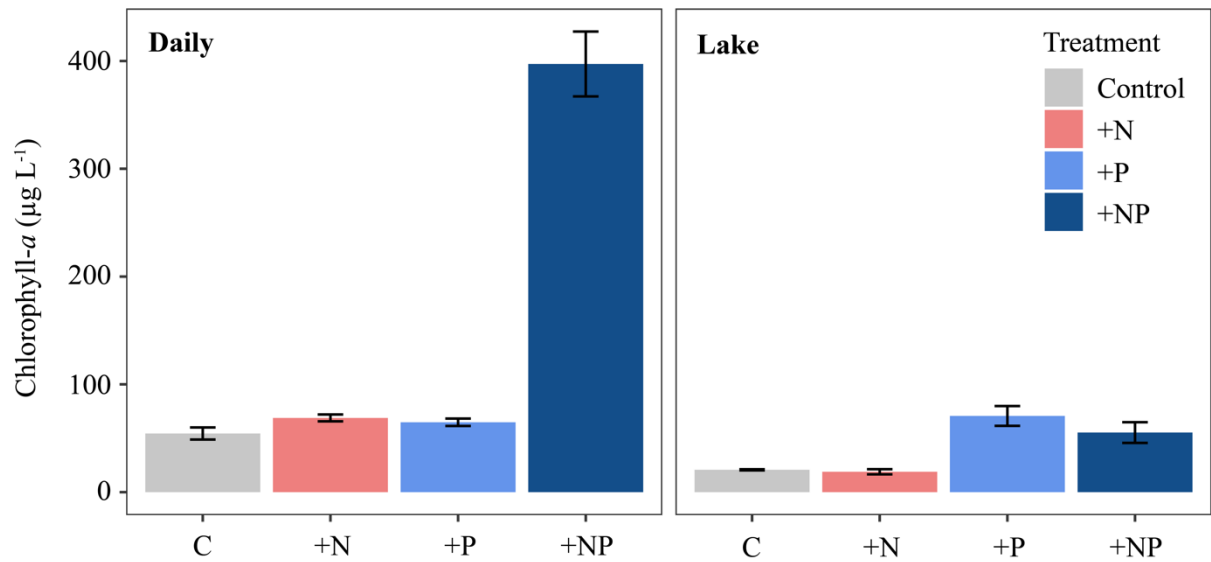


**Figure S2:** Nutrient limitation bioassay. Chlorophyll-a at the endpoint is presented for the different nutrient additions: control with no additions (C), nitrogen addition (N), phosphorus addition (P), or an addition of both nitrogen and phosphorus together (NP). The left panel shows the response of the plankton community taken from a pooled sample of the daily mesocosms and the right side represents a community originating from the lake.

## APPENDIX PUBLICATION IV

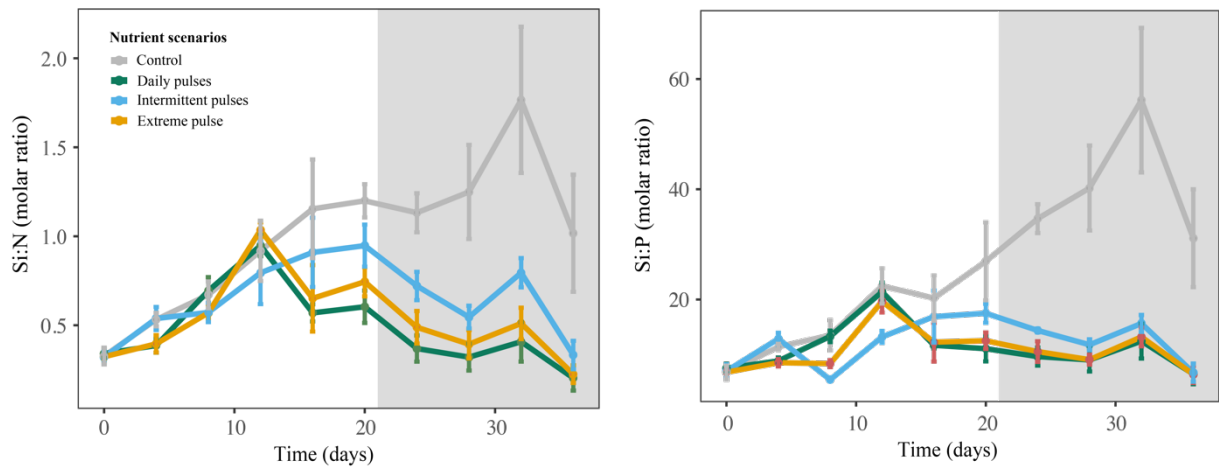


**Figure S3:** Time series of particulate molar ratios of Si:P and Si:N. The grey background represents the recovery period. Time series are given for the control (C), the daily pulses (D), intermittent pulses (I) and the extreme pulse (E).

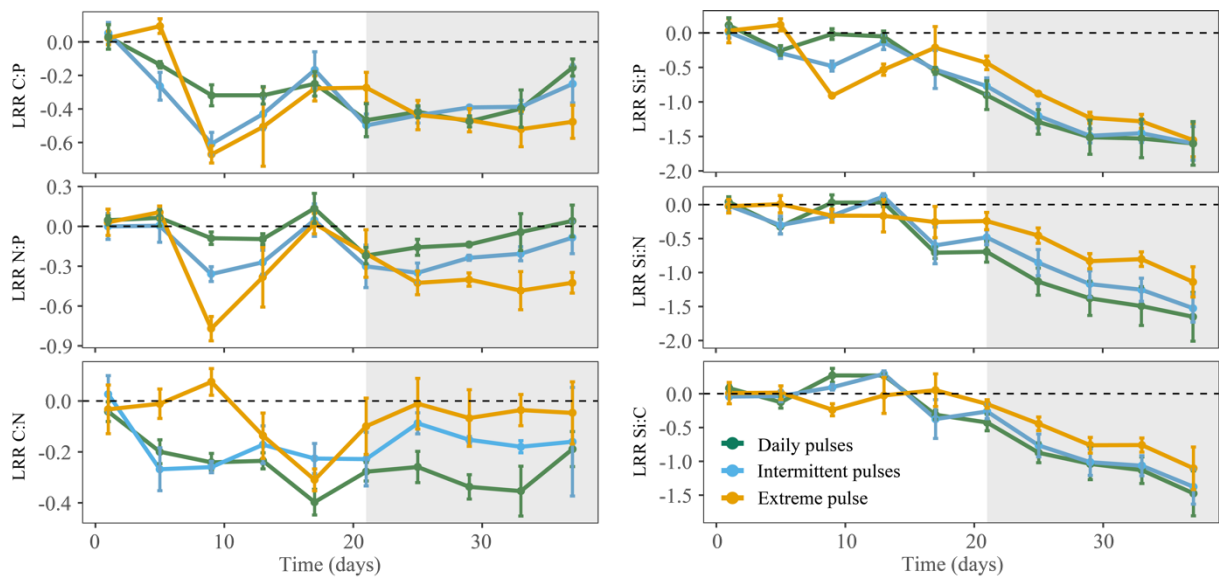


**Figure S4:** Log-response ratios over time for the cellular C:P, N:P, C:N, Si:P, Si:N and Si:C ratio of phytoplankton. The grey area represents the recovery period. Time series are given for the daily pulses (green), intermittent pulses (blue) and the extreme pulse (orange).

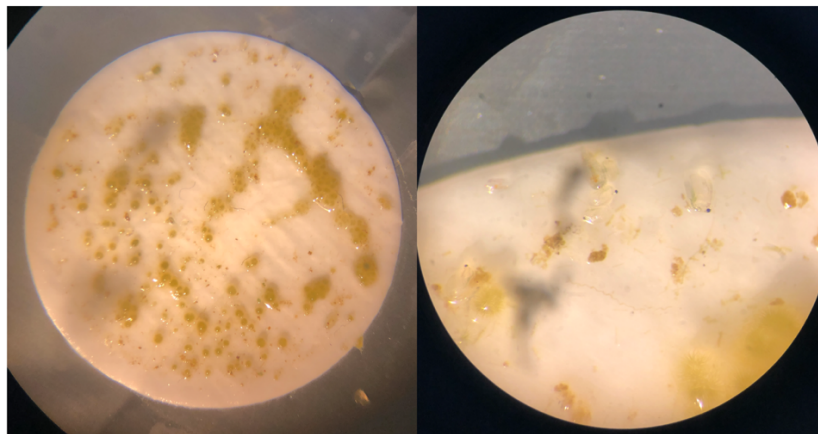


**Figure S5.5:** Photograph of a CN filter under the binocular during sampling 5 in mesocosm #9 (extreme).

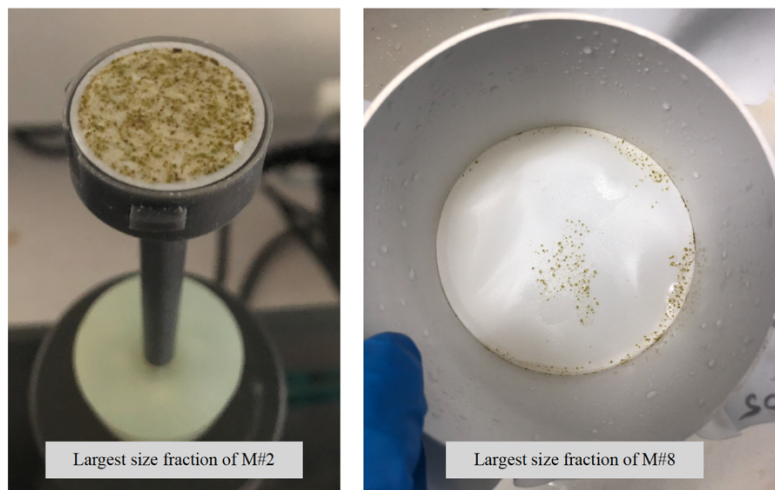


**Figure S6:** Photograph of a CN filter for mesocosm #2 (daily), and mesocosm #8 (daily) during sampling #3.

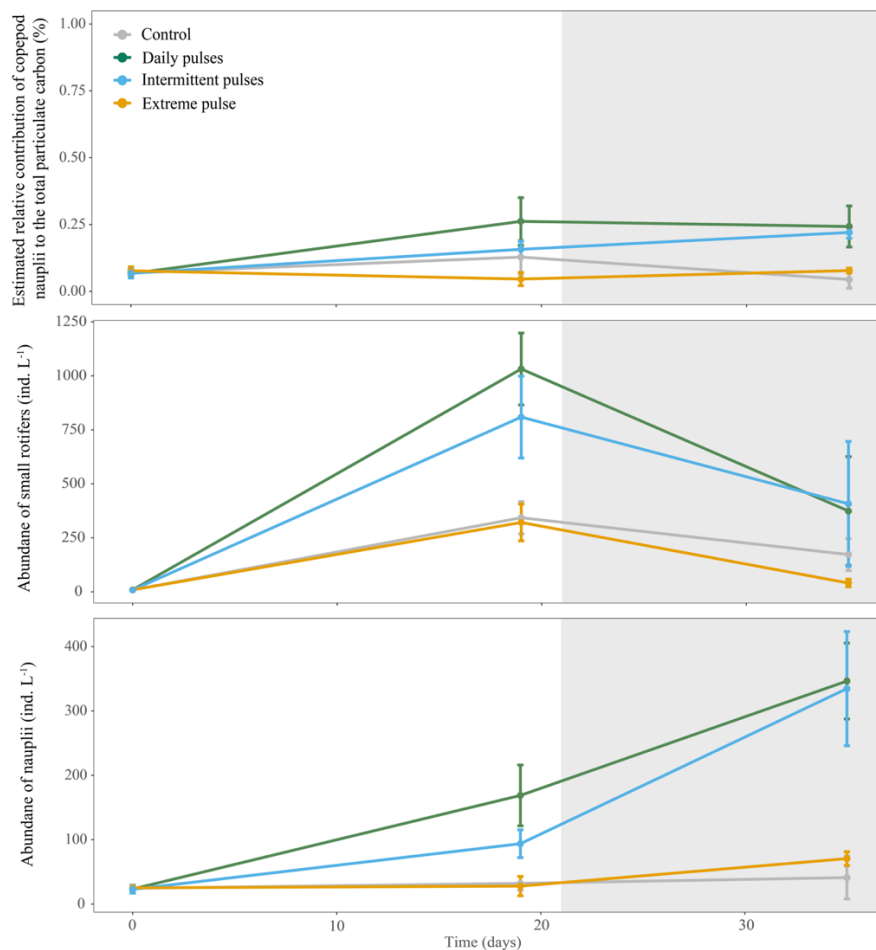


**Figure S7:** Time series of the estimated relative copepod nauplii contribution to the total particulate organic carbon of the small size class ( $< 105 \mu\text{m}$ ) (not that the y-axis only ranges from 0 to 1 %), as well as copepod nauplii and small rotifer abundances. Carbon-based biomass contribution of the copepod nauplii to the total particulate carbon in this size class was calculated based on a regression between body length and carbon weight for *Acartia steuerii* nauplii (Natori and Toda 2018). For this calculation, a body length of  $105 \mu\text{m}$  has been assumed (which represents the upper limit of the size class). Due to the assumption of maximum size in this size class and that all copepod nauplii were present in the small size class, the calculated carbon-based biomass contribution is likely over-estimated and thus, even more supports that copepod nauplii only had a minor influence on the results of this size class. Time series are given for the control (grey), the daily pulses (green), intermittent pulses (blue) and the extreme pulse (orange).

## APPENDIX PUBLICATION IV

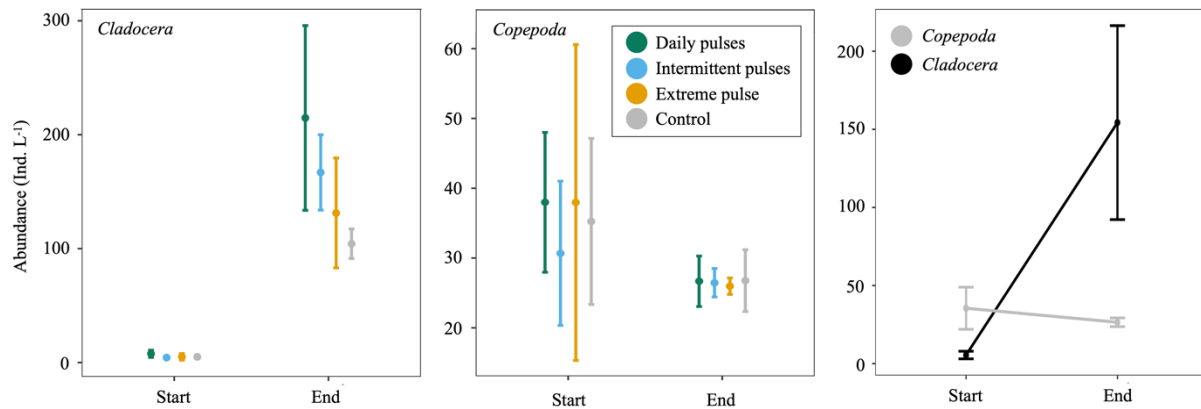


**Figure S8:** Abundance of *Cladocera* and *Copepoda* at the start and end of the experiment. The color in the left and middle box represents the applied treatments, whereas the shades in the right box show the major zooplankton group. The right box shows mean abundances across all treatments. Error bars represent standard deviations.

**Table S1:** Results of the Kruskal-Wallis and Conover's multiple comparisons test for the nutrient limitation bioassay after the simulated rainfall period with lake water (Lake) and water from the daily-pulsed mesocosms (Daily). Abbreviations for the nutrient treatments are control (C), nitrogen addition (N), phosphorus addition (P), nitrogen and phosphorus addition (NP). Significant p-values are indicated by an asterisk (\*) for  $p < 0.05$ . Mean rank differences (MRD) are reported.

	Lake			Daily	
	MRD	p-value		MRD	p-value
<b>N-C</b>	-1.000	0.511		5.333	0.011 *
<b>NP-C</b>	4.333	0.053		9.000	<0.005 *
<b>P-C</b>	6.667	0.009 *		3.667	0.047 *
<b>NP-N</b>	5.333	0.025 *		3.667	0.047 *
<b>P-N</b>	7.667	0.005 *		-1.667	0.203
<b>P-NP</b>	2.333	0.294		-5.333	0.011 *

## References

Natori N, Toda T (2018) A multi-factor empirical model for calculation of naupliar ingestion rate of the embayment copepod *Acartia steueri* Smirnov (Copepoda: Calanoida). Mar Biol 165:1–11. <https://doi.org/10.1007/s00227-018-3378-z>



## **Appendix Publication V**

The effects of nutrient pulse scenarios on the  
stoichiometry of a freshwater plankton community  
across sites and seasons

*Supplementary material*

## APPENDIX PUBLICATION V

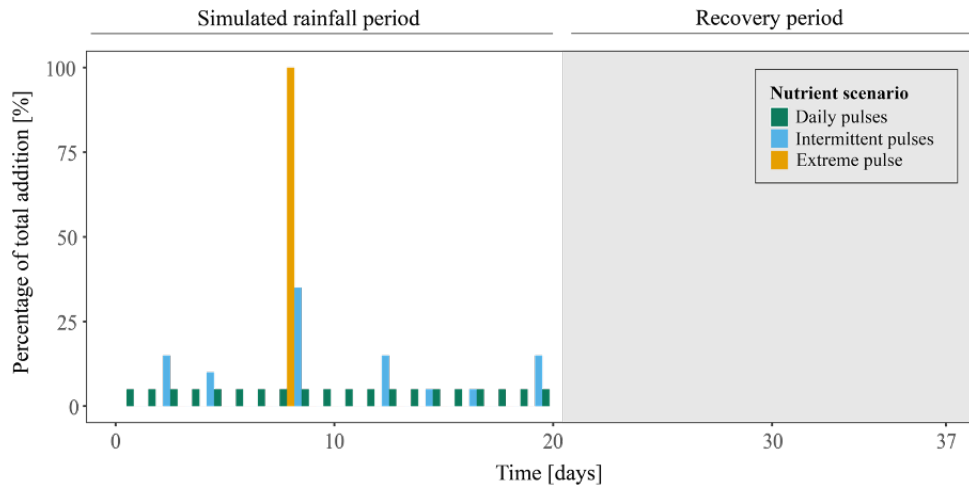


**Fig. S1:** Experimental nutrient and cDOM additions and timeline of the mesocosm experiment. The total additions (100 %) refer to 2 mg L<sup>-1</sup> colored dissolved organic matter (cDOM), 50 µg L<sup>-1</sup> phosphorus primarily added as KH<sub>2</sub>PO<sub>4</sub> and 500 µg L<sup>-1</sup> primarily added as nitrogen NaNO<sub>3</sub>. The experiment ended after 37 days. The grey shaded area represents the recovery period. This figure is taken from Happe et al. (2024).

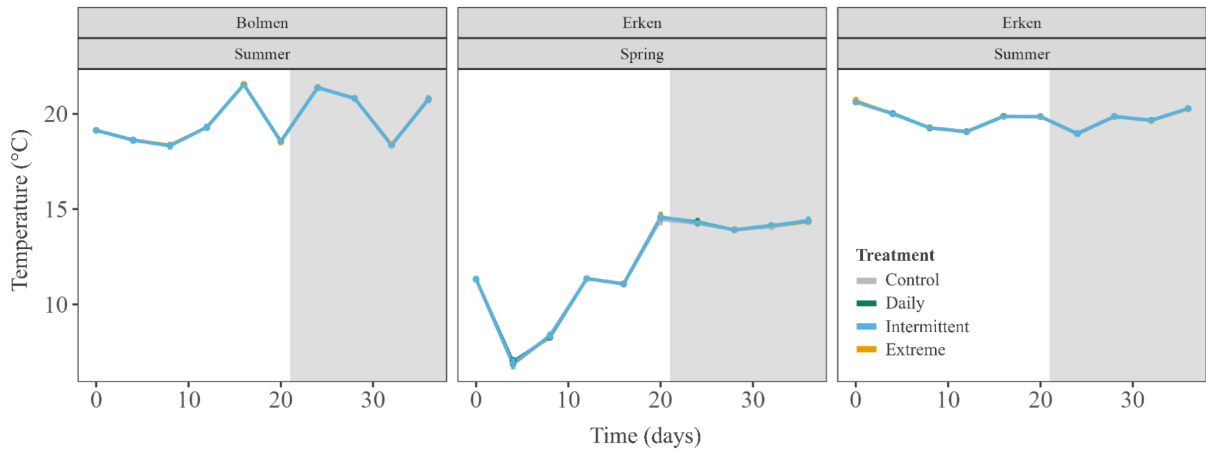


**Fig. S2:** Temporal development of temperature over the duration of the experiments at Lake Erken and Lake Bolmen in Sweden. The summer experiments lasted from 7<sup>th</sup> of July until 11<sup>th</sup> of August 2022. The spring experiment at Lake Erken from 2<sup>nd</sup> of May to 8<sup>th</sup> of June 2023. The lines for the different treatments are very similar and thus, overlay each other.

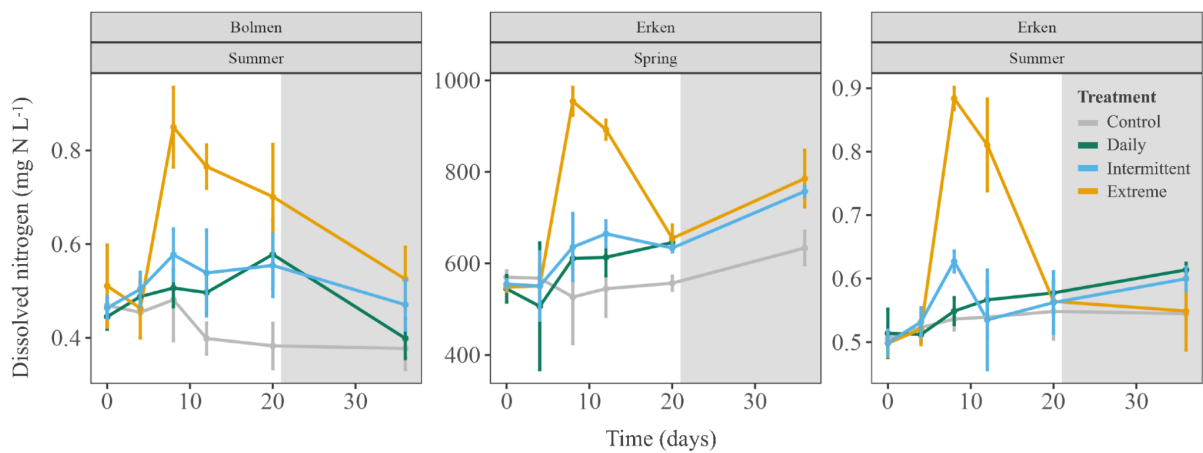


**Fig. S3:** Temporal development of dissolved nitrogen over the duration of the mesocosm experiments at Lake Erken and Lake Bolmen in Sweden. The error bars represent the standard deviation. The dark grey background represents the recovery period.



## APPENDIX PUBLICATION V

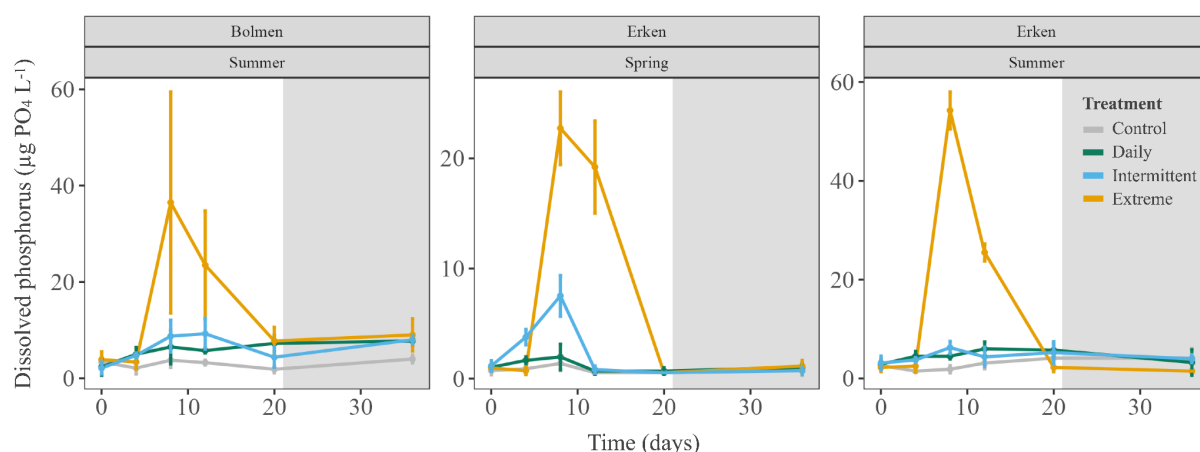


**Fig. S4:** Temporal development of dissolved phosphorus over the duration of the experiments at Lake Erken and Lake Bolmen in Sweden. The error bars represent the standard deviation. The dark grey background represents the recovery period.

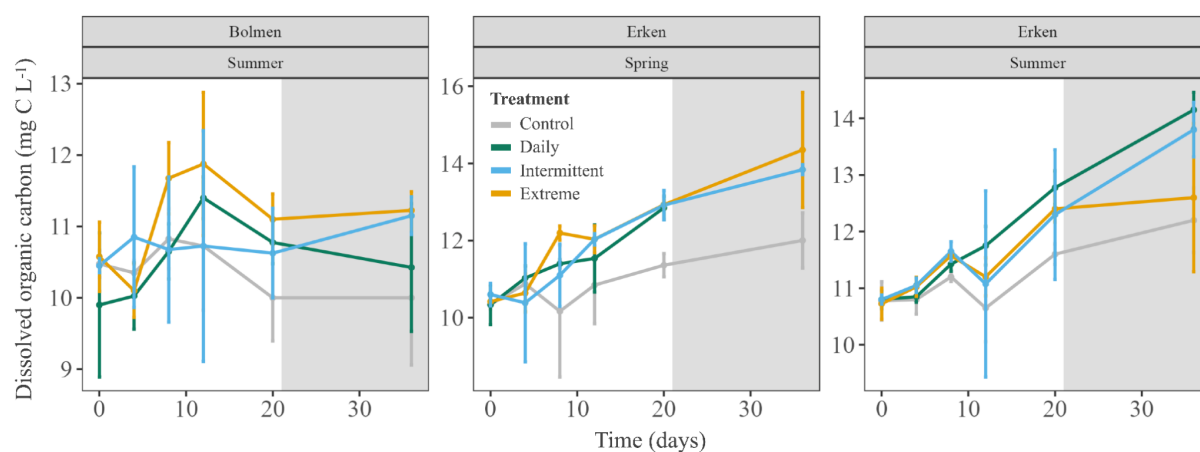


**Fig. S5:** Temporal development of dissolved organic carbon over the duration of the experiments at Lake Erken and Lake Bolmen in Sweden. The error bars represent the standard deviation. The dark grey background represents the recovery period.

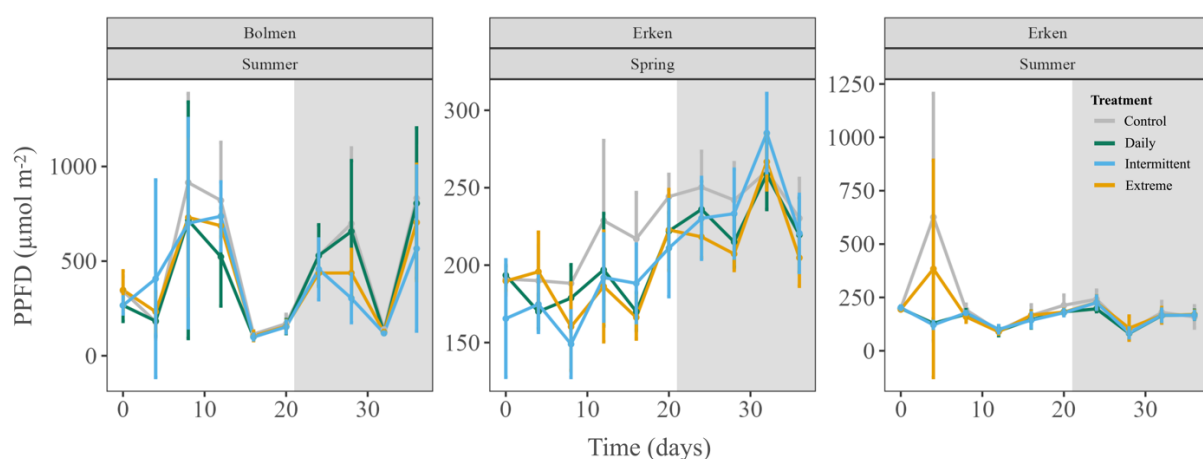


**Fig. S6:** Temporal development of photosynthetic photon flux density (PPFD) of the water surface (-5 cm) throughout the duration of the experiments at Lake Erken and Lake Bolmen in Sweden. The error bars represent the standard deviation. The dark grey background represents the recovery period.

## APPENDIX PUBLICATION V

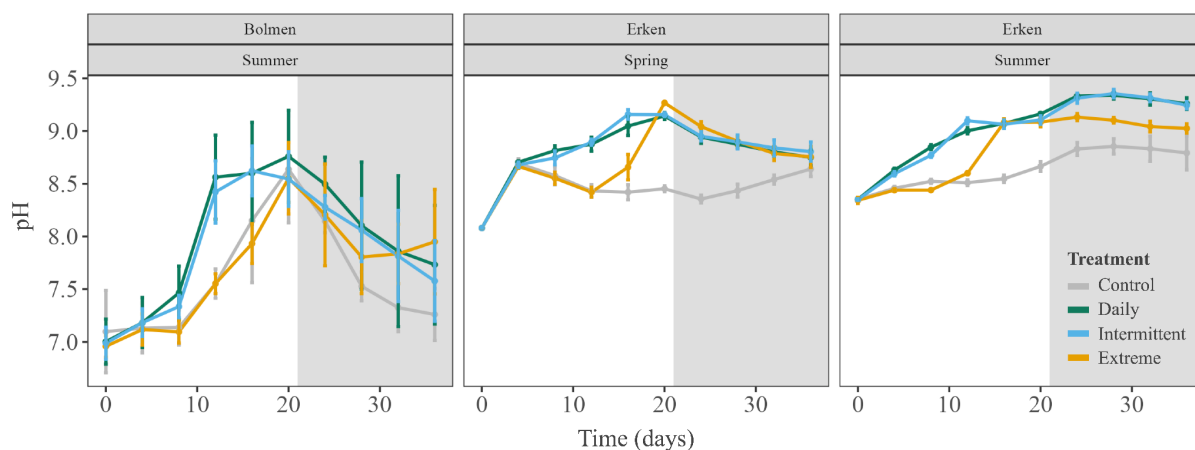


**Fig. S7:** Temporal development of pH over the duration of the experiments at Lake Erken and Lake Bolmen in Sweden. The error bars represent the standard deviation. The dark grey background represents the recovery period.

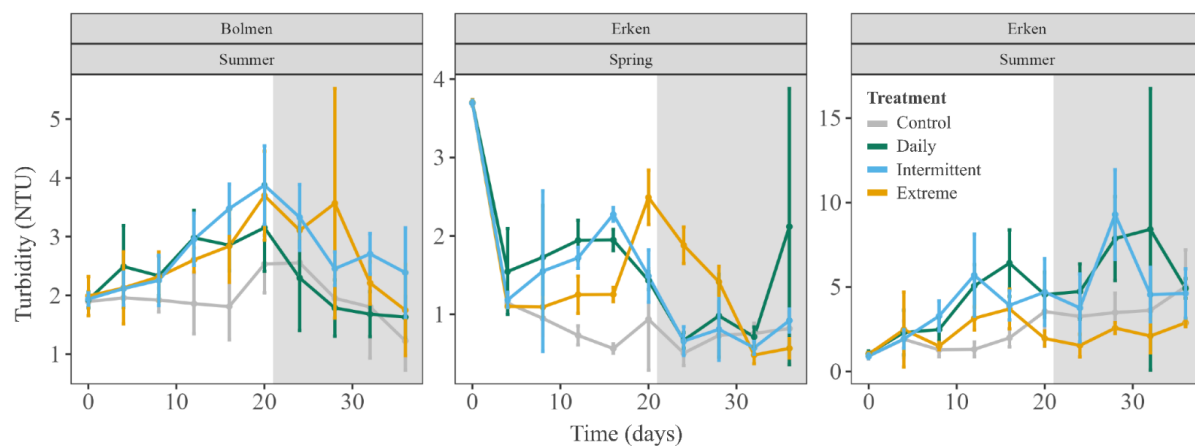


**Fig. S8:** Temporal development of turbidity (in NTU as Nephelometric Turbidity Unit) over the duration of the experiments at Lake Erken and Lake Bolmen in Sweden. The error bars represent the standard deviation. The dark grey background represents the recovery period.

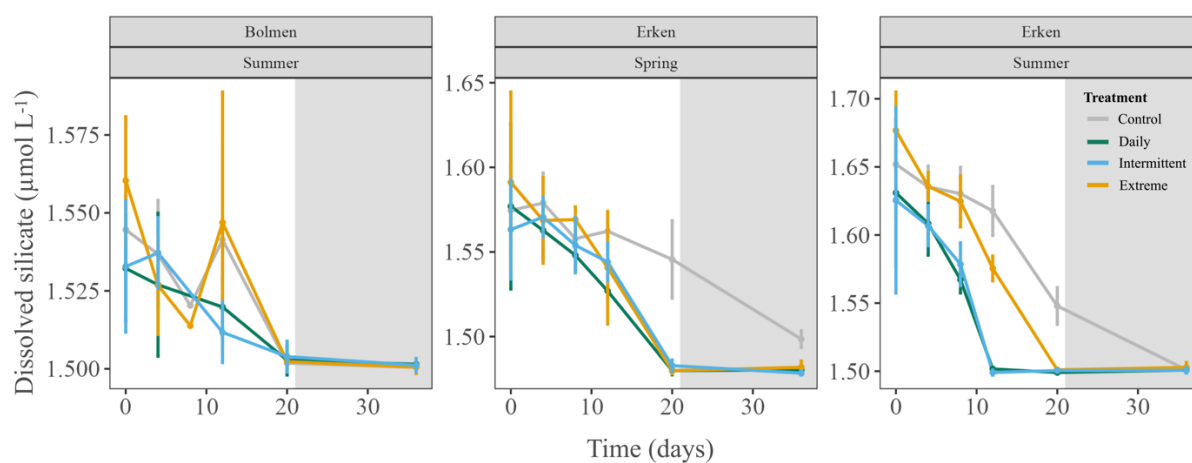


**Fig. S9:** Temporal development of dissolved silicate over the duration of the experiments at Lake Erken and Lake Bolmen in Sweden. The error bars represent the standard deviation. The dark grey background represents the recovery period.

# APPENDIX PUBLICATION V

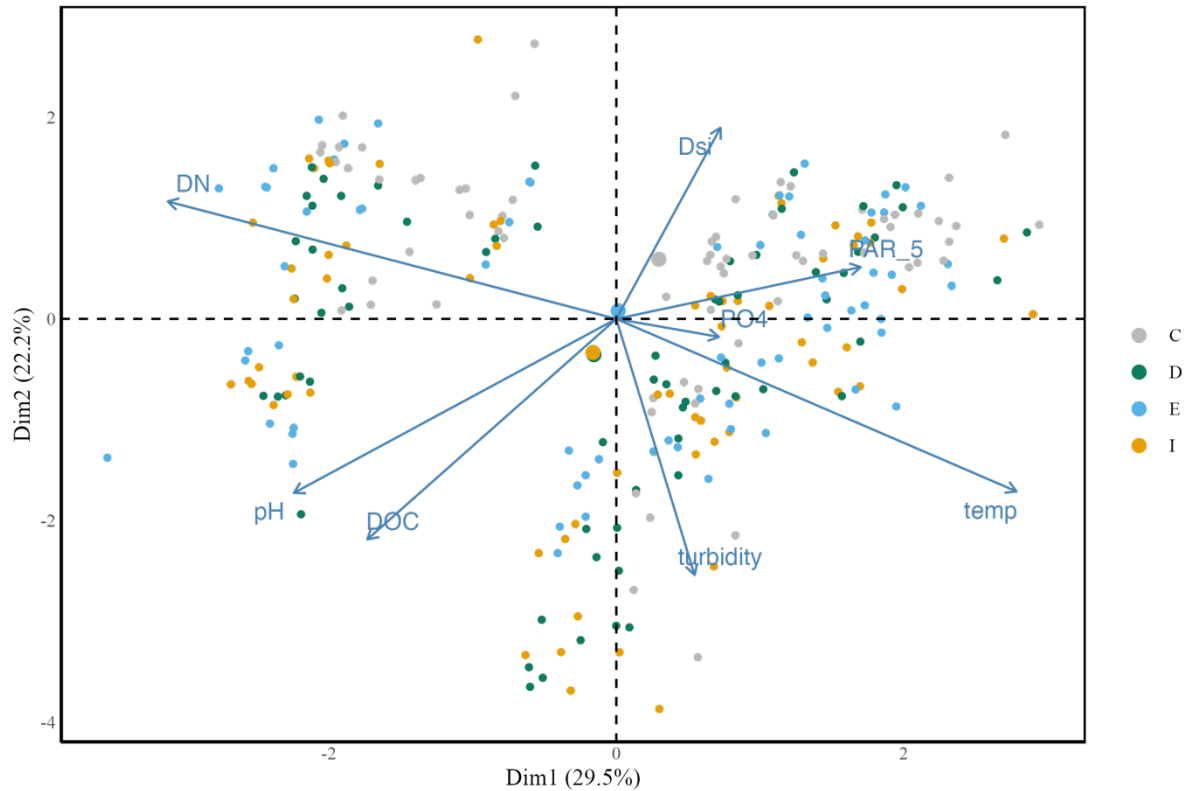


**Fig. S10:** Environmental principal component analysis (PCA) of the abiotic conditions during the experiments at Lake Erken and Bolmen in summer and Lake Erken in spring. The summer experiments at Lake Bolmen and Erken lasted from 7th of July to 11th of August 2022, followed by the spring experiment at Lake Erken from 2nd of May to 8th of June 2023. The symbols indicate the different treatments i.e., control (C), daily pulses (D), intermittent pulses (I), and the extreme pulse (E).

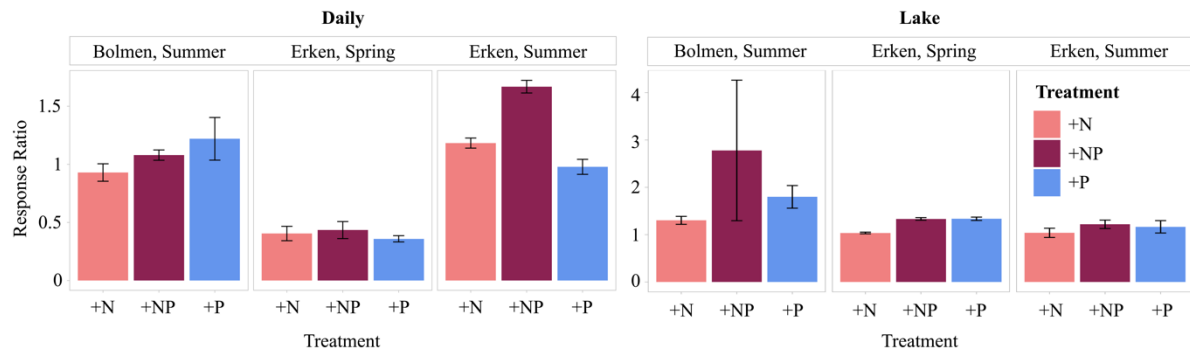


**Fig. S11:** Response ratios (RR) calculated as the ratio between the treatments and the control based on particulate organic carbon as a proxy for biomass at the end (day 4) of the nutrient limitation bioassays. The colors refer to the nutrient addition treatment with either the addition of nitrogen only (+N), the addition of phosphorus only (+P) or the addition of both nitrogen and phosphorus (+NP). The upper row represents communities originating from the daily-pulsed mesocosms after the simulated rainfall period, while the lower row refers to the community originating from the lake. The error bars display standard deviations. Note: Due to the opening of the lid, two bottles (one replicate of the daily mesocosm water as a control and one replicate of the lake water with the phosphorus addition) were lost during the spring experiment at Lake Erken and thus, excluded from the analysis.

# APPENDIX PUBLICATION V

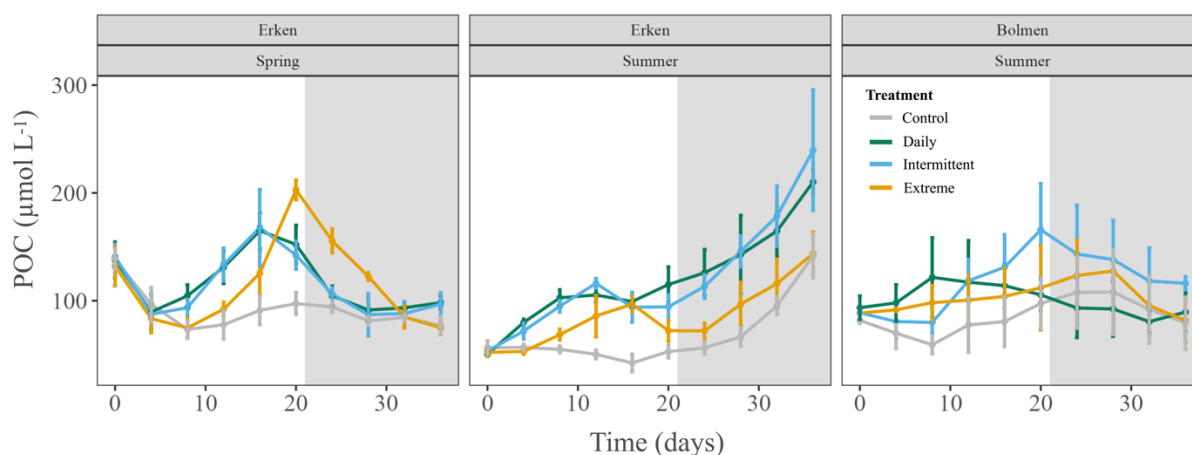


**Figure S12:** Temporal development of particulate organic carbon (POC, as a proxy for plankton biomass) of the **small size fraction (< 105 µm)** during mesocosm experiments at the SITES facilities separated by site (Erken vs. Bolmen) and season (spring vs. summer). Error bars represent standard deviations. The grey background represents the recovery period.

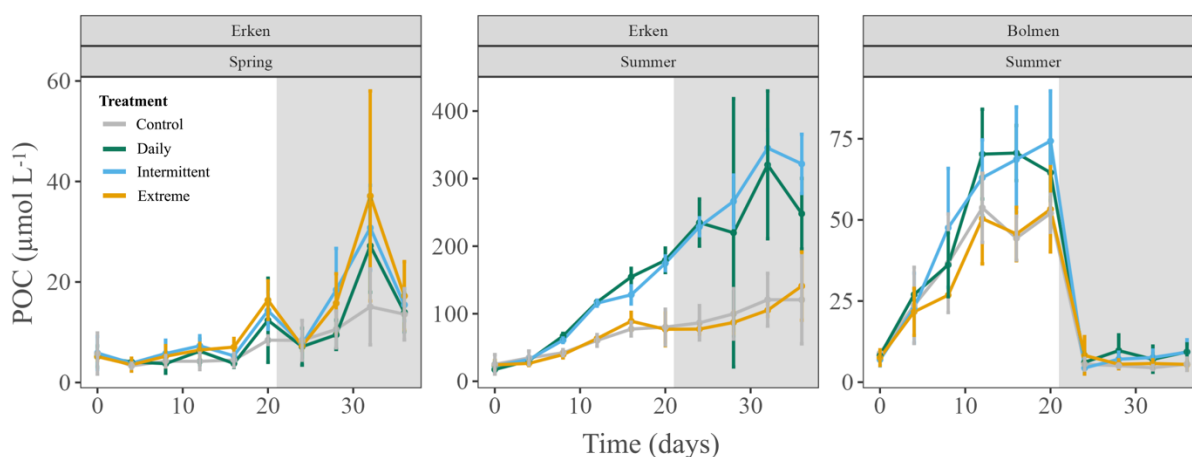


**Figure S13:** Temporal development of particulate organic carbon (POC, as a proxy for plankton biomass) of the **large size fraction (> 105 µm)** during mesocosm experiments at the SITES facilities separated by site (Erken vs. Bolmen) and season (spring vs. summer). Error bars represent standard deviations. The grey background represents the recovery period.

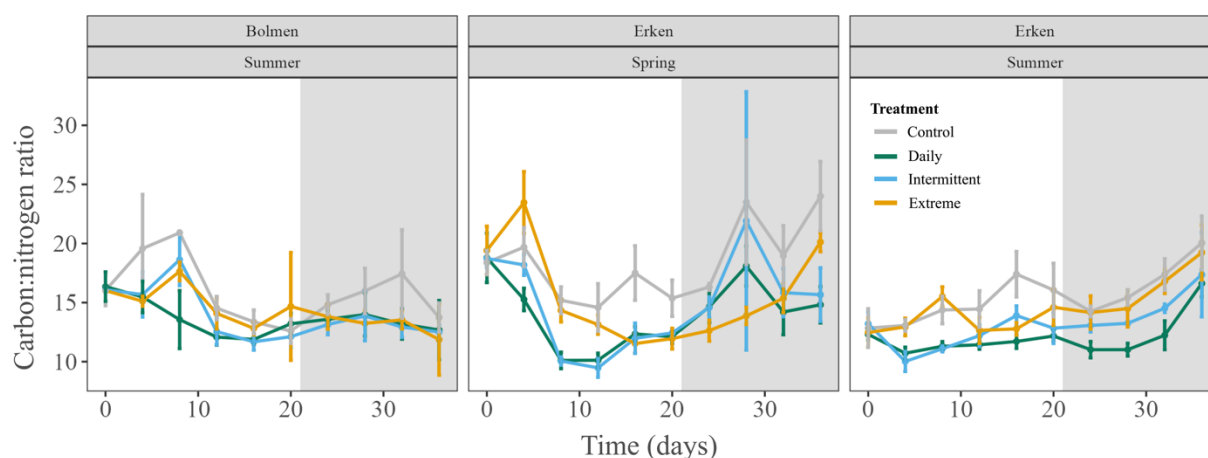


**Figure S14:** Temporal development of the particulate organic carbon to nitrogen molar ratio (C:N ratio) in the small size fraction separated by site (Erken vs. Bolmen) and season (spring vs. summer). The grey background represents the recovery period.

## APPENDIX PUBLICATION V

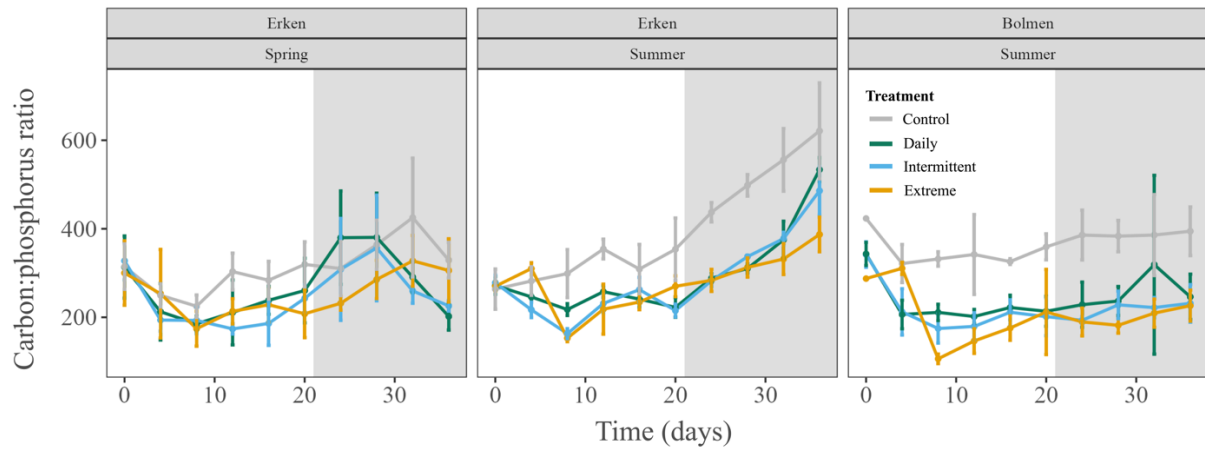


**Figure S15:** Temporal development of the particulate organic carbon to phosphorus molar ratio (C:P ratio) in the small size fraction separated by site (Erken vs. Bolmen) and season (spring vs. summer). The grey background represents the recovery period.

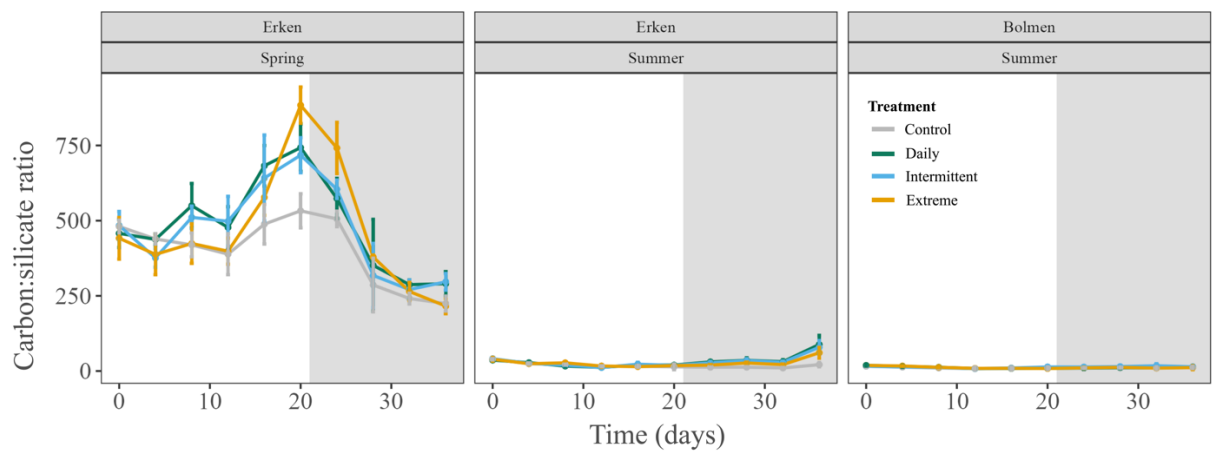


**Figure S16:** Time series of the particulate organic carbon to silicate molar ratio (C:Si ratio) in the small size fraction separated by site (Erken vs. Bolmen) and season (spring vs. summer). The grey background represents the recovery period.

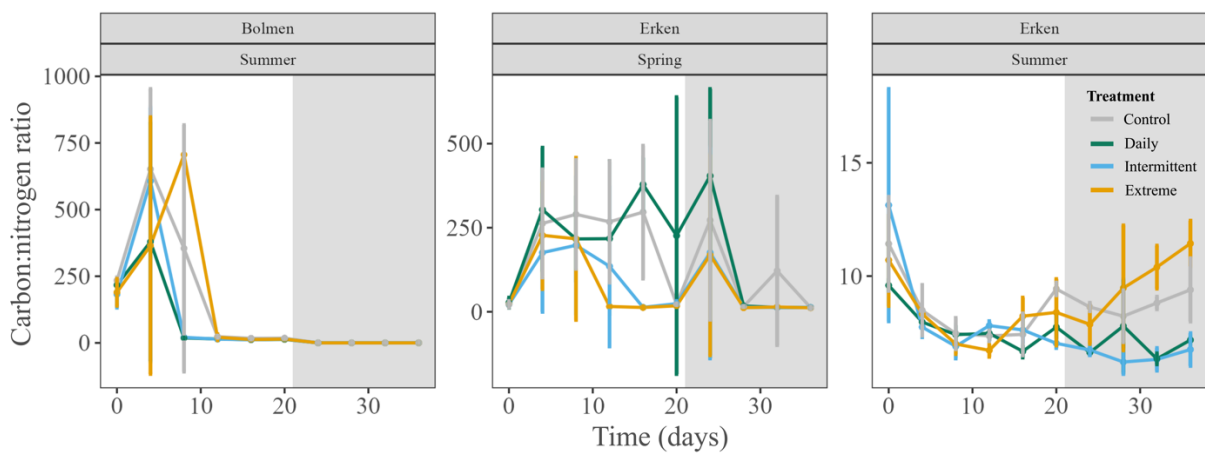


**Figure S17:** Time series of the particulate organic carbon to nitrogen molar ratio (C:N ratio) in the large size fraction separated by site (Erken vs. Bolmen) and season (spring vs. summer). The grey background represents the recovery period.

# APPENDIX PUBLICATION V

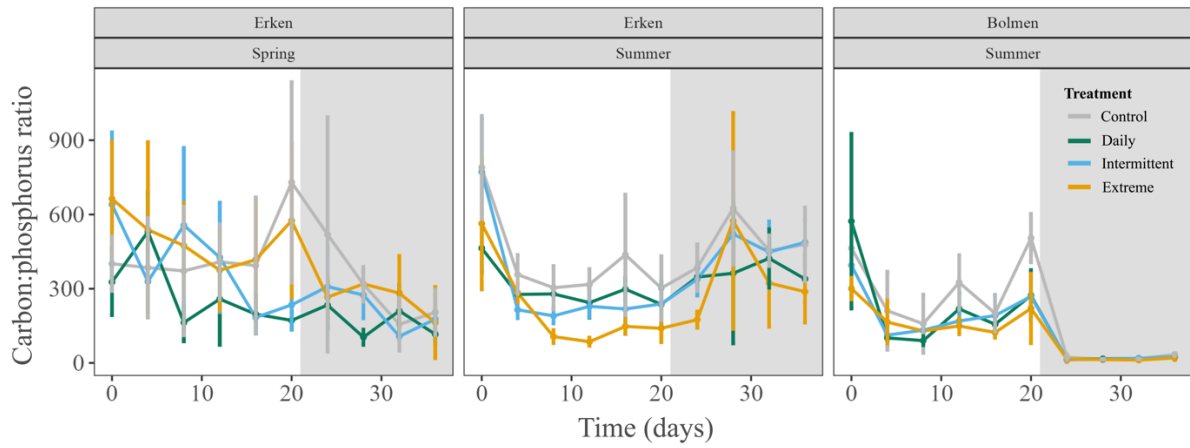


**Figure S18:** Time series of the particulate organic carbon to phosphorus molar ratio (C:P ratio) in the large size fraction separated by site (Erken vs. Bolmen) and season (spring vs. summer). The grey background represents the recovery period.

**Table S1:** Statistical results of the nutrient limitation bioassays obtained from the Kruskal-Wallis tests with the number of observations (n), the degree of difference between the groups (statistic), the degrees of freedom (df) and the p-value with a significance level of 0.05.

Site	Season	Origin	Response	n	Statistic	df	p-value
Erken	Summer	Lake	RR	9	3.47	2	0.177
Erken	Summer	Mesocosm	RR	9	7.20	2	0.027 *
Erken	Spring	Lake	RR	8	5.14	2	0.077
Erken	Spring	Mesocosm	RR	9	2.49	2	0.288
Bolmen	Summer	Lake	RR	9	5.96	2	0.051
Bolmen	Summer	Mesocosm	RR	9	5.96	2	0.051

**Table S2:** Results of the Tukey's HSD post-hoc test for the overall ecological vulnerability (OEV) of carbon concentration (C) of the small size fraction. Contrasts are presented between seasons for the same treatment and between treatments of the same season. Abbreviations for the nutrient scenarios are daily pulses (D), intermittent pulses (I), and one extreme pulse (E). Standard errors (SE) and degrees of freedom (df) are reported. Contrasts between the seasons of the same treatment are highlighted in bold.

OEV: C for Season					
Contrast	Estimate	SE	df	t-ratio	p-value
D Spring - E Spring	-0.002	0.361	17	-0.006	1.000
D Spring - I Spring	0.147	0.361	17	0.407	1.000
<b>D Spring - D Summer</b>	<b>-3.158</b>	<b>0.389</b>	<b>17</b>	<b>-8.109</b>	<b>&lt;0.001</b>
E Spring - I Spring	0.149	0.361	17	0.412	1.000
<b>E Spring - E Summer</b>	<b>-0.255</b>	<b>0.361</b>	<b>17</b>	<b>-0.707</b>	<b>1.000</b>
<b>I Spring - I Summer</b>	<b>-3.000</b>	<b>0.361</b>	<b>17</b>	<b>-8.318</b>	<b>&lt;0.001</b>
D Summer - E Summer	2.902	0.389	17	7.450	<0.001
D Summer - I Summer	0.305	0.389	17	0.784	1.000
E Summer - I Summer	-2.596	0.361	17	-7.199	<0.001

## APPENDIX PUBLICATION V

**Table S3:** Results of the Tukey's HSD post-hoc test for the overall ecological vulnerability (OEV) of carbon concentration (C) of the small size fraction. Contrasts are presented between sites for the same treatment and between treatments of the same site. Abbreviations for the nutrient scenarios are daily pulses (D), intermittent pulses (I), and one extreme pulse (E). Standard errors (SE) and degrees of freedom (df) are reported. Contrasts between the sites of the same treatment are highlighted in bold.

OEV: log(C) for Site					
Contrast	Estimate	SE	df	t-ratio	p-value
D Bolmen - E Bolmen	1.379	0.583	19	2.364	0.433
D Bolmen - I Bolmen	-0.243	0.583	19	-0.417	1.000
<b>D Bolmen - D Erken</b>	<b>-2.036</b>	<b>0.471</b>	<b>19</b>	<b>-4.325</b>	<b>0.005</b>
E Bolmen - I Bolmen	-1.622	0.563	19	-2.883	0.143
<b>E Bolmen - E Erken</b>	<b>-2.036</b>	<b>0.471</b>	<b>19</b>	<b>-4.325</b>	<b>0.005</b>
<b>I Bolmen - I Erken</b>	<b>-2.036</b>	<b>0.471</b>	<b>19</b>	<b>-4.325</b>	<b>0.005</b>
D Erken - E Erken	1.379	0.583	19	2.364	0.433
D Erken - I Erken	-0.243	0.583	19	-0.417	1.000
E Erken - I Erken	-1.622	0.563	19	-2.883	0.143

**Table S4:** Results of the Tukey's HSD post-hoc test for the overall ecological vulnerability (OEV) of the particulate carbon:nitrogen ratios (C:N) of the small size fraction. Contrasts are presented between seasons for the same treatment and between treatments of the same season. Abbreviations for the nutrient scenarios are daily pulses (D), intermittent pulses (I), and one extreme pulse (E). Standard errors (SE) and degrees of freedom (df) are reported. Contrasts between the seasons of the same treatment are highlighted in bold.

OEV: C:N for Season					
Contrast	Estimate	SE	df	t-ratio	p-value
D Spring - E Spring	0.538	0.153	17	3.507	0.041
D Spring - I Spring	0.154	0.153	17	1.003	1.000
<b>D Spring - D Summer</b>	<b>0.148</b>	<b>0.166</b>	<b>17</b>	<b>0.892</b>	<b>1.000</b>
E Spring - I Spring	-0.384	0.153	17	-2.504	0.342
<b>E Spring - E Summer</b>	<b>1.121</b>	<b>0.153</b>	<b>17</b>	<b>7.306</b>	<b>&lt;0.001</b>
<b>I Spring - I Summer</b>	<b>0.733</b>	<b>0.153</b>	<b>17</b>	<b>4.774</b>	<b>0.003</b>
D Summer - E Summer	1.512	0.166	17	9.119	<0.001
D Summer - I Summer	0.739	0.166	17	4.456	0.005
E Summer - I Summer	-0.773	0.153	17	-5.036	0.002

## APPENDIX PUBLICATION V

**Table S5:** Results of the Tukey's HSD post-hoc test for the overall ecological vulnerability (OEV) of the particulate carbon:nitrogen ratios (C:N) of the small size fraction. Contrasts are presented between sites for the same treatment and between treatments of the same site. Abbreviations for the nutrient scenarios are daily pulses (D), intermittent pulses (I), and one extreme pulse (E). Standard errors (SE) and degrees of freedom (df) are reported. Contrasts between the sites of the same treatment are highlighted in bold.

OEV: C:N for Site					
Contrast	Estimate	SE	df	t-ratio	p-value
D Bolmen - E Bolmen	0.258	0.180	17	1.430	1.000
D Bolmen - I Bolmen	0.169	0.180	17	0.936	1.000
<b>D Bolmen - D Erken</b>	<b>-0.905</b>	<b>0.195</b>	<b>17</b>	<b>-4.648</b>	<b>0.003</b>
E Bolmen - I Bolmen	-0.089	0.180	17	-0.494	1.000
<b>E Bolmen - E Erken</b>	<b>0.348</b>	<b>0.180</b>	<b>17</b>	<b>1.932</b>	<b>1.000</b>
<b>I Bolmen - I Erken</b>	<b>-0.335</b>	<b>0.180</b>	<b>17</b>	<b>-1.860</b>	<b>1.000</b>
D Erken - E Erken	1.512	0.195	17	7.761	<0.001
D Erken - I Erken	0.739	0.195	17	3.793	0.022
E Erken - I Erken	-0.773	0.180	17	-4.286	0.007

**Table S6:** Results of the Tukey's HSD post-hoc test for the recovery of the particulate carbon:phosphorus ratios (C:P) of the small size fraction. Contrasts are presented between seasons for the same treatment and between treatments of the same season. Abbreviations for the nutrient scenarios are daily pulses (D), intermittent pulses (I), and one extreme pulse (E). Standard errors (SE) and degrees of freedom (df) are reported. Contrasts between the seasons of the same treatment are highlighted in bold.

OEV: C:P for Season					
Contrast	Estimate	SE	df	t-ratio	p-value
D Spring - E Spring	-0.224	0.268	17	-0.835	1.000
D Spring - I Spring	-0.535	0.268	17	-1.994	0.936
<b>D Spring - D Summer</b>	<b>-0.491</b>	<b>0.290</b>	<b>17</b>	<b>-1.694</b>	<b>1.000</b>
E Spring - I Spring	-0.311	0.268	17	-1.159	1.000
<b>E Spring - E Summer</b>	<b>-0.780</b>	<b>0.268</b>	<b>17</b>	<b>-2.904</b>	<b>0.148</b>
<b>I Spring - I Summer</b>	<b>-0.401</b>	<b>0.268</b>	<b>17</b>	<b>-1.493</b>	<b>1.000</b>
D Summer - E Summer	-0.513	0.290	17	-1.768	1.000
D Summer - I Summer	-0.445	0.290	17	-1.534	1.000
E Summer - I Summer	0.068	0.268	17	0.253	1.000



## APPENDIX PUBLICATION V

**Table S7:** Results of the Tukey's HSD post-hoc test for the recovery of the particulate carbon:phosphorus ratios (C:P) of the small size fraction. Contrasts are presented between sites for the same treatment and between treatments of the same site. Abbreviations for the nutrient scenarios are daily pulses (D), intermittent pulses (I), and one extreme pulse (E). Standard errors (SE) and degrees of freedom (df) are reported. Contrasts between the sites of the same treatment are highlighted in bold.

OEV: log(C:P) for Site					
Contrast	Estimate	SE	df	t-ratio	p-value
D Bolmen - E Bolmen	-0.201	0.113	17	-1.768	1.000
D Bolmen - I Bolmen	-0.127	0.113	17	-1.116	1.000
<b>D Bolmen - D Erken</b>	<b>0.392</b>	<b>0.123</b>	<b>17</b>	<b>3.202</b>	<b>0.078</b>
E Bolmen - I Bolmen	0.074	0.113	17	0.652	1.000
<b>E Bolmen - E Erken</b>	<b>0.432</b>	<b>0.113</b>	<b>17</b>	<b>3.804</b>	<b>0.021</b>
<b>I Bolmen - I Erken</b>	<b>0.374</b>	<b>0.113</b>	<b>17</b>	<b>3.300</b>	<b>0.063</b>
D Erken - E Erken	-0.161	0.123	17	-1.316	1.000
D Erken - I Erken	-0.145	0.123	17	-1.179	1.000
E Erken - I Erken	0.017	0.113	17	0.148	1.000

**Table S8:** Results of the Tukey's HSD post-hoc test for the recovery of the particulate carbon:silicate ratios (C:Si) of the small size fraction. Contrasts are presented between seasons for the same treatment and between treatments of the same season. Abbreviations for the nutrient scenarios are daily pulses (D), intermittent pulses (I), and one extreme pulse (E). Standard errors (SE) and degrees of freedom (df) are reported. Contrasts between the seasons of the same treatment are highlighted in bold.

OEV: C:Si for Season					
Contrast	Estimate	SE	df	t-ratio	p-value
D Spring - E Spring	-0.121	0.347	17	-0.350	1.000
D Spring - I Spring	-0.092	0.347	17	-0.265	1.000
<b>D Spring - D Summer</b>	<b>-3.243</b>	<b>0.375</b>	<b>17</b>	<b>-8.655</b>	<b>&lt;0.001</b>
E Spring - I Spring	0.029	0.347	17	0.084	1.000
<b>E Spring - E Summer</b>	<b>-1.544</b>	<b>0.347</b>	<b>17</b>	<b>-4.450</b>	<b>0.005</b>
<b>I Spring - I Summer</b>	<b>-2.681</b>	<b>0.347</b>	<b>17</b>	<b>-7.727</b>	<b>&lt;0.001</b>
D Summer - E Summer	1.578	0.375	17	4.212	0.009
D Summer - I Summer	0.470	0.375	17	1.255	1.000
E Summer - I Summer	-1.108	0.347	17	-3.193	0.080

## APPENDIX PUBLICATION V

**Table S9:** Results of the Tukey's HSD post-hoc test for the recovery of the particulate carbon:silicate ratios (C:Si) of the small size fraction. Contrasts are presented between sites for the same treatment and between treatments of the same site. Abbreviations for the nutrient scenarios are daily pulses (D), intermittent pulses (I), and one extreme pulse (E). Standard errors (SE) and degrees of freedom (df) are reported. Contrasts between the sites of the same treatment are highlighted in bold.

OEV: C:Si for Site					
Contrast	Estimate	SE	df	t-ratio	p-value
D Bolmen - E Bolmen	-0.090	0.560	17	-0.161	1.000
D Bolmen - I Bolmen	-0.311	0.560	17	-0.556	1.000
<b>D Bolmen - D Erken</b>	<b>-3.359</b>	<b>0.605</b>	<b>17</b>	<b>-5.551</b>	<b>0.001</b>
E Bolmen - I Bolmen	-0.221	0.560	17	-0.394	1.000
<b>E Bolmen - E Erken</b>	<b>-1.691</b>	<b>0.560</b>	<b>17</b>	<b>-3.018</b>	<b>0.116</b>
<b>I Bolmen - I Erken</b>	<b>-2.577</b>	<b>0.560</b>	<b>17</b>	<b>-4.601</b>	<b>0.004</b>
D Erken - E Erken	1.578	0.605	17	2.608	0.276
D Erken - I Erken	0.470	0.605	17	0.777	1.000
E Erken - I Erken	-1.108	0.560	17	-1.977	0.967

**Table S10:** Results of the Tukey's HSD post-hoc test for the recovery of the carbon concentration (C) of the small size fraction. Contrasts are presented between seasons for the same treatment and between treatments of the same season. Abbreviations for the nutrient scenarios are daily pulses (D), intermittent pulses (I), and one extreme pulse (E). Standard errors (SE) and degrees of freedom (df) are reported. Contrasts between the seasons of the same treatment are highlighted in bold.

Recovery: log(C) for Season					
Contrast	Estimate	SE	df	t-ratio	p-value
D Spring - E Spring	2.362	0.601	13	3.933	0.026
D Spring - I Spring	0.214	0.490	13	0.436	1.000
<b>D Spring - D Summer</b>	<b>-0.501</b>	<b>0.530</b>	<b>13</b>	<b>-0.946</b>	<b>1.000</b>
E Spring - I Spring	-2.149	0.601	13	-3.578	0.051
<b>E Spring - E Summer</b>	<b>-1.638</b>	<b>0.693</b>	<b>13</b>	<b>-2.361</b>	<b>0.517</b>
<b>I Spring - I Summer</b>	<b>-0.759</b>	<b>0.490</b>	<b>13</b>	<b>-1.547</b>	<b>1.000</b>
D Summer - E Summer	1.226	0.633	13	1.936	1.000
D Summer - I Summer	-0.044	0.530	13	-0.082	1.000
E Summer - I Summer	-1.270	0.601	13	-2.114	0.816

## APPENDIX PUBLICATION V

**Table S11:** Results of the Tukey's HSD post-hoc test for the recovery of the carbon:nitrogen ratio (C:N) of the small size fraction. Contrasts are presented between seasons for the same treatment and between treatments of the same season. Abbreviations for the nutrient scenarios are daily pulses (D), intermittent pulses (I), and one extreme pulse (E). Standard errors (SE) and degrees of freedom (df) are reported. Contrasts between the seasons of the same treatment are highlighted in bold.

Recovery: C:N for Season					
Contrast	Estimate	SE	df	t-ratio	p-value
D Spring - E Spring	-0.310	0.092	17	-3.365	0.055
D Spring - I Spring	-0.052	0.092	17	-0.568	1.000
<b>D Spring - D Summer</b>	<b>-0.298</b>	<b>0.099</b>	<b>17</b>	<b>-2.994</b>	<b>0.122</b>
E Spring - I Spring	0.257	0.092	17	2.797	0.186
E Spring - E Summer	-0.130	0.092	17	-1.412	1.000
I Spring - I Summer	-0.274	0.092	17	-2.980	0.126
D Summer - E Summer	-0.142	0.099	17	-1.429	1.000
D Summer - I Summer	-0.029	0.099	17	-0.291	1.000
E Summer - I Summer	0.113	0.092	17	1.229	1.000

**Table S12:** Results of the Tukey's HSD post-hoc test for the recovery of the carbon:phosphorus ratio (C:P) of the small size fraction. Contrasts are presented between seasons for the same treatment and between treatments of the same season. Abbreviations for the nutrient scenarios are daily pulses (D), intermittent pulses (I), and one extreme pulse (E). Standard errors (SE) and degrees of freedom (df) are reported. Contrasts between the seasons of the same treatment are highlighted in bold.

Recovery: C:P for Season					
Contrast	Estimate	SE	df	t-ratio	p-value
D Spring - E Spring	-0.403	0.099	17	-4.075	0.012
D Spring - I Spring	-0.120	0.099	17	-1.215	1.000
<b>D Spring - D Summer</b>	<b>-0.345</b>	<b>0.107</b>	<b>17</b>	<b>-3.232</b>	<b>0.073</b>
E Spring - I Spring	0.283	0.099	17	2.861	0.162
<b>E Spring - E Summer</b>	<b>0.381</b>	<b>0.099</b>	<b>17</b>	<b>3.862</b>	<b>0.019</b>
<b>I Spring - I Summer</b>	<b>-0.127</b>	<b>0.099</b>	<b>17</b>	<b>-1.287</b>	<b>1.000</b>
D Summer - E Summer	0.324	0.107	17	3.034	0.112
D Summer - I Summer	0.098	0.107	17	0.916	1.000
E Summer - I Summer	-0.226	0.099	17	-2.288	0.528

## APPENDIX PUBLICATION V

**Table S13:** Results of the Tukey's HSD post-hoc test for the recovery of the carbon:phosphorus ratio (C:P) of the small size fraction. Contrasts are presented between sites for the same treatment and between treatments of the same site. Abbreviations for the nutrient scenarios are daily pulses (D), intermittent pulses (I), and one extreme pulse (E). Standard errors (SE) and degrees of freedom (df) are reported. Contrasts between the sites of the same treatment are highlighted in bold.

Recovery: C:P for Site					
Contrast	Estimate	SE	df	t-ratio	p-value
D Bolmen - E Bolmen	0.078	0.104	17	0.751	1.000
D Bolmen - I Bolmen	0.057	0.104	17	0.544	1.000
<b>D Bolmen - D Erken</b>	<b>-0.335</b>	<b>0.113</b>	<b>17</b>	<b>-2.968</b>	<b>0.129</b>
E Bolmen - I Bolmen	-0.022	0.104	17	-0.207	1.000
<b>E Bolmen - E Erken</b>	<b>-0.089</b>	<b>0.104</b>	<b>17</b>	<b>-0.856</b>	<b>1.000</b>
<b>I Bolmen - I Erken</b>	<b>-0.294</b>	<b>0.104</b>	<b>17</b>	<b>-2.814</b>	<b>0.179</b>
D Erken - E Erken	0.324	0.113	17	2.871	0.159
D Erken - I Erken	0.098	0.113	17	0.867	1.000
E Erken - I Erken	-0.226	0.104	17	-2.165	0.674

**Table S14:** Results of the Tukey's HSD post-hoc test for the recovery of the carbon:silicate ratio (C:Si) of the small size fraction. Contrasts are presented between seasons for the same treatment and between treatments of the same season. Abbreviations for the nutrient scenarios are daily pulses (D), intermittent pulses (I), and one extreme pulse (E). Standard errors (SE) and degrees of freedom (df) are reported. Contrasts between the seasons of the same treatment are highlighted in bold.

Recovery: C:Si for Seasons					
Contrast	Estimate	SE	df	t-ratio	p-value
D Spring - E Spring	0.294	0.158	17	1.859	1.000
D Spring - I Spring	-0.025	0.158	17	-0.160	1.000
<b>D Spring - D Summer</b>	<b>-1.135</b>	<b>0.171</b>	<b>17</b>	<b>-6.643</b>	<b>&lt;0.001</b>
E Spring - I Spring	-0.319	0.158	17	-2.019	0.894
<b>E Spring - E Summer</b>	<b>-1.058</b>	<b>0.158</b>	<b>17</b>	<b>-6.687</b>	<b>&lt;0.001</b>
<b>I Spring - I Summer</b>	<b>-1.012</b>	<b>0.158</b>	<b>17</b>	<b>-6.397</b>	<b>&lt;0.001</b>
D Summer - E Summer	0.371	0.171	17	2.173	0.663
D Summer - I Summer	0.098	0.171	17	0.572	1.000
E Summer - I Summer	-0.274	0.158	17	-1.729	1.000

## APPENDIX PUBLICATION V

**Table S15:** Results of the Tukey's HSD post-hoc test for the recovery of the carbon:silicate ratio (C:Si) of the small size fraction. Contrasts are presented between sites for the same treatment and between treatments of the same site. Abbreviations for the nutrient scenarios are daily pulses (D), intermittent pulses (I), and one extreme pulse (E). Standard errors (SE) and degrees of freedom (df) are reported. Contrasts between the sites of the same treatment are highlighted in bold.

Recovery: C:Si for Site					
Contrast	Estimate	SE	df	t-ratio	p-value
D Bolmen - E Bolmen	0.233	0.252	17	0.927	1.000
D Bolmen - I Bolmen	-0.087	0.252	17	-0.344	1.000
<b>D Bolmen - D Erken</b>	<b>-1.330</b>	<b>0.272</b>	<b>17</b>	<b>-4.895</b>	<b>0.002</b>
E Bolmen - I Bolmen	-0.320	0.252	17	-1.271	1.000
<b>E Bolmen - E Erken</b>	<b>-1.191</b>	<b>0.252</b>	<b>17</b>	<b>-4.737</b>	<b>0.003</b>
<b>I Bolmen - I Erken</b>	<b>-1.145</b>	<b>0.252</b>	<b>17</b>	<b>-4.554</b>	<b>0.004</b>
D Erken - E Erken	0.371	0.272	17	1.367	1.000
D Erken - I Erken	0.098	0.272	17	0.360	1.000
E Erken - I Erken	-0.274	0.252	17	-1.088	1.000

**Table S16:** Results of the Tukey's HSD post-hoc test for the OEV of the particulate organic carbon (POC) of the large size fraction. Contrasts are presented between seasons for the same treatment and between treatments of the same season. Abbreviations for the nutrient scenarios are daily pulses (D), intermittent pulses (I), and one extreme pulse (E). Standard errors (SE) and degrees of freedom (df) are reported. Contrasts between the sites of the same treatment are highlighted in bold.

OEV: C <sup>2</sup> for Season					
Contrast	Estimate	SE	df	t-ratio	p-value
D Spring - E Spring	-3.595	5.118	17	-0.702	1.000
D Spring - I Spring	-3.194	5.118	17	-0.624	1.000
<b>D Spring - D Summer</b>	<b>-28.593</b>	<b>5.528</b>	<b>17</b>	<b>-5.172</b>	<b>0.001</b>
E Spring - I Spring	0.402	5.118	17	0.078	1.000
<b>E Spring - E Summer</b>	<b>10.467</b>	<b>5.118</b>	<b>17</b>	<b>2.045</b>	<b>0.850</b>
<b>I Spring - I Summer</b>	<b>-23.220</b>	<b>5.118</b>	<b>17</b>	<b>-4.536</b>	<b>0.004</b>
D Summer - E Summer	35.465	5.528	17	6.415	<0.001
D Summer - I Summer	2.180	5.528	17	0.394	1.000
E Summer - I Summer	-33.285	5.118	17	-6.503	<0.001

## APPENDIX PUBLICATION V

**Table S17:** Results of the Tukey's HSD post-hoc test for the OEV of the particulate organic carbon (POC) of the large size fraction. Contrasts are presented between sites for the same treatment and between treatments of the same site. Abbreviations for the nutrient scenarios are daily pulses (D), intermittent pulses (I), and one extreme pulse (E). Standard errors (SE) and degrees of freedom (df) are reported. Contrasts between the sites of the same treatment are highlighted in bold.

OEV: log(C) for Site					
Contrast	Estimate	SE	df	t-ratio	p-value
D Bolmen - E Bolmen	0.422	0.186	17	2.274	0.543
D Bolmen - I Bolmen	0.033	0.186	17	0.179	1.000
<b>D Bolmen - D Erken</b>	<b>-0.778</b>	<b>0.201</b>	<b>17</b>	<b>-3.880</b>	<b>0.018</b>
E Bolmen - I Bolmen	-0.389	0.186	17	-2.095	0.772
<b>E Bolmen - E Erken</b>	<b>0.284</b>	<b>0.186</b>	<b>17</b>	<b>1.528</b>	<b>1.000</b>
<b>I Bolmen - I Erken</b>	<b>-0.814</b>	<b>0.186</b>	<b>17</b>	<b>-4.381</b>	<b>0.006</b>
D Erken - E Erken	1.485	0.201	17	7.400	<0.001
D Erken - I Erken	-0.002	0.201	17	-0.010	1.000
E Erken - I Erken	-1.487	0.186	17	-8.004	<0.001

**Table S18:** Results of the Tukey's HSD post-hoc test for the recovery of the particulate organic carbon (POC) of the large size fraction. Contrasts are presented between seasons for the same treatment and between treatments of the same seasons. Abbreviations for the nutrient scenarios are daily pulses (D), intermittent pulses (I), and one extreme pulse (E). Standard errors (SE) and degrees of freedom (df) are reported. Contrasts between the sites of the same treatment are highlighted in bold.

Recovery: C <sup>2</sup> for Season					
Contrast	Estimate	SE	df	t-ratio	p-value
D Spring - E Spring	-0.098	0.126	17	-0.778	1.000
D Spring - I Spring	0.014	0.126	17	0.111	1.000
<b>D Spring - D Summer</b>	<b>-0.470</b>	<b>0.136</b>	<b>17</b>	<b>-3.459</b>	<b>0.045</b>
E Spring - I Spring	0.112	0.126	17	0.888	1.000
<b>E Spring - E Summer</b>	<b>0.050</b>	<b>0.126</b>	<b>17</b>	<b>0.398</b>	<b>1.000</b>
<b>I Spring - I Summer</b>	<b>-0.917</b>	<b>0.126</b>	<b>17</b>	<b>-7.297</b>	<b>&lt;0.001</b>
D Summer - E Summer	0.422	0.136	17	3.108	0.096
D Summer - I Summer	-0.434	0.136	17	-3.194	0.080
E Summer - I Summer	-0.856	0.126	17	-6.806	<0.001

## APPENDIX PUBLICATION V

**Table S19:** Results of the Tukey's HSD post-hoc test for the recovery of the particulate organic carbon (POC) of the large size fraction. Contrasts are presented between seasons for the same treatment and between treatments of the same seasons. Abbreviations for the nutrient scenarios are daily pulses (D), intermittent pulses (I), and one extreme pulse (E). Standard errors (SE) and degrees of freedom (df) are reported. Contrasts between the sites of the same treatment are highlighted in bold.

Recovery: C for Site					
Contrast	Estimate	SE	df	t-ratio	p-value
D Bolmen - E Bolmen	0.536	0.221	15	2.427	0.424
D Bolmen - I Bolmen	0.030	0.221	15	0.136	1.000
<b>D Bolmen - D Erken</b>	<b>-0.216</b>	<b>0.221</b>	<b>15</b>	<b>-0.979</b>	<b>1.000</b>
E Bolmen - I Bolmen	-0.506	0.236	15	-2.143	0.733
<b>E Bolmen - E Erken</b>	<b>-0.154</b>	<b>0.221</b>	<b>15</b>	<b>-0.699</b>	<b>1.000</b>
<b>I Bolmen - I Erken</b>	<b>-0.514</b>	<b>0.221</b>	<b>15</b>	<b>-2.331</b>	<b>0.512</b>
D Erken - E Erken	0.597	0.221	15	2.707	0.243
D Erken - I Erken	-0.268	0.221	15	-1.216	1.000
E Erken - I Erken	-0.866	0.204	15	-4.238	0.011

**Table S20:** Results of the Tukey's HSD post-hoc test for the OEV of the particulate C:N ratio of the large size fraction. Contrasts are presented between seasons for the same treatment and between treatments of the same seasons. Abbreviations for the nutrient scenarios are daily pulses (D), intermittent pulses (I), and one extreme pulse (E). Standard errors (SE) and degrees of freedom (df) are reported. Contrasts between the sites of the same treatment are highlighted in bold.

OEV: log(CN) for Season					
Contrast	Estimate	SE	df	t-ratio	p-value
D Spring - E Spring	-0.598	0.225	17	-2.660	0.248
D Spring - I Spring	-0.530	0.225	17	-2.357	0.460
<b>D Spring - D Summer</b>	<b>1.495</b>	<b>0.243</b>	<b>17</b>	<b>6.157</b>	<b>&lt;0.001</b>
E Spring - I Spring	0.068	0.225	17	0.303	1.000
<b>E Spring - E Summer</b>	<b>2.507</b>	<b>0.225</b>	<b>17</b>	<b>11.149</b>	<b>&lt;0.001</b>
<b>I Spring - I Summer</b>	<b>1.887</b>	<b>0.225</b>	<b>17</b>	<b>8.390</b>	<b>&lt;0.001</b>
D Summer - E Summer	0.414	0.243	17	1.703	1.000
D Summer - I Summer	-0.139	0.243	17	-0.572	1.000
E Summer - I Summer	-0.552	0.225	17	-2.456	0.376

## APPENDIX PUBLICATION V

**Table S21:** Results of the Tukey's HSD post-hoc test for the OEV of the particulate C:N ratio of the large size fraction. Contrasts are presented between sites for the same treatment and between treatments of the same site. Abbreviations for the nutrient scenarios are daily pulses (D), intermittent pulses (I), and one extreme pulse (E). Standard errors (SE) and degrees of freedom (df) are reported. Contrasts between the sites of the same treatment are highlighted in bold.

OEV: log(CN) for Site					
Contrast	Estimate	SE	df	t-ratio	p-value
D Bolmen - E Bolmen	0.347	0.279	17	1.243	1.000
D Bolmen - I Bolmen	0.392	0.279	17	1.403	1.000
<b>D Bolmen - D Erken</b>	<b>1.074</b>	<b>0.301</b>	<b>17</b>	<b>3.564</b>	<b>0.036</b>
E Bolmen - I Bolmen	0.045	0.279	17	0.160	1.000
<b>E Bolmen - E Erken</b>	<b>1.141</b>	<b>0.279</b>	<b>17</b>	<b>4.089</b>	<b>0.011</b>
<b>I Bolmen - I Erken</b>	<b>0.544</b>	<b>0.279</b>	<b>17</b>	<b>1.949</b>	<b>1.000</b>
D Erken - E Erken	0.414	0.301	17	1.372	1.000
D Erken - I Erken	-0.139	0.301	17	-0.461	1.000
E Erken - I Erken	-0.552	0.279	17	-1.980	0.962

**Table S22:** Results of the Tukey's HSD post-hoc test for the recovery of the particulate C:N ratio of the large size fraction. Contrasts are presented between seasons for the same treatment and between treatments of the same season. Abbreviations for the nutrient scenarios are daily pulses (D), intermittent pulses (I), and one extreme pulse (E). Standard errors (SE) and degrees of freedom (df) are reported. Contrasts between the sites of the same treatment are highlighted in bold.

Recovery: CN for Season					
Contrast	Estimate	SE	df	t-ratio	p-value
D Spring - E Spring	0.069	0.075	17	0.925	1.000
D Spring - I Spring	-0.015	0.075	17	-0.194	1.000
<b>D Spring - D Summer</b>	<b>0.310</b>	<b>0.081</b>	<b>17</b>	<b>3.822</b>	<b>0.020</b>
E Spring - I Spring	-0.084	0.075	17	-1.118	1.000
<b>E Spring - E Summer</b>	<b>-0.223</b>	<b>0.075</b>	<b>17</b>	<b>-2.969</b>	<b>0.129</b>
<b>I Spring - I Summer</b>	<b>0.389</b>	<b>0.075</b>	<b>17</b>	<b>5.179</b>	<b>0.001</b>
D Summer - E Summer	-0.463	0.081	17	-5.715	<0.001
D Summer - I Summer	0.064	0.081	17	0.794	1.000
E Summer - I Summer	0.528	0.075	17	7.030	<0.001



## APPENDIX PUBLICATION V

**Table S23:** Results of the Tukey's HSD post-hoc test for the recovery of the particulate C:N ratio of the large size fraction. Contrasts are presented between sites for the same treatment and between treatments of the same site. Abbreviations for the nutrient scenarios are daily pulses (D), intermittent pulses (I), and one extreme pulse (E). Standard errors (SE) and degrees of freedom (df) are reported. Contrasts between the sites of the same treatment are highlighted in bold.

Recovery: CN for Site					
Contrast	Estimate	SE	df	t-ratio	p-value
D Bolmen - E Bolmen	0.026	0.078	15	0.328	1.000
D Bolmen - I Bolmen	-0.034	0.078	15	-0.435	1.000
<b>D Bolmen - D Erken</b>	<b>0.432</b>	<b>0.078</b>	<b>15</b>	<b>5.543</b>	<b>0.001</b>
E Bolmen - I Bolmen	-0.060	0.083	15	-0.714	1.000
<b>E Bolmen - E Erken</b>	<b>-0.057</b>	<b>0.078</b>	<b>15</b>	<b>-0.726</b>	<b>1.000</b>
<b>I Bolmen - I Erken</b>	<b>0.530</b>	<b>0.078</b>	<b>15</b>	<b>6.803</b>	<b>&lt;0.001</b>
D Erken - E Erken	-0.463	0.078	15	-5.941	<0.001
D Erken - I Erken	0.064	0.078	15	0.825	1.000
E Erken - I Erken	0.528	0.072	15	7.308	<0.001

**Table S24:** Results of the Tukey's HSD post-hoc test for the OEV of the particulate C:P ratio of the large size fraction. Contrasts are presented between seasons for the same treatment and between treatments of the same season. Abbreviations for the nutrient scenarios are daily pulses (D), intermittent pulses (I), and one extreme pulse (E). Standard errors (SE) and degrees of freedom (df) are reported. Contrasts between the sites of the same treatment are highlighted in bold.

OEV: C:P for Season					
Contrast	Estimate	SE	df	t-ratio	p-value
D Spring - E Spring	3.053	0.514	17	5.942	<0.001
D Spring - I Spring	2.199	0.514	17	4.281	0.008
<b>D Spring - D Summer</b>	<b>4.482</b>	<b>0.555</b>	<b>17</b>	<b>8.078</b>	<b>&lt;0.001</b>
E Spring - I Spring	-0.853	0.514	17	-1.661	1.000
<b>E Spring - E Summer</b>	<b>-2.992</b>	<b>0.514</b>	<b>17</b>	<b>-5.825</b>	<b>&lt;0.001</b>
<b>I Spring - I Summer</b>	<b>1.561</b>	<b>0.514</b>	<b>17</b>	<b>3.039</b>	<b>0.111</b>
D Summer - E Summer	-4.422	0.555	17	-7.970	<0.001
D Summer - I Summer	-0.722	0.555	17	-1.301	1.000
E Summer - I Summer	3.700	0.514	17	7.203	<0.001

## APPENDIX PUBLICATION V

**Table S25:** Results of the Tukey's HSD post-hoc test for the OEV of the particulate C:P ratio of the large size fraction. Contrasts are presented between sites for the same treatment and between treatments of the same site. Abbreviations for the nutrient scenarios are daily pulses (D), intermittent pulses (I), and one extreme pulse (E). Standard errors (SE) and degrees of freedom (df) are reported. Contrasts between the sites of the same treatment are highlighted in bold.

OEV: C:P for Site					
Contrast	Estimate	SE	df	t-ratio	p-value
D Bolmen - E Bolmen	-0.605	0.579	17	-1.044	1.000
D Bolmen - I Bolmen	0.107	0.579	17	0.184	1.000
<b>D Bolmen - D Erken</b>	<b>1.443</b>	<b>0.626</b>	<b>17</b>	<b>2.307</b>	<b>0.509</b>
E Bolmen - I Bolmen	0.711	0.579	17	1.228	1.000
<b>E Bolmen - E Erken</b>	<b>-2.375</b>	<b>0.579</b>	<b>17</b>	<b>-4.100</b>	<b>0.011</b>
<b>I Bolmen - I Erken</b>	<b>0.614</b>	<b>0.579</b>	<b>17</b>	<b>1.061</b>	<b>1.000</b>
D Erken - E Erken	-4.422	0.626	17	-7.069	<0.001
D Erken - I Erken	-0.722	0.626	17	-1.154	1.000
E Erken - I Erken	3.700	0.579	17	6.389	<0.001

## Acknowledgements

Coming to an end, I would like to express my deepest gratitude to all those who supported me in all various ways throughout my journey! First and foremost, I would like to thank my supervisors Maren Striebel and Helmut Hillebrand for a perfect balance of guidance, freedom, endless support and creation of opportunities. I am beyond thankful to have experienced such amazing supervision and to have learned from such inspiring scientists and role models.

Furthermore, I would like to thank my further thesis committee members – Miriam Gerhard, Silke Langenheder and Jan Freund – for dedicating their time to extremely productive discussions and constructive feedback on my chapters and thesis.

Moreover, I would like to thank all members of the Plankton Ecology working group for creating such a warm, welcome and supportive working atmosphere. I truly feel honored to have been part of this amazing group! Especially, I want to thank Heike Rickels and Christian Spindler as none of my experimental work would have been possible without your excellent technical assistance, and my fellow PhD students – Charlotte Kunze, Anna Lena Heinrichs, Sebastian Neun and Mike Smykala – for a lot of smart advice in the lab and about coping with life as a PhD student, for your positivity, humour and genuine joy for each other.

Throughout this journey, I also worked with many great and inspiring scientists on various mesocosm experiments and am extremely grateful for all the wonderful memories that were made during long hours in the lab and field. I found great friends in the most unexpected place and am very grateful for monthly online meetings with Katerina Symiakaki, Sarah Hasnain, Varsha Rani, Katalin Patonai and Alexis Guislain in which sharing life updates (rightfully so) often received more time than actual discussions.

Additionally, I found a truly wonderful group of friends in Bremen on the way and am deeply thankful for all your encouragement, optimism, and genuine support throughout my journey. Thank you so much, Antonia Ahme, Benjamin Ahme, Linda Rehder, Carla Pein, Joel Bose and Ruben Schulte-Hillen.

I also want to thank my family – my mum, my dad, my brother and our dog – for always supporting me with all you can give and always welcoming me back home with the loveliest dinners and game nights when all I needed was a mental break.

Finally, I am beyond grateful for having such a supportive, loving and brilliant partner on my side. I do not know how to thank you enough, Jakob, for navigating this crazy time with me.

## **Declaration**

### **Versicherung an Eides Statt**

Ich, Anika Happe,

Hiermit versichere ich, dass ich die von mir vorgelegte Dissertation zum Erlangen des Grades eines Doktor rerum naturalium (Dr. rer. nat.) selbstständig verfasst und keine anderen als die angegebenen Hilfsmittel und Quellen genutzt habe. Alle Tabellen und Graphiken sowie alle wörtlich oder dem Sinn entnommenen Stellen sind von mir als solche gekennzeichnet. Des Weiteren versichere ich, dass Dritte von mir weder unmittelbar noch mittelbar geldwerte Leistungen erhalten haben, die im Zusammenhang mit dem Promotionsverfahren stehen könnten. Ich versichere, dass diese Dissertation weder in ihrer Gesamtheit noch in Teilen einer anderen Hochschule zur Begutachtung in einem Promotionsverfahren vorliegt oder vorgelegen hat.

Im Zusammenhang mit dem Promotionsvorhaben wurden keine kommerziellen Vermittlungs- oder Beratungsdienste (Promotionsberatung) in Anspruch genommen. Diese Arbeit ist noch nicht veröffentlicht worden, angegebene Teile sind jedoch zur Publikation einreicht. Die Leitlinien guter wissenschaftlicher Praxis an der Carl von Ossietzky Universität Oldenburg wurden befolgt. Die Satzungen der Promotionsordnung sind mir bekannt und von mir eingehalten worden.



---

Ort, Datum, Unterschrift



2025

ANIKA HAPPE